ABSTRACT

TRANDEL, MARLEE ANNE. Cell Wall Polysaccharides in Grafted and Non-Grafted 'Liberty' Watermelon with Hollow Heart (Under the direction of Dr. Penelope Perkins-Veazie)

Triploid (seedless) watermelon [*Citrullus lanatus* (Thunb. Mastum and Nakai).] is prone to hollow heart (HH), a disorder expressed as a crack in the flesh expanding to an open cavity in the fruit. Watermelon genetics, environmental conditions, and pollen deficit can induce HH, and fruit with lower tissue firmness are more susceptible. Grafting watermelon to cucurbit rootstocks (RS) can increase tissue firmness, possibly from increased cell density, changes in cell wall pectins, or a combination of these. Cell wall pectins play an important role in cell wall strength, internal flesh quality and plant defense.

Since HH is sporadic, affecting 0 to 65% of fruit in a season, watermelon cultigen data from previous three-year studies was subjected to logistic regression to identify genetic sources of HH. In the first field study, HH was induced by using 'Liberty' watermelon and reduced diploid pollen. Rootstock (RS) cultivars grafted to 'Liberty' were used in a second field study to follow HH. Interspecific squash hybrid (*C. maxima* x *C. moschata*) RS 'Carnivor' and 'Kazako', bottle gourd (*Lageneria siceraria*) RS 'Emphasis', and non-grafted plants were used as controls. Flesh firmness was increased by 1 N for fruit from interspecific RS. Using confocal microscopy, cells from fruit with HH had increased area, decreased number of cells, and areas of cell wall breakage. Cell density was increased in fruit grafted onto 'Carnivor' compared to non-grafted fruit.

In a final field study with non-grafted 'Liberty' or grafted to 'Carnivor', HH incidence was 34% less and tissue firmness was increased by 3 N in grafted fruit compared to non-grafted fruit. Heart tissue firmness was lower in fruit with HH (15.9 N) compared to those no HH (19.1 N). Compositional changes in fruit were not significantly different with graft or HH. Placental fruit tissue was used for extraction of alcohol insoluble residues which were then subjected to total pectin sequential extraction or were reduced, methylated, hydrolyzed and acetylated followed by GC-MS analysis. Among pectic fractions, water soluble fractions were lowest and carbonate soluble fractions were reduced with HH. Twelve monosaccharides were identified in fruit from grafted plants with and without HH. Glucose and galactose were highest in abundance followed by xylose and arabinose. Meso-erythritol, fucose, rhamnose, arabinose and 2-deox-d-

glucose were highest in fruit with HH at 0.32, 2.36, 3.38, 21.29 and 0.55 $\mu g \cdot mg^{-1,}$ respectively. Ribose and allose were highest in fruit from grafted plants with no HH at 1.27 and 0.64 $\mu g \cdot mg^{-1}$, respectively. Degree of methylation (e.g. % of cell wall degradation) or uronic acid concentrations did not differ. Using methylation linkage assembly, 34 partially methylated alditol acetates were detected. Three linkages, 4-Glc(p), 3-Glc(p) and 2,4-Glc(p), were highest in grafted fruit with no HH.

HH could be successfully induced in watermelon fruit by limiting the amount of pollen (with fewer pollinator plants) and using a triploid watermelon cultivar known to be susceptible to HH. 'Liberty' fruit from those grafted onto an interspecific squash hybrid RS reduced HH incidence, increased tissue firmness and cell density. The interaction of RS and scion graft appears to protect fruit from HH by increasing tissue firmness. Watermelon with HH had higher meso-erythritol, fucose, rhamnose, and arabinose. Although fruit textural characteristics were different between grafting treatments, no clear trends were identified in cell wall composition and the current analyses could not fully explain the increased fruit tissue firmness. In future watermelon research, exploring the relationships among fruit tissue microstructure, middle lamella separation, degree of polymerization and enzyme activity may help link textural changes to cell wall composition.

Cell Wall Polysaccharides in Grafted and Non-Grafted ‘Liberty’ Watermelon with Hollow Heart

by
Marlee Anne Trandel

A dissertation submitted to the Graduate Faculty of
North Carolina State University
in partial fulfillment of the
requirements for the degree of
Doctor of Philosophy

Horticultural Science

Raleigh, North Carolina
2020

APPROVED BY:

Dr. Penelope Perkins-Veazie Committee Chair	Dr. Suzanne Johanningsmeier
Dr. Jonathan Schultheis	Dr. Chris Gunter

DEDICATION

First and foremost, I dedicate this dissertation and all of my doctoral work to my beautiful mother in heaven, Jody Trandel. Mom, even though I lost you at such a young age, I know you never really left me. You have had a hand on my shoulder and served as my guardian angel and protector. In my darkest days, I could feel you steering me in the right direction reminding me to believe in myself. I hope you know the strength and persistence you have given me. Secondly, I dedicate this dissertation to my grandmother in heaven, Marlene DeVito. Through losing both of you, I was able to find my life purpose which is to spread knowledge and love among all. In my hardest times, my prayers were answered by both women as they are a strong reason for not only my determination but my passion and enthusiasm. It is in their memory that I dedicate and give much credit for not only these advances in my academic career but also my future professional career.

BIOGRAPHY

Marlee Trandel is doctoral candidate in the Department of Horticultural Sciences from North Carolina State University (NCSU). She works as a research assistant in the postharvest physiology lab at the Plants for Human Health Institute (PHHI). She has experience in watermelon field production, postharvest physiology and plant cell wall chemistry. Before joining NCSU, Marlee completed a BS in Animal Science from the College of Agricultural Sciences, a BA in Chemistry, from the College of Biochemistry and Chemistry in 2014 and a MS in Horticulture Sciences in the College of Agricultural Sciences in 2016 from Southern Illinois University Carbondale.

Marlee is researcher and scientist in horticulture with an emphasis on food chemistry, specifically cell wall polysaccharides. She has an extensive background in organic and sustainable horticulture production, plant physiology/biochemistry and plant stable isotopes. Her current research is focused on changes in postharvest physiology of grafted and non-grafted triploid (seedless) watermelon with an internal fruit disorder known as hollow heart. She combines plant physiology with food chemistry to relate fruit quality attributes to total cell wall pectins and plant cell wall polysaccharide strength and integrity.

ACKNOWLEDGMENTS

I would like to express my deepest gratitude to my major advisor Dr. Penelope Perkins-Veazie, for her undeniable support, expertise, guidance, understanding and time. Without her daily encouragement and knowledge the depth and novelty of my research would be lacking. She pushed both myself and my research to levels I thought were uncappable. Dr. Perkins-Veazie is a woman I give utmost respect to. Her consistent support made a tremendous difference in the course of my PhD and she positively impacted my life and future career.

I would also like to express appreciation towards Dr. Jonathan Schultheis, a committee member who played a pivotal role in designing my field experiments. His knowledge of watermelon production and hollow heart disorder was a leading factor in obtaining watermelon material. I thank Dr. Suzanne Johanningsmeier, who served on my committee as the expert in cell wall polysaccharides. She spent countless hours with me helping to set up instrumentation, discussing our findings and guiding my method optimization. Her guidance is a major reason for my cell wall polysaccharide discoveries and she gave me passion to understand as much as possible in plant cell wall chemistry. I thank Dr. Chris Gunter for serving on my committee. He brought a depth of knowledge to my research and served as my extension mentor. I thank Dr. Eva Johannes for her knowledge and training on confocal microscopy.

I thank the field crew from the Cunningham Research Station, Central Crops Research Station and Cherry Farms Research Station for helping to manage my watermelon trials. I thank Dr. Schultheis's 2017 and 2019 summer work crew for helping to harvest and collect all field data on my watermelon.

To my fiancé, Tyler Hayse, you have given never-ending love and encouragement. You have consistently been there to lift me up - thank you so much for believing in me when I forgot to believe in myself. I thank Joyce Edwards and Erin Deaton for their help preparing and running my samples in the laboratory. I thank Joy Smith and Alex Long for their statistical analysis help. Finally, I give a special thanks to my fellow graduate students in the Department of Horticultural Sciences, who encouraged me throughout the challenges, along with the faculty and staff at the Raleigh and Kannapolis campuses from North Carolina State University. A very special thanks also goes out to my numerous friends who encouraged me as they watched me chase my dreams.

TABLE OF CONTENTS

LIST OF TABLES

LIST OF FIGURES

CHAPTER 1

LITERATURE REVIEW

Globally, watermelon is the largest produced fruit crop (Tlili et al., 2011), with1.7 million tonnes produced in 2018 (USDA, 2019). China dominates world production and the U.S. is 7th with 39,0545 hectares planted annually (National Agriculture Survey, 2019). Watermelon is consumed by many around the world for its seeds, juice, or as a dessert fruit. The fruit has a high nutritional value, containing the mineral salts (Ca, K, Fe and Mg) and vitamins (A, B, C and E), and also contains compounds with antioxidant properties such as lycopene, citrulline, and some complex polyphenols (Dammak et al., 2019).

Seeded (diploid) watermelon are the most common genotype grown worldwide. In the U.S., seedless (triploid) watermelon now make up 90-95% of the U.S. market (Levi et al., 2014). Seedless watermelon are triploid hybrids resulting from a cross between diploid (paternal) and tetraploid (maternal) lines. The lack of large seed locules and possibly increased cell density is thought to improve the firmness of triploid watermelons. Production of triploids is challenging because of susceptibility to soil-borne diseases and nematodes, the lack of highly effective soil fumigation, and the need for diploid plants for pollination within the same field (Levi et al., 2014).

Triploid watermelon are also more prone than diploid fruit to an internal fruit disorder known as hollow heart (HH). This internal fruit disorder is exhibited as a cavity or void air space in the center of the fruit (Johnson 2014; 2015). HH is a difficult disorder to study because incidence is highly variable from season to season and multiple factors seem to initiate or aggravate the disorder. To date, little is known about the disorder relative to fruit quality and compositional attributes.

Grafting watermelon onto *Cucurbita* rootstocks is increasingly being used as a means to reduce damage caused by soil-borne diseases (e.g., *Fusarium*, *Verticillium*, *Phytophthora*, *Pseudomonas* etc.) (Mohamed et al., 2012). Grafting has been reported to change fruit quality attributes, including tissue firmness, rind thickness, lycopene, and citrulline (Davis et al., 2008). Rootstocks from interspecific hybrid squash (*Cucurbita maxima* x *C. moschata*), bottle gourd (*Laginaria siceraria*) and wildtype (*C. lanatas var. citroides*) are commonly used in watermelon grafting (Hassell et al., 2008). Significant fruit quality improvements appear to be especially prevalent when watermelon scions are grafted onto interspecific hybrid rootstocks. Such

improvements include increased tissue firmness (e.g., tissue density), rind thickness, and postharvest shelf life (Soteriou et al., 2014; 2017).

The changes in fruit quality, specifically in fruit firmness and the onset of HH, indicate that fruit cell wall strength and subsequent integrity of watermelon tissue may be at play. In dicots (e.g., cucurbits), cell walls consist of the hemicellulose/cellulosic and pectin networks (Pettolino et al., 2012). The pectin network includes various polysaccharide classes which are made up of 17 monosaccharide building blocks (Houben et al., 2011). Monosaccharide analysis and linkage assembly is a useful technique to elucidate the various polysaccharide classes. Advantages of obtaining monosaccharaide concentrations and linkage composition of the cell wall include the potential to estimate the relative proportions of different polysaccharide classes, uronic acid concentration (galacturonic and glucuronic acids) and degree of methylation (cell wall degradation) (Pettolino et al., 2012). Understanding pectic polysaccharides may help explain changes in fruit tissue firmness (Brummell, 2006) and obtain unknown information on cell wall disassembly in fruit with HH.

Botany of watermelon

Watermelons are defined as globular pepos that are smooth with a hard outer rind (Lebo, 1932). The hard outer portion is the pericarp, consisting of successive layers of the following: 1) epidermis that is one cell thick, transparent and has thickened outer walls with many stomata; 2) hypoderm that is comprised of many cells with chlorophyll, responsible for the green exterior color; 3) mesocarp (outer and middle), which is traversed with vascular bundles and sieve tubes; and 4) endocarp consisting of one layer of small, thin, elongated cells (Lebo, 1932; Sedgley et al., 1977). The greater portion of the fruit is the edible flesh derived from the placentae (heart tissue). Locules are known as areas in the fleshy part (placenta) that hold the endocarp and seeds (or seed traces in triploid fruit).

Within the locule is the ovule, which is made up of fused carpels and septa (Johnson, 2015). Before pollination, the ovule initially begins as the ovary located below pistillate flowers and petals (Sungiyama et al., 2014). After pollination, tissue differentiation begins with the ovule, carpels and septa. Around 2 to 3 dap, fruit placental and rind tissue begin to develop (Sungiyama et al., 2014). These various tissues types can be used to identify differences in the physical (e.g., tissue firmness and tissue density) and chemical (e.g., phytonutrients, sugars, vitamins and cell wall polysaccharides) qualities of watermelon fruit.

Watermelon fruit contains tissue types that play important roles in developing specific physicochemical and phytochemical qualities. The watermelon rind and flesh contain mineral salts, proteins, carbohydrates (sugars and pectins), lipids, vitamins, and citrulline (Petkowicz et al., 2016; USDA Food composition database, 2020). The flesh consists of highly developed placental (heart) tissue, which is known as the edible part of the fruit (Tarazona-Diaz et al., 2010).

Watermelon pollination and fruit development

Watermelon fruit development begins with fertilization (pollination). Watermelon plants produce separate male and female flowers and require insects, such as honey bees, for successful pollination. Bees visit staminate (male) flowers and transfer pollen to open pistillate (female) flowers (Walters, 2005). The amount of pollen transferred to the female pollen and viability of pollen play important roles in fruit development and subsequent onset of fruit disorders (Johnson, 2014). It has been reported that pollinators need to visit a seeded (2N) watermelon flower between 7-9 to ensure proper pollination, which increases to14-16 visitations for a seedless (3N) watermelon flower (Johnson, 2014; Walters et al., 2009).

Watermelon flowers open in the morning and the stigma is receptive to pollination for only a few hours (Walters, 2005). Within 24 to 36 hours of pollen deposit on the stigma, pollen grains germinate and pollen tubes penetrate the ovary, swelling begins and the ovule is produced. This is when fruit tissue differentiation and development begin (Kano, 1993). As the fertilized ovule develops, cytokinin, gibberellins and plant signals are released which stimulate the division and expansion of fruit cells (Nistch, 1970).

Watermelon fruit growth is slow until 2 days post anthesis (dpa), then increases rapidly and consists of cell division. Between 7-10 dpa, cell division in the placental tissue slows and instead the mesocarp (placental) cells increase in size and volume. Conversely, cell division in the heart region of the watermelon fruit stops when the ovary diameter reaches roughly 35 mm, which is between days 7 to 10 after fruit set (Nitsch, 1970). In contrast, cell division continues in the fruit rind until removal from the vine at about 40 dpa (Kano, 1993; Johnson, 2014).

About halfway through fruit growth the mesocarp starts to change to thickened and pitted cells. This tissue consists of very large cells encompassed by a primary cell wall and separated by intercellular spaces. As the fruit continue to uptake nutrients and photosynthesize, these intercellular spaces fill with sugars and water that are translocated from the epidermis through

the tracheary elements (Wechter et al., 2008). Around 36 days after pollination (DAP), the transitional phase begins and fruit will start to change color due to plastid accumulation in the placental tissue. Fruit tissue is white (10 dpa) and transition to mature placental tissue can be seen as the appearance of pink at 12 dpa then red color around 30 dap (Perkins-Veazie et al., 2001; 2006). The carotenoid pathway shifts from lutein production to phytofluene at the white-flesh stage. Lutein plays an important role in the photosynthetic light-harvesting assembly and plays an role in protection of protoplasts during immature fruit stages (Guo et al., 2018; Grassi et al., 2013). With the onset of the white-pink stage, the carotenoids phytoene and phytofluene increase (Wechter et al., 2008; Zhu et al., 2017) and lycopene synthesis and accumulation is promoted into the red-ripe stage at 36-45 dap (Tadmor, 2005). In red-fleshed watermelon fruit, trans-lycopene content can range from 20 to 150 mg/kg, depending on cultivar while beta carotene is present in much lower amounts, from 1 to 6 mg/kg (Perkins-Veazie et al., 2006). Trans-lycopene content tends to decrease in overripe watermelon while beta carotene increases. (Perkins-Veazie et al., 2006).

Citrulline and arginine are important amino acids found in watermelon; citrulline is unusually high in watermelon fruit (Rimando and Perkins-Veazie, 2005). Citrulline biosynthesis is from the breakdown of glutamate and is a precursor to arginine (Joshi et al., 2019). Three substrates are thought to promote plant citrulline synthesis, including ornithine carbomoyltransferase, arginase and nitric oxide synthase (Domingos et al., 2015). Citrulline content in leaves, roots and shoots is lower than in fruit flesh for all development stages. Citrulline biosynthesis occurs in the watermelon plant chloroplasts of leaves and rind. Citrulline is mobile and the watermelon rind may act as a gatekeeper in regulating citrulline content to the placental tissue (Yuan et al., 2016; Joshi et al., 2019), as the ratio of citrulline in placental to rind tissue decreases with fruit maturity (Joshi et al., 2019). Generally citrulline starts to increase in watermelon leaves and fruit flesh at around 20-25 dap and citrulline and arginine concentration is highest at 40 dap (red ripe) (Joshi et al., 2019). Relative amounts of citrulline and arginine vary greatly among watermelon cultivars (Joshi et al., 2019).

Sweetness of watermelon is a pivotal factor for consumer fruit quality and is determined by the soluble solids content (°Brix) and total soluble sugar content (Yativ et al., 2010). The developmental stage influences sugar pattern and accumulation. In watermelon fruit, the soluble sugars are primarily sucrose, glucose and fructose. Gao et al. (2018) reported both soluble solids

content and sucrose begin to peak around 26 dpa (3-4 weeks after pollination). Accumulation of glucose begins early and peaks at around 18 dpa, while fruicose and sucrose peak around 34 dpa (Gao et al., 2018). The rate of sugar accumulation increases as fruit approach 40 dpa (Grassi et al., 2013). Watermelon can vary widely in presence and amount of sucrose, with a range of 0 to 76% of total sugars depending on cultivar (Elmstrom and Davis, 1981; Gao et al., 2018). In mature (commercial) watermelon, proportions of sucrose and glucose are generally found in the range of 20-40% of total sugars and fructose is between 30-50% (Yativ et al., 2010).

Another pertinent biochemical pathway during the development and maturation of watermelon fruit is the primary plant cell wall. Cell wall metabolism has important roles in cell definition, expansion, regulation of plant development, fruit ripening and fruit senescence (Karakurt and Huber, 2009). Changes in tissue firmness during maturation and postharvest softening is attributed to hydrolysis (disassembly) of the cell wall (Huber, 1983; Elkashif and Huber, 1988; Brummell, 2006). Elkashif and Huber (1988) reported progressive breakdown and dissolution of the middle lamella and gradual separation of cell wall fibrils increased tissue softening in watermelon placental tissue. Cell wall enzymes, specifically polygalacturonase, have been associated to fruit softening (Karakurt and Huber, 2009).

Hollow heart formation in watermelon

HH, also known as internal cracking, is a physiological disorder most commonly found in seedless watermelon. This internal split or void that develops in the placental tissue is caused by the separation of three internal fruit compartments; ovule, locule and septum (Johnson, 2015). Although the cause of HH has not been definitively determined, watermelon genetics, lack of adequate pollination and environment and water stress appear to play definitive roles (Johnson, 2014; 2015). Watermelon cultivars (or cultigens) vary considerably in their susceptibility to HH, and this may be from different rates of internal flesh expansion or from differences in flower pollen receptivity (Walters et al., 2009).

Increased HH has been loosely associated with cold or rainy weather, low bee activity, and lack of staminate flowers (Johnson, 2014; 2015). Events which ultimately reduce bee visits and indicate that inadequate pollination is a primary cause of HH. Inferior pollination may be from a lack of viable pollen, a need for more pollen in some genotypes than others to stimulate hormone secretion, or a problem in the receptiveness of the stigma of some genotypes (Walters, 2005; Sugiyama et al., 2008). Triploid watermelon require diploid counterparts for viable pollen.

To achieve optimal fruit yields, a rule of thumb is to plant between 25-33% of a field with diploid plants (Brusca et al., 2013). This is generally done by interplanting a seeded watermelon cultivar in the same field- either in the same row as triploid plants or as a dedicated row only for diploid pollinizers (Freeman et al., 2007). Generally, anything less than 20% of a field (i.e. four triploid watermelon planted to one diploid interplanted) increases HH formation in fruit. Inadequate rates (or amounts) of proper pollination is one of the leading causes with the onset of HH in watermelon (Freeman et al., 2007).

Internal cracking starts at the epidermal layers within the carpels, ovule and septum (e.g., mesocarp or placental tissue). Kano (1993) and Johnson (2015) reported HH may develop due to differences in growth rates of the rind and flesh, and where rates are most different, softer flesh and decreased cell numbers have been found. The watermelon rind continues to expand and differentiate during the entire time the fruit is attached to the vine (i.e., the rind grows fast). In contrast, mesocarp tissue division stops at days 7-10 after fruit set, and tissue growth slows as cells enlarge with water, sugars, proteins and nutrients. If the relative rates of rind and mesocarp growth are too far apart, the three internal fruit compartments will separate, leading to HH (Kano, 1993; Johnson, 2015).

Although internal cracking has no negative effects on sweetness, it has been associated with the overall quality of the harvested fruit including differences in tissue firmness and cell size (Kano, 1993). Researchers have reported watermelon cultivars with lower density flesh have been shown to have a higher incidence of HH (Kano, 1993; Johnson, 2014; 2015). Density is related to the number of fruit cells in the heart tissue and the size of cells. Generally, fruit with larger cells (less dense) have lower tissue firmness and are more susceptible to hollow heart (Johnson, 2015; Kano, 1993).

Watermelon grafting

Breeding for watermelon resistance to soil borne diseases and nematodes takes many years. More immediate means to keep these problems under control have been soil fumigation or land rotation, but loss of effective fumigants and of inexpensive agricultural land has driven interest in other approaches, such as grafting (Davis et al., 2008). Grafting involves placement of a scion (e.g., a young watermelon shoot) that will produce fruit with desired qualities onto a disease-resistant rootstock. A number of plant and fruit traits (morphological and compositional)

can be affected with this technique, some of which are undesirable (Lee and Oda, 2003; Davis et al., 2008; Soteriou et al., 2014; 2017).

Rootstock-scion combinations affect plant production and often result in enhanced plant vigor and increased disease resistance. Grafting with certain rootstocks, such as interspecific hybrid squash (*Cucurbita maxima* x *C. moschata*), increase fruit firmness and cell density. It has been observed that watermelon cultigens with decreases in tissue firmness are more susceptible to HH disorder (Johnson, 2014; 2105). Grafting onto rootstocks that increase fruit tissue firmness may be useful for HH susceptible scions, but this area has not been explored.

Grafted plants also show an increased uptake of water and nutrient use efficiency and have a more vigorous root system when compared to non-grafted plants (Martinez-Bellasta et al., 2010). It has been reported that rootstocks enhance nitrogen shuttling, nitrate reductase activity and nitrate accumulation in watermelon and tomato (Kawagauchi et al., 2008; Martinez-Bellasta et al., 2010). In tomato, grafting also increased leaf water content by ~35%, which increases leaf size and plant photosynthetic capacity, protein synthesis and osmotic/turgor pressure (Martinez-Bellasta et al., 2010). A similar phenomena may be happening in watermelon. The improved performance of grafted plants can also affect fruit quality and compositional attributes (Soteriou et al., 2017). The precise mechanisms that influence rootstock-scion interactions are not well understood, and may take place at the cellular or molecular level, as suggested by Soteriou et al. (2017).

For watermelon, the rootstocks that appear to work best to achieve desired quality traits include wild watermelon (*C. lanatas* var. *citroides*), bottle gourd (*Lagenaria siceraria*), and interspecific squash hybrids (*Cucurbita maxima* x *C. moschata*) (Thies et al, 2010; Soteriou et al., 2014; 2017). A range of watermelon fruit traits have been reported to be affected by rootstock, including marketable yields, fruit shape, rind thickness, placental flesh firmness, flavor, carotenoid content, sugars, organic acids, and amounts of certain amino acids (Davis et al., 2008; Yuan et al., 2016). Several of these traits influence consumer appeal and postharvest shelf life; grafting with interspecific hybrids and bottle gourd rootstocks enhanced fruit physical qualities (e.g., increasing yields, soluble solids and fruit shape) (Yetisir et al., 2003). Obstacles to use of wild type rootstocks were problems with abnormal fruit quality (e.g., insipid taste, poor texture and decreased firmness) (Yetisir et al., 2003). Newer releases of wild type rootstocks

appear to be increasing the postharvest quality of grafted watermelon without texture and off flavor issues (Fredes et al., 2016).

Physiochemical differences between grafted and non-grafted watermelon

Watermelon fruit are often harvested before lycopene or red color is at the maximum (Perkins-Veazie et al., 2006b; Collins et al., 2006). The soluble solids (sugars) (SSC) can reach an acceptable level of 10% before fruit are fully red, and flesh firmness is often highest at this point. When stored past 7 days, the rind thins, flesh firmness declines, pH increases, soluble sugars decrease, fruit color starts to develop an orange hue, and flavor can become unacceptable (Bangalore, 2008; Perkins-Veazie et al., 2006a). Ripening was delayed by about 5 days in grafted watermelon fruit compared to non-grafted fruit, and was thought to be from extended accumulation of soluble sugars, ultimately leading to increased flesh firmness, rind thickness and chroma (Ozdemir et al., 2016). The soluble sugars are located and stored in plant vacuole; increasing the accumulation in the vacuoles may decrease intercellular air spaces and increase firmness and rind thickness (Gao et al., 2018). As a delay in ripening is common with watermelon, Soteriou et al (2014; 2017) allowed for the ripening delay before harvesting grafted fruit. In their studies, grafting with interspecific hybrid rootstocks improved watermelon flesh firmness, rind thickness, fruit yields, and flesh color intensity (chroma), and increased the concentration of lycopene and citrulline. In contrast, soluble carbohydrates, hue, and titratable acidity were not significantly affected by grafting. Soteriou et al. (2014) also found that flesh firmness was maintained in grafted fruit well beyond 40 dpa, whereas the firmness of non-grafted watermelons plateaued at 40 dpa (Soteriou et al., 2014).

In the U.S., acceptable watermelon flavor is primarily dictated by sweetness, e.g., soluble solids content (SSC), with 10% SSC required by the USDA. Titratable acidity is very low in watermelon (<0.1% malic acid equivalents). The fruit pH generally is high relative to other fruits, being between 5 and 6. The characteristic watermelon flavor is from the aldehydes of the nonenals and this flavor can quickly disappear or change in the presence of lipoxygenases (Xiao et al., 2019). The sugars in watermelon consist of fructose, glucose, and sucrose. The relative amount of sucrose appears to depend on the watermelon germplasm and the underlying presence of enzymes like sucrose synthase and sucrose phosphate synthases that synthesize and convert sucrose (Yativ et al., 2009). Balancing sweetness and acidity together is crucial to fruit flavor Yativ et al., 2009).

In general, SSC was increased with ripening time but not with grafting, and grafted fruit displayed a delay in the accumulation of solids (Perkins-Veazie et al., 2006a). Although titratable acidity is very low in watermelon (<0.2 mg/100 g malic acid equivalents), it may affect flavor. Ozdemir et al. (2015) found that grafting increased titratable acidity. An increase in titratable acidity might own to "diminishing flavor" in some grafted fruits because it is generally accompanied with a decrease in pH (Soteriou et al., 2014).

Phytochemicals found in watermelon and response to grafting

Some plant compounds play multiple roles in fruit, used for plant growth, reproduction or plant defense activities (Bennet and Wallsgrove, 1994). These compounds can also be important in human health, either for normal growth and development or for prevention of chronic diseases (Kong et al., 2016). Watermelon fruit provides a source of vitamin C, potassium, pro-retinol, lycopene, citrulline, and phenolic compounds.

Previous research suggested that grafting with interspecific rootstocks enhanced carotenoid and nutritional content (e.g., vitamin C) of watermelon fruit (Proietti et al., 2008). Lycopene (cis or trans) is a fat-soluble carotenoid that provides the red color of tomato and red fleshed watermelon. Although it is not a pro-retinol itself, lycopene is a precursor to β-carotene in plants and has at least twice the antioxidant capacity of β-carotene (Fish et al., 2003). Lycopene may also deactivate DNA chain-breaking agents that are implicated in some cancers (Perkins-Veazie et al., 2006b; Collins et al., 2006). The lycopene content and subsequent red color have been reported to increase with grafting, especially with the interspecific rootstocks (Bangalore, 2008; Soteriou et al., 2014; Ozdemir et al., 2016). β-carotene content also increased with grafting (Zhong et al., 2018).

As mentioned previously, citrulline (D- or L-citrulline) is a non-essential amino acid and has been isolated from cucurbitaceous fruits including watermelon, bitter melon, cucumber, muskmelon, bottle gourd and wax gourd (Rimando and Perkins-Veazie, 2005; Dane and Liu, 2006; Joshi and Fernie, 2017). It is a co-product of the nitric oxide cycle generated from the oxidation of arginine catalyzed by nitric oxide synthase. Citrulline aids in vasodilation, cardiac contractile dysfunction and acts as a strong antioxidant and hydroxyl scavenger (Rimando and Perkins-Veazie, 2005; Soteriou et al., 2014). In watermelon, this amino acid is found in the rind and flesh of the fruit (Rimando and Perkins-Veazie; Perkins-Veazie et al., 2006b). There have been mixed reports on the effect of grafting and citrulline content (Davis et al., 2008).

Other carotenoids are present in watermelon flesh, but in much lower amounts than lycopene or beta carotene. Phytoene and phytofluene are the precursors of lycopene and beta carotene (Tomes et al., 1963; Tadmor, 2012) and are reported to be synthesized in the chloroplast then transported to various tissues during the fruit maturation process (Kong et al., 2016). Lutein, which originates from the alpha carotene branch point, has not been found to be abundant in red fleshed watermelon. In yellow fleshed watermelon, where lycopene is lacking, the xanthophylls such as violaxanthin and neoxanthin appear to be more prevalent than lutein or α-carotene.

Other phytochemicals such as flavonoids, flavanols, and isoflavones are also considered beneficial to human health. Tlili et al. (2011) reported that phenolic compounds may be the principal hydrophilic compound contribution to the hydrophilic antioxidant activity of watermelon. While widely reported in berries, phenolic compound quantification and identification in watermelon has been challenging as phenolics tend to be in low amounts, highly complex, and lacking in standards for identification (Abu-Reidah, 2013). Using mass spectrometry, Abu-Reidah et al. (2013) identified saligenin glycopyranoside, cimifugin, hydroquinone glucouronide, glehlinoside C, leachionol G and shikoninie from freeze dried watermelon flesh.

Cucurbitacins are a group of highly substituted bitter-tasting oxygenated tetracyclic triterpenes that are produced in the cucurbitaceae family. Over 20 isomers have been identified, are generally toxic to many organisms and can act as defense compounds against pathogens and pests (Torkey et al., 2009). Cucurbitacins have many reported pharmaceutical attributes, including anti-cancer, anti-inflammatory and cytotoxic properties (Davidovich-Rikanati et al., 2015). Cucurbitacins can also impart bitter taste and can be toxic, depending on the isomer and amount (Davidovich-Rikanati et al., 2015). In watermelon, reported cucurbitacins include B, I and E. Rootstock influence on cucurbitacins appears to be minimal (Fallik and Ilic, 2014). However, very little information is available concerning grafted watermelon species with various rootstocks (interspecific and wild type rootstocks) and their contribution to the metabolic processes that affect the postharvest quality of the fruit.

Changes in fruit firmness

Watermelon grafting and HH disorder are related to changes in fruit quality. Grafting onto interspecific hybrid rootstocks increases rind and tissue firmness. Brummell (2006) speculated that changes in fruit quality (and fruit ripening) are largely related to the plant cell

wall. In the cell wall the three main classes of components, cellulose, hemicellulose and pectin, contribute to intercellular adhesion and cell wall strength and integrity. Although the structure of the primary cell wall is generally understood – cellulose microfibrils are embedded in pectin and glycan polysaccharides - little is known about the interpolymer pectic interactions (Pauly et al., 1999). These interactions and/or changes in monosaccharide linkage assembly may be most responsible for the onset of HH by changing the cell wall network and increasing cell wall degradation.

Watermelon cell wall

To protect the cell, plants have developed primary and secondary cell walls (Padayachee et al., 2017). A primary cell wall is ubiquitous among all plant tissues, although secondary cell walls are not found in high quantities in fleshy fruits and vegetables like watermelon. Instead, the secondary cell wall is associated more with high lignin plants, and is deposited on the primary cell wall in fruits and vegetables like asparagus or celery as well as woody plants (Taylor, 2006).

The primary cell wall protects intracellular contents and also provides a porous medium to exchange material (Brummell, 2006). Cell walls are extremely complex and dynamic as they change throughout the processes of cell division, differentiation and cell growth. The cell wall is exterior to the plasma membrane and is considered to be part of the apoplast (most outer part of the cell), which hosts the middle lamella, intercellular air spaces, water and solutes (Fisher, 2000). The primary cell wall is composed of polysaccharides (90% dry weight), structural glycoproteins (2-5%), phenolic esters (<2%) and minerals (5%) (Rose et al., 2003). The cell wall polysaccharides include cellulose, hemicellulose and pectin (Fig 2.1), utilize covalent and non-covalent bonding, and also interact with proteins and lignin via plasmodesmata.

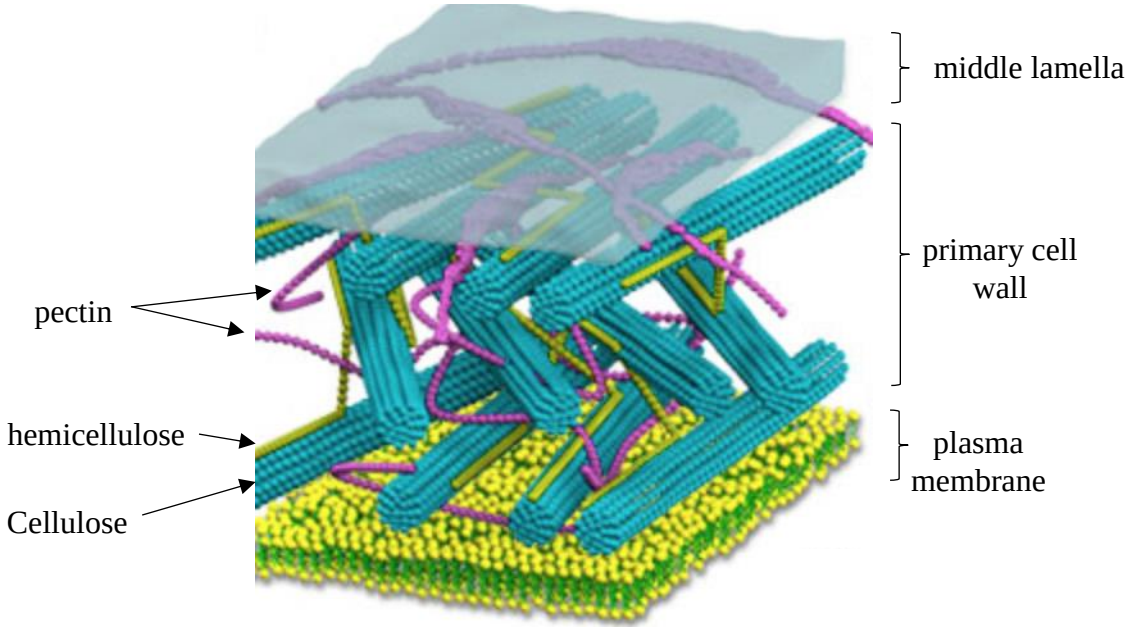

Figure 1.1. Plant cell wall structural components protecting intracellular content and aiding in plant defense and fruit quality (figure credit: Davidson, M.W. 2019, Florida State University https://micro.magnet.fsu.edu/cells/plants/cellwall.html).

Cell Wall Components

The most abundant polysaccharide in the cell wall is cellulose and was initially considered the main load-bearing constituent of the plant cell wall. It is located in the matrix of hemicellulose and pectins (Padayachee et al., 2017). Cellulose is a simple polymer made up of unbranched β-1,4-linked glucan chains (which are hundreds to thousands of glucose monomers) (Taylor, 2006). Individual cellulose molecules are held together by repeating hydrogen bonding through hydroxyl (-OH) groups. Primary cell wall cellulose has a molecular weight of 8,000 (Brown, 2004). Cellulose is hydrophobic and insoluble in water, though it serves as a skeletal network in the cell wall (Broxterman and Schols, 2018). Glycan chains, around 36 cellulose polysaccharides, will crystalize together to form a microfibril (Taylor, 2006).

Hemicelluloses are a heterogenous group of polysaccharides. Hemicellulose is similar to cellulose in that the polysaccharides are β-1,4-linked but are composed of a glucose, xylose and mannose backbone (Scheller and Ulvskov, 2010). Hemicellulose polysaccharides are predominantly composed of xylogucans (α-D-Xyl-(1,6)-glucose) and xylans, which are not water soluble and have little enzymatic degradation (Pena et al., 2008). Xylans are very similar to xyloglucans but have galacturonic acids, which embed the pectic network (Scheller and

Ulvskov, 2010). In Arabidopsis, xylans have been found to have repeating xylose monomers (β-D-Xyl(p)-(1,4)- β-D-Xyl(p)) with rhamnose and galactose monosaccharides attached (e.g. Xyl-Xyl-Rha-Gal). Mannans, glucomannans and mixed-link glycans are other types of hemicellulose. Mannans are found primarily on seed coats and are in mosses and lycophytes, glucomannans are much less abundant as a hemicellulose but also play a role in seed coats (Goubet et al., 2003).

The cellulose and hemicellulose network provide communication and interaction while pectin is used for load-bearing and is important for plant defense, protection and internal flesh quality (Hofte et al., 2012). Pectins are known to be crucial to plant cell wall strength and integrity and are of major importance for intercellular adhesion, middle lamella adhesion and overall tissue structure (Mort et al., 2008; Houben et al., 2011). Pectin also plays important roles in the lipid membrane and cell wall metabolism of fruits. Pectins are galacturonic acid-rich polysaccharides covalently linked to each other, with composition and structure strongly dependent on the pectin source and fruit developmental stage (Petkowicz et al., 2016). Cell wall disassembly and enzymatic degradation begins with enzymes targeting the glycosidic bonds of pectin (Karakurt et al., 2008).

Classes of pectic polysaccharides

Pectic polysaccharides are deposited early, during the formation of new cell walls in the process of cell plate formation (Amos and Mohnen, 2019). The plate occurs in an equatorial plane between two daughter nuclei; the cell plate and its membranes are assembled by fusion of membrane-bound vesicles derived by Golgi dictyosomes (Tanner and Loewus, 2012). The plate persists during deposition of the primary cell wall, with layers of polysaccharides secreted and the layers pushed outward via internal cell pressure (Tanner and Loewus, 2012). The cell plate is then recognized as the middle lamella and pectic polysaccharides embed into the middle lamella, aiding in intercellular junction (Amos and Mohnen, 2019).

Five major pectic structures that can be detected in plant cell walls include homogalacturonan (HG), xylogalacturonan (XG), apiogalcturonan (APG), rhamnogalacturonan I (RGI), and rhamnogalacturonan II (RGII). RGI, XG and HG and are linked by either α-(1-4) or β-(1-3) to galacturonic acid residues with a calcium core (Mort et al., 2008) (Fig 1.2).

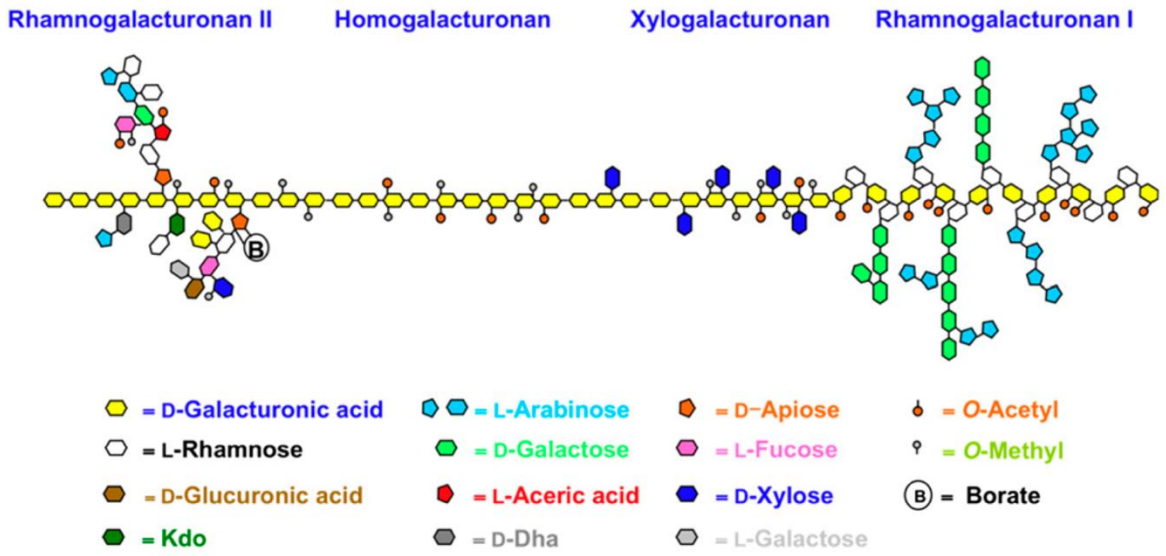

Figure 1.2. Structures of the major pectic polysaccharide classes. Pectin consists of 4 major polysaccharides found in plant cell walls. Kdo is 3-Deoxy-D-manno-oct-2-ulosonic acid and D-Dha is dihydoroxyacetone. (Figure credit Petkowicz et al., 2016).

The structural characteristics of heterogalacturonans are diverse and include pectic polysaccharides of xylogalacturonan (XG), apiogalacturonan (APG), rhamnogalacturonan I and II (RG I and II) and arabinogalacturonans (AG) (Yang et al., 2018). Their structural characteristics are based on a α-(1-4)-D-galacturonan backbone with main distinctions arising from the side chains (Paniagua et al., 2017). Homogalacturonan (HG) is considered more of a simple polysaccharide comprised of α-(1-4) galacturonic acid residues with a calcium core (Mort et al., 2009). Pectic ratios tend to vary between HG, XG, APG, Type I and II AG, RGI, and RGII. HG is the most abundant polysaccharide and constitutes roughly 60% of the pectin content found in cell walls. RGI and RGII are next, with around 30% of the pectin content (Verhertbruggen et al., 2009). Generally, APG and XG are minor components and have a ratio of 10% or less (Harholt et al., 2017).

Pectic arabinogalactans are split into type I and type II arbinogalacturonan (Type I and II AG). Type I AG consist of 1,4-β-linked-D-GalA(p) backbone with occasional interspersed 1,3-β-links and can be substituted at oxygen-3 or 2 with arabinose residues (Hinz et al., 2005). Type I AG may contain other monosaccharides like fucose and glucuronic acid. In contrast, Type II arabinogalactan has a 1,3-β-L -D-GalA(p) backbone, which is substituted with short side chains consisting of 1,6-β-linked-GalA(p) (Verhertbruggen et al., 2009). Another class of

polysaccharides, pectic arabinans, are composed of a 1,5-α- L-arabinofuranosyl reside also branched on O-2 or O-3. However, arabinans (1,5-linked) may also exist as free polymers unattached to pectic domains (Verhertbruggen et al., 2009).

Pectin content in watermelon

Pectin can be analyzed by extraction of total pectins or via intensive wet chemistry to characterize cell wall polysaccharides (Soteriou et al., 2017; Pettolino et al., 2012). Total pectin content is assessed via sequential fractions of total cell wall material. The fractions are water soluble (WSF), carbonate soluble (CSF), alkali soluble (ASF) and unextractable fractions. WSF yield pectins "freely bound" in the plant cell well and are also freely soluble in the apoplast (Panigua et al., 2014). CSF are considered to be enriched in de-esterified pectins covalently bound to the cell wall and are enriched in homogalacturonan (Panigua et al., 2014; Soteriou et al., 2017). ASF are derived from matrix glycans that are tightly attached to the cell wall via hydrogen bonds, and are generally the hardest to solubilize (Brummell and Harpster, 2001). ASF are also considered to have a low degree of methylesterification (Soteriou et al., 2017) and high polyuronide (uronic acid) concentrations compared to WSF and CSF (Soteriou et al., 2017).

Soteriou et al. (2017) performed total pectin extraction on watermelon placental tissue to explore fruit texture differences. Fruit from non-grafted watermelon (lower heart firmness) and or from watermelon grafted onto interspecific hybrid rootstocks (higher tissue firmness) were used. Pectin solubilization of total cell wall material was very low at around 0.65% and no differences were found among the sequential pectic fractions. Generally, watermelon is known to have a low degree of pectin solubilization, meaning it is difficult to extract pectin from the cell wall and place it into solution (Brummell, 2006). In watermelon, WSF was the lowest fraction at 23.0% of total cell material. The amount of CSF recovered was 37% and ASF was 40% of total cell wall material, respectively. Since no differences were found in the WSF, this implies that the firmness differences identified between grafted and non-grafted watermelon could not be explained by WSF (Soteriou et al., 2017). However, a positive correlation was seen between the combination of insoluble pectic fractions (e.g., %CSF + %ASF) and tissue firmness. This correlation suggests that changes in fruit textural characteristics may be associated with fractions containing de-esterified pectins bound to the cell wall by covalent bonds, and matrix glycans tightly attached to the cell wall by hydrogen bonds (Brummell and Harpster, 2001).

Cell wall polysaccharide composition uses quantification of polysaccharides coming from cellulose, hemicellulose and pectin and is far more robust than total pectin extractions. The various pectic classes can also be deduced by combining monosaccharide composition with linkage assembly (Pettolino et al., 2012). Previous research in watermelon used enzymatic hydrolysis (endo-polygalacturonase) to depolymerize cell walls prior to pectin fraction extraction and quantification of matrix glycans and xylogalacturonan monomers (Brummell, 2006; Karakurt and Huber, 2009; Mort et al., 2008). Additionally, ethylene, which induces polygalacturonase activity in watermelon, was used to induce tissue softening and assess cell wall depolymerization to follow the differences in fruit textural characteristics. Although fruit treated with ethylene had lower tissue firmness, no differences in matrix glycans were found (Karakurt et al., 2008; Mort et al., 2008). Monosaccharides of glucose, xylose, galactose, arabinose, galacturonic acid and glucuronic acid were calculated on a %mol basis after hydrolyzing the cell wall with endo-polygalcturonase. Karakurt et al. (2008) found approximately 95% of the watermelon matrix glycans consisted of 40% glucose, 30% xylose, 15% arabinose and 14% galactose. Mort et al. (2008) focused on xylosyl linked residues of matrix glycans from watermelon placental tissue. Hydrogen and carbon (^{1}H and ^{13}C) shifts were measured after xylosyl oligomers were treated with endo-polygalacturonase to depolymerize polysaccharide chains. Nine linkage residues were identified in matrix glycan oligomers consisting of xylose (1-Xyl(p) and galacturonic acid (3-GalA(p), 4-GalA(p) and 3,4-GalA(p)) linkages (Mort et al., 2008).

Researchers propose that crosslinking of homogalacturonan and rhamnogalacturonan II within the middle lamella strongly controls cellular adhesion and differences in fruit textural characteristics (Daher and Braybrok, 2015; Amos and Mohnen, 2019). In previous studies, only xylogalacturonan was extracted not all polysaccharides were characterized. A more thorough characterization of the cell wall in watermelon can be done. Instead of enzymatic depolymerization of the cell wall, Saemen hydrolysis can be used to quantitatively measure 12 neutral monosaccharide building blocks (Pettolino et al., 2012). Complete methylation of the cell wall can be used to deduce linkage residues and calculate the amount of polysaccharide classes. Understanding the composition of the cell wall with these methods could lead to a better understanding of general fruit textural changes and may be useful in elucidating how HH forms in watermelon.

Summary

Watermelon fruit is a high value crop yet has had relatively little research on processes controlling fruit growth, ripening, or changes pertinent to defects. Hollow heart is an internal defect characterized by a void in the placental tissue of the fruit (Johnson, 2015). Hollow heart is found predominantly in triploid watermelon types, and cannot be visually distinguished from normal fruit unless cut. The incidence of hollow heart can be 0 to 65% of watermelon in a growing season, making it difficult for breeders to develop screening strategies for the disorder. Proper pollination, watermelon genetics and environment are some of the important factors involved with the onset of HH. Triploid cultivars with higher tissue firmness are thought to also be less prone to HH (Johnson 2014; 2015).

Grafting watermelon onto soil-borne pathogen resistant rootstocks is a growing practice world-wide. Grafting is useful as an alternative to soil fumigation and protects plants from disease, nematodes, abiotic stresses, temperature fluctuation and drought stress. Cucurbit rootstocks of interspecific hybrid squash (*Cucurbita maxima* x *C. moschata*), bottle gourd (*Laginaria sicaria*) and wild type are most commonly used (Davis et al., 2008, Soteriou et al., 2014; 2017). Rootstock/scion combinations affect the yield and fruit quality attributes (e.g., increased tissue firmness, rind thickness and tissue density). Currently, the effects of rootstock/scion on HH are unknown for susceptible triploid cultivars. Tissue density (the number and size of cells in the heart tissue) was positively correlated to tissue firmness in watermelon (Kano, 1993). Understanding the role of cell wall polysaccharides (specifically total pectin and pectic polysaccharides) can give a better understanding of the onset of hollow heart and grafting effects on fruit quality.

Research Hypothesis and Objectives

The overarching hypothesis for this project is that grafting a watermelon cultivar susceptible to hollow heart protects fruit cell walls from degradation/disassembly by increasing total pectin content and pectic polysaccharides of homogalacturonan, rhamnogalacturonan I and II (e.g., increases in monosaccharides of glucose, galactose, xylose, arabinose and rhamnose). A series of experiments were done to follow and initiate incidence of hollow heart, quantitate quality changes in tissues, cell morphology and cell wall composition. Objectives of the research were 1) to establish ways to effectively induce hollow heart, 2) to use generated material to

analyze tissue composition, cell morphology, and cell wall pectins, and 3) to characterize the assembly of monosaccharides in cell wall pectins.

In the first objective, data from three years of North Carolina triploid watermelon cultivar trials were analyzed to determine the relative susceptibility of watermelon cultivars to development of hollow heart, and to look for a relationship between fruit tissue firmness and hollow heart. A predictive model was be used to determine the susceptibility (e.g., odds) of a given cultivar to develop hollow heart.

Next, a watermelon cultivar susceptible to hollow heart was grafted to various rootstocks to determine if grafting could reduce hollow heart. Fewer seeded (diploid) plants were used in field plantings to reduce viable diploid pollen and induce hollow heart. Using this combined system of susceptible scion and reduced pollen, hollow heart incidence was successfully increased, occurring in 20 to 40% of the resulting fruit. This provided sufficient fruit for determining fruit composition, and conducting cell microscopy and cell wall polysaccharide studies. Cell microscopy and cell wall polysaccharide studies were done to determine cell density, relative types of pectins, and polysaccharide assembly of the pectins.

References

1. Amos, R.A and D. Mohnen. 2019. Critical review of plant cell wall matrix polysaccharide glycosyltransferase activities verified by heterologous protein expression. Frontiers Plant Sci. 10:1-2.

2. Abdu-Reidah, I. 2013. Profiling of phenolic and other polar constituents from hydro-methanolic extract of watermelon (*Citrullus lanatas*) by means of accurate-mass spectrometry. Food Res. Intl. 51:354-362.

3. Bangalore, D. 2008. Effects of fruit maturity on watermelon ultrastructure and intracellular lycopene distribution. J. Food Sci. 73:222-228.

4. Bennett, R. and R.M. Wallsgrove. 1994. Secondary metabolites in plant defense mechanisms. New Phytol. 127:617-633.

5. Brown RM Jr. 2004. Cellulose structure and biosynthesis: what is in store for the 21st century? J. Poly Sci. Part A-Pol Chem. 42:487–495.

6. Broxterman, S.E. and H.A. Schols. 2018. Interactions between pectin and cellulose in primary plant cell walls. Carbohydrate Polymers 192:263-272.

7. Brusca, J. and X. Zhang. 2013. United States Patent: Watermelon Pollinizer SP6. US., 8, 212,118 B1

8. Brummell, D.A. 2006. Cell wall disassembly in ripening. Funct. Plant Biol. 33:103-119.

9. Brummell, D.A. and M.H. Harpster. 2001. Cell wall metabolism in fruit softening and its manipulation in transgenic plants. Plant Mol. Bio. 47:311-340.

10. Collins, J.K. and P. Perkins-Veazie. 2006. Flesh quality and lycopene stability of fresh-cut watermelon. Postharvest Biol. Tech. 31:159-166.

11. Daher, F.B and S.A. Braybrook. 2015. How to let go: pectin and plant cell adhesion. Front Plant Sci. 6:523-540.

12. Dane, F. and J. Liu. 2006. Diveristy and orgicn of cultivated citron type watermelon (*Citrullus lanatus*). Genet. Resour. Crop Evol. 54:1255-1265.

13. Davis, A. R., P. Perkins-Veazie, Y. Sakata, S. Lopez-Galarza, J.V. Maroto, S.G. Lee, Y.C. Huh, Z. Sun, A. Miguel, S.R. King, R. Cohen and J.M. Lee. 2008. Cucurbit Grafting. Critical Rev. Plant Sci. 27:50-74.

14. Dammak, M.I., Y.B. Salem, A. Belaid, H.B. Mansour, S. Hammami, D. Le Cerf and H. Majdoub. 2019. Partial characterization and antitumor activity of a polysaccharide isolated from watermelon rinds. Intl. J. Biol. Macro Molec. 136:632-641.

15. Davidovich-Rikanati, R., L. Shalev, N. Barabes, A. Meir, M. Itkin, S. Cohen, K. Zimbler, V. Portnoy, Y. Ebizuka, M. Shibuya, Y. Burger, N. Katzir, A.A. Schaffer, E. Lewisohn and Y. Tadmor. 2015. Recombinant yeast as a functional tool for understanding bitterness and cucurbitacin biosynthesis in watermelon (*Citrullus* spp.). Yeast 32:103-114.

16. Domingos, P., A.M. Prado, A. Wong, C. Gehring and J.A. Feijo. 2016. Nitric oxide: A ultitasked signaling gas in plants. Molec. Plant 8:506-520.

17. Elkashif, M.E. and D.J. Huber. 1988. Enzymic hydrolysis of placental cell wall pectins and cell separation in watermelon (*Citrullus lanatus*) fruits exposed to ethylene. Physol. Planta. 73:432-439.

18. Elmstrom, G.W. and P.L. Davis. 1981. Sugars in developing and mature fruits of several watermelon cultivars. J. Amer. Soc. Hortic. Sci. 106:330-333.

19. Fallik, E. and Z. Ilic. 2014. Grafted vegetables – the influence of rootstock and scion on postharvest quality. Folia Hortic. 26:79-90.

20. Fish, W.W. and A.R. Davis. 2003. The Effects of frozen storage conditions on lycopene stability in watermelon tissue. J. Agric. Food Chem. 51:3582-3585.

21. Fredes, A. S. Rosello, J. Beltran, J. Cebolla-Cornejo. A. Perez-de-Castro, C. Gisbert and M.B. Pico. 2016. Fruit quality assessment of watermelons grafted onto citron melon roostock. J. Sci. Food Agric. 97:1646-1655.

22. Freeman, J. and Olson, S. 2007. Characteristics of watermelon pollinizer cultivars for use in triploid production. Intl J. Vegetable Sci. 13:73-78.

23. Gao, L., S. Zhao, X. Lu, N. He, H. Zhu, J. Dou and W. Liu. 2018. Comparative transcriptome analysis reveals key genes potentially related to soluble sugar and organic acid accumulation in watermelon. Plo S One 13:1-22.

24. Grassi, S. G. Piro, J.M. Lee, Y. Zheng, Z. Fei, G. Dalessandro, J.J. Giovannoni and M.S. Lenucci. 2013. Comparative genomics reveals candidate carotenoid pathway regulators of ripening watermelon. BMC Genomics 14:781-801.

25. Goubet, F., A. Misrahi, S.K. Park, Z.N. Zhang and D. Twell. 2003. At CSLA7, a cellulose synthase-like putative glycosyltransferase, is important for pollen tube growth and embryogenesis in *Arabidopsis.* Plant Physiol. 131:547–57

26. Guo, S. J. Liu. Y. Zheng. M. Huang, G. Gong, H. He, Y. Ren, S. Zhong, Z. Fei and Y. Xu. 2011. Characterization of transcriptome dynamics during watermelon fruit development: sequencing, assembly annotation and gene expression profiles. BMC Genomics 12:454-467.

27. Hassell, R., F. Memmott, D.G. Liere. 2008. Grafting methods for watermelon production. Hortic. Sci. 43:1677-1679.

28. Harholt, J., A. Suttankakul and H.V. Scheller. 2010. Biosynthesis of pectin. Plant Physiol. 153:384-395.

29. Hinz, S.W.A., R. Verhoef, H.W. Schols, J.P. Vincken and A.G.J. Voragen. 2005. Type 1 arabinogalactan contains β-D-Galp-(1,3)-β-D-Galp structural elements. Carbohydr. Res. 340:2135-2143.

30. Hofte, H., A. Peaucelle and S. Braybrook. 2012. Cell wall mechanics and growth control in plants: the role of pectins revisited. Front. Plant Sci. 3:121-130.

31. Houben, K., R.P. Jollie, I. Fraeye, A.M. Van Loey, and M. Hendrick. 2011. Comparative study of the cell wall composition of broccoli, carrot, and tomato: Structural characterization of the extractable pectins and hemicelluloses. Carbohydrate Poly. 346:1105-1111.

32. Huber, D.J. 1983. Polyuronide degradation and hemicellulose modifications in ripening tomato fruit. J. Amer. Soc. Hortic. Sci. 73:432-438.

33. Johnson, G. 2014. These beautiful watermelon patterns are driving everyone crazy. [Online]. https://www.boredpanda.com/weird-watermelons-beautiful-hollow-heart/

34. Johnson, G. 2015. Research finds potential cause of hollow heart disorder in watermelon. PhysOrg. [Online]. https://phys.org/news/2015-06-potential-hollow-heart-disorder-watermelons.html

35. Joshi, V. and A.R. Fernie. 2017. Citrulline metabolism in plants. Amino Acids 49:1543-1559.

36. Joshi, V., M. Joshi, D. Silwal, K Noonan, S. Rodriguez and A. Penalosa. 2019. Systemized biosynthesis and catabolism regulate citrulline accumulation in watermelon. Phytochemistry 162:129-140.

37. Karakurt, Y. and D.J. Huber. 2009. Purification and partial characterization of xyloglucan-hydrolyzing enzymes from watermelon placental tissue. J. Sci. Food Agric. 89:645-652.

38. Kano, Y. 1993. Relationship between the occurrence of hollowing in watermelon and the size and the number of fruit cells and intercellular air space. J. Japan Soc. Hort. Sci. 62:103-112

39. Kawaguchi, M., A. Taji, D. Backhouse and M. Oda, M. 2008. Anatomy and physiology of graft incompatibility in solanaceous plants. J. Hortic. Sci. Biotechnol. 83:581–588.

40. Kong, Q., J. Yuan, L. Gao, P. Liu, L. Cao, Y. Huang, L. Zhao, H. Lv, and Z. Bie. 2016. Transcriptional regulation of lycopene metabolism mediated by rootstock ripening of grafted watermelon. Food Chem. 214:406-411.

41. Lebo, M.B. 1932. Maturity and Quality in Watermelon. Texas A&M, Thesis.

42. Lee, J.M and M. Oda. 2003. Grafting of herbaceous vegetable and ornamental crops. Hortic. Rev. 28:61-124.

43. Levi, A., J.A. Thies, P.W. Wechter, . Farnham, Y. Weng and R. Hassell. 2014. USVL-360, a novel watermelon tetrapoid germplasm line. J. Amer. Hortic. Sci. 49:354-357.

44. Martinez-Bellasta, M., C. Alcaraz-Lopez, C. Monta-Cadenas and M. Carvajal. 2010. Physiological aspects of rootstock-scion interactions. Scientia Hortic. 127:112-118.

45. Mort, A., Y. Zeng, F. Qiu, M. Nimtz, and G. Bell-Eunice. 2008. Structure of xylogalacturonic fragments from watermelon cell-wall pectin. Endopolygalacturonase can accommodate a xylosyl residue on the galacturonic acid just following the hydrolysis sight. Carbohydrate Res. 434:1212-1221.

46. Mohamed, F.H., E. Khalid, A. El-Hamed, M.W.M. Elwan and N.E. Hussien. 2012. Impact of grafting on watermelon growth, fruit yield and quality. Veg. Crops Res. Bull. 76:99-118.

47. National Agriculture Statistics Survey. 2019. Statistics on vegetables and melons. [Onine]. https://www.nass.usda.gov/Publications/Ag_Statistics/2019/chapter04.pdf

48. Nitsch, J. P. Hormonal factors in growth and development. 1970. In : A. C. Hulme (ed.). Biochemistry of fruits and their products. I. Academic Press, London. p.427-472.

49. Ozdemir, A.H, E. Candir, H. Yetisir, V. Aras, O. Arslan, O. Baltaer, D. Utsun, and M. Unlu. 2016. Effects of rootstocks on storage and shelf life of grafted watermelons. Appl. Bot. Food Qual. 89:191-201.

50. Padayachee, A., L. Day, K. Howell and M.J. Gidley. 2017. Complexity and health functionality of plant cell wall fibers from fruits and vegetables. Crit. Rev. Food Sci. 57:59-81.

51. Paniagua, C., N. Santiago-Domenech, A.R. Kirby, A.P. Gunning, V.J Morris, M.A. Quesada, A.J. Matas and J.A. Mercado. 2017. Structural changes in cell wall pectins during strawberry fruit development. Plant Physiol. Biochem. 118:55-63.

52. Pauly, M., P. Albersheim, A. Darvill and W.S. York. 1999. Molecular domains of cellulose/xylogucan network in the cell wall of higher plants. Plant J. 20:629-639.

53. Pena M.J., A.G. Darvill, E.S. Berhard, W.S. York and M.A. O'Neill. 2008. Moss and liverwort xyloglucans contain galacturonic acid and are structurally distinct from the xyloglucans synthesized by hornworts and vascular plants. Glycobiology 18:891–904.

54. Perkins-Veazie P, J.k. Collins, S.D. Pair and W. Roberts. 2001. Lycopene content differs among red-fleshed watermelon cultivars. J. Sci. Food Agric. 81:983–987.

55. Perkins-Veazie, P and J.K. Collins. 2006a. Carotenoid changes of intact watermelon after storage. J. Agric. Food Chem. 54:2593-2597.

56. Perkins-Veazie, P., J.K. Collins, A.R. Davis, and W. Roberts. 2006b. Carotenoid content of 50 watermelon cultivars. J. Agric. Food Chem. 54:2593-2597.

57. Petkowicz, C.L.O, L.C. Vriesmann, and P.A. Williams. 2016. Pectins from food waste: Extraction, characterization and properties of watermelon rind pectin. Food Hydrocolloids 65:57-67.

58. Pettolino, F.A., C. Walsh, G.B. Fincher and A. Bacic. 2012. Determining the polysaccharide composition of plant cell walls. Nat. Protoc. 9:1590-1607.

59. Proietti, S., Y. Rouphael, G. Colla, M. Cardarelli, M. DeAgazio, M. Zacchini, E. Rea, S. Moscatello and A. Battistelli. 2008. Fruit quality of mini-watermelon as affected by grafting and irrigation regimes. J. Sci. Food Agric. 88:1107-1114.

60. Rimando, A.M. and P. Perkins-Veazie. 2005. Determination of citrulline in watermelon rind. J. Chromatography A. 1078:196-200.

61. Rose, J.K.C. 2003. The plant cell wall. Annual plant reviews, volume 8. Blackwell publishing, pp 45-49.

62. Scheller, H.V. and P. Ulvskov. 2010. Hemicellulose. Annu. Rev. Plant Biol. 61:263-289.

63. Sedgley, M. H.J. Newbury and J.V. Possing. 1977. Early fruit development in the watermelon: Anatomical comparison of pollinated, auxin-induced parthenocarpic and unpollinated fruit. Ann. Bot. 41:1345-1355.

64. Soteriou, G.A., M.C. Kyriacou, A.S. Simons, and D. Gerasopoulos. 2014. Evolution of watermelon fruit physicochemical and phytochemical composition during ripening as affected by grafting. Food Chem. 165:282-289.

65. Soteriou, G.A., M.C. Kyriacou, A.S. Simons, and D. Gerasopoulos. 2017. Rootstock-Mediated Effects on Watermelon Ripening Behavior and Fruit Physicochemical and Phytochemical Composition. Acta Hort. 1079:707-714.

66. Sugiyama, K., D. Kami and T. Muro. 2014. Induction of parthenocarpic fruit set in watermelon by pollination with bottle gourd (*Lagenaria sicararia* (Molina) Stdl.) pollen. Sci. Hort. 171:1-5.

67. Tadmor, Y. 2005. Comparative fruit coloration in watermelon and tomato. Food Res. Int. 38:837-841.

68. Tanner, W. and F.A. Loewus. 2012. Plant Carbohydrates II. Cell wall in higher plants. Springer-Verlag Berlin Heidleberg, New York.

69. Tarazona-Diaz, M.P., J. Viegas. M. Moldao-Martins, and E. Aguayo. 2010. Bioactive compounds from flesh and by-product of fresh-cut watermelon cultivars. J. Sci. Food Agric. 91:805-812.

70. Taylor, N.G. 2006. Cellulose biosynthesis and deposition in higher plants. New Phytol. 178:239–252.

71. Thies, J.A., J.J. Ariss, R.L. Hassell, S. Olson, C.S. Kousik, and A. Levi. 2010. Grafting for management of southern root-knot nematode, Meloidogyne incognita, in watermelon. Plant Dis. 94:1195-1199.

72. Tlili, I., C. Hdider, M. Lenucci, S. Ilahy and G. Dalessandro. 2011. Bioactive compounds and antioxidant activities during fruit ripening of watermelon cultivars. J. Food Comp. Anal. 34:923-928.

73. Tomes, M.L., K. Johnson, and M. Hess. 1963. The carotene pigment content of certain red fleshed watermelons. Proc. Amer. Soc. Hort. Sci. 83:460-464.

74. Torkey, H.M., H.M. Abou-Yousef, A.Z. Abdel-Azeiz and E.A. Farid-Hoda. 2009. Insecticidal effect of cucubitacin E glycoside isolated from *Citrullus colocynthis* against *Aphis craccivora.* J. Basic Appl. Sci. 3(4):4060-4066.

75. USDA. 2019. Specialty Crop Market News. Seeded and Seedless Watermelon Production. [Online]. https://www.ams.usda.gov/mnreports/wa_fv456.txt

76. USDA National Agriculture Library. 2020. Food Composition database. [Online]. https://www.nal.usda.gov/fnic/vitamins-and-minerals

77. Verhertbruggen, Y., S.E. Marcus, A. Haeger, R. Verhoef, H.A. Schols, B.V. McCleary, L. McKee, H.J. Gilbert and J.P. Knox. 2009. Developmental complexity of arabinan polysaccharides and their processing in plant cell walls. Plant J. 59:413-425.

78. Walters, S.A. 2005. Honey bee requirements for triploid watermelon. HortScience 40:1268-1270.

79. Walters, A. and J. Schultheis. 2009. Directionality of pollinator movement in watermelon plantings. HortScience 44:49-52.

80. Wechter, P.W., A. Levi, K.R. Harris, A.R. Davis, Z. Fei, N. Katzir, J.J Giovannoni, A. Salman-Minkov, A. Hernandez, J. Thimmapuram, Y. Tadmor, V. Portnoy and T. Trebitsh. 2008. Gene expression in developing watermelon fruit. BMC Genomics 9:275-280.

81. Xiao, Z., H. Wenjing, Y. Kang, Y. Niu and X. Kou. 2019. Encapsulation and sustained release properties of watermelon flavor and its characteristic aroma compounds from gamma-cyclodextrin inclusion complexes. Food Hydro. 97:105-112.

82. Yang, Y., Y. Mo, X. Yang, H. Zhang, Y. Wang, H. Li, C. Wei and X. Zhang. 2016. Transcriptome profiling of watermelon root response to short-term osmotic stress. Plo S One 11:1-19.

83. Yativ, M, I. Haray and S. Wolf. 2010. Sucrose accumulation in watermelon fruits: Genetic variation and biochemical analysis. J. Plant Physiol. 167:589-596.

84. Yetisir, H., N. Sari, and S. Yucel. 2003. Rootstock resistance to Fusarium wilt and effect on watermelon fruit yield and quality. Phytoparasitica 31:163-169.

85. Yuan, H. Z. Liqiang, K. Qiusheng, C. Fei, N. Mengliang, X. Junjun, M.A. Nawaz and B. Zhilong. 2016. Comprehensive mineral nutrition analysis of watermelon grafted onto two different rootstocks. Hort. Plant J. 2:105-113.

86. Zhong, Y., C. Chen, M.A. Nawaz, Y. Jiao, Z. Zheng, X. Shi, W. Xie, Y. Yu, J. Guo, S. Zhu, M. Xie, Q. Kong, F. Cheng, Z. Bie and Y. Huang. 2018. Using rootstock to increase watermelon yield and quality at low potassium supply: A comprehensive analysis from agronomic, physiological and transcriptional perspective. Scientia Hort. 241:144-151.

87. Zhu, Q. P., S. Gao, Z. Liu, S. Zhu, A. Amanullah, A.R. Davis, and F. Luan. 2017. Comparative transcriptome analysis of two contrasting watermelon genotypes during fruit development and ripening. BMC Genomics 18:1-3.

CHAPTER 2

PREDICITING HOLLOW HEART INCIDENCE AND TISSUE FIRMNESS IN TRIPLOID WATERMELON (*CITRULLUS LANATUS*)

Abstract

In triploid (seedless) watermelon [*Citrullus lanatus* var. lanatus (Thunb. Matsum.and Nakai)], hollow heart (HH) is a disorder that is expressed as a crack in the center of the fruit that expands to an open cavity. Although HH incidence and severity is part of a screening process for marketable watermelon fruit in cultigen evaluations, HH incidence is highly variable with growing season even when the best cultural practices are utilized. Placental tissue firmness is also measured since firmness is related to marketability of watermelon and may also be related to HH. Genetic and environmental factors can influence watermelon HH development, including plant genetics, pollen amount and viability, pollinator activity, and temperature and rainfall fluctuations. We utilized seedless watermelon cultigen evaluation data collected over three years (2012-2014) to determine the relationship between germplasm HH and tissue firmness. Transplanted watermelon representing 30 to 44 cultigens per year were grown at the Central Crops Research Station, Clayton, NC and interplanted with pollenizers 'Ace' or 'SP-6'. Harvested fruit were cut length-wise and rated for HH incidence and severity. Flesh firmness was determined by a handheld penetrometer at five locations in the flesh (stem end, top side, ground spot, blossom end and heart). A common cultigen subset, consisting of 13 cultigens that were grown in all three experiments, was used for analysis of HH severity and incidence, and placental firmness. The presence of HH was negatively correlated with tissue firmness in both the large multi-year cultigen set (R^2 = -0.32, p-value = 0.0001) and the common cultigen set (R^2 = -0.78, p-value = 0.0001). Cultigens with lower watermelon tissue firmness values had higher HH severity. By using multi-year cultigen studies and logistic regression, we were able to detect trends for cultigen susceptibility to this highly variable disorder. Using logistic regression, the probability to develop HH was found to be highest for 'Bold Ruler', 'Liberty' and 'Affirmed' and lowest for 'Maxima' and 'Captivation'. Identification of cultigens with a tendency for more or less HH incidence will be useful for further research into the causes of HH. Measurement of placental flesh firmness may be a useful indicator of susceptible cultigens.

Introduction

Globally, watermelon is the largest produced fruit crop (Tlili et al., 2011), with18.1 MT produced in 2018 (USDA, 2019). In the U.S., seedless (triploid) watermelon makes up 95% of the market (USDA, 2019). One of the USDA grade defects in triploid watermelon is the appearance of hollow heart (HH), also known as internal cracking (USDA, 2006). Hollow heart occurs as an internal split or void that usually starts in the placental (heart) tissue of the watermelon and can extend through the carpels into the epidermal (rind) layers (Johnson, 2014; 2015). Depending on the season and demand for seedless watermelon, fruit rated with moderate to severe HH will be rejected for marketability (USDA, 2006), ultimately resulting in significant monetary losses for both growers and industry (Fig. 2.1).

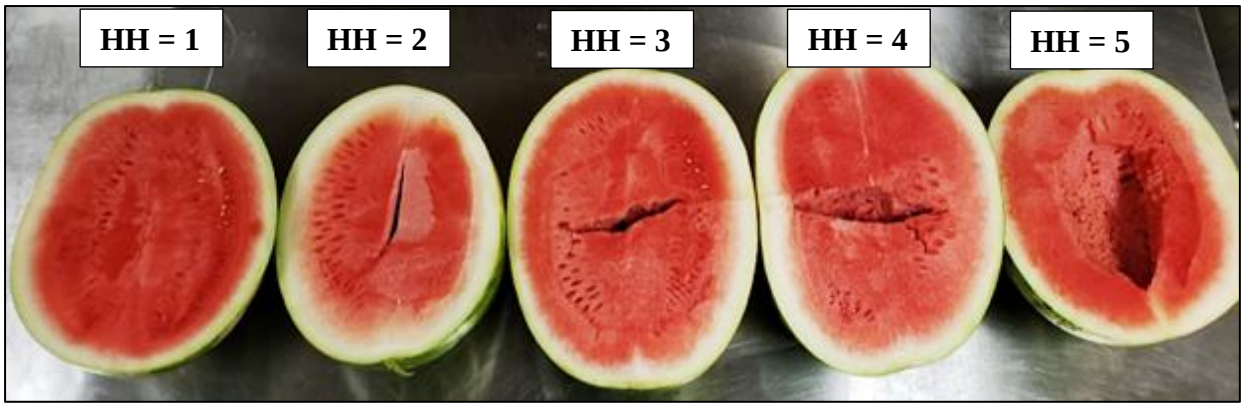

Figure 2.1. Hollow heart rated on a 1 to 5 scale (1 = no or very minor HH and 5 = severe). Fruit with moderate to severe levels of HH (rated 2 to 5 in severity) do not meet USDA grade for watermelon marketability.

Hollow heart is thought to develop as a result of unequal expansion of placental and rind tissues (Kano, 1993) and most often occurs in fruit from the crown set (or first harvested fruit) (Diezma-Iglesias et al., 2004). The watermelon rind continues to expand and differentiate during fruit growth and maturation. Placental tissue cells stop dividing at 7 days post anthesis and cells begin to enlarge with the accumulation of water, sugars, proteins and nutrients accumulate (Kano, 1993; Elmstrom and Davis, 1981). A rapid change in water potential between placental cells and rind cells can lead to a separation of the carpels, ovule and placental tissue, causing a hollowing or cavity (Kano, 1993; Johnson, 2014; 2015).

Inadequate pollination is thought to be one of the leading causes of HH in watermelon and may be worse in triploid (seedless) watermelons since they require a diploid (seeded) pollenizer, with viable pollen (Diezma-Iglesias et al., 2004). Inadequate pollination can come from improper choice of diploid pollenizer-triploid combination (McGregor and Waters, 2014), reduced bee visits, or unfavorable weather conditions (e.g., decrease in pollen viability and/or pollinator activity) (Pisanty et al., 2016). Additionally, cytokinin known to promote cell division, can affect watermelon flesh firmness and cell density (Soteriou et al., 2017), and may contribute to inadequate pollination.

Previous studies have reported that watermelon fruit from plantings with lower diploid-to-triploid ratios have a higher incidence of HH (Fiacchino and Walters, 2003; Freeman et al., 2007c). Generally, any diploid to triploid ratio less than 20% of a field (e.g., four triploid to one interplanted diploid pollenizer) increases HH formation (Freeman et al., 2007c). To achieve optimal fruit yields and high watermelon fruit quality, 25 to 33% of a field should be planted with diploid plants (Fiacchino and Walters, 2003; Freeman and Olson, 2007a). This is done by interplanting a seeded watermelon cultigen or diploid pollenizer in the same field, either in the same row as triploid plants or as a dedicated row only for diploid pollenizers (Freeman et al., 2007c).

In watermelon cultigen evaluations, HH incidence is highly variable even when planted at the same geographic location (Seminis Seeds, 2019) which increases breeder difficulty for screening germplasm for the disorder. The relationship of watermelon fruit firmness and incidence of HH has not been studied, although researchers have suggested fruit tissue firmness may give some indication of HH disorder (Guan, 2018). Cultigen evaluations for watermelon productivity and fruit traits are routinely conducted across the United States (Coolong, 2015; Johnson, 2017; Schultheis and Thompson, 2014). Fruit firmness and HH incidence are collected as part of these evaluations in North Carolina and offers datasets that might be useful in detecting relationships. In this study, three years of seedless watermelon cultigen evaluation data were used to determine possible germplasm trends for high and low HH incidence with tissue firmness.

Materials and Methods

Experimental site

The three watermelon cultigen evaluations were conducted in a field experiment at the Central Crops Research Station (35.6507^{o}N, -78.4962^{o}W) located in Clayton, North Carolina (North Carolina State University) from May to September in 2012, 2013 and 2014. The soil type was sandy clay loam (80% sand, 5% clay, low organic matter (1 to 1.5%) and low acid retention) (Kleiss, 1981). The average max/min temperatures, rainfall and cumulative rainfall from May to September 2012 to 2014 are provided in Table 2.1. Day and night temperatures and daily rainfall during peak pollination and fruit set are reported in Figure 2.2, three to six weeks after transplanting.

Table 2.1. Average day and night temperatures, minimum and maximum temperatures and average daily and cumulative rainfall for each cultigen evaluation, May to September.

Growing season	Day temp. (^{o}C)	Night temp. (^{o}C)	Max temp. (^{o}C)	Min temp. (^{o}C)	Rainfall (cm)	Cumulative Rainfall (cm)
2012	29.7	19.5	39.7	10.6	0.25	31.5
2013	28.9	19.5	35.1	11	1.19	131.8
2014	29.5	19.3	35.1	8.6	0.38	42.5

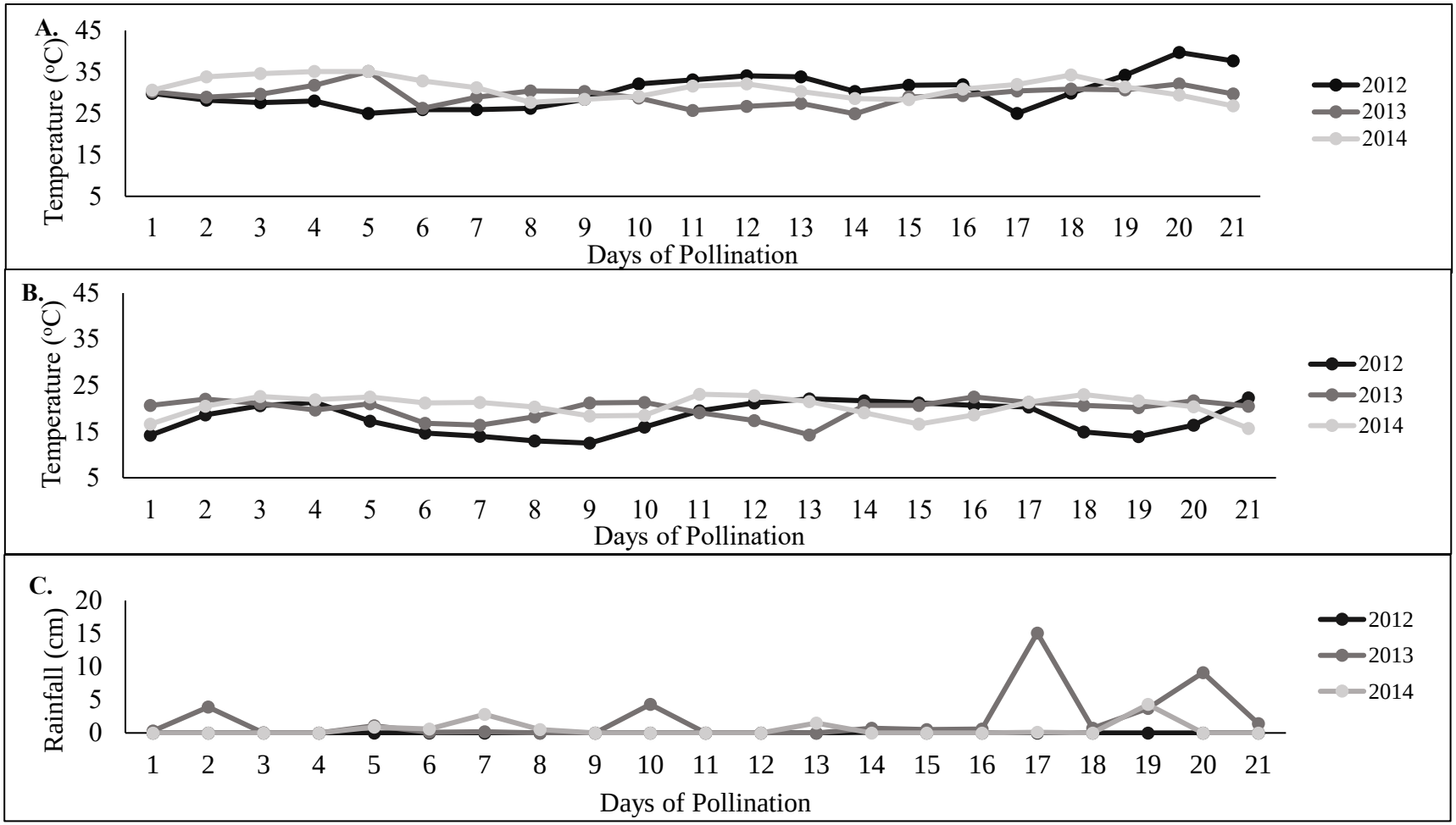

Figure 2.2. Maximum (A) and minimum (B) temperatures, and daily rainfall (C) recorded during the estimated time of fruit set (from 3 to 6 weeks after transplanting) among the 2012, 2013 and 2014 triploid watermelon evaluations. The x-axis represents the estimated number of days of pollination. In 2012, diploid flowers opened ~8 June, climate data shown from 8 June to 1 July; in 2013 diploid flowers opened ~9 June, climate data shown from 9 June to 2 July; and in 2014 diploid flowers opened and pollination occurred ~15 June, climate data shown from 15 June to 7 July.

Experimental design

A randomized complete block design (RCBD) with four replications was used for each watermelon cultigen evaluation in 2012 and 2014, with five fruit randomly collected from each plot (20 fruit/entry) used as the experimental unit for evaluations. Excessive rainfall occurred in the 2013 growing season, and one replication of the triploid study was lost, with only replications 2-4 used for analysis (Schultheis and Thompson, 2013). New seed were obtained each year and consisted of 44, 40, and 30 entries for 2012, 2013, and 2014 respectively. Additionally, 13 cultigens were present each year of the evaluations and are denoted as the common cultigen set. The common cultigens and fruit characteristics are listed in Table 2.2.

Table 2.2. Cultigen names of the thirteen common cultigens used in 2012, 2013 and 2014 and their relative fruit characteristics.

Cultigen name	Fruit description
ACX 6177	Indistinct medium wide green stripes; long round fruit shape; medium fruit size
7197	Indistinct medium to dark green stripes on light green background; long round to blocky shape; medium to large fruit size
SV0241	Indistinct medium dark green stripes on medium green background; short blocky to oval fruit; variable size; distinct red flesh
Affirmed	Indistinct medium wide, dark green strips on light green background; short blocky shape; medium to large fruit size
Bold Ruler	Indistinct medium wide, medium/dark green stripes on light green background; short blocky to oval shape; medium to large fruit size
Captivation	Indistinct medium/wide, dark green stripes, light green background; short blocky shape; fruit size medium to large; excellent rind/flesh delineation; hardcore found
Crunchy Red	Indistinct medium wide, medium green stripes on light green background; small fruit are round while large are elongated; mainly large fruit; very thick fruit rind
Declaration	Indistinct medium width dark green strips on light green background; uniform oval blocky fruit; uniform medium to large size; indistinct rind delineation
Fascination	Indistinct medium width, dark green stripes on light green background; oval and blocky shape; medium to large size; very dark red flesh
Liberty	Indistinct medium wide, medium to dark green stripes on light green background; oval to short blocky fruit with small fruit more round in shape; generally medium to large fruit size

Table 2.2 (continued)

Maxima	Distinct, medium width, very dark green stripes; short oval to round shape; medium to large fruit size
Secretariat	Indistinct medium width, medium to dark green stripes on light green background; blocky fruit with uniform shape; medium to large size fruit; indistinct rind flesh delineation; good red flesh color
Tri-X-313	Indistinct medium wide, medium to dark green stripes on light green background; oval to short blocky fruit shape; medium to larger fruit size; thick rind

Seedling and field preparation

Seed of triploid cultigens and diploid pollenizer plants were sown 3-5 April, 2012, 3-5 April, 2013 and 15 April, 2014. Seed were placed into poly transplant trays (Hummert Int.; Earth City, MO) filled with commercial soilless mix (Fine Germinating Mix, Carolina Greenhouse and Soil Company, Kinston, NC) were held under greenhouse conditions (ranging from 24 to 30 °C). About 3 weeks after seeding, watermelon transplants were placed either in a cold frame or high tunnel to harden off. Transplants were field planted 8 May 2012, 14 May, 2013 and 19 May, 2014, respectively. Granular fertilizer was the same for each year, and were applied at 33.6 $kg \cdot ha^{-1}$ N and 74.1 $kg \cdot ha^{-1}$ K. Granular fertilizers were incorporated into the beds prior to laying black polyethylene plastic (0.70 mm thick high density plastic film, 1.2 m wide; B.B. Hobbs, Clinton, NC).

The field studies were fumigated with Telone C-17 (Dow AgroSciences, Indianapolis IN) via broadcast application at 93.4 $kg \cdot ha^{-1}$ on 14 Nov. 2011, and the same rate was applied on 9 Nov, 2012 and 7, Nov. 2013, respectively. Ethalfluralin (4.7 $kg \cdot ha^{-1}$), N,N′-dimethyl-4,4′-bipyridinium dichloride (3.5 $kg \cdot ha^{-1}$) and bensulide (5.8 $kg \cdot ha^{-1}$) (Dow AgroSciences, Indianapolis, IN) were applied between plastic beds for weed control in May (prior to planting) and June (before watermelon started to vine out) for all triploid watermelon evaluations (Schultheis and Thompson, 2012; 2013; 2014).

Crop production

Spacing between rows was 3.1 m with in-row plant spacing 0.8 m. Plots were one row, 7.6 m long allowing 10 plants to be grown for each experimental unit. A 3.1 m alley was maintained between plots. At the time of transplant, a liquid fertilizer was 20-20-20 (20.0N-8.7P-

16.5K, Peters Professional General Purpose Fertilizer, Clayton, NC) at 0.01 kg·ha^{-1} with Coragen® (DuPont™, Wilmington, DE) at 0.07 kg·ha^{-1} applied at the same time for insect control. Plots with missing transplants were replanted approximately 7 d after planting to achieve 100% stand count in all three experimental (Schultheis and Thompson, 2012; 2013; 2014).

Pollenizer plants

For the 2012 growing season, the diploid pollenizer 'Ace' was interplanted after triploid plants 1, 4, and 7 in each plot. In 2013, two pollenizer cultigens ('Ace' and 'SP-6') were used, with 'SP-6' interplanted after triploid plants 1 and 10, and 'Ace' interplanted after triploid plants 4 and 7. 'SP-6' was used as the sole pollenizer source in 2014 and was interplanted between plants after triploid plants 1, 4 , 8 and 10.

Trickle irrigation (NETAFIM, 197 mL, 1.09 x10^{3} mL·hr^{-1}; NETAFIM, Tel Aviv, Israel) was utilized over the course of each growing season. Fertigation started two weeks after planting and was drip applied weekly over the course of the growing seasons using a 4-0-8 (4.0N-0.0P-6.6K) liquid fertilizer (Harrell's Max® Potassium plus Calcium, Lakeland, FL). Cumulative amounts of liquid fertilizer applied through the growing seasons were 146.1 kg·ha^{-1} N, 0.0 kg·ha^{-1} P and 259.9 kg·ha^{-1} K.

A conventional spray program for North Carolina was used for crop production (Schultheis and Thompson, 2012; 2013; 2014). Insecticide, fungicide and/or miticide applications were applied every week starting from the first week of June through the second week of Aug. The products were alternated during consecutive spray applications among the evaluations to avoid pest resistance. Acramite (Arysta, Tokyo, Japan), a miticide was applied in 2012, while the fungicide and insecticide programs utilized during each of the growing seasons are listed in Table 2.3.

Table 2.3. Fungicide, insecticide and miticide program utilized in the 2012, 2013 and 2014 watermelon evaluations.

2012		2013		2014	
Pesticide	Fungicide	Pesticide	Fungicide	Pesticide	Fungicide
Acramite 'Arysta'	Chlorothalonil 'Bravo'	Esenvalerate 'Asana'	Chlorothalonil 'Bravo'	Esenvalerate 'Asana'	Chlorothalonil 'Bravo'
Esenvalerate 'Asana'	Copper hydroxide 'Kocide'	Bifenthrin 'Fan Fare'	Copper hydroxide 'Kocide'	Bifenthrin 'Fan Fare'	Copper hydroxide 'Kocide'

Table 2.3. (continued)

Bifenthrin 'Fan Fare'	Pyraclostribin 'Prisitine'	Permethrin 'Perm Up'	Pyraclostribin 'Prisitine'	Permethrin 'Perm Up'	pyraclostribin 'Prisitine'
Permethrin 'Perm Up'	Propamocarb 'Previcur Flex'	Endosulfan 'Phaser'	Propamocarb 'Previcur Flex'	Carabaryl 'Sevin'	Propamocarb 'Previcur Flex'
Bifenthrin 'Sniper'	Mancozeb 'Penncozeb'		Mancozeb 'Penncozeb'		Mancozeb 'Penncozeb'
Endosulfan 'Thionex'	Cyazofamid 'Ranman'		Cyazofamid 'Ranman'		Cyazofamid 'Ranman'

List of chemicals and associated company/locations: Acramite (Arysta, Tokyo, Japan), Esenvalerate (DuPont, Willimington, DE), Bifenthrin (FMC Co., Philadelphia, PA), Permethrin (Bayer, USA, Hanover, NJ), Bifenthrin (FMC Co., Philadelphia, PA), Endosulfan (Velsicol Chemical Co., Chicago, IL), Chlorothalonil (ISK Biotech Corp., Painsville, OH), Copper hydroxide (Kocide Chemical Corp., Houston, TX), Pyraclostribin (Bayer, USA, Hanover, NJ, Midland, MI), Cyazofamid (ISK Biotech Corp., Painsville, OH), Carabaryl (Bayer, USA, Hanover, NJ).

Crop harvest and data collection

Four watermelon harvests were made in 2012 and 2014 and five harvests in 2013. The first harvests were done on 17 July, 2012; 18 July, 2013; and 24 July, 2014, respectively. Each of the fruit were harvested at about 65 days post anthesis when ripe, weighed and rated for the incidence and severity of HH. Hollow heart was rated on a 0-4 scale in 2012 (0 being none, 1= little HH and 4 being severe) and a 1-5 scale in the 2013 and 2014 trials (1= no HH, 2= little HH and 5= severe) (USDA, 2006). For uniform comparison, HH ratings for 2012 were converted to a 1-5 scale. Other evaluations for each entry included yield, fruit shape and size, rind pattern, occurrence of hard seeds, flesh color, and soluble solids content (NC state extension website, https://cucurbits.ces.ncsu.edu/growing-cucurbits/variety-trials/).

Flesh firmness in pounds was determined using a Penetrometer FT 011 (1-11 lb/4.4-44 N range) with a 1.11 cm diameter plunger tip, (QA Supplies LLC, Norfolk, VA). Firmness readings were taken at five locations in the placental material (flesh) (Fig. 2.3) at the ground spot side, opposite (top) side, blossom end, stem end, and heart and are presented as means for 20 fruit per cultigen per year, primarily from first or second harvests.

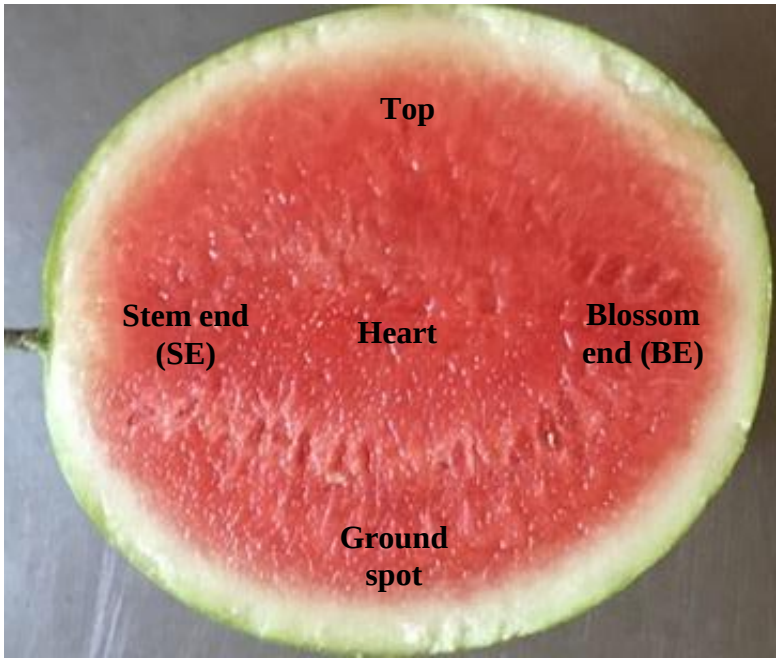

Figure 2.3. Location of firmness readings taken in longitudinally cut triploid watermelon.

Data analysis

All statistical analysis of HH percent (incidence), severity, and tissue firmness were conducted using SAS 9.4 (SAS Institute, Cary, NC). Linear regression was run on the overall and common cultigen sets, and coefficient of determination (R^2) values were used to assess the relationship between tissue firmness and the incidence of HH. An ANOVA was generated on mean tissue firmness and mean HH severity ratings for all cultigens by year for all cultigens, across the years for 13 common cultigens and by year for the 13 common cultigen set. Logistic regression was run to indicate the HH percent for all cultigens by year, across the years for the 13 common cultigens and by year for the 13 common cultigen set. Logistic regression was also done to identify the predictive odds of a watermelon cultigen developing HH in a given year. Mean separations were performed using Tukey-Kramer ($p < 0.05$) on average tissue firmness (N), average HH severity rating and HH percent among the three cultigen evaluations and common cultigens.

Results and Discussion

Incidence and severity of HH

Logistic regression indicated incidence of HH did not differ by year for the large multi-year cultigen evaluation (Fig. 2.4). Within the years, the range of HH incidence was highest in

2012 from 0-65%, lowest in 2013 ranging from 0-35% and intermediate in 2014 from 0-50%, respectively (Fig 2.4).

In the 13 common cultigens, the interaction of year and cultigen was not significant ($p > 0.9567$). By year, incidence of HH did not differ in the 13 common cultigens ($p < 0.1221$; $p < 0.3387$; $p < 0.2327$ for 2012, 2013, and 2014, respectively). The three years of data for the 13 common cultigens were combined and subjected to logistic regression, which yielded significant cultigen differences in the incidence of HH ($p < 0.0001$) (Table 2.5). The 13 common cultigens did not differ in HH severity across the years or by year (data not shown) ($p > 0.05$).

Tissue firmness and hollow heart

Mean tissue firmness in the large multi-year cultigen evalution differed by year ($p < 0.05$) (Fig. 2.4). In 2012, average tissue firmness ranged from 11.0 to 17.6 N, with lowest values for 'Gilboa' and 'Affirmed' (11.0 and 11.2 N, respectively), and the highest value for 'Fusion' (17.6 N). In 2013, the average tissue firmness ranged from 10.3 to 16.2 N, with the lowest value for 'Tri-X-313' (10.3 N) and highest value for 'LaJuva' (17.2 N). The average tissue firmness was 9.1 to 16.4 N in 2014, and was lowest for 'Harvest Moon' (9.1 N) and highest for 'Premont' (16.4 N), 'Captivation' (16.3 N), 13-13077 (16.1 N), 'Crunchy Red' (16.0 N), 'Exclamation' (15.6 N), 'Secretariat' (15.3 N) and 'ACX 6177 '(15.3 N).

Coefficient of determinations indicated that the incidence of HH was positively correlated to the severity of HH (0.96, $r^2 = 0.92$) and mean fruit tissue firmness was negatively correlated to the incidence of HH (0.55, $r^2 = -0.32$) (data not shown). In 2012 and 2013, cultigens that had the lowest mean tissue firmness ('Affirmed', 'Gilboa' and 'Tri-X-313') were in the top 25% for HH incidence. Conversely, cultigens with the highest tissue firmness ('Fusion' and 'LaJuya') were in the lower 10% for incidence of HH. No trends were found in 2014 for cultigen flesh firmness and HH incidence.

In the common cultigen set, mean tissue firmness differed across the years ($p > 0.0001$) (Fig. 2.5) and within years ($p < 0.0001$ for 2012, 2013, 2014) (data not shown). Cultigens with higher tissue firmness values had less HH incidence. Cultigens with an average HH incidence of 20% or less such as 'Crunchy Red', 'Maxima' and 'Captivation' had firmness values of 15 to 16 N. Conversely, tissue firmness was 11 to 12 N for 4 of 6 cultigens with HH incidence above 20%. Mean tissue firmness was negatively correlated to the incidence of HH (0.88 $R^2 = -0.78$). Mean tissue firmness was also negatively correlated to the severity of HH (0.62, $R^2 = -0.39$,

respectively). In contrast, the correlation of HH incidence and severity was positively correlated (0.96, $R^2 = 0.92$).

Linear regression

In the common cultigen set, linear regression was used to determine the relationship of tissue firmness to HH percent (Fig. 2.7). Fruit with lower tissue firmness generally indicate a higher percentage of HH. 'Bold Ruler', 'Liberty' and 'Affirmed' had both low tissue firmness (~12 N) and a high probability of developing HH. Conversely, 'Maxima' and 'Captivation' had the lowest probability of developing HH and higher tissue firmness (15 N). Utilizing average tissue firmness for 2012-2014 in the common cultigen data set, the incidence of HH was predicted using the formula: $y = -6.6152(N) + 115.29$, where y = %HH and N represents firmness (newtons). The general trends to higher firmness and less HH incidence also indicate that selection for higher firmness may reduce HH incidence and severity.

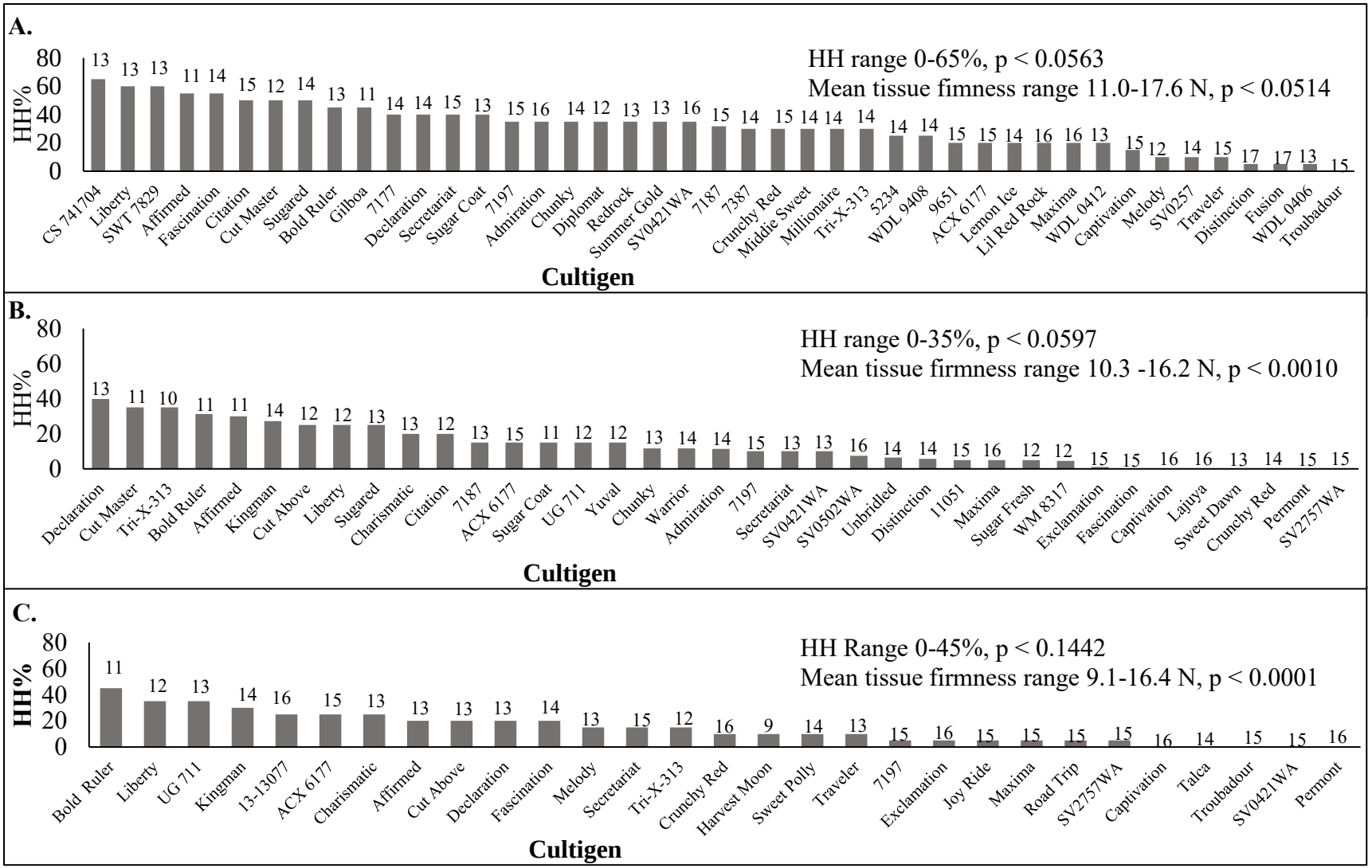

Figure 2.4. Percentage (%) of HH with mean tissue firmness in newtons (N), LS-means given above the bars in 2012 (A), 2013 (B) and 2014 (C). Differences were found in fruit mean tissue firmness within the 2012, 2013 and 2014 evaluations ($p < 0.05$).

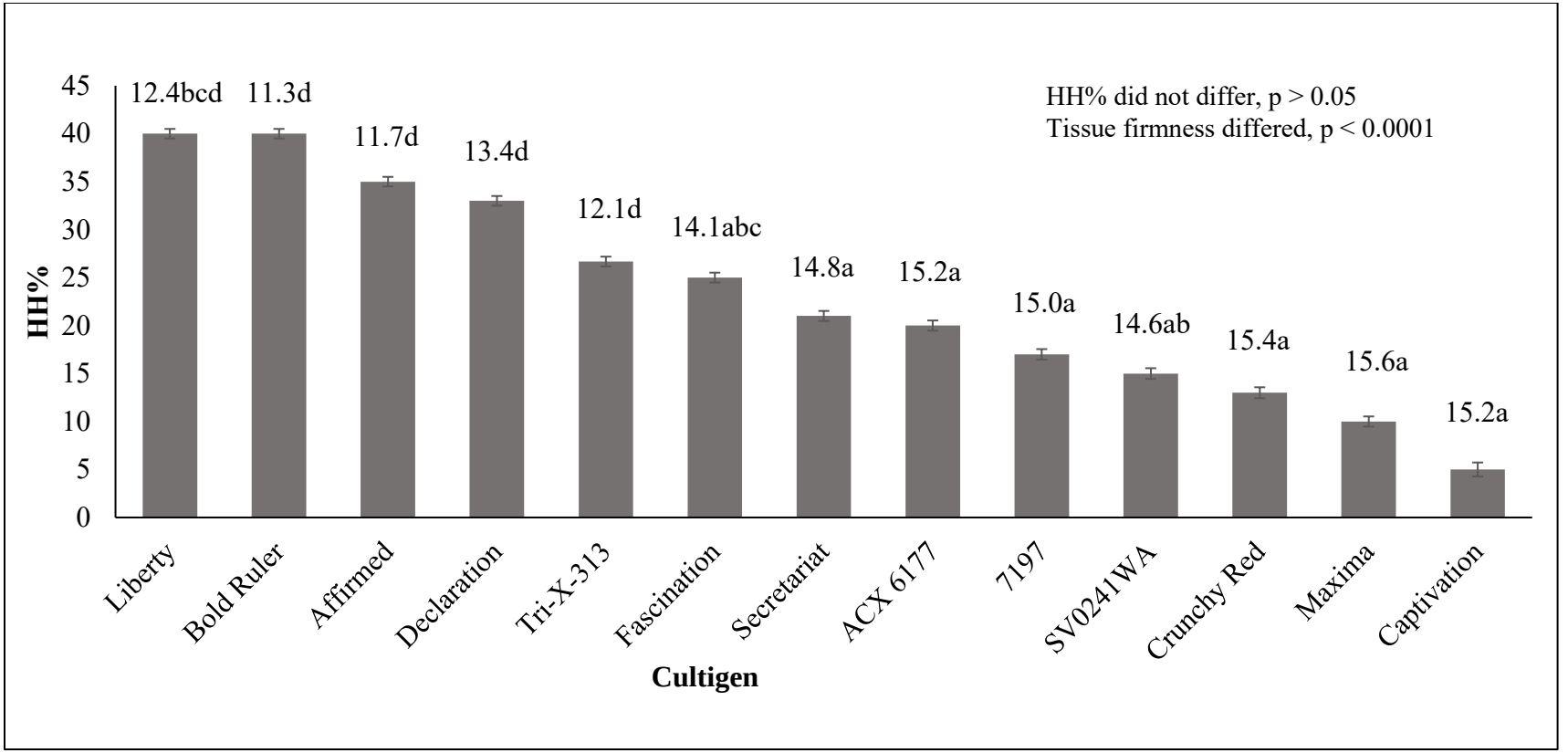

Figure 2.5. Percentage (%) of hollow heart in the common cultigen set averaged over the three growing seasons 2012, 2013, and 2014; differences among cultigens were not significant at $p < 0.05$. Tissue firmness (N) as LS-means values are provided above the bars and values are separated by Tukey Kramer honest significant difference, $p < 0.05$, with differences indicated by different letters.

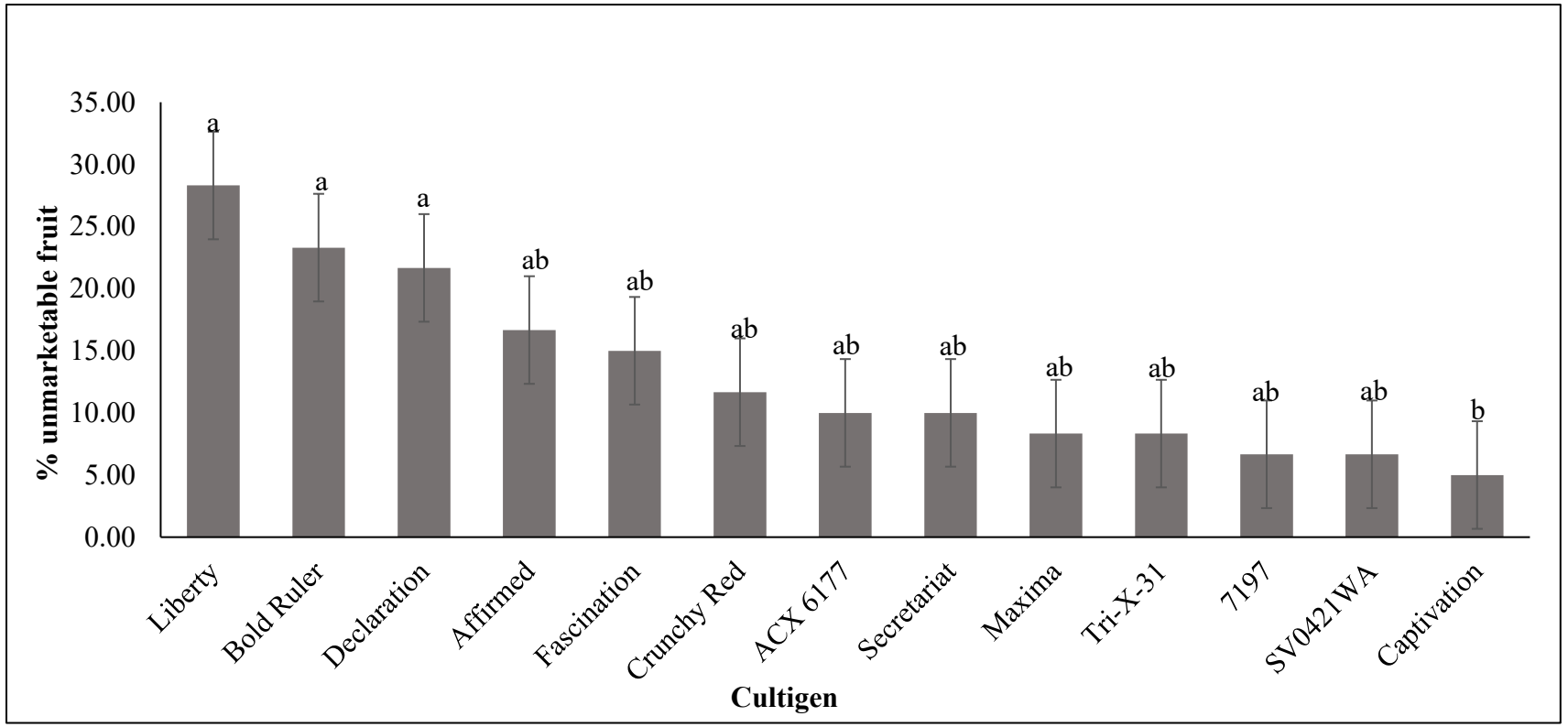

Figure 2.6. Percentage (%) of unmarketable fruit in the 13 common cultigens rated with a hollow heart severity > 2 (considered unmarketable) averaged across the 2012-2014 growing seasons. Means were separated by Tukey Kramer honest significant difference, $p < 0.05$, and differences are indicated by different letters. Fruit tissue firmness values specific for unmarketable fruit (HH > 2) were not measured.

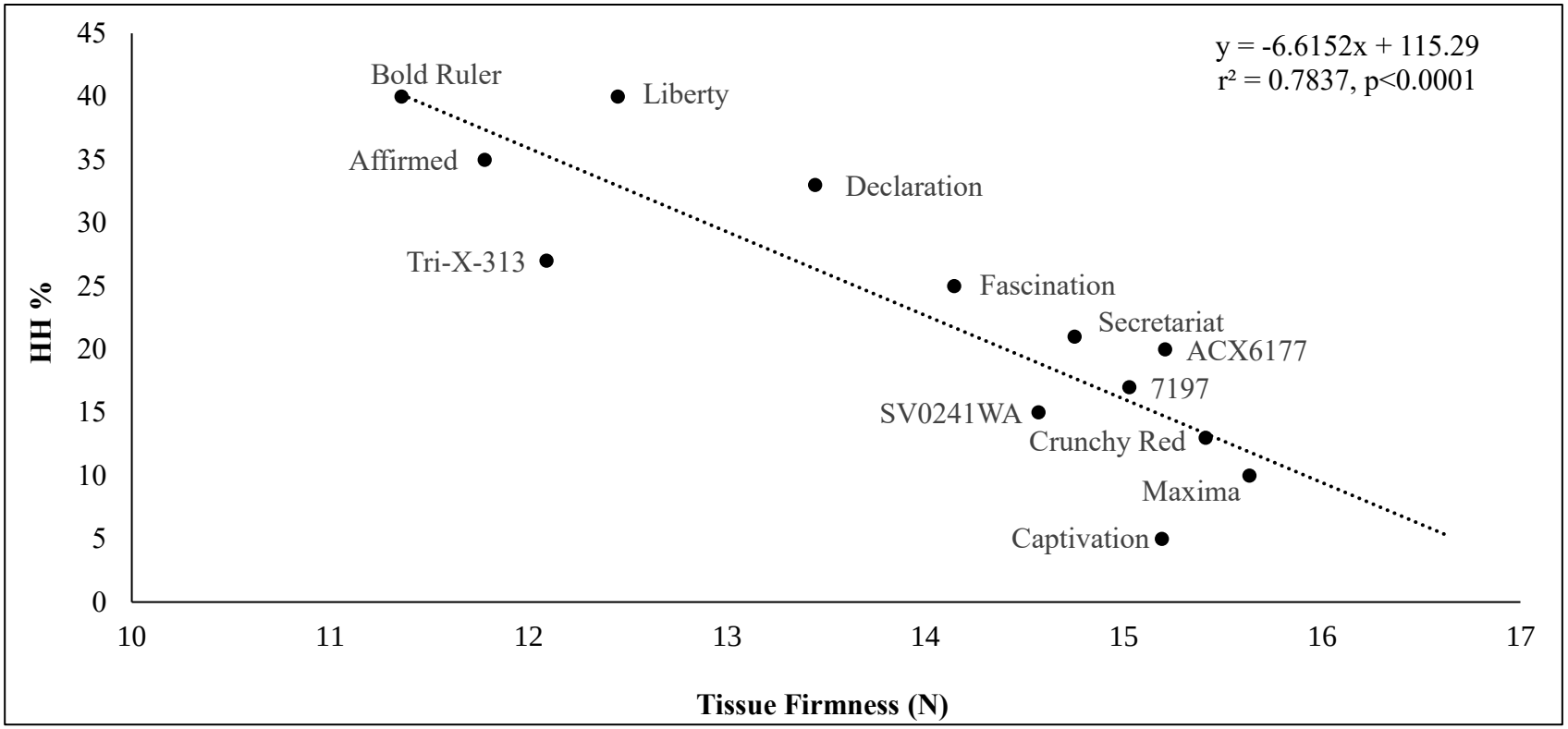

Figure 2.7. Linear regression of tissue firmness (N) and incidence of hollow heart (%) in the 13 common cultigen data set, averaged over the three growing seasons.

Since HH incidence is unpredictable within a growing season, factors that might contribute to this disorder have been explored. Although HH disorder is found in diploid (seeded) fruit, it is more prevalent in triploid watermelons, which cannot produce sufficient viable pollen for fruit set. Additionally, pollen viability, pollinator activity, and watermelon bloom receptivity are highly influenced by environmental factors such as rainfall and fluctuations in day and night temperatures. Peak watermelon flowering and pollination generally starts to occur about 2 to 3 weeks after field transplanting and up to 7 weeks after transplant when air temperatures exceed 25 °C (Freeman et al., 2007c). Pollinators need to visit a triploid flower 16 to 24 times in order to achieve adequate pollen grain transfer and fruit set (Johnson 2014; Fiacchino and Walters, 2003; Walters, 2005). Pollen tetrad development decreases with temperature stress (below 15°C), ultimately decreasing pollen count (Lyu et al., 2019). Pollen viability can also decrease as temperature increases (above 30 °C) (Lyu et al., 2019). Additionally, high day time temperatures and low morning temperatures, or fluctuations in humidity shortly after anthesis, can decrease pollen viability and trigger the onset of HH (Lyu et al., 2019).

Staminate watermelon flowers shed pollen for only a few hours early in the day, requiring temperatures above 15 °C (Stanghellini and Schultheis, 2005; Lyu et al., 2019). Additionally, watermelon pistillate flower stigmas are most receptive to pollen from 15 to 26 °C, and senesce within a few hours where temperatures reach 30 °C (Lyu et al., 2019). In our study, average day and night temperatures were similar during the three growing seasons (May-September), although cumulative rainfall was considerably higher in 2013 compared to 2012 or 2014 (Table 2.1). However, periods of low air temperature (under 15°C) occurred during the early fruit set period in 2012, followed by several days of high daily temperatures (34-39.7 °C) also occurred (Fig. 2.2). It is possible that these low/high temperatures contributed to the higher incidence and severity of HH in 2012. Although 2013 had large rainfall events (which could impact insect pollen transfer) the events were near the end of the pollination period and may be why HH incidence was low in 2013.

Choice and placement of diploid pollinators may also affect HH incidence. The cultigen evaluations had diploid pollenizers interplanted with triploid plants an average of 43% per plot, above the recommended 25% (Freeman et al., 2007c) to reduce HH incidence. Diploids ‘Ace’ and ‘SP-6’ were used in two seasons, but only ‘Ace’ was utilized in 2012, where HH incidence

was highest and pollenizer ratio was lowest (Fig. 2.4). 'Ace' has a very early flowering date and an elongated pollination period, making pollen available for the first female triploid watermelon pistillate flowers as well as those produced later (Sakata Vegetables, 2018). In comparison, 'SP-6' has high pollen release/quantity, thin branches and small, deep lobed leaves to increase flower visibility to honey bees (Brusca and Zhang, 2012). The use of an increased ratio of diploid to triploid plants and multiple diploid cultigens for pollen viability would reduce potential diploid effects and HH incidence.

Pollination in seedless watermelon depends on the number of pollen grains transferred to pistillate flowers and the growth regulators produced by the developing ovule after fertilization (Walters and Schultheis, 2009). As a fertilized ovule develops, hormones are released that stimulate the division and expansion of fruit cells (Kano, 1993). Inadequate amounts of pollen can limit plant hormones, cause underdeveloped, misshapen fruit (Walters, 2005) ultimately leading to HH. Cell wall polysaccharide structure may also be affected with adverse hormone production, causing uneven cell growth, cell wall weakening, and cell breakage (Karakurt et al., 2008; Mort et al., 2008).

The watermelon rind continues to expand and differentiate during fruit growth and maturation. Placental tissue cells stop dividing at 7 days post anthesis and cells begin to enlarge with the accumulation of water, sugars, proteins and nutrients accumulate (Kano, 1993; Elmstrom and Davis, 1981). A rapid change in water potential between placental cells and rind cells can lead to a separation of the carpels, ovule and placental tissue, causing a hollowing or cavity (Kano, 1993; Johnson, 2014; 2015).

Results from the common cultigen evaluation data indicate that some germplasm is more susceptible to HH, possibly resulting from receptivity to pollen or amount of hormone released, or to relative cell growth rates. The three cultigens showing consistently high HH may differ from other cultivars in earliness of bloom (before adequate pollen is available), or blooms may require more pollen than other cultivars in order to set fruit and grow normally.

Rapid and irregular fruit growth can also be from reduced fruit tissue firmness or cell density (Kano, 1993). The common cultigen set indicates that higher HH incidence is associated with lower tissue firmness values (Fig. 2.5 and 2.7). Correlation of the incidence of HH disorder and fruit firmness from 2012, 2013 and 2014 data and the 13 common cultivar set provided a

negative correlation between fruit firmness and %HH (Figs. 2.4, 2.5, and 2.7). This suggests that fruit with lower tissue firmness are more susceptible to HH.

Logistic regression

When a dependent variable is categorical, a logistic regression provides a more robust statistical comparison than linear regression (Lever et al., 2016). Logistic regression was useful in this study as a means to indicate the 'predicative odds' of a cultigen to develop HH. Logistic regression was run separately by year for the complete cultigen set, since the cultigens used varied considerably across years. No differences were found among cultigens for predicted HH incidence (Table 2.4), probably from the high amount of variation within and across replicates, and the change in cultigens utilized in each year.

Table 2.4. Logistic regression showing the incidence of HH among 2012, 2013 and 2014 in the large multi-year cultigen evluations.

Cultigen	2012 HH incidence (%)[Z]	2013 HH incidence (%)[Z]	2014 HH incidence (%)[Z]
5234	24.2a	-	-
7177	39.6a	-	-
7187	29.3a	12.4a	-
7197	34.5a	7.9a	4.7a
7387	29.3a	-	-
9651	19.2a	-	-
11051	-	3.8a	-
13-13077	-	-	24.3a
ACX 6177	19.2a	12.4a	24.3a
Admiration	34.5a	9.1a	-
Affirmed	55.3a	27.9a	19.3a
Bold Ruler	44.8a	27.9a	44.8a
Captivation	14.3a	0.0a	0.0a
Charismatic	-	17.3a	24.3a
Chunky	34.5a	7.9a	-
Citation	50.0a	17.3a	-
Crunchy Red	29.3a	0.0a	9.5a
CS 741704	65.6a	-	-
Cut Above	-	22.5a	19.3a
Cut Master	50.0a	33.4a	-
Declaration	39.6a	33.4a	19.3a
Diplomat	34.5a	-	-
Distinction	4.6a	3.8a	-
Exclamation	-	0.0a	4.7a
Fascination	55.3a	0.0a	19.3a
Fusion	4.6a	-	-
Gilboa	44.8a	-	-
Harvest Moon	-	-	9.5a

Table 2.4. (continued)

Joyride	-	-	4.7a
Kingman	-	22.5a	29.4a
LaJuya	-	0.0a	-
Lemon Ice	19.2a	-	-
Liberty	60.4a	22.5a	34.5a
Lil Red Rock	19.2a	-	-
Maxima	19.2a	3.8a	4.7a
Melody	9.4a	-	14.3a
Middie Sweet	29.3a	-	-
Millionaire	29.3a	-	-
Permont	-	0.0a	0.0a
Red Rock	34.5a	-	-
Road Trip		-	4.7a
Secretariat	39.6a	7.9a	14.3a
Sugarcoat	39.6a	12.4a	-
Sugar Fresh	-	3.8a	-
Sugared	50.0a	22.5a	-
Summer Gold	34.5a	-	-
SV0257	9.4a	-	-
SV0421WA	34.5a	7.9a	0.0a
SV0502WA	-	3.8a	-
SV2757WA	-	0.0a	4.7a
Sweet Dawn	-	0.0a	-
Sweet Polly	-	-	9.5a
SWT 7829	60.4a	-	-
Talca	-	-	0.0a
Traveler	9.4a	-	9.5a
Tri-X-313	29.3a	33.4a	14.3a
Troubadour	0.0a	-	0.0a
UG 711	-	12.4a	34.5a
Unbridled	-	3.8a	-
Warrior	-	7.9a	-
WDL0406	4.6a	-	-
WDL0412	19.2a	-	-
WDL9408	24.2a	-	-
WM 8317	-	3.8a	-
Yuval	-	12.4a	-
P-value	0.0563	0.0142	0.1442

[z] = incidence of HH is reported as LS-means ($\alpha = 0.05$); means separated by Tukey Kramer honestly significant difference test.

With the common cultigen data set, logistic regression indicated differences in HH incidence were found among the 13 cultigens averaged over the 2012, 2013 and 2014 (Table 2.5). Cultigens with a tendency to develop HH could be clearly identified, even with large year to year differences in environmental conditions and HH incidence; and the odds of developing

HH for each cultigen were compared against ‘Maxima’. Logistic regression also allowed identification of germplasm that was more likely to develop HH. ‘Bold Ruler’ and ‘Liberty’ had a 7.0 and 6.9 times more likely to develop HH, while ‘Maxima’ and ‘Captivation’ were 1.0 and 0.4 times more likely to develop HH in a given year (Table 2.5). These cultigens could be useful as markers for susceptibility and resistance to HH disorder in different production sites and seasons.

Table 2.5. Incidence of HH and predictive odds of a cultigen in the common cultigen data set for developing hollow heart in any given year.

Cultigen	HH incidence (%)	Predictive Odd[z]
Bold Ruler	39.2a	7.0a
Liberty	39.2a	6.9a
Affirmed	34.0ab	5.5ab
Declaration	30.0abc	4.8ab
Tri-X-313	25.0abcd	3.7ab
Fascination	23.0bcde	3.1ab
ACX 6177	18.1bcde	2.5ab
7197	14.9cde	2.5ab
Secretariat	13.3d	1.6ab
SV0241WA	13.0de	1.6ab
Crunchy Red	12.0de	1.3ab
Maxima	8.5e	1.0a
Captivation	4.1e	0.4a
p value	0.0001	0.0093

LS-means of HH incidence were separated by Tukey Kramer honestly significant difference test, $p < 0.05$ and dissimilar letters indicate significance.
[z] Odds of developing HH (%) reported as LS-means. The predictive odds of the 13 common cultigens were generated by comparisons to ‘Maxima’; ‘Bold Ruler’ is 7.0 times more likely to develop HH in a given year than ‘Maxima’.

In the common cultigen set, linear regression was used to see the relationship of tissue firmness values to the percent fruit with HH (Fig. 2.7). Fruit with lower tissue firmness generally indicate a higher probability of developing HH. ‘Bold Ruler’, ‘Liberty’ and ‘Affirmed’ had both low tissue firmness (~12 N) and a high probability of developing HH. Conversely, ‘Maxima’ and ‘Captivation’ had the lowest probability of developing HH and higher tissue firmness (15 N). Utilizing common cultigen average tissue firmness for 2012-2014, the incidence of HH was predicted using the formula: $y = -6.6152(N) + 115.29$, where y = %HH and N represents

firmness (newtons). The general trends to higher firmness and less HH incidence also indicate that selection for higher firmness may reduce HH incidence and severity.

Conclusion

Utilizing watermelon cultigen evaluation data collected over three years, cultigen tendencies could be found for developing HH, despite the unpredictable nature of this disorder. Tissue firmness was negatively correlated to the incidence of HH in both the multi-year and common cultigen evaluations, indicating that triploid cultigens with lower tissue firmness may be more likely to develop HH. This information provides a means for cultigen screening for HH even in seasons where HH is not prevalent. Applying logistic regression to HH incidence and tissue firmness yielded the predictive odds (probability) for watermelon cultigens to develop HH. This approach indicates cultigens ‘Bold Ruler’, ‘Liberty’, ‘Affirmed’, ‘Maxima’ and ‘Captivation’ can be used as benchmarks for high and low incidence in cultigen studies where HH incidence is being screened.

References

1. Brusca, J. and X. Zhang. 2012. United States Patent: Watermelon Pollenizer SP-6. Patent No. US 8,212,118 B1. [Online]. https://patentimages.storage.googleapis.com/0f/d4/dd/c7678b0b5e70ca/US8212118.pdf

2. Coolong, T. 2015. 2014/2015 University of Georgia vegetable crops research report. UGA Cooperative Extension Annual Publication. Pp 61-69. [Online]. https://secure.caes.uga.edu/extension/publications/files/pdf/AP%20115_2.PDF

3. Diezma-Iglesias, B., M. Ruiz-Altisent and P. Barreiro. 2004. Detection of internal quality in seedless watermelon acoustic impulse response. Biosystems Eng. 88(2):221-230.

4. Elmstrom, G.M. and P.L. Davis. 1981. Sugars in developing and mature fruits of several watermelon cultivars. J. Amer. Soc. Hortic. Sci. 106:330-333.

5. Freeman, J. and S. Olson. 2007a. Characteristics of watermelon pollinizer cultivars for use in triploid production. Intl. J. Veg. Sci. 13:73-78.

6. Freeman, J. and S. Olson. 2007b. Competitive effect of in-row diploid watermelon pollinizers on triploid watermelon yield. HortScience 42:1575-1577.

7. Freeman, J., G.A. Miller, S.M. Olson and W.M. Stall. 2007c. Diploid watermelon pollenizer cultivars differ with respect to triploid watermelon yield. HortTechnology 17:518-523.

8. Fiacchino, D.C and S.A. Walters. 2003. Influence of diploid pollenizer frequencies on triploid watermelon quality and yields. HortTechnology 13:58-61.

9. Guan, W. 2018. Hallowheart of watermelons. Purdue Agriculture. [Online]. https://ag.purdue.edu/btny/ppdl/Pages/POTW2018/POTW09042018.aspx

10. Johnson, G. 2014. These beautiful watermelon patterns are driving everyone crazy. [Online]. https://www.boredpanda.com/weird-watermelons-beautiful-hollow-heart/

11. Johnson, G. 2015. Research finds potential cause of hollow heart disorder in watermelon. PhysOrg. [Online]. https://phys.org/news/2015-06-potential-hollow-heart-disorder-watermelons.html

12. Johnson, G. 2017. Seedless watermelon trials 2017. Weekly crop update. UD Cooperative Extension. [Online]. https://sites.udel.edu/weeklycropupdate/?p=11482

13. Kano, Y. 1993. Relationship between the occurrence of hollowing in watermelon and the size and the number of fruit cells and intercellular air space. J. Japan Soc. Hortic. Sci. 62:103-112.

14. Kleiss, S. 1981. Soils of Central Crops Research Station: their technical and usability classification. Soil Science Society of North Carolina. [Online]. http://agronomy.agr.state.nc.us/sssnc/index.htm

15. Lever, J., M. Krzywinski, and N. Altman. 2016. Logistic regression: regression can be used on categorical responses to estimate probabilities and to classify. Nature Methods 13:541-548.

16. Lyu, X., S. Chen, N. Liao, J. Liu, J. Yang and M. Zhang. 2019. Characterization of watermelon anther and its programmed cell death- associated events during dehiscence under cold stress. Plant Cell Reports 38:1551-1561.

17. McGregor, C. and V. Waters. 2014. Flowering patterns of pollenizer and triploid watermelon cultivars. HortScience 49:714-721.

18. Pisanty, G., O. Afik, E. Wajnberg and Y. Mandelik. 2016. Watermelon pollinators exhibit complementary in both visitation rate and single-visit pollination. J Applied Ecol. 53:360-370.

19. Sakata Vegetables. 2018. 'Ace Plus'. Sakata Seed America©. [Online]. https://sakatavegetables.com/vegetable/watermelon/ace-plus/

20. Schultheis, J.R. and B. Thompson. 2012. Watermelon Cultivar Trials NCSU. No. 203. Pp 1-55. [Online]. https://cucurbits.ces.ncsu.edu/wp-content/uploads/2017/03/2012-WM-Cultivar-Booklet-Final.pdf?fwd=no

21. Schultheis, J.R. and B. Thompson. 2013. Watermelon Cultivar Trials. NCSU. No. 207. Pp 1-56. [Online]. https://cucurbits.ces.ncsu.edu/wp-content/uploads/2017/03/2013-WM-Cultivar-Evaluation-Booklet.pdf?fwd=no

22. Schultheis, J.R. and B. Thompson. 2014. North Carolina State University Watermelon Cultivar Trials. No. 210. Pp 1-39. [Online]. https://gates.ces.ncsu.edu/wp-content/uploads/2015/01/NCSU-Watermelon-Cultivar-Booklet_2014.pdf?fwd=no

23. Seminis Seeds. 2019. Agronomic Spotlight. Hollow heart of watermelon. [Online]. https://seminisus.s3.amazonaws.com/app/uploads/2019/11/5070_SE_S1_Hollow-Heart-of-Watermelon.pdf

24. Soteriou, G.A., A.S. Siomos, D. Gerasopoulous, Y. Rouphael, S. Georgiadou, and M.K. Kyriacou. 2017. Biochemical and histological contributions to textural changes in watermelon fruit modulated by grafting. J. Food Chem. *2*37:133-140.

25. Stanghellini, M. and J. Schultheis. 2005. Genotype variability in staminate flower and pollen grain production of diploid flowers. HortScience 40:752-755.

26. Walters, A. 2005. Honey bee pollination requirements for triploid watermelon. HortScience 40:1268-1270.

27. USDA. 2006. US Standards for Grades of Watermelon. Agricultural Marketing Services, Fruit and Vegetable Program, pp. 1-11.

28. USDA. 2019. Specialty Crop Market News. Seeded and Seedless Watermelon Production. [Online]. https://www.ams.usda.gov/mnreports/wa_fv456.txt

CHAPTER 3

GRAFTING WATERMELON ONTO INTERSPECIFIC HYBRID SQUASH REDUCES HOLLOW HEART DISORDER

Abstract

Hollow heart (HH) fruit disorder develops predominantly in triploid (seedless) watermelon. Incidence of HH can range from 0 to over 60%, depending upon the season, making it difficult to predict or control. Fruit genetics, pollination, and other environmental factors are thought to contribute to the onset and development of HH. Previous research indicates that watermelon cultivars with lower tissue firmness have a higher incidence of HH. Grafting a watermelon scion to a hybrid squash rootstock has been shown to increase tissue firmness and may decrease HH in susceptible cultivars. In this study, 'Liberty', a HH susceptible cultivar, was grafted onto the interspecific hybrid (*Cucurbita maxima* × C. *moschata*) rootstocks (RS) 'Carnivor' and 'Kazako', or to 'Emphasis' (*Lageneria siceraria*, bottle gourd RS). Fruit HH incidence was reduced by 28% when grafted onto 'Carnivor' RS compared to non-grafted fruit. Flesh firmness was increased by 1 N in fruit from 'Kazako' or 'Carnivor' RS. The soluble solids content was lowest in fruit from the 'Carnivor' RS (11.7) or from fruit with HH (11.9), respectively. Fruit pH was slightly higher in those without HH and those from 'Emphasis' or non-grafted RS. Lycopene, total sugars, citrulline, or arginine content among the grafting RS were not significantly different. Confocal micrographs from ripe heart tissue showed fewer fruit cells in watermelon exhibiting HH from non-grafted or with 'Carnivor' RS plants, and cell number was higher in fruit from 'Emphasis' RS. Cell area was largest in fruit without HH grafted to 'Emphasis' (117,100 μm^2). Fruit without HH grafted to 'Carnivor' had the smallest cell area. Our results show that grafting produced fruits with higher firmness and lower incidence of hollow heart. These results indicate that grafting may be a useful technique to reduce HH disorder in seedless watermelon cultivars susceptible to HH.

Introduction

Watermelon [*Citrullus lanatas* var. lanatus (Thunb. Matsum.and Nakai)] is a fruit of great economic importance with 457,200 metric tons produced globally (USDA, 2019a). In the U.S., seedless (triploid) watermelon cultivars make up 95% of the market (USDA, 2019b). A disorder found mostly in seedless watermelon genotypes is hollow heart (HH), which causes an internal split or void in the placental tissue (Johnson, 2014). Although there is no definitive cause of HH, multiple factors have been implicated, including watermelon genetics, pollination, pollen viability, flower bloom time, lower fruit tissue firmness and environmental stressors (Johnson, 2014, 2015; Kano, 1993).

Grafting watermelon onto squash RS has provided a means of combating soil-borne diseases and nematodes and for changing the fruit quality attributes of tissue firmness, rind thickness, lycopene, and citrulline (Davis et al., 2012). The morphological characteristics of fruit cells can affect cell wall strength, firmness of fruit, and tissue density (Kano, 1993). Tissue density is related to the number of fruit cells in the heart tissue and the subsequent cell size. Fruit with larger cells generally have lower tissue firmness (Kano, 1993; Soteriou et al., 2014), and tend to be more susceptible to HH disorder (Johnson, 2015). Grafting onto interspecific hybrid RS has been shown to increase tissue firmness in harvested fruit and may decrease the susceptibility of HH formation in triploid watermelon (Davis et al., 2012). Gaining a better understanding of tissue density via confocal microscopy can better elucidate cell morphological differences (Huitron et al., 2007) and may be useful to follow cell area and number in placental tissue of grafted and non-grafted watermelon.

The objectives of this study were to determine grafting effects on HH incidence, compositional changes, and fruit cells.

Materials and methods

Plant material and grafting

‘Liberty’ triploid (Nunhems USA Inc, Parma ID) was used as the watermelon scion. This scion was non-grafted or grafted onto the interspecific hybrid RS (*Cucurbita maxima* × *C. moschata*) ‘Carnivor’ and ‘Kazako’ (Syngenta AG, Wilmington, DE), or onto the bottle gourd (*Lagenaria siceraria)* RS ‘Emphasis’ (Syngenta AG, Wilmington, DE). ‘Liberty’ seed was sown on 24 April 2017, 7 d prior to ‘Carnivor’ and 4 d prior to ‘Kazako’ and ‘Emphasis’ RS. ‘SP-6’

(Syngenta AG, Basal Switzerland) was used as the diploid pollenizer and was sown on 16 April 2017.

A one-cotyledon graft method was utilized on 5 May 2017 following the method of Hassell et al. (2008). Grafted plants were placed into a healing chamber at a constant 27 $^{\circ}$C, with 100% humidity provided by a Trion Comfortbreeze CB777 Atomizing Hurmidifier (Trion, Sanford NC, USA). Following a 7 day graft union healing interval, the plants were held in an open wall greenhouse to harden off for 4 to 6 d prior to field planting.

Field establishment

Four watermelon beds (rows) were used, with each grafting treatment assigned to one bed. Rows were 100 m long, with 3.1 m between row spacing and 0.8 m in-row spacing for watermelon plant treatment. The rows were then split into 3 tiers, each 33.3 m long, to impose different diploid pollenizer ratios. The diploid pollenizer 'SP-6' was planted 6, 9, and 12 m apart in row (tiers 1, 2, and 3 respectively), yielding diploid:triploid pollenizer ratios of 1:5, 1:9 and 1:12. Typically a 1:4 ratio is used by growers.

Any rows with missing transplants were replanted about 7 d after planting to achieve 100% stand count. Trickle irrigation (NETAFIM, 197 ml, 0.24 gph; NETAFIM, Tel Aviv, Israel) was utilized over the course of the growing season. Fertigation started two weeks after planting and was applied weekly using a 4.5-0-9 kg/ha liquid fertilizer (Harrell's Max® Potassium plus Calcium, Lakeland, FL, USA). Crop production followed a conventional spray program (Schultheis et al., 2014) to decrease pest and weed pressure. Fruits were harvested between 64 and 78 days from transplanting.

Quality evaluation

Fruit were taken to the laboratory and fruit weight (kg) was determine with an electronic scale (Ohaus RC31P6 Counting Scale, Parsippany, NJ, USA). Fruit length (cm) from stem to blossom end and maximum fruit diameter (cm) were determined using calipers (Precise Heavy Large Vernier Caliper 40/1000MM-LC-040, Penn Tool Co., Maplewoood, NJ, USA). Length and diameter were converted to volume (cylinder) as L using the equation: $\pi hr^2*0.001$, where h is fruit length and r (radius) is fruit diameter divided by 2 and cm^3 is converted to L by multiplying by 0.001.

Fruit were then cut longitudinally from stem to blossom end and rated for the incidence and severity of HH. Hollow heart was rated on a 1-5 scale (1= no HH to minor crack and 5=

severe cavity) (USDA grading standards, 2006). Tissue firmness (N), was assessed as maximum resistance to puncture (5 mm depth) at two locations near or in heart tissue using a stationary firmness tester equipped with a Force One FDIX Digital Force Gauge (Wagner Instruments, Greenwich, CT, USA) and a 0.8 cm plunger tip (Perkins-Veazie et al., 2016). Soluble solids (°Brix) were measured with a Digital Brix Refractometer, 0 to 85% (Southern LabWare, Cumming, GA, USA). Tissue samples (100 g) were taken from the heart area, frozen, thawed, and pureed for determination of pH, soluble sugars (sucrose, fructose, and glucose), citrulline, arginine, and lycopene following methods of Fall et al. (2019).

Confocal microscopy

Fruit halves of non-grafted and grafted treatment with 'Carnivor' and 'Emphasis' rootstocks were held at 5 ºC up to 24 h to provide confocal samples. Heart tissue was extracted in 5 x 5 x 10 cm portions using a sanitized laboratory knife. Where HH was severe, tissue was excised from areas nearest the cavity. Three subsamples (10 x 10 x 2 mm) were further excised from each of the heart samples. Subsamples were steeped for 10 min in 10% calcofluor white dye (Sigma-Aldrich, St. Louis, MO, USA).

Subsamples were analyzed with a Zeiss LSM 880 Confocal workstation with Airyscan (Carl Zeiss Ag., Oberkochen, Germany). Subsamples were placed on a cell imaging dish, 170 μm, 35 x 10 mm (Eppendorf Biotech Co., Hamburg, Germany) and analyzed with 5 x 5 tile scans, z-stacking (~20 planes) and image stitching. ImageJ (Public Domain, https://imagej.nih.gov/ij/download.html) was utilized to obtain the number of cells and average surface area (μm^2) of the cells.

Data analysis

All data were analyzed using SAS 9.4 (SAS Institute, Cary, NC, USA). A one-way ANOVA was run to determine significance of diploid pollenizer distance (m), HH incidence and severity, fruit weight, tissue firmness, soluble solids, pH, lycopene, and citrulline. The relation of percent HH, tissue firmness, soluble solids and pH were determined using Pearson's correlation. A nested ANOVA was used to analyze confocal microscopy data of cell number and cell area (μm^2) and to compare cell area and cell number to HH and were subjected to Pearson's correlation. Where significance was found, separation of means was done using Tukey's honest significant difference (HSD) test at $p \leq 0.05$.

Results and Discussion

Pollenizer Spacing and Fruit Attributes

Distance from the diploid pollenizer plant (6, 9, or 12 m) did not affect the incidence or severity of HH and data were pooled to determine RS effects. The total percentage of fruit with HH differed with RS. Fruit from 'Carnivor' and 'Kazako' grafted plants had the lowest incidence of HH, with 32 and 38%, respectively (Fig 3.1). Fruit volume were lowest for 'Carnivor' compared to other RS (Table 3.1). Fruit volume was significantly increased in all watermelons with HH compared to no HH fruit (7.53 and 6.96 L), respectively. Heart tissue firmness was lower in fruit with HH compared to those without HH, averaging 16N and 18N, respectively (Fig. 3.2). Heart tissue firmness (N) in watermelons without HH differed with RS, and was highest in fruit from interspecific squash hybrids 'Carnivor' and 'Kazako' compared to non-grafted or 'Emphasis' (Fig. 3.2).

Effect of grafting and hollow heart incidence on fruit composition

Soluble solids content was lowest in fruit from 'Carnivor' grafted plants (11.7) (Fig. 3.3). Soluble solids content (ºBrix) was slightly but significantly reduced in fruit with HH (11.9) compared to those without HH (12.6). Fruit pH was higher in non-grafted or 'Emphasis' and just slightly higher in fruit with HH (Fig 3.4). A positive correlation of fruit pH to soluble solids content ($r^2 = 0.50$) was the only significant correlation found (data not shown). Lycopene, citrulline, arginine, and total sugars were similar for ripe watermelons regardless of RS or HH (Table 3.1). No differences were found in glucose or fructose concentration among fruit regardless of RS or HH incidence. Although HH incidence did not affect sucrose concentration, fruit from 'Emphasis' RS had the highest amount relative to other RS (Table 3.1).

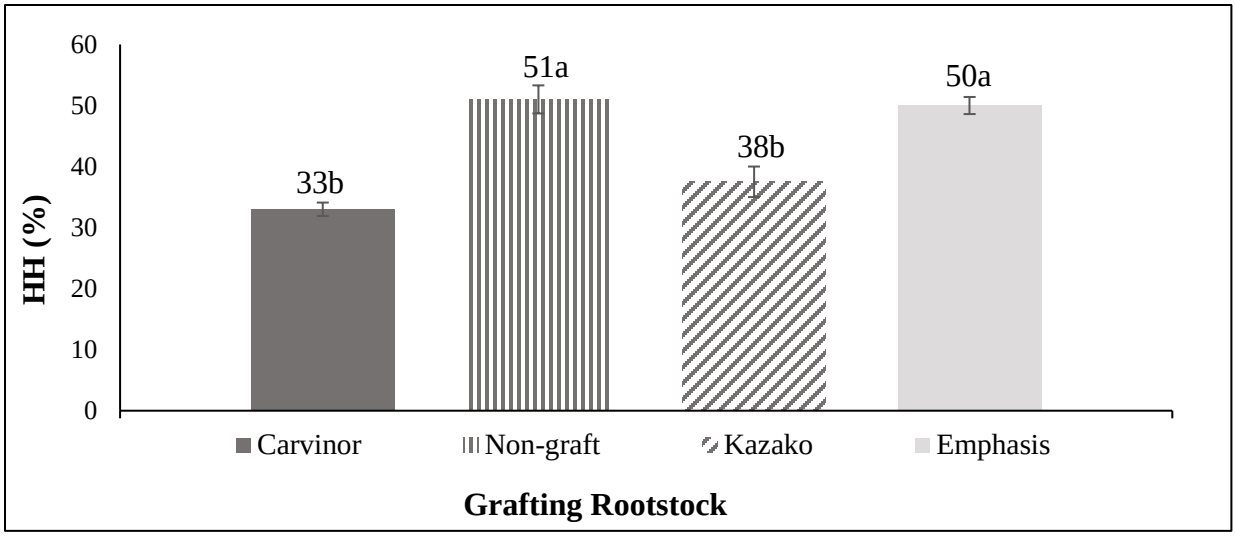

Figure 3.1. Percent (%) of watermelon fruit with hollow heart among the plants grafted with different rootstocks in comparison with non-grafted plants. Data area reported as LS-means with standard error bars. Tukey's honestly significant difference test (HSD) was done to separate the means ($p \leq 0.05$) with significant differences indicated by dissimilar letters.

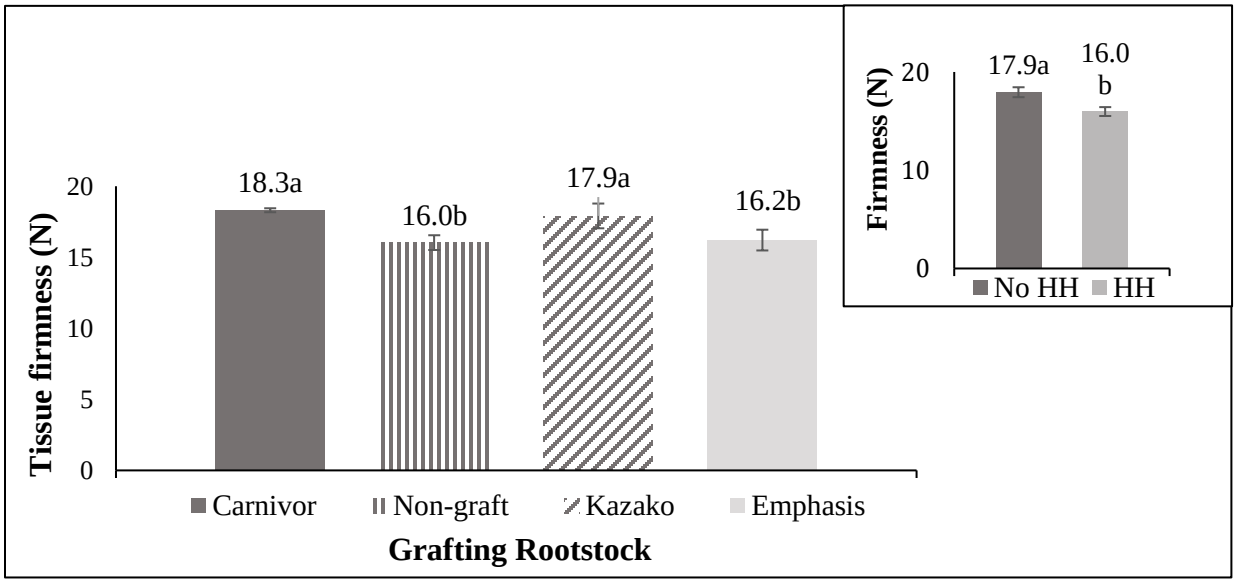

Figure 3.2. Heart tissue firmness in fruit without HH from plants grafted with different rootstocks in comparison with non-grafted plants ($p < 0.0001$) and in fruit with and without hollow heart ($p < 0.032$). Data are reported as LS-means with standard error bars. Tukey's HSD was done to separate the means ($p \leq 0.05$) with significant differences indicated by dissimilar letters.

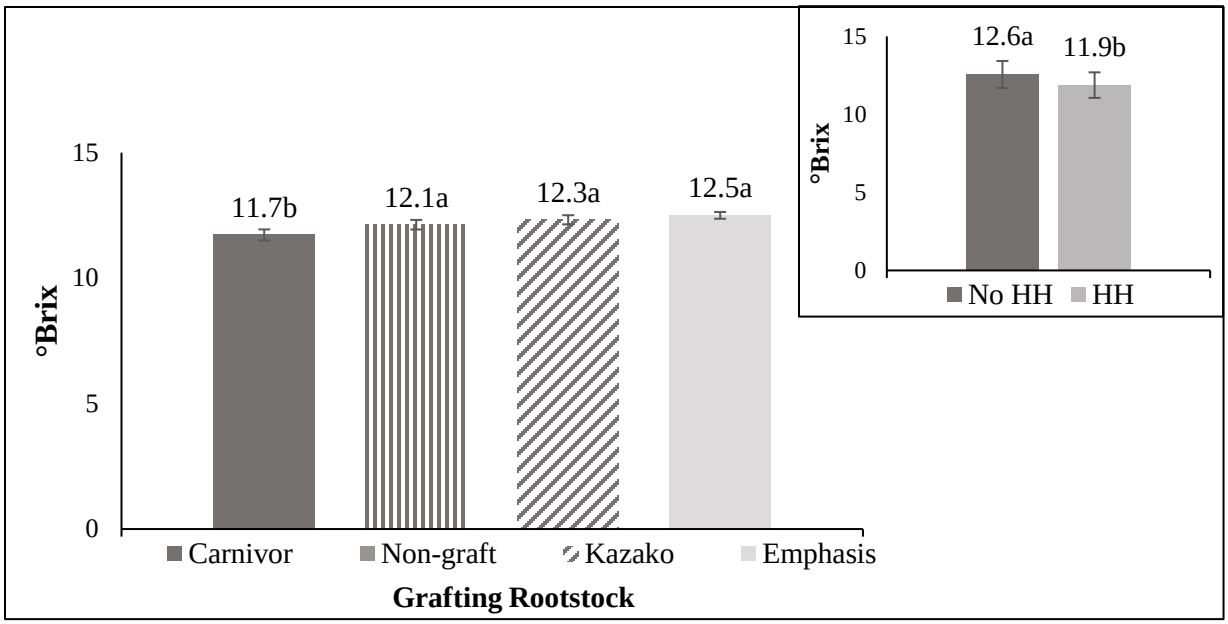

Figure 3.3. Soluble solids content (°Brix) in fruit from plants grafted with different rootstocks ($p < 0.0032$) in comparison with non-grafted plants and in fruit with and without hollow heart ($p < 0.0412$). Data are reported as LS-means with standard error bars and mean separation was done using Tukey's HSD ($p \leq 0.05$) with significant differences indicated by dissimilar letters.

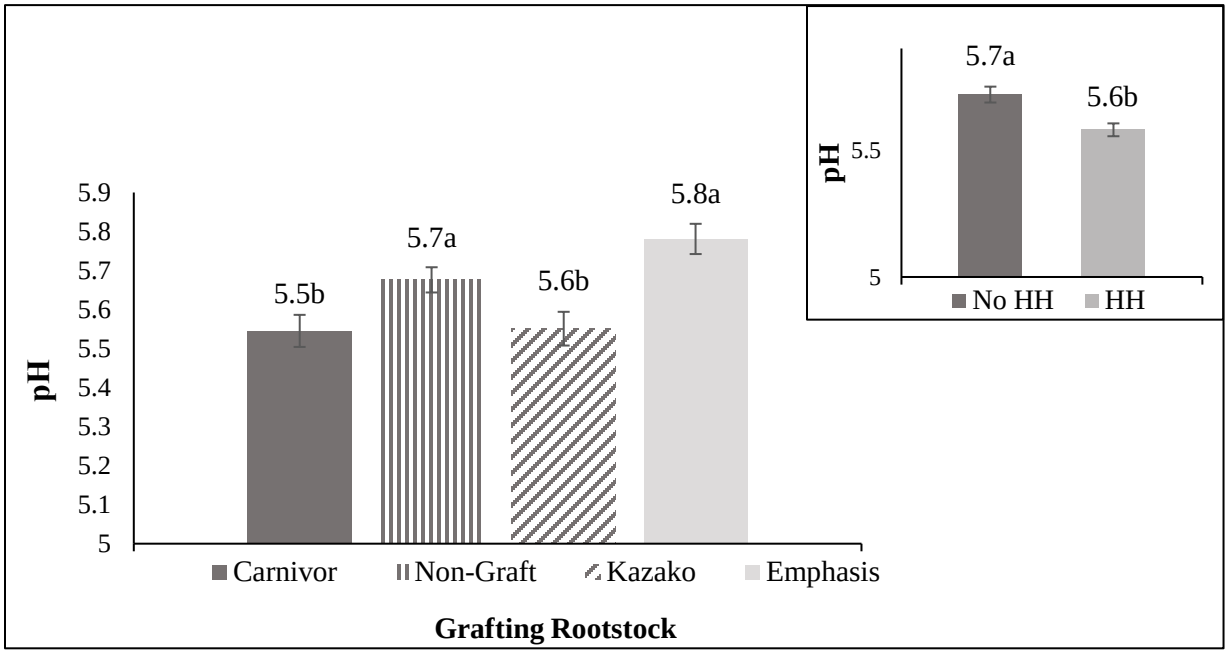

Figure 3.4. Fruit pH of grafted treatments with rootstocks compared to non-grafted plants and in fruit across rootstocks ($p < 0.0418$) with and without hollow heart ($p < 0.0132$). Values represent LS-means ± standard error bars and mean separation was done using Tukey's HSD ($p \leq 0.05$) with significant differences indicated by dissimilar letters.

Table 3.1. Fruit quality and composition among the treatments grafted with different rootstocks in comparison with non-grafted plants.

Measurement	Non-grafted	'Carnivor'	'Kazako'	'Emphasis'	p-value
Weight (kg·fruit^{-1})	7.0 ± 0.23a	5.7 ± 0.4a	6.8 ± 0.4a	6.7 ± 0.4a	0.5290
Volume (L)	7.8 ± 0.7a	5.7 ± 0.5b	7.2 ± 0.6b	7.8 ± 0.8a	0.0421
Composition					
Lycopene (mg·kg^{-1})	50.5 ± 1.3a	52.2 ± 2.0a	54.3 ± 1.9a	53.7 ± 1.3a	0.1315
Arginine (g·kg^{-1})	1.06 ± 0.41a	0.98 ± 0.49a	1.01 ± 0.54a	0.93 ± 0.06a	0.2335
Citrulline (g·kg^{-1})	2.92 ± 0.15a	2.86 ± 0.12a	3.07 ± 0.17a	2.74 ± 0.12a	0.7776
Total sugars (mg·g^{-1})	62.9 ± 8.4a	66.7 ± 6.1a	67.9 ± 6.1a	68.6 ± 4.9a	0.3211
%sucrose	43.1 ± 2.1b	46.5 ± 2.8b	44.9 ± 2.3b	52.7 ± 2.1a	0.0322
%glucose	17.9 ± 1.0a	18.0 ± 1.2a	18.8 ± 1.1a	15.1 ± 1a	0.4654
%fructose	35.3 ± 1.7a	35.3 ± 1.7a	35.8 ± 1.4a	32.4 ±1.2a	0.1746

Values represent LS-means ± standard error. Means separated within rows using Tukey's HSD, $p \leq 0.05$, with differences indicated by different letters.

Confocal microscopy results. Cell number did not differ among RS or HH severity ($p>0.05$). Although, the interaction of RS and HH indicated cell number was lowest in fruit from 'Carnivor' with moderate to severe HH and in non-graft fruit with moderate HH. Cell number was highest in fruit from 'Emphasis' with severe HH (Table 3.2). Cell size was largest in fruit from 'Emphasis' (mean of 108.2 x 10^3 μm^2). Fruit with severe HH from 'Carnivor' and non-graft RS had larger cell areas. Cell number was inversely correlated to cell size ($r^2 = -0.8598$, $p < 0.001$).

Table 3.2. Confocal microscopy data of fruit heart cell number and size among the grafting treatments with different rootstocks in comparison with non-grafted plants and at varying levels of hollow heart.[1]

Rootstock	Hollow Heart severity	Number of Cells (5x5 mm tile)	Size of cells ($\mu m^2 x 10^3$)
'Carnivor'	None	279 ± 20a	92.7 ± 11.2b
	Moderate	261 ± 35a	97.7 ± 8.0b
	Severe	255 ± 4a	108.8 ± 6.9a
	Mean	266A	99.7A
Non-graft	None	272 ± 56a	94.3 ± 6.8b
	Moderate	251 ±35a	103.3 ± 6.6a
	Severe	-	-
	Mean	263A	99.1A
'Emphasis'	None	240 ± 18a	117.1 ± 7.4a
	Moderate	228 ± 21a	115.5 ± 6.8a
	Severe	276 ± 40a	91.9 ± 6.8b
	Mean	248A	108.2A
p-value (HH severity)		0.1280	0.0001
p-value (RS)		0.4305	0.4194
p-value (RS*HH)		0.4380	0.0001

[1]Significance of HH severity on number or size of cells within rootstock is indicated by differences in small letters using Tukey's HSD test at $p \leq 0.05$. Significance of cell number and size across rootstocks is indicated by differences in capital letters using Tukey's HSD test ($p \leq 0.05$).

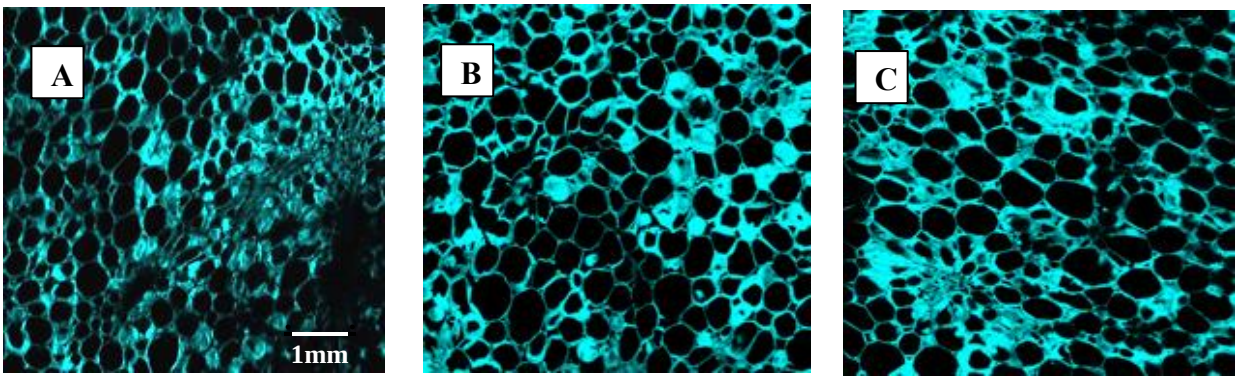

Figure 3.5. Confocal micrographs of non-graft (A), 'Carnivor' (B) and 'Emphasis' (C) grafting treatments with and without hollow heart.

Triploid watermelon does not produce sufficient viable pollen and requires diploid (seeded) pollen sources (Maynard, 1992). Generally, between 25-33% of a field needs to be planted with diploids to achieve fruit set and high quality fruit (Freeman and Olson, 2007). Our study showed no pollenizer spacing effect on the incidence of HH where the average percentage

of diploid pollenizers was 13% (below the 25% threshold). This result suggests that lowering the amount of diploid pollenizers/viable pollen below 25% may not induce additional HH.

Among the grafting treatments, HH incidence was reduced by 25-30% in fruit from the interspecific hybrid RS 'Carnivor' and 'Kazako' compared to non-grafted fruit (Fig 3.2). Fruit firmness of 'Carnivor' and 'Kazako' was increased by 1 N compared to non-grafted fruit. Across all HH severities, fruit volume was smallest in fruit from 'Carnivor' and in fruit without HH. Researchers have hypothesized that fruit with lower tissue firmness are often more affected by internal fruit disorders compared to dense fruit types (Johnson, 2014; 2015) and our study supports this hypothesis. Fruit cells expressing HH are thought to have uneven tissue expansion of flesh and rind during fruit growth, causing larger volume fruit with lower cell density leading to lower tissue firmness (Kano, 1993). Alternatively, the interspecific squash hybrid RS may alter cell wall composition, slowing the rate of cell growth and equalizing relative rates of cell expansion in flesh and rind tissues.

In this study, moderate infestation with root-knot nematode was found in 'Carnivor' and 'Kazako' grafted plant roots, which reduced relative fruit dimensions (Table 3.1) and can decrease soluble solids content (Liu et al., 2015). Total sugar content or relative amounts of glucose and fructose did not differ with RS or with HH. Sucrose was the dominant soluble sugar and was highest in fruit from 'Emphasis' but was similar with HH incidence. In ripening watermelon, fruit pH tends to increase after soluble solids content and lycopene development (Corey and Schlimme, 1988). Fruit from the interspecific squash RS 'Carnivor' and 'Kazako' were lowest in pH, similar to results of Soteriou et al. (2014), and in fruit with HH (Fig. 3.4). Grafting to the interspecific hybrid RS has been shown to slow ripening (Fallik et al., 2014) and it is possible that fruit with HH also have slightly delayed ripening.

Confocal microscopy was utilized as a means of assessing watermelon flesh density and its relationship to firmness and HH (Fig 3.5). The HH disorder is thought to be related to rapid and irregular fruit growth, lowering cell density (fewer cells per unit and increased cell area) (Johnson, 2015; Kano, 1993). Soteriou et al. (2017) reported that fruit grafted onto squash RS had increased tissue firmness and cell number and decreased cell area. In our study, confocal micrographs indicated cell area decreased with increasing HH severity in fruit when grown without grafting or on 'Carnivor' RS; but was the opposite for fruit from 'Emphasis' (*Laginaria siceraria*) and may be due to the generally lower fruit density.

Conclusion

In this study, we were able to effectively induce HH in triploid watermelon by utilizing a susceptible scion and decreasing pollinizing plants. Soluble solids content was slightly higher and pH slightly lower in fruit with HH. The size of fruit cells deceased and number of cells increased with interspecific hybrid RS, however, confocal microscopy data from ‘Emphasis’ was inconclusive. Grafting onto interspecific squash hybrid RS of ‘Carnivor’ and ‘Kazako’ increased tissue firmness and decreased HH incidence. This technique provides a means to combat the disorder if growing susceptible triploid cultivars.

References

1. Corey, K.A. and D.V. Schlimme. 1988. Relationship of rind gloss and groundspot color to flesh quality of watermelon fruits during maturation. Sci. Hortic. 34:11-214.

2. Davis, A.R., P. Perkins-Veazie, Y. Sakata, S. Lopez-Galarza, J.V. Maroto, S.G. Lee, Y.C. Huh, Z. Sun, A. Miguel, S.R. King, R Cohen, and J.M. Lee. 2012. Cucurbit grafting. Cr. Rev. Plant Sci. 27:50-74.

3. Fall, L.A., P. Perkins-Veazie, G. Ma and C. McGregor. 2019. QTLs associated with flesh quality traits in an elite x elite watermelon population. Euphytica 215:xx-xx.

4. Fallik, E. and Z. Ilic. 2014. Grafted vegetables – The influence of rootstock and scion on postharvest quality. Folia Hortic. 26:79-90.

5. Freeman, J. and S. Olson. 2007. Characteristics of watermelon pollinizer cultivars for use in triploid production. Intl. J. Vegetable Sci. 13:73-78.

6. Hassell, R., F. Memmott and D.G. Liere. 2008. Grafting methods for watermelon production. Hort 43:1677-1679.

7. Huitron, M.V., M. Diaz, F. Dianez and F. Camacho. 2007. Texture of fresh fruit. Hortic. Rev. 20:121-224.

8. Johnson, G. 2014. These beautiful watermelon patterns are driving everyone crazy. [Online]. https://www.boredpanda.com/weird-watermelons-beautiful-hollow-heart/

9. Johnson, G. 2015. Research finds potential cause of hollow heart disorder in watermelon. PhysOrg. [Online]. https://phys.org/news/2015-06-potential-hollow-heart-disorder-watermelons.html

10. Kano, Y. 1993. Relationship between the occurrence of hollowing in watermelon and the size and the number of fruit cells and intercellular air space. J. Japan Soc. Hortic. Sci. 62:103-112

11. Liu, B., J. Ren, Y. Zhang, J. An, M. Chen, H. Chen, C. Xu and H. Ren. 2015. A new grafted rootstock against root-knot nematode for cucumber, melon and watermelon. Agron. Sustain. Dev. 35:251-259.

12. Perkins-Veazie, P., J. Lotito, R. Hassell. 2016. Development of a firmness tester designed for large watermelon. HortScience S250.

13. Rimando, A.M. and P. Perkins-Veazie. 2005. Determination of citrulline in watermelon rind. J Chromatogr A. 1078:196-200.

14. Schultheis, J.R. and B. Thompson. 2014. North Carolina State University Watermelon Cultivar Trials. No. 210. Pp 1-39. [Online]. https://gates.ces.ncsu.edu/wp-content/uploads/2015/01/NCSU-Watermelon-Cultivar-Booklet_2014.pdf?fwd=no

15. Soteriou, G.A., M.C. Kyriacou, A.S. Simons, and D. Gerasopoulos. 2014. Evolution of watermelon fruit physicochemical and phytochemical composition during ripening as affected by grafting. J. Food Chem. 165:282-289.

16. Soteriou, G.A., A.S. Siomos, D. Gerasopoulous, Y. Rouphael, S. Georgiadou, and M.K. Kyriacou. 2017. Biochemical and histological contributions to textural changes in watermelon fruit modulated by grafting. J. Food Chem. 237:133-140.

17. USDA. 2019a. Agricultural Marketing Service. National Watermelon Report. [Online]. https://www.ams.usda.gov/mnreports/fvdtvmelon.pdf

18. USDA. 2019b. Specialty Crop Market News. Seeded and Seedless Watermelon Production. [Online]. https://www.ams.usda.gov/mnreports/wa_fv456.txt

CHAPTER 4

METHOD DEVELOPMENT FOR CELL WALL EXTRACTION TO ANALYZE PECTIC POLYSACCHARIDES AND TOTAL PECTIN IN WATERMELON

Abstract

Understanding the differences that occur in watermelon cell wall polysaccharides can help researchers answer questions regarding postharvest quality of the fruit. Cell walls are highly complex, composed of polysaccharides including cellulose, hemicellulose and pectin. Enzymatic hydrolysis (endo-polygalacturonase) has been used to depolymerize cell walls prior to pectin fraction extraction and quantification of matrix glycans (e.g., xylogalacturonan monomers). To date, full pectin assembly has not been done on watermelon flesh tissue, although a detailed protocol were published for Arabidopsis and methods can be adapted for use on watermelon flesh tissue. The objectives of this research were to apply and optimize pectin extraction and cell wall polysaccharide composition methods to watermelon placental tissue A randomized complete block design was set up to develop optimal hydrolysis and alcohol insoluble residue (AIR) grinding conditions for cell wall polysaccharide analysis. Watermelon placental tissue was frozen in liquid nitrogen, packed into 50 mL test tubes and ground with or without 80% ethanol in a bead homogenizer, followed by methanol and acetone rinses to yield AIR. Hydrolysis optimization consisted of 63, 126, 189, and 252 μL of 72% sulfuric acid applied to ~3-5 mg AIR in 2 ml vials with seals. AIR samples were re-ground with 6 x 2.8 mm steel balls in a bead mill homogenizer for 0, 30, 60, or 90 seconds prior to acid hydrolysis. A subset of re-ground AIRs were analyzed for particle size. Total sugar content was used as a measure of the effectiveness of the acid hydrolysis and AIR re-grinding treatments. The total sugar yield was highest with 126 or 252 μL sulfuric acid addition to AIR. Variability among replicates was high in samples with the highest volume of acid (252 μL), indicating possible monomer break down. These results showed that at least 126 μL sulfuric acid is needed for complete hydrolysis of 3 mg watermelon AIR. Re-grinding AIR for 60 seconds resulted in smaller particle size (55.3 μm) and higher total sugars (2.28 nmole·mg^{-1}). Unlike Arabidopsis, watermelon AIR requires re-grinding to achieve proper particle size for hydrolysis. Increasing the amount of 72% sulfuric acid applied to watermelon was critical to achieve full hydrolysis. Applying these adapted methods for hydrolysis and methylation analysis enabled quantification of 12 neutral sugars and linkage assembly of watermelon cell wall polysaccharides.

Introduction

The plant cell wall is highly complex as it is dynamic and continually changing through growth and development. For example, as fruit start to mature, cell expansion begins and intercellular spaces fill with air, and tissue firmness and cell density change. Brummell (2006) states that the cell wall is crucial for internal fruit qualities, and disassembly or degradation is responsible for diminishing crop qualities (e.g., softening of fruit tissues). Plant cell wall composition varies depending on both crop and type of plant tissue (Pettolino et al., 2012). Cell wall composition includes structural proteins, polysaccharides, and aromatic and aliphatic compounds (Caffal and Mohnen, 2009). The primary cell wall is composed primarily of polysaccharides (90% dry weight) (Mohnen, 2008), which are associated via covalent and non-covalent bonding (Caffal and Mohnen, 2009). Plants also have secondary cell walls, which are not usually found in appreciable amounts in vegetables and fleshy fruits like watermelon. Instead, the secondary cell wall is associated more with high lignin plants, and is deposited on the primary cell wall in vegetables like asparagus or celery as well as woody plants (Taylor, 2006).

The main polysaccharide components of the primary cell wall include cellulose, hemicellulose and pectin. The cell wall is thought to be composed of two separate interconnected networks-a pectin network and hemicellulose/cellulose network (Cosgrove, 2005). Pectin has long been thought to be important in load-bearing cell wall structures and increasing evidence supports this conclusion (Hofte et al., 2012). Pectins act as the glue between the cellulose/hemicellulosic network and aid in cell wall strength, communication, adherence and internal flesh qualities (Karakurt et al., 2008). Cell wall degradation starts with an enzymatic attack of the glycosydic bonds of pectin (Karakurt and Huber, 2008).

Flesh firmness was increased in grafted watermelon and observed to be lower in flesh of fruit with hollow heart disorder (refer to Chapters 2 and 3). The differences in grafted fruit and fruit with HH are hypothesized to be related to differences in pectic architecture and assembly. Pectin is the more likely target because the hemicellulose and cellulose network are less inclined to enzymatic degradation and are less associated with cell wall load-bearing (Broxterman and Schols, 2018). To date, cell wall components and the exact nature of their interactions are still unknown (Broxterman and Schols, 2018). However, Pettolino et al. (2012) was able to develop qualitative methods to analyze the composition and linkages of cell wall pectic polysaccharides.

The methods were developed for Arabidopsis leaves, which differ considerably compared to cucurbit fruit. Thus, method optimization is crucial to achieve pectin extraction in watermelon placental tissue.

Background on methodology and GC-MS

To distinguish various small and volatile compounds, gas chromatography mass spectrometry (GC-MS) is a preferred analytical technique. GC-MS begins with gas chromatography, where the sample is volatized (Gates, 2008). The sample then becomes vaporized (the gas phase) and its various components are separated using a capillary column coated with a stationary phase. The components elute from the column at different times, allowing for different compounds to be identified via their retention times. Once the compounds leave the column, they are ionized and separated based on their (*m/z*) ratios or mass spectra (Gates, 2008). For the purpose of exploring watermelon cell wall polysaccharides, various wet chemistry steps are done to produce small, monomeric building blocks that are chemically derivatized to produce volatile compounds suitable for GC-MS analysis. Due to the size of the compounds being identified (monosaccharides) and complexity of the chemistry, GC-MS provides a means to properly identify watermelon cell wall constituents.

Methods for preparing and fractionating plant cell walls range from rapid alcohol-insoluble residues (AIR) to more complicated detergent- and salt-containing aqueous buffer extractions (Pettolino et al., 2012). For the purpose of watermelon cell wall extraction, AIRs were prepared via mass spectrophotometer grade solvent extraction to yield well defined chromatograms.

Carboxyl reduction is a key step in preparing cell wall material for analysis following collection of AIR. Watermelon mesocarp cells have galacturonic acid (uronic acid) and this interferes with colorimetric assays. Glycosidic linkages are adjacent to the uronic acids and do not hydrolyze efficiently unless the uronic acid residues are reduced (Kim and Carpita, 1992). The carboxylic esters are first reduced with sodium borodeuteride and generate 6,6'-dideuterio-sugars, then free uronic acids are activated by carbodiimide and reduced again via sodium borodueteride and hydride. These dideuterio sugars are distinguished from neutral sugars via GC-MS by the presence of a fragment ion with increased quant masses ($M^+ + 2$) (Pettolino et al., 2012). Alditol acetates are generated after carboxyl reduction and hydrolysis of polysaccharides to monomeric building blocks. Acetylation is a crucial step for monosaccharide identification by

GC-MS. Carboxyl reduction steps are critical to this experiment as the split samples will be used to deduce neutral sugar concentration, degree of methylation and uronic acid (galacturonic and glucuronic) acid concentrations. Therefore, it is extremely important to handle samples quantitatively as the dideuterio alditol acetates will be compared to the singly deuterated alditol acetates to calculate degree of methylation.

Methylation analysis is used for elucidation of polysaccharide structure. Methylation allows for the identification of linkage residues in the cell wall which is critical when calculating relative amounts of polysaccharide classes. The resulting partially methylated alditol acetates can be separated, identified and quantified via the GC-MS. The linkage positions of each sugar will be apparent by use of their relative retention times (rrt) and mass spectral data compared to the Complex Carbohydrate Research Database (Georgia, USA). Methylation principles follow those developed by Ciucanu and Kerek (1998) in order to generate a cleaner chromatogram. A perfect methylation of branched of substituted polysaccharides will have terminal-to-branch point ratios at approximately 1:1. One disadvantage to methylation via GC-MS analysis is that the polysaccharides may be inadequately solubilized and under methylated (Pettolino et al., 2012). Failure to fully methylate the polysaccharides will lead to issues identifying linkage residues and inability to fully characterize polysaccharide classes. Polysaccharide composition estimation occurs by obtaining monosaccharide building blocks and linkage compositions using GC-MS. The monosaccharide information can be used to group linkages into polysaccharide classes and it also enables common linkage derivatives that are found in different polysaccharide classes (e.g., 4-GalA(p) is found in both rhamnogalacturonan I and homogalacturonan) to be properly calculated for the different classes.

Advantages of GC-MS

GC-MS offers very good sensitivity and instrumentation is reliable, rugged and user friendly. When run as a full scan analysis, the data acquisition is non-targeted. This means that the researcher will gain a response from any compound that gets into the MS, ionizes and falls into the selected mass range. Multiple other methods use only targeted analytes, meaning molecules can be missed, particularly if the researcher doesn't know exactly what they are looking for (Worrell and Newton, 2004). For cell wall composition, this distinction is important due to the inherent complexity of the polysaccharide linkages.

Quantitative cell wall analysis

Understanding pectin and cell wall metabolism is challenging due to the complex molecular structures and difficulty in assembling the arrangement of polysaccharides. As previously mentioned, Pettolino et al. (2012) was able to develop qualitative methods to analyze cell wall pectic polysaccharides. The methods were developed for Arabidopsis, which is very different than the cucurbit family with respect to tissue type. Thus, method optimization is crucial to achieve pectin extraction in watermelon placental tissue.

Understanding the differences that occur in watermelon cell wall polysaccharides can help researchers answer many questions regarding postharvest quality of the fruit (Petkowicz et al., 2016). Cell wall structure and network interactions were determined using a series of chemical methods and extraction protocols to hydrolyze cell wall fibers, followed by identification and quantification of the monosaccharide molecules (Pettolino et al. 2012). This approach required some means of optimization for a successful quantitative analysis of cell wall constituents.

Grinding and particle size

The first step of cell wall preparation is grinding of the plant sample. In this step, temperature during preparation and type and degree of grinding can greatly affect results (Pettolino et al., 2012). Keeping samples at or below 4 ºC during grinding helps stop enzymatic degradation (Pettolino et al., 2016). Broxterman and Schols (2018) applied microwave heating to tomato to stop enzymatic degradation of pectinases. Keeping samples cold through use of -80 ºC stored samples and preparation with liquid N is probably the simpler of these two methods. Samples too coarsely ground or homogenized will contain a lot more intracellular material, which is difficult to remove and can cause contamination to the sample (Pettolino et al. 2012).

Broxterman and Schols (2018) prepared alcohol insoluble residues from carrot, strawberry, or microwaved tomato by blending 400 g in a 1:3 w/v ratio in 96% ethanol. Samples were then milled for 30 seconds in a Retch Cryomill MM440 at a frequency of 20 Hz to obtain a homogeneous material. To further study the effect of milling on sample hydrolysis, Broxterman and Schols (2018) milled samples at 0 sec, 30 sec, 15 min, 45 min and 90 min in 96% ethanol. Samples were filtered and the residue was washed with 70% ethanol and dried. Their research showed that increased milling time resulted in decreased average particle size (or molecular weight of the sample particles). A plateau was found after 15 min grinding in all three tissue

types (strawberry, tomato and carrot), indicating that milling time of 15 min or more led to depolymerization of polysaccharides to ~10 kDa, thus increasing subsequent sample hydrolysis when using 72% sulfuric acid.

It would be most helpful to have a means to look at particle size before proceeding with hydrolysis and derivatization steps. Some researchers have attempted to estimate particles using methods that are relatively simple to those that are complex. Mesh or nylon screens were used to control size and uniformity of particles from woody/lignified samples (sugar maple, Arabidopsis and wheat straw). Screen mesh sizes ranged from 0.4 mm for freeze dried sweet potato to 10 mm for sugar maple (Willfor et al., 2009; Lareo et al., 2013).

Blankenly et al. (1983) determined that the particle size Italian ryegrass was 0.62×10^7 nm^2 using electron microscopy. Also, grinding of the plant sample followed by re-grinding of alcohol insoluble residues with mortar and pestle was done by McFeeters et al. (1984) to achieve a smaller particle size. Key points for grinding include selection of appropriate mechanism, speed of grinding, grinding time, and ball size and volume of container relative to sample size. Particles need to be small to enhance surface area for reaction with acid in the hydrolysis steps.

Hydrolysis of cell wall polysaccharides

Monosaccharide analysis is helpful in the characterization of cell wall polysaccharides. The qualitative and quantitative analysis of sugars is based on the monosaccharides released from polysaccharide structure (Wang et al., 2018). Acid hydrolysis is a critical step to disperse acid into the polysaccharides ultimately cleaving glycosidic bonds. This reaction breaks long complex chains into short fractions leaving behind the backbone structures for further identification via GC-MS, HPAEC or Maldi-TOF (Al-Dulaimi et al., 2015; Pettolino et al., 2012). The most commonly used hydrolysis acids are triflouroacetic acid, maleic acid, hydrochloric acid and sulfuric acid (Al-Dulaimi et al., 2015; Pettolino et al., 2012, Broxterman and Schols, 2018). Trifluoroacetic acid hydrolysis was commonly used as a ‘routine’ method for monosaccharide release from soluble polysaccharides (e.g., total pectin fractions or secreted polysaccharides). The release of monosaccharides heavily depends on the cleavage/hydrolysis of glycosidic bonds (Haranzo et al. 2011) and sulfuric acid (Saeman hydrolysis) is used for more complex polysaccharides from intact cell walls (e.g., AIR from watermelon flesh).

Saeman hydrolysis is a widely used procedure utilized to breakdown intact cellulose, hemicellulose and pectin using a strong acid. Sulfuric acid hydrolysis is used for intact cell walls

coming straight from the plant or sample material. A concentrated sulfuric acid solution is generally directly applied to the prepared cell wall followed by a second hydrolysis step incorporating diluted sulfuric acid (Saeman et al., 1954). To aid hydrolysis, the sample will generally be placed into an oven or autoclave ranging from 85-121 $^{\circ}$C for one to four hours (Pettolino et al., 2016; Jung et al., 2012; Broxterman and Schols 2018).

Crop-specific hydrolysis experiments

Jung et al. (2012), prepared stover corn samples with 80% (vol/vol) alcohol to yield 200 mg alcohol insoluble residues samples. The residues were then treated with concentrated sulfuric acid solution (12 M) at room temperature for 3 hour. The acid was then diluted to 0.4 M and samples were autoclaved at 121 ºC. Neutral sugar polysaccharide components (glucose, xylose, arabinose, galactose, mannose, rhamnose, and fucose) were measured by gas chromatography as alditol acetates. Total uronic acids were measured in an aliquot of the dilute acid solution by colorimetry. The stover sample set showed large variation in neutral sugar concentrations from sample to sample.

Al-Dulaimi et al. (2015) utilized sulfuric acid hydrolysis on nanocrystalline cellulose which was treated with 58% (wt/wt) sulfuric acid concentration at four time periods (40, 60, 80 and 100 min) and at a fixed temperature of 45 ºC. The acid/cellulose ratio was 1 part acid to 12 parts cellulose (1:12). His results indicated no significant hydrolysis changes after 60 min of reaction time at 45 ºC. Hu et al. (2010) used sugar maple wood as the sample matrix. The hydrolysis was performed at three temperatures treatments of 85 ºC, 95 ºC and 105 ºC, with 15%, 31% and 62% concentrated sulfuric acid at each temperature. Samples were collected at 2, 5, 10, 15, 20, 30, 50, 80, 120 and 180 min, respectively. Hu found that xylose concentration generally increased with increased hydrolysis time, temperature (105 ºC) and concentration (62%). The addition of 62% sulfuric acid yielded the highest concentration of xylose. At higher sulfuric acid concentrations (31% and 62%) the xylose monomer initially increased with increased hydrolysis time at 105 ºC, and then leveled off (or had a small reduction) after 120 mins of the reaction. In contrast, the addition of 15% sulfuric acid caused increased xylose concentrations over the 3 h of hydrolysis, suggesting that using lower concentrations of sulfuric acid will need longer hydrolysis times.

Blankenly et al. (1983) obtained monosaccharides and alditols from two sources, commercial sources used as the control and plant cell walls of Italian ryegrass as the sample

matrix. Ryegrass samples were prepared separately from commercial sources and were ground by two passages through a 'French pressure-mill' to particle size 0.62 x 10^7 nm^2 then collected and washed with ethanol, methanol, and pentane. Alcohol insoluble residues were collected on nylon mesh (10 μm pore size) and dried. The cell wall residues (10 mg samples) were then treated with 72% sulfuric acid solution (125 microliter/sample). Samples were flushed with argon gas and fitted with Teflon-lined caps then vortexed intermittently for 45 min at room temperature. After 45 min the acid was diluted to 1 M by adding 1.35 mL di-water to each sample and were heated under argon at; a) 1 hr, 121ºC b) 2 hr, 120 ºC and c) 3 hr, 100 ºC. Hydrolysis at 120 ºC resulted in the lowest recovery of arabinose and xylose. In contrast, 93% of monosaccharides were recovered after hydrolysis for 3 hr at 100 ºC in both commercial and ryegrass samples, respectively.

Broxterman and Schols (2018) sequentially extracted pectic fractions from carrots, strawberry and tomato. A preparation of alcohol insoluble residues was done first, then were sequentially extracted into water soluble, chelate soluble and alkali soluble fractions. Fractions were collected and dried, then treated with 72% (w/w) sulfuric acid for one hour at 30 °C, followed by hydrolysis with 1 M sulfuric acid at 100 °C for 3 hours. Grinding time of material was done prior to pectin extraction (samples were milled at 0 sec, 30 sec, 15 min, 45 min and 90 min in 96% ethanol). Isolation of cell wall material occurred by use of Saemen hydrolysis via application of 72% sulfuric acid to hydrolyze the cell wall into monomeric building blocks. Carrot monosaccharide concentrations were comprised of 8 mol% arabinose, 1 mol% rhamnose, ~20 mol%, galactose, ~30 mol% glucose, 2 mol% xylose and 5 mol% mannose, respectively. Similar concentrations were found in strawberry and tomato for most monosaccharides; however, tomato had a lower relative concentration of galactose at 8 mol% and higher glucose at 42 mol%, respectively.

Determining effective grinding and hydrolysis by total sugars assay

Estimation of effective grinding and hydrolysis steps can be done by determining total sugar composition. This can be done with relatively general tests, such as a colorimetric protocol, or with more extensive methods involving derivatization and analysis with GC, HPAEC, or MS.

Li et al., (2018) performed acid hydrolysis to determine total sugar composition on sorghum juice extract. Juice (20 μL sample) was hydrolyzed with 100 μL of concentrated

sulfuric acid and incubated at 95 °C for 15 min followed by 25 °C for 5 min. Phenol (20 μL of 2% (v/v)) was added to each well, fully mixed and transferred to a 96-well microplate. The absorbance values were measured at 490 nm using a Sunrise microplate reader after shaking the plate for 10 min and resting for 5 min. The standard curve for each plate was calculated by averaging the absorbance values of the three technical replicates. The total sugar concentration in sorghum juice extracts was calculated from the standard curve.

This total sugar assay has several challenges. First, there is a possibility that dilutions will be needed as the linear range for the phenol-sulfuric acid assay is 0–1 $\mu g \cdot \mu L^{-1}$ of glucose and it will be important to identify the total sugar content for watermelon. If the total sugar concentration of watermelon exceeds that of 1 $\mu g \cdot \mu L^{-1}$, a dilution will be needed for accurate quantification. Another challenge is to choose an appropriate sugar for the standard curve. Cell walls of different crops can be composed of higher concentrations of galactose or glucose. It is important to choose the monomer in highest concentration to give a more robust conclusion about total sugars in the cell wall. Li et al. (2018) recommends that the most representative carbohydrate in the measured samples should be used as the standard.

Optimization objectives for quantitative cell wall polysaccharide composition analysis in watermelon

1. Test various grinding times and ball mill sizes on fresh watermelon flesh to achieve proper particle size.
2. Optimize the amount of sulfuric acid for seaman hydrolysis to achieve complete hydrolysis of cell wall polysaccharides to produce monomeric building blocks.
3. Apply the optimized grinding and hydrolysis methods to the cell wall protocol from Pettolino et al. (2012).

Objective 1- Grinding and ball mill size

Heart tissue samples (10 g) were cut from commercially available triploid watermelon, frozen with liquid N, and held at -80 ºC until grinding. Frozen watermelon was placed into plastic conical test tubes (50 mL, Falcon, VWR) and variables of time, ball size steel balls magnetic, high carbon (4RJH5) (Grainger, Lake Forest, IL), and 80% HPLC grade ethanol evaluated for grinding (Table 4.1). All samples were immersed in liquid N for 15-20 sec, transferred to a cold aluminum block, and ground at 1,200 strokes$\cdot$min^{-1} with a Geno/Grinder (Model SN 10592, SPEX, NJ).

Heart tissue samples (10 g) were cut from commercially available triploid watermelon, frozen with liquid N, and held at -80 ºC until grinding. Frozen watermelon was placed into Falcon conical test tubes (50 mL) and grinding levels were tested. Frozen watermelon samples were ground using several grinding treatments: 1) 3 x 9 mm steel balls magnetic, high carbon (4RJH5) (Grainger, Lake Forest, IL) for 15 min at 1200 strokes, 2) 4 x 6.5 mm steel balls for 12 min at 1,200 strokes and 3) 6 x 5 mm steel balls at 1,200 strokes for 12 min. A second set of watermelon samples were ground in 10 mL of 80% ethanol held at 4 ºC with the following grinding treatments; 1) 3 x 9 for 12 min at 1200 strokes $\cdot min^{-1}$, 2) 4 x 6.5 mm steel balls magnetic, high carbon for 8 min at 1,200 strokes and 3) 6 x 5 mm steel balls magnetic, high carbon at 1,200 strokes$\cdot min^{-1}$ for 8 min. All samples were dropped in liquid N for 15-20 sec, transferred to a cold aluminum block, and ground at 1,200 strokes$\cdot min^{-1}$ with a Geno/Grinder (Model SN 10592, SPEX, NJ).

Results for cell wall disruption

All watermelon samples ground without 80% ethanol had temperatures higher than 4 $^{\circ}$C after 6 min of grinding, while samples ground in ethanol held temperatures at or below 4 $^{\circ}$C. The increased temperature in the absence of ethanol indicates that grinding in 80% ethanol is preferred to keep watermelon tissue temperatures below 4 ºC, decreasing the chances of enzymatic degradation of the samples.

All samples ground with 9 mm steel balls were contaminated or lost as the steel balls broke the falcon test tubes. Samples ground in 80% ethanol with either four 6.5 mm steel balls or six 5 mm steels were analyzed via compound light microscopy (Ken-a-vision, Kansas City, MO) to visually assess if cell walls were disrupted. Samples ground with the 5 mm steel balls had intact cell walls and watermelon cells were still clearly visible, while samples ground with 6.5 mm steel balls showed complete disruption of cell walls (e.g., could not see whole watermelon cells) (Table 4.1).

Complete cell wall disruption is crucial for hydrolysis and clean chromatograms for linkage assembly (Pettolino et al., 2012). It appears that best disruption of watermelon cell walls (10 g tissue in 50 ml polypropylene tubes) is achieved by grinding flash frozen samples with 10 mL of 80% ethanol with four 6.5 mm steel balls at 1,200 strokes$\cdot min^{-1}$ for 8 min.

Table 4.1. Optimization of grinding and ball mill size on watermelon placental tissue.

Magnetic steel ball diam. (mm)	no. minutes grinding	+/- 80% ethanol (10 mL)	Sample maintained below 4 ºC	Observations
3 x 9	15	-	no	Broken test tubes
3 x 9	12	+	yes	Broken test tubes
4 x 6.5	15	-	no	Did not check cell wall disruption; samples above 4 ˚C
4 x 6.5	8	+	yes	Cell walls completely disrupted
6 x 5	12	-	no	Did not check cell wall disruption; samples above 4 ˚C
6 x 5	8	+	yes	Some cell wall still intact/no complete disruption

Objective 2 – Hydrolysis testing and re-grinding of AIR

After grinding, samples were held for 30 min on ice and centrifuged in a Benchtop Sorval Legend RT Centrifuge, Model D-37520 Osterode (Thermal Electron Corporation, Watham, MA) for 5 min (4,000*g* at 4 ºC). Pellets were washed a total of three times with cold ethanol (4 ºC, HPLC grade) and centrifuged for 5 min (4,000*g* at 4 ˚C). Cell wall material was collected on nylon mesh filters (60 µm, 47 mm diam., Millipore/Sigma, Germany) and supernatants discarded between the washes. To the same pellets, 10 mL of room temperature acetone were added, held for 10 min (20 ºC), centrifuged for 5 min (4,000*g* at 20 ºC) and supernatant discarded. Finally, 10 mL of methanol was added to pellets and held for 10 min at 20 ºC, centrifuged (5 min, 4,000 *g*, 20 ˚C) and supernatant discarded. Pellets were placed in an oven (30 ºC) for 12-14 hours, then stored with a desiccant. The final cell wall material was an alcohol insoluble residue (AIR) of roughly 10-15 mg dry weight.

The standard hydrolysis method for cell wall AIR uses 63 to 252 µl of 72% sulfuric acid for 3 to 5 mg AIR (Saemen et al., 1954). Hydrolysis treatments consisting of 63, 126, 189, and 252 µL of 72% sulfuric acid were applied to 3-5 mg of watermelon AIR in 2 ml microcentrifuge tubes with screw caps (product no. PFSS 2800 50 20U) (OPS Diagnostics, Lebanon, NJ), incubated for 1 h at 20 ºC, with 1 min vortex intervals per 10 min incubation. After 1 h, each hydrolysis treatment was diluted to 1 M and samples transferred to acid washed 12 ml borosilicate culture glass test tubes (Fisher Scientific, Hampton NH). All samples were held for 3 h in a FED Fan-forced drying and heating oven (Binder, Camarillo, CA) at 100 ºC. Samples were

cooled to room temperature then stored in microcentrifuge tubes at -80 ºC until ready for analysis.

Total sugar content was used as a measure of effectiveness of the acid hydrolysis and grinding treatments. Standards consisted of D-(+)-glucose, >99.5% (GC Grade) (Sigma-Aldrich, St. Louis, MO) at 120, 300, 600 and 900 nmol. The phenol-sulfuric acid colorimetric assay for total sugar content was used as outlined in the method of Masuko et al. (2005). In brief, hydrolyzed AIR samples were diluted 1:10 with 1 M sulfuric acid. Aliquots of this (150 μL) were pipetted into 2 mL tubes, followed by addition of 450 μL of concentrated sulfuric acid and 90 μL of 5% phenol. Samples were held at 90 ºC for 5 min in a water bath then cooled in a room temperature water bath for 5 min. Absorbance at 490 mm was determined using a UV-2450 Spectrophotometer equipped with UVProbe 2.34 software (Shimadzu Corp., Kyoto Japan).

Hydrolysis results

Primary cell walls of dicots (i.e. cucurbit plants) consist of the hemicellulose/cellulosic and pectin networks (Pettolino et al., 2012). The polysaccharides are composed of pectic substituents which are made of 17 various monosaccharide building blocks (Houben et al., 2011). Monosaccharide analysis is extremely important for the structural characterization of cell wall polysaccharides. Acid hydrolysis is a critical step to disperse acid into the polysaccharides and cleave glycosidic bonds. Sulfuric acid hydrolysis (Saeman hydrolysis) is used for more complex polysaccharides, such as watermelon cell walls, and is applied directly to the prepared cell walls (Saeman et al., 1954).

The total sugar yield was found to be similar between 126 and 252 μL sulfuric acid addition to AIR (Fig 4.1). Total sugar yield was lowest with the lowest volume of acid, 63 μL. These results indicate that at least 126 μL sulfuric acid is needed for complete hydrolysis of 3 ± 0.21 mg watermelon AIR. At the highest volume of acid (252 μL), variability among replicates was high. These results showed that at least 126 μL sulfuric acid is needed for complete hydrolysis of 3 mg watermelon AIR.

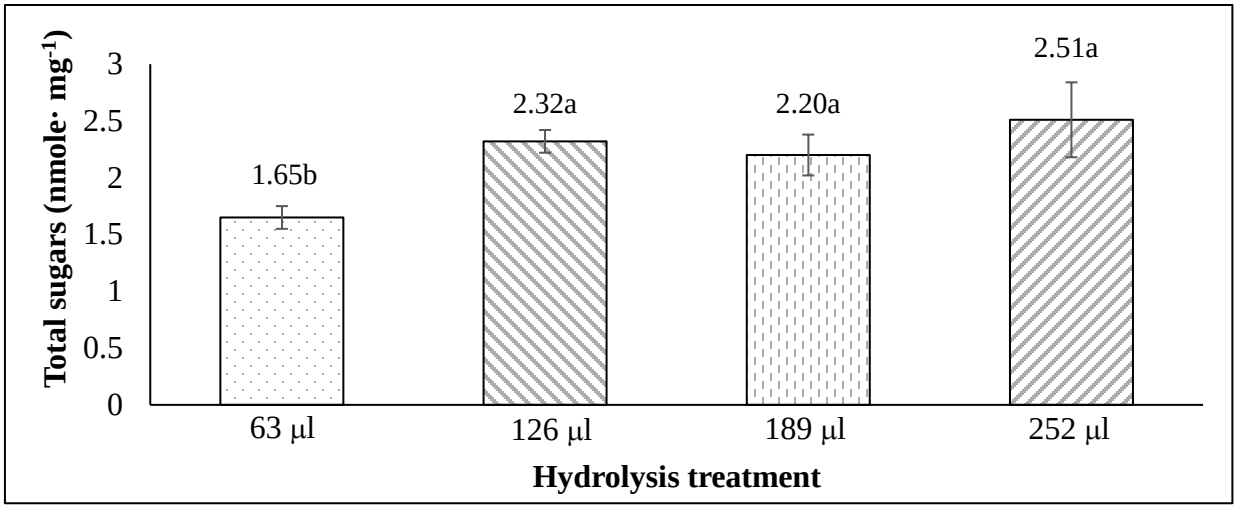

Figure 4.1. Total sugars (nmole·mg^{-1}AIR) relative to volume of added 72% sulfuric acid during hydrolysis of watermelon AIR.

Regrinding of AIR

After identifying the appropriate hydrolysis acid ratio, regrinding of the AIR was tested for proper particle size. Four levels of grinding were tested. The experiment was set up as a randomized complete block design, The AIR was used as the block by aliquoting each AIR into four grinding levels done using a Omni Bead Ruptor Homogenizer (Southern Labware, Cumming GA). Final particle size of extracted watermelon AIR desired was between 50 to 100 µm (Lareo et al., 2013). The grinding treatments were: 1) control, no grinding of the AIR, 2) grinding of AIR for 30 sec, 3) grinding of AIR for 60 sec and 4) grinding of AIR for 90 sec.

Three mg of AIR were aliquoted into labeled 2 mL centrifuge tubes. To each tube, 6 x 2.8 mm steel beads were added and ground (4,000 strokes/min). One set of replicates from each of the grinding treatments were stored in desiccant until analyzed at a Sympatec particle analysis demonstration held at North Carolina State University in the Food Science Department. The rest of the samples were hydrolyzed with 126 µL of 72% sulfuric acid and incubated at room temperature for 1 hr and vortexed every 10 min for 60 sec. After 1 hr, the sulfuric acid concentration was brought up to 1 M by adding 1.38 ml of di-water and placed into an oven set at 100 ºC for 3 hrs. Samples were pulled and cooled to room temperature then stored in microcentrifuge tubes at -80 ˚C until ready for analysis.

AIR re-grinding results

Unground AIR yielded the highest amount of total sugars (2.51 nmol mg^{-1}) but particle size was very large (972.8 μm) (Table 4.2). After re-grinding the AIR, cell wall particles became hydrostatic and clung to the sides of the test tube. When applying the 126 μL of 72% sulfuric acid, some cell wall particles were not submerged even after samples were vortexed, resulting in lack of complete hydrolysis. Furthermore, although the control sample indicated the highest total sugar concentration it also had the highest variability, which may suggest that particle size was too large and some particles may not have fully hydrolyzed.

Table 4.2. Total sugar concentration of watermelon flesh after various AIR grinding levels and Saeman hydrolysis.

Treatment[x]	**grinding time (min)**	**Total sugars (nmol·mg^{-1} AIR)** [x]	**Particle size (μm)**
Control	0	2.70 ± 0.34a	972.8 ± 0.63
1	30	2.28 ± 0.12b	230.3 ± 0.59
2	60	2.28 ± 0.13b	55.3 ± 0.43
3	90	2.00 ± 0.22b	8.4 ± 0.09

[x] Control = no grinding after extraction of alcohol insoluble residue
1 = grinding alcohol insoluble reside with 4 x 2.8 mm steel balls, 30 sec. at 400 strokes/min
2 = grinding alcohol insoluble reside with 4 x 2.8 mm steel balls, 60 sec. at 400 strokes/min
3 = grinding alcohol insoluble reside with 4 x 2.8 mm steel balls, 90 sec. at 400 strokes/min
[y] Means with different letters indicate significant differences based on Tukey's Honest Significant different test at $p \leq 0.05$.

Discussion – Objective 2

Identification of sugars in cell wall polysaccharides is done using chromatograms generated by GC-MS. Optimal yields and quality of cell wall residues is critical for accurate linkage construction. The type of cell wall material, acid concentration and acid amount dictate the release of monosaccharides in the polysaccharide structures (Broxterman et al., 2018). Crude cell wall materials need a more robust hydrolysis via sulfuric acid to cleave the monosaccharides. While pectic fractions and solubilized cell wall componenets require a more gentle hydrolysis (e.g., trifluoracetic acid) (Pettolino et al., 2012). Results for watermelon indicate that 126 μL of 72% sulfuric acid, applied to a 3-5 mg alcohol insoluble residue, is optimal (Figure 4.1). Although application of 252 μL of 72% sulfuric acid gave the highest total sugars, it also resulted in the highest variability among samples. This variability could also

indicate that some monosaccharides, such as xylose and arabinose, were broken down into smaller units (Blankenly et al., 1983).

Particle size of the AIR is crucial to ensure complete hydrolysis and four levels of re-grinding were evaluated. Pure cellulose samples and delignified loblolly pines were ball milled for different times to assess particle size and release of monosaccharides from cellulose. Results indicated that particle size ranging between 55-73 μm completely hydrolyzed as glucose concentration was highest at 93 mol%. When particles were <55 μm the concentration of glucose decreased to around 80 mol% (Agarwal et al., 2011). This suggests that regrinding is needed for watermelon AIR as particle size was too large without regrinding. This may also create further problems not only when quantifying neutral sugars, but can also be a reason for improper methylation because cell wall material with large particle size will not fully solubilize in dimethyl sulfoxide (Broxterman and Schols, 2018; Pettolino et al., 2012). Re-grinding for 60 seconds resulted in smaller particle size (55.3 μm) and higher total sugars compared to those ground for 90 seconds (2.28 vs 2.00 $nm \cdot mg^{-1}$) suggesting this optimization may be best for watermelon cell wall polysaccharide characterization (Table 4.2).

This objective was to optimize the cell wall polysaccharide analysis method based on Pettolino et al. (2012) to determine cell wall polysaccharide composition in grafted and non-grafted watermelon with or without HH. Various wet chemistry steps are required including Saeman hydrolysis for neutral sugar components, methanolysis and trifluoracetic acid (TFA) hydrolysis for pectic linkage assembly, reduction of monosaccharides to tag the anomeric carbon on hydrolyzed sugars and acetylation for volatility of watermelon cell wall tissue.

Approach

The extraction of watermelon cell wall material and methods for quantitative identification of polysaccharides are outlined in Fig 4.2. Specific steps are reported in the protocol including preparation of watermelon plant material, preparation of alcohol insoluble residues (AIR), carboxyl reduction, Saeman hydrolysis and methanolysis with trifluoracetic acid hydrolysis and acetylation steps are reported. Equipment and materials needed are provided in Tables 4.4 and 4.5.

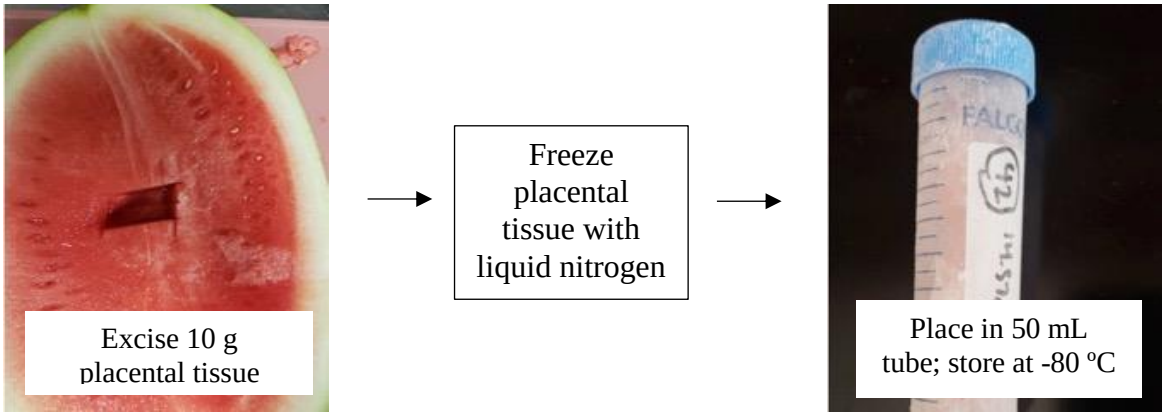

Figure 4.2. Schematic showing how placental tissue from whole watermelon was excised and stored for cell wall polysaccharide extractions.

Table 4.3. Preparation and sampling of fresh watermelon fruit tissue for cell wall extraction.

Steps	Description
1	Clean the exterior of the fruit by wiping away any dirt or remining debris left on the fruit.
2	Rinse the fruit with tap water and then spray a 5% bleach solution on the fruit. Carefully wipe the exterior of the fruit.
3	Completely dry the fruit
4	Longitudinally cut the fruit (stem to blossom end) to expose watermelon flesh
5	Excise the heart tissue from the watermelon using a scalpel or sharp knife, avoiding seed cavity areas and seed traces. Aim for ~10 grams fresh weight (Fig 4.2).
6	Place the heart tissue into weigh boats and immediately pour ~10 mL of liquid N over the sample. Apply more liquid N if needed to freeze the sample.
7	As samples are freezing with liquid N, label a disposable 50 mL Falcon test tube with sample name or number. Obtain test tube weight and recorded to 4 decimals. Tare the tube, transfer frozen watermelon to tube and record the watermelon weight in grams to four decimal places and immediately place into a -80 $^{\circ}$C freezer (Fig 4.2).

Equipment set up follows Pettolino et al., 2012

A GC-MS was used for watermelon analysis and methodology adapted from Pettolino et al. (2012) was used. To access instrument control, open MSD 5975 Chemstation (Agilent, Santa Clara, CA), which is the program on the computer connected to the GC-MS. Use helium as the carrier gas with a flow rate of 1 mL·min^{-1}. Inject 1 µL of sample with a split (1/10) injection using an autosampler, inject samples with the temperature at 240 ºC. Perform 5 syringe washes with dichloromethane between each sample. Set the oven conditions to an initial temperature of

170 ºC, hold for 2 min, and then ramp at 3 ºC min^{-1} to 260 ºC. Hold for 3 min and maintain mass selective detector (MSD) transfer line at 260 ºC.

The MS quad was maintained at 106 ºC and the MS source at 230 ºC, use 70 eV electron impact ionization and acquire the data in scan mode from 100 to 350 m/z at 2.14 scans per 1 s and with a solvent delay of 3 min. Trim and purge the BPX 70 column before starting sample injections. Be sure to change the injector syringe, septa (premium inlet septa, part no. 5183-4757, Agilent, Santa Clara, CA) and inlet liners (liner 4 mm, part no. 5181-3316, Agilent, Santa Clara, CA) from the autosampler to the GC system every 50 injections. This is critical as remaining water in the sample can corrode the injector syringe and cause faulty injections. As well, water can contaminate the inlet liner and septa causing artifacts in the chromatograms.

Cell wall polysaccharide flowchart

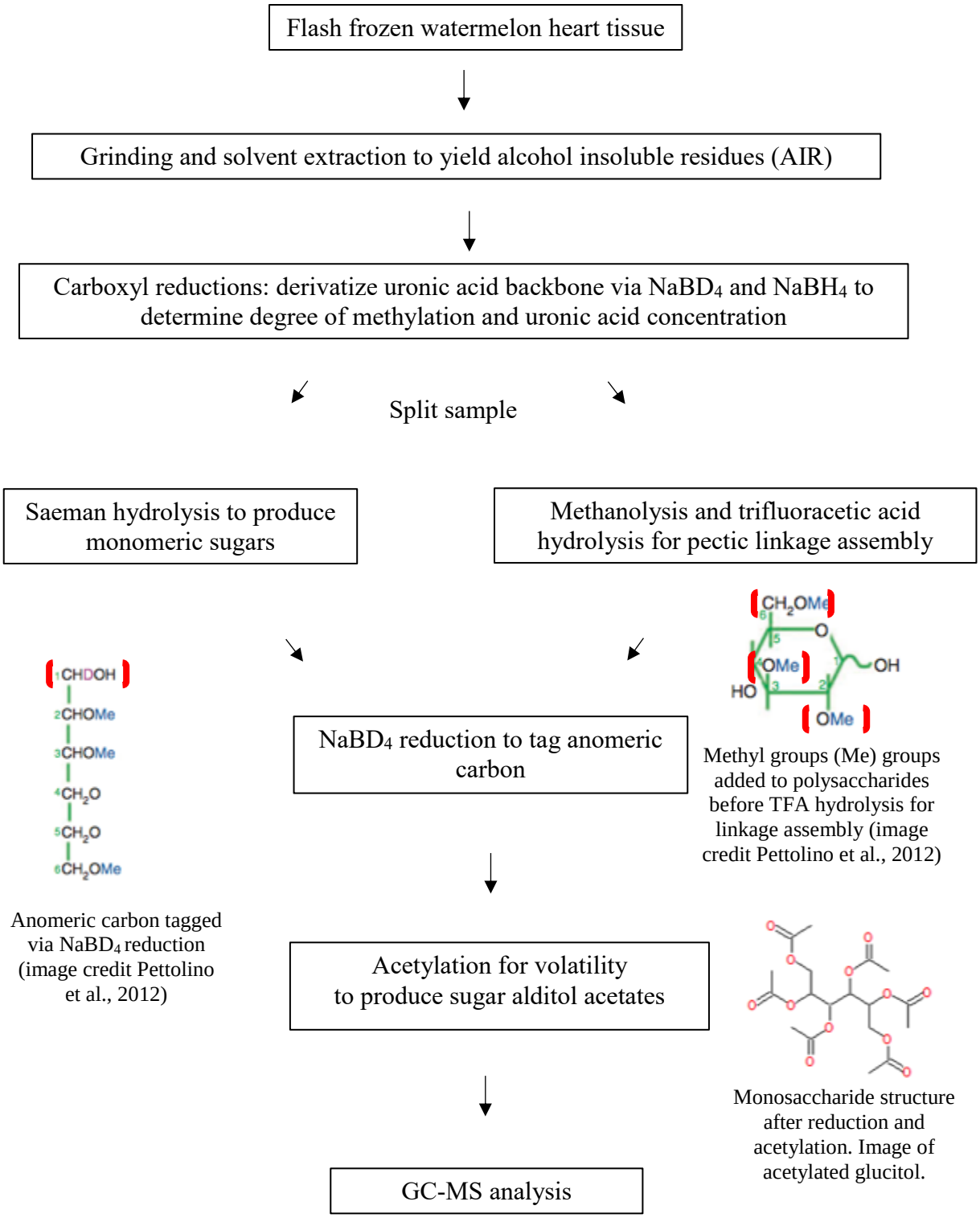

Figure 4.3. Flow chart of cell wall polysaccharide analysis methods following extraction and freezing of watermelon flesh tissue.

Materials List

Table 4.4. Chemical list required for cell wall polysaccharide composition analysis of watermelon placental tissue.

Chemical	Company	Cas no	Grade	Quantity
Sodium hydroxide	Sigma-Aldrich	1310-73-2	Analytical, ≥99.8%	500 g
Immidazole	Sigma-Aldrich	288-32-4	Analytical, ≥99%	50 g
Hydrochloric acid	Sigma-Aldrich	7647-01-0	ACS reagent, 37%	500 mL
2-[*N*-Morpholino] ethane sulfonic acid (MES)	Sigma-Aldrich	1266615-59-1	Titration, ≥99.5%	25 g
1-Cyclohexyl-3-(2-morpholinoethyl) carbodiimide-metho-*p*-toluene sulfonate (carbodiimide)	Sigma-Aldrich	2491-17-0	≥95%	25 g
Glacial acetic acid	Sigma-Aldrich	64-19-17	Reagent plus, ≥99.5%	500 mL
Triflouracetic acid	Fisher Scientific	76-05-1	Optimal, LC/MS	10 mL
Sulfuric acid	Sigma-Aldrich	7664-93-9	Airstar	1 L
Ammonia solution (32%)	Millipore sigma	105428	Suprapur	1 L
Sodium borodeuteride	Sigma-Aldrich	15681-89-7	≥98%	25 g
Sodium borohydride	Sigma-Aldrich	16940-66-2	purum p.a., ≥96%	25 g
Acetic anhydride	Fisher Scientific	108-24-7	LC/MS	2.5 L
Dichloromethane	Sigma-Aldrich	75-09-2	Anhydrous, ≥99.8%	1 L
Methanol	Fisher Scientific	67-56-1	HPLC	16 L
Dioctylamine	Sigma-Aldrich	1120-48-5	97%	50 g
Chloroform	Sigma-Aldrich			4 L
Meso-erythritol	BDH	5328-37-0	Aristar, ≥99%	25 g
2-deoxy-d-ribose	Fisher Scientific	533-67-5	Aristar, ≥99%	5 g
L-Rhamnose	Sigma-Aldrich	R3875	≥99%	5 g
L-Fucose	Sigma Aldrich	F-2252	≥99%	5 g
D-Ribose	Sigma Aldrich	R-7500	≥99%	5 g
L+Arabinose	BDH	5328-37-0	Airstar	5 g
D+Xylose	Sigma-Aldrich	58-86-6	GC, ≥99%	50 mg
2-deoxy-d-Glucose	Sigma- Aldrich	D6134	GC, ≥99%	1 g
d-allose	Fisher Scientific	2595-9-3	GC, ≥99%	1 g
D+mannose	Sigma Aldrich	M-4625	Airstar	1 g
D-Glucose	Sigma Aldrich	47829	Analytical	1 g
D-Galactose	Sigma-Aldrich	59-23-4	Analytical	10 g
Myo-Inositol	Sigma-Aldrich	87-89-8	Airstar	50 g
Dimethyl sulfoxide	Sigma-Aldrich	67-68-5	GC, ≥99.5%	1 L
Iodomethane	Sigma-Aldrich	74-88-4	ReagentPlus, ≥99%	100 g
Ethanol	Fisher Scientific	64-17-5	Analytical	16 L

Table 4.4. (continued)

Acetone	Millipore Sigma	67-64-1	HPLC	16 L
α-amylase	Sigma-Aldrich	9000-90-2		5 mL
Maleic acid	Sigma-Aldrich	110-16-7	≥99%	100 g
Sodium sulfate, granular	Sigma Aldrich	7757-82-6	Anhydrous, ≥99%	500 g
Liquid Nitrogen	Airgas			t-tank
Nitrogen gas	Airgas			t-tank

Equipment List

Table 4.5. Equipment and Instrumentation required for cell wall polysaccharide analysis.

Equipment	Company	Company Headquarters
Geno/Grinder 2010, Model SN 10592	Spex Sample Prep	USA, Metuchen, NJ
Nitrogen Evaporator, Model TM 111	Organomation Associates INC	USA, Berlin, MA
Vivaspin turbo 15 mL Centrifugal Ultrafiltration Filters (3 KDa)	Sartorius	*Bought by Sigma
BeadBug Microtube Homogenizer, Model D1030	Sigma-Aldrich	Germany, Darmstadt
Benchtop Sorval Legend RT Centrifuge, Model D-37520 Osterode	Thermo Electron Corporation	Waltham, MA
Borosilicate Culture Test Tubes, 16x100 mm N16100) with PTFE caps	Scientific Specialties INC	USA, Hanover, MD
Borosilicate Culture Test Tubes, 13x100 mm (N13100) with PTFE caps	Scientific Specialties INC	USA, Hanover, MD
50 mL Falcon sterile conical test tubes (Item # 1495949a)	Fisher Scientific	USA, Hampton, NH
BPX70 column (25 m x 0.22mm inner diameter, film = 0.25 μm)	SGE Analytical Science	Australia
Ultrasonic cleaner, Sonicator, Model 3510R-MT	Branson Ultrasonics Corporation	USA, Danbury, CT
Universal pH paper (0-10 pH)	Precision Labs, INC	USA Cottonwood, AZ
Nichipet ECO Positive displacement micro-dispenser pipet (1000 μL)	Nichiryo CO., LTD	Japan, Saitama, Koshigaya City
Glass tip pipet (100-1000 μL)	Nichiryo CO., LTD	Japan, Saitama, Koshigaya City
Pipet-aid with tissue culture nose piece, Model 4-00-101	Drummond	USA, Broomall, PA
5/3" Glass Pasteur Pipets (Cat # 13-678-61), 1000	Fisher Scientific	USA, Hampton, NH
FED Fan-forced drying and heating oven, 5-300 C	Binder	USA, Camarillo, CA
Freeze dryer, Model 24DX48GPFD, 25 L, EL-85	Virtis	USA, Houston, TX
Isotemp 637D Incubator	Fisher Scientific	USA, Hampton, NH
Pulsing Vortex Mixer, Deluxe Pulse, Model E19371	Fisher Scientific	USA, Hampton, NH
5 mL glass mortar and pestle	Laboratory Product Experts	USA, Vernon Hills IL
Steel beads, 6.5 and 2.8 mm, magnetic, high carbon (4RJH5)	Grainger	USA, Lake Forest, IL
2 mL Microcentrifuge tubes with screw cap (PFSS 2800 50 20U)	OPS Diagnostics	USA, Lebanon, NJ
Isotemp Vacuum oven, Model 285A	Fisher Scientific	USA, Hampton, NH
GC 7098A system with MSD VL 5975C system	Agilent	USA, Santa Clara, CA
Autosampler N10149, 0-50 vials	Agilent	USA, Santa Clara, CA
Injector syringe, gold standard, 10 μL (item # 9301-0713)	Agilent	USA, Santa Clara, CA
Vials (part no. 5182-0543) and crimp caps (part no. 5182-0552)	Agilent	USA, Santa Clara, CA
Inset vials, 250 μL, deactivated glass, polymer feet (part no. 5181-8872)	Agilent	USA, Santa Clara, CA
Nylon mesh filters, 60 μm, 47 mm diam.	Millipore/Sigma	Germany, Darmstadt

Table 4.6. Comprehensive cell wall polysaccharide analysis methods for watermelon (6-8 hrs).

Steps	Description of methods
1	Using the same 50 mL tubes that watermelon was stored in, record the weight of the watermelon tissue plus tube and sample. Add four 6.5 mm steel beads and 15 mL of 80% ethanol.
2	Flash freeze samples by immersing tubes in liquid N for 30-45 sec. Transfer the tubes to a pre chilled aluminum block (chilled at -80 ºC), then transfer to a Geno/Grinder and grind sample for 8 min at 20 Hz. Be sure to check temperature of matrix, keep below 4 ºC. Remove the steel beads using a magnetic stir bar retriever and rinse the stir bar with deionized distilled water (ddw) 3x between samples.
3	Put tubes on ice for 30 min to extract, then centrifuge samples for 5 min at 4,000*g* at 4 ºC. Collect CWM on 60 µm nylon mesh filters and discard the supernatant. Be extremely careful to keep all CWM for quantification purposes.
4	For the 2nd and 3rd ethanol extraction use 20 mL of 80% ethanol each time. Be sure to vortex all samples for 45-60 sec after each addition of ethanol. Centrifuge for 5 min at 4,000 *g*. Collect CWM on 60 µm mesh and discard the supernatant. Repeat until a clean sample is obtained. Discard supernatant between washes. **Three ethanol washes are required in total.**
5	Add 20 mL of room temperature acetone at room temperature. Vortex sample for 45-60 seconds. Extract material for 10 min at room temperature. Centrifuge for 5 min at 4,000*g* and discard the supernatant being sure to collect any CWM that isn't pelletized on 60 µm nylon mesh filters.
6	Add 20 mL of methanol. Vortex the sample for 45-60 seconds. Centrifuge (8 min, 4,000*g*, room temperature) and discard the supernatant. Be sure to collect any CWM that isn't pelletized on 60 µm mesh.
7	Add 20 mL of acetone at room temperature. Vortex sample for 45-60 seconds. Extract material for 10 min. Centrifuge for 5 min at 4,000*g* and discard the supernatant being sure to collect any CWM that isn't pelletized on 60 µm mesh.
8	Add 20 mL of methanol. Vortex the sample for 45-60 seconds. Centrifuge for 5 min at 4,000*g* and discard the supernatant. Be sure to collect any CWM that isn't pelletized on 60 µm mesh.
9	Repeat acetone and methanol extraction steps. **Three total acetone and methanol extractions are required**
10	Dry samples in a fan forced oven at 37 ºC for ~16 hours (overnight). Then remove samples and obtain the weights of the AIR. Pack all AIR samples into labeled 2 mL microcentrifuge tubes with screw caps and store in desiccants until ready to preform carboxyl reductions.

Carboxyl reduction methods

Watermelon contains both neutral sugars and uronic acids (galacturonic and glucuronic acids). Carboxyl reduction is a useful technique for determining neutral and acidic sugars simultaneously. However, quantitative transfers are crucial between each subsequent step in order to quantify the differences in content of these polysaccharide constituents and to calculate degree of methylation.

Table 4.7. Carboxyl reduction of prepared AIR from watermelon flesh (4.5 days).

Steps	Description of methods
1	Prior to starting carboxyl reduction, select the sample/batch of choice. If samples are frozen, pull from the -80 ºC freezer and bring to room temperature. As samples are warming up, add 6 x 2.8 mm steel balls to each watermelon AIR sample and grind samples with bead bug at 4,000 strokes/min for 60 s. The samples are already packed into 2 mL microcentrifuge tubes. **Critical step:** Further grinding of AIR helps with quantitative transfer issues and is done in order to achieve full carboxyl reduction
2	**Reduction I** Label, weigh and record the weight of the 12 mL glass test tube, and tare the test tube. Add roughly 5 mg of ground watermelon AIR to the test tube. Record sample weight in mg to 2 decimal places using an analytical scale. Then hydrate the sample by pipetting 5 mL of 1 M cold (4 °C) imidazole in each test tube with sample (imidazole is stored in a laboratory refrigerator) and place all the samples on ice. After about 10 min vortex the sample for 30 sec. Pellet hydration has occurred when the cell wall particles fall to the bottom of the test tube (samples are generally cooled for 20-30 min.)
3	As samples are cooling make fresh 100 mg·mL^{-1} sodium borodeuteride ($NaBD_4$) **100 mg·mL^{-1} $NaBD_4$ (freshly prepare)** A. Weigh out 100 mg of $NaBD_4$ per each mL of ddw, 2.5 mL of 100 mg·mL^{-1} are added to each cell wall sample B. Pour $NaBD_4$ into volumetric flask (each time the reducing agent is made to a different volume; volume depends on amount of samples being processed at one time. Generally each batch has 8 watermelon samples prepared at one time. 8 samples require 20 mL of $NaBD_4$) C. Add ddw to final volume and mix **Critical step:** Place $NaBD_4$ on ice and cool for 10 min before pipetting into the samples.

Table 4.7. (continued)

4	In a fume hood, pipet 2.5 mL of 100 mg·mL^{-1} $NaBD_4$, and wait for the fizzing to stop. Vortex for 30 seconds and cool on ice for 2.5 hours. Make sure to keep samples on ice for the duration of the first reduction. Check the samples periodically as the reducing agent will cause sample to fizz. If this happens carefully shake the sample to suspend the cell wall particles in the solution. Again, cell wall particles should fall to the bottom of the test tube as reduction I occurs. *Place glacial acetic acid on ice 30 min prior to the end of 2.5 hour incubation. Destroy excess $NaBD_4$ by slowly adding 100 μL aliquots of cooled glacial acetic acid; keeping samples on ice. Add acid slowly until sample stops fizzing. Roughly 500-700 μL of acetic acid are needed per sample in this step.
5	**Dialysis I** Ultrafiltration centrifugal filters, pore size 3 kD and 50 mL total volume are used with a 5 mL starting sample volume. Label centrifugal filters. Carefully pour reduced sample into 15 mL centrifugal filter within a 50 mL test tube to capture the filtrate. Rinse the sample test tube 3-4 times with 500 μL of ddw. Pipet ddw in a circular fashion around the test tube and then vortex to ensure no cell wall residue remains on the test tube.
6	Centrifuge samples at 4,000*g* for 1.5 hour (or until ~200 μL of retentate remains in the filter). Then add 2 x 200 μL of ddw to the filtrate. Centrifuge for a further 60 min between each addition (or until only ~200 μL of retentate remains). **Goal:** Remove small molecules and retain the large molecules; ddw rinses help to pull all small molecules out of the sample matrix
7	**Quantitative transfer I:** Remove samples from centrifuge. Using the same 12 mL glass test tube with weight recorded, transfer the sample by pipetting with a 200 μL and pipet tip from centrifugal filter into the glass test tube. To make pipetting easier, the tips the plastic pipets may need to be cut to obtain a slightly larger tip opening for easier sample uptake. To further achieve quantitative transfer, add 3x200 μL of ddw to centrifugal filter and pipet the rinse into the same glass test tube. Place the samples with caps into freezer (small holes are pre-drilled into the caps to prevent pressure build up during freeze drying, see photo). Once samples are fully frozen at -80 ºC, place samples in the freeze dryer and dry the sample overnight, at least 16 hours. Freeze dry shelf parameters were held at -25 ºC, for 240 mins and 50 μtorr, then -20 ºC for 500 mins at 200 μtorr, then -10 ºC at 190 μtorr until pulled from the freeze dryer. The condenser was held at -60 ºC during each freeze drying step.

Table 4.7. (continued)

8 Add 1 mL of ddw to the freeze dried samples and hydrate the sample for 10 min. Vortex well.

9 As samples are hydrating freshly prepare a 500 mg·mL^{-1} carbodiimide reagent.

500 mg·mL^{-1} carbodiimide (freshly prepare)

A. Weigh out 500 mg·mL^{-1} of carbodiimide
B. Place into a volume flask (again since this is freshly made, volume will change dependent upon the amount of samples being processed)
C. Fill to volume with ddw
D. Heat in a warm water bath (40 ºC) to fully dissolve

Add 200 µL 0.2 M Mes hydrate and 400 µL 500 mg·mL^{-1} carbodiimide to each of the samples and incubate for 3 hr at 30 ºC. Then remove the samples from the incubator.

10 **Quantitative transfer II**

Split the sample (1.6 mL aqueous solution). To achieve a quantitative transfer, gently vortex the sample to ensure a homogenous suspension. Label and pre-weigh 7 mL glass test tubes and record the weight. Using a glass pipet tip transfer ~800 µL of the mixed sample into a clean and labeled test tubes (see picture). Check the weights between sample split, samples should be homogenously suspending in solution and should weigh the same amount once they are split. Record the weight of the sample in solution. At this point one test tube will be denoted (D/D) and the other will be (D/H).

11 **Reduction II**

Add 500 µL of cold 4 M imidazole) to each sample (imidazole is refrigerated during storage. Then place all samples on ice to cool the samples. While the samples are cooling, prepare fresh $NaBD_4$ and $NaBH_4$.

Freshly prepare 70 mg $NaBD_4$ and 70 mg $NaBH_4$ (Freshly prepare)

1. Weigh out 70 mg·mL^{-1} of both $NaBD_4$ and $NaBH_4$
2. Total weight will be equivalent to the number of samples processing at the time
3. Pour into a volumetric flask
4. Fill to volume and mix well

Table 4.7. (continued)

12 Add 1 mL of 70 mg·mL^{-1} $NaBD_4$ to the test tubes labeled (D/D). Cap immediately. Add 1 mL of 70 mg·mL^{-1} $NaBH_4$ to the test tubes labeled (D/H). Cap immediately. Further reduce the samples at room temperature overnight (16 hours).

13 Working temperature and in a fume hood, place the samples on ice. Destroy excess $NaBD_4$ and $NaBH_4$ by slowly adding 100 μL glacial acetic acid. Add acid until sample stops fizzing. Roughly 300-400 μL acetic acid are needed in this step.

14 **Dialysis II**
With new, labeled 50 mL centrifugal filters, carefully pour reduced sample into 15 mL centrifugal filter held in a 50 mL test tube. To further achieve quantitative transfer, add 3 to 4 volumes of 500 μL of ddw to test tube and pour the rinse into the centrifugal filter.

15 Centrifuge samples at 4,000*g* for 60 min (or until 200 μL of filtrate remains in the filter). Then add 2 x 200 μL of ddw to the filtrate. Centrifuge for a further 60 min between each addition (or until only 200 μL of filtrate remains).
Goal: Remove small molecules and retain the polysaccharides

16 **Quantitative Transfer III**
At this point the samples will all be split again! Using 7 mL glass test tubes label the test tubes with sample name: sample # (D/D) hydrol., sample # (D/H) hydrol,. sample # (D/D) methyl. and sample # (D/H) methyl., and then weigh the test tubes and record the weight.

As before, obtain the weight of each labeled test tube and record in mg. Mix the sample in the centrifugal filter gently by shaking. Using a 200 μL pipet, transfer all of the sample into one test tube either (D/D) or (D/H). Rinse the centrifugal filter by pipetting 3x100 μL ddw into the filter, shake to mix and then pipet the rinse into the same test tube.

Then split the samples as previously done, start by gently mixing the sample to ensure a homogenous suspension, then transfer 250 μL of the sample to its sister test tube. Then weigh the sample and test tube (subtracting test tube weight) to ensure samples have the same weight once split

Table 4.7. (continued)

17	**PAUSE POINT: CAN STORE SAMPLES AT -80 ºC UNTIL READY FOR METHYLATION OR HYDROLYSIS STEPS.** All samples are were freeze dried for ~56 hrs (generally through the weekend). Freeze dry shelf parameters were held at -25 ºC, for 240 mins and 50 mtor, then -20 ºC for 500 mins at 200 mtor, then -10 ºC for 1200 min at 190 mtor and -5 ºC for 1200 min at 100 mtor. The condenser was held at -60 ºC during each freeze drying step. Samples were pulled from the freeze dryer after ~56 hrs. Weigh all the samples on an analytical scale after removing from freeze dryer. Subtract the weight of the test tube and record the weight of the reduced and freeze dried AIR pellets. Add 20 μL of methanol to the samples that will be methylated to further dehydrate the sample, then freeze dry for 3 more hours using the same parameters as mentioned above.

Methylation/trifluoroacetic acid hydrolysis occurs simultaneously with Seamen hydrolysis

Monosaccharide composition from alditol acetates is done to determine neutral and acidic monosaccharides composition. There are two options for hydrolysis: 1) TFA hydrolysis for soluble polysaccharides which is used on the methylated samples or 2) Sulfuric acid hydrolysis for insoluble polysaccharides. Hydrolyzed watermelon samples are treated with sulfuric acid hydrolysis as the cell wall polysaccharides came from intact cell walls that were mechanically disrupted in the laboratory by a grinding.

Methylation steps are performed on the same samples after the carboxyl reduction steps. Methylation is a critical step to this protocol as it is used to determine bot neutral and acidic monosaccharide linkages.

Table 4.8. Saeman hydrolysis and methylation with TFA hydrolysis are done side by side (1.5 days)

Steps	Methylation/TFA Hydrolysis	Saemen Hydrolysis
1	To the samples undergoing methylation, add 20 μL of methanol to dehydrate the samples and further freeze dry for 3 hours	Remove samples intended for hydrolysis from freeze dryer and obtain sample and test tube weight. Subtract the weight of the test tube to obtain pellet weight. Then place into -80 ºC overnight.

Table 4.8. (continued)

2	Remove samples from the freeze dryer and obtain the sample and test tube weight. Subtract the weight of the test tube to obtain pellet weight. Flush the test tubes with nitrogen.	
3	Add 200 µL of dimethyl sulfoxide (DMSO) to the samples. Flush the samples one more time with nitrogen. Cap the samples and sonicate for 30 min. Then let solubilize overnight (~16 hours). **Note:** Samples have solubilized when the cell wall material turns glassy/clear.	
4	Prepare a slurry of DMSO and 50% (wt/wt) with sodium hydroxide pellets. For each 1 mL of DMSO add 4 pellets of NaOH. Grind in mortar and pestle To each of the solubilized samples, add 200 µL of DMSO/NaOH slurry **Critical Step:** It's important to evenly suspend the slurry directly to the sample. If any slurry should get on the side of the test tube the reagent will be limiting.	Remove the sample from the freezer and bring to room temp and turn the oven to 100 ºC. For the samples that are to be hydrolyzed prepare 72% sulfuric acid **72% (wt/wt) sulfuric acid** A. Working in a fume hood B. Cool ddw and sulfuric acid on ice C. Weigh out 20 g ice cold ddw D. Add cold sulfuric acid to 93.2 g (73.2 g sulfuric acid) E. Add cold ddw to 100 g F. Transfer to a storage glass bottle, label. Store at room temp for 12 months Add 126 µL of 72% sulfuric acid to the sample. Vortex every 10 min for 30 sec, do this for 1 hr. keeping them at room temperature. **Notes:** the samples should be completely dissolved and turn a brown to black color. If this color change has not occurred then hydrolysis is not complete

Table 4.8. (continued)

5	Cap and sonicate the samples for 50 mins. Be sure to check the temperature of the sonicating water and keep the water at about 10 ºC by adding ice during sonication.	Dilute the acid to 1 M by adding 1.38 mL of ddw to the sample. Vortex the sample for 30 seconds. Then place into the oven set at 100 ºC for 3 hours to complete hydrolysis.
6	Add 10 μL of iodomethane Cap and sonicate the samples for 10 min	Samples are still in oven at 100 ºC
7	Add 10 μL of iodomethane Cap and sonicate the samples for 10 min	Samples are still in oven at 100 ºC
8	Add 20 μL of iodomethane Cap and sonicate the samples for 20 min. Make sure sonicating water stays cold throughout methylation. **Note:** Samples should have a milky appearance after the third addition of iodomethane, this is a good indicator that the samples are fully methylated	Samples are still in oven at 100 ºC. After the last methylation event, about half way through heated hydrolysis, vortex the hydrolyzed samples for 30 sec and place back into the oven.
9	To all the methylated samples: add 1 mL of ddw and vortex about 15 sec/sample. Then add 500 μL DCM. Cap samples and vortex well (~60 sec/sample). **Repeat** this by washing the samples in dichloromethane with 3 x1 mL of ddw. Remove and discard the upper aqueous phase with a glass pasture pipet. Keeping the lower organic phase	Remove all samples from the oven. Cool during lunch.
10	Dry all of the samples under a stream of N in warm water bath held at 35 ºC. Then cap samples and let set during lunch.	Turn the oven to 121 ºC and let warm up during lunch break.

Table 4.8. (continued)

11	**<u>Start TFA hydrolysis</u>**	
	After samples have dried under nitrogen, add 200 µL of 2 M triflouroacetic acid (TFA) **2 M TFA** A. Using a 50 mL volumetric flask B. Pipet 7.42 mL of TFA into the cleaned flask C. Fill the flask to volume with ddw D. Mix well. Transfer to a glass storage bottle. **E.** Label and store for up to 6 months	Neutralize the samples by adding 1 mL of 20% (vol/vol) dioctylamine in chloroform. Vortex the samples for 60 seconds. **20% (vol/vol) dioctylamine in chloroform** A. Using a 100 mL volumetric flask B. Pipet 20 mL of dioctylamine into flask C. Bring up to volume with chloroform D. Mix well E. Transfer to a glass storage bottle. Label. Store for 6-12 months
12	Hydrolyze all samples for 90 min at 121 ºC in a fan forced oven. **Critical step:** Check the samples periodically to make sure that the TFA has not evaporated off. If so, add 50 µL more of TFA to the sample to complete hydrolysis	Centrifuge samples at 2,200 *g* for 3 min. Remove the lower organic phase with a glass pasture pipet. Repeat by adding 3 x 1 mL 20% dioctyl amine in chloroform with centrifugation. Samples should all be at pH 6 at this point. **Critical step:** Be sure to remove only the lower organic phase, leave a little bit of the organic phase in the bottom of the test tube as to not pull any of the aqueous phase.
13	Pull the samples from the oven and let come to room temperature.	Remove excess amine by washing upper aqueous phase with 4 x 1 mL aliquots of chloroform. Check the pH of upper aqueous phase with pH paper. pH should now be ~4-5. With a glass pasture pipet the lower organic phase between each wash and after the last wash.
14	Add internal standard by pipetting **10 µL of 13.561 mg·mL^{-1}** myo-inositol (about 1/20th of total carbohydrate) into each sample.	Add internal by pipetting in **10 µL of 13.561 mg·mL^{-1}** myo-inositol (about 1/20th of total carbohydrate) into each sample.

Table 4.8. (continued)

15	Dry down the upper aqueous phase (with internal standard) under a stream of nitrogen (using a warm water bath ~35 ºC). Notes: At this point can proceed forward to the next reduction (step 53) or can pause experiment by placing the samples in -20 ºC freezer overnight.	Dry down the upper aqueous phase (with internal standard) under a stream of nitrogen (using a warm water bath ~35 ºC). Notes: At this point can proceed forward to the next reduction (step 53) or can pause experiment. **PAUSE POINT:** Add 200 μL of methanol and store samples in labeled test tubes in a -20 ºC freezer overnight.

Prior to starting the next steps there are 12 other sugar standards (meso-erythritol, 2-deoxy-d-ribose, rhamnose, fucose, ribose, arabinose, xylose, 2-deoxy-d-glucose, allose, mannose, galactose and glucose) that should have also been dried at the same time as the internal standard. Again they are dried in a vacuum oven at 40 ºC overnight in the presence of desiccant.

Independent sugar standard solutions (0.1 M)

A. After drying down all of the sugars and transferring to a labeled storage test tube
B. Remove sugar standards from desiccator, using 1 mL volumetric flasks, label each flask.
C. Tare the 1 mL volumetric flask and weigh out ~20 mg of each sugar and be sure to record the weight to 2 decimal places
D. Bring to volume with ddw
E. Mix well. To ensure all sugar has gone into solution, sonicate for 5 min
F. Transfer to a labeled 2.0 mL microcentrifuge tube
G. Store at -80 ºC for ~12 months

Once all the sugar standards have been made its time to make a stock sugar mix

Stock sugar mix

A. DO NOT add 20 $mg \cdot mL^{-1}$ of myo-inositol to the stock sugar mix. Myo-inositol is the internal standard and is used to normalize the calibration curve and sample data
B. To the 12 other sugar standards, measure 100 μL of each sugar
C. Pipet into a 2 mL microcentrifuge tube
D. Mix well, vortex 30-60 seconds
A. Label microcentrifuge tube as "stock sugar mix" and store at -80 °C for ~12 months

Perform dilutions on the stock sugar mix to generate a standard curve

Sugar standards dilution methods

The stock sugar mix will be diluted into a labeled 2 mL microcentrifuge tube and then stored at -80 °C

- Take stock sugar mix out of freezer and bring to room temp (20 °C)

- 1:5 (100 μL stock sugar mix into 400 μL ddw)
- 1:10 (100 μL stock sugar mix into 900 μL ddw)
- 1:15 (100 μL stock sugar mix into 1.4 mL ddw)
- 1:20 (100 μL stock sugar mix into 1.9 mL ddw)
- Vortex well, 60 sec, and store at -80 °C for ~12 months

Note: Once standard curve samples have been generated, there is no need to prepare standard curve every batch of experimental samples

Myo-inositol (internal standard) dilution methods

- Take the 20 $mg \cdot mL^{-1}$ (0.1 M) myo-inositol from freezer, bring to room temp. (20 °C)
- Pipet 100 μL internal standard into 2 mL microcentrifuge tube
- Dilute with 1.9 mL ddw and vortex for 60 sec to give a 1:20 dilution
- Store at -80 °C until ready to add to samples or calibration curve

Critical step: The 1:20 myo-inositol solution will be used as the internal standard. To each sample add 10 μL of 13.561 $\mu g \cdot mL^{-1}$ myo-inositol ($1/20^{th}$ of total carbohydrate) to the samples. It is critical to use the same 10 μL pipettor when adding the internal standard to the samples. This will decrease variability of internal standard and increase accuracy and precision.

Extended Calibration

If the watermelon sample chromatogram peak intensities exceed the calibration curve it is important to extend the calibration curve. In watermelon the dominant sugars are glucose, galactose, xylose and arabinose. After running batch 1, many of the peaks in the chromatograms exceeded those of the diluted sugar mixes.

Extended calibration curve methods:

- 10 μL stock sugar mix added to 7 mL borosilicate glass test tubes (final stock sugar concentration around ~30 $\mu g \cdot mL^{-1}$)
- 50 μL stock sugar mix added to 7 mL borosilicate glass test tubes (final stock sugar concentration around ~111 $\mu g \cdot mL^{-1}$)
- 100 μL stock sugar mix added to 7 mL borosilicate glass test tubes (final stock sugar concentrations around ~222 $\mu g \cdot mL^{-1}$)
- 150 μL stock sugar mix added to 7 mL borosilicate glass test tubes (final stock sugar concentrations around ~333 $\mu g \cdot mL^{-1}$)
- Add 10 μL of 1:20 diluted myo-inositol
- Dry all samples down in a warm water bath around 35 °C
- Proceed to steps 42

At this point ALL cell walls samples and standards are treated the same!

Table 4.9. Further Reduction of Monosaccharides to tag the anomeric carbon (5 hrs).

Steps	Description of methods
1	At this point, the stock sugar mix/calibration curve mixes will be reduced and acetylated with the sample batch. Pipet 10 μL of the diluted sugar mixes or to extend the curve pipet 10, 50, 100 and 150 μL "stock sugar mix" into the 7 mL culture tubes. Add 10 μL 1:20 myo-inositol to each of the tubes.
2	Dry down all sugar standards and watermelon samples stored in methanol under a stream of nitrogen **Critical step:** For sugar standards and samples make sure to use a warm water bath at 35 ºC (do not let the water bath warm about 40 ºC as monosaccharides can be lost at warmer temperatures. The wm were stored overnight methanol; methanol evaporates rapidly under nitrogen so no warm water bath is necessary.
3	**2 M Ammonia** A. Using a clean 50 mL volumetric flask and in a fume hood B. Pipet 5.52 mL of 32% ammonia in flask C. Bring to volume with ddw D. Transfer to a glass storage bottle. Label and store at room temp. for 6-12 months. After samples have been dried, pipet 100 μL of 2 M ammonia to dissolve the residue.
4	As the residues are dissolving **Freshly prepare 1 M $NaBD_4$ in 2 M ammonia solution** A. Weigh out 41.87 mg of $NaBD_4$ B. Add exactly 41.87 mg to each 1 mL of 2 M ammonia C. The total volume prepared will change depending upon the amount of samples being processed at one time D. Bring up to volume. Mix well and use fresh Pipet 100 μL of NaBD4 in ammonia to each sample. Sonicate the samples for 2 min. Incubate all samples at room temperature for 2.5 hours
5	Destroy excess reductant by adding 50 μL of glacial acetic acid. Add additional acid in increments of 50 μL until the sample stops fizzing.
6	Place all samples in a shallow water bath maintained at about 35 ºC and evaporate with a stream of nitrogen.
7	Rise each sample with 2 x 250 μL of 5% (vol/vol) acetic acid and methanol and then 2 x 250 μL methanol

Table 4.9. (continued)

	5% vol/vol acetic acid and methanol A. Use a 100 mL clean, volumetric flask B. Pipet 5 mL acetic acid into flask C. Fill to volume with methanol D. Mix well, transfer to a glass storage container and label (store at ambient temp for 12 months)
8	Proceed to acetylation step 55 or use this as a pause point **PAUSE POINT:** Can store the samples overnight in 250 μL methanol only after they have been washed and evaporated 2 x 250 μL methanol.

All steps to this point were performed at the NC research campus in Kannapolis, NC. The last steps to this protocol were performed in Raleigh where the GCMS is located. To the reduced samples stored in methanol, place them into a secondary container for the drive to Schaub Hall. It is very important that samples are gently moved and samples are kept upright during travel as to not lose any sample during transportation.

Table 4.10. Acetylation for generating volatile alditol acetates for GC-MS analysis (5-6 hr).

Steps	Description of methods
1	Dry the samples and sugar standard down with a stream of nitrogen.
2	Acetylate samples by adding 250 μL of acetic anhydride. Sonicate the samples for 5 min and place into an oven at 100 ºC for 2.5 hrs
3	Remove samples and cool at ambient temperature by placing samples in a fume hood for 10-15 min. Then destroy acetic anhydride by adding 2 mL of ddw to each sample. Vortex for 60 secs/sample. Let stand for 10 min.
4	Extract the partially acetylated alditols with 750 μL of dichloromethane (DCM). Vortex well (2 min/sample). Centrifuge at 2,200*g* for 4 min at room temperature. Remove the top aqueous phase with a glass pipet
5	Wash the DCM phase with 2x2 mL aliquots of ddw. Removing the top aqueous phase with a glass pasture pipet. **Notes:** Be extremely careful to not pipet out any of the DCM as the sample may be lost.

Table 4.10. (continued)

6	Label small glass vials from Agilent with sample name. Pack about 0.1 to 0.2 g of sodium sulfate into the vials. This is done to pull any excess water from the sample as to not disrupt the GC-MS system(s) or chromatograms. Then Transfer the DCM phase into the vial (2 mL, screw, clr, WrtOn, cert, part no. 5182-0715, Agilent, Santa Clara CA) and close with a screw cap (9 mm, blue, PTFE/RS, part no. 5185-5820, Agilent, Santa Clara CA) **PAUSE POINT:** Store samples at -80 ºC until ready to run on the GC-MS **Notes:** Make sure to only store the DCM phase in glass vials (never use plastic microcentrifuge tubes)
7	Remove samples from -80 ºC and bring to room temperature. Transfer 150 µL of the sample into vials with insert vials. Use crimp cap vials with crimp cap tops with samples placed into autosampler to decrease variability due to DCM volatility. Be sure to cap each sample prior to transferring the next sample. Only 16 watermelon cell wall polysaccharide samples can be run per batch/run time due to volatility issues with DCM. **Critical Step:** Run a DCM blank, alkane series and the same QC sample with each batch/run to identify any variability from day to day.

Alditol acetate (monosaccharide analysis) data processing (15 min per chromatogram)

All data will be integrated and quantitated via 5975C Data Analysis MSD chemstation (Agilent, Santa Clara, CA). A labeled chromatogram of sugar standards is found in Figure 4.4.

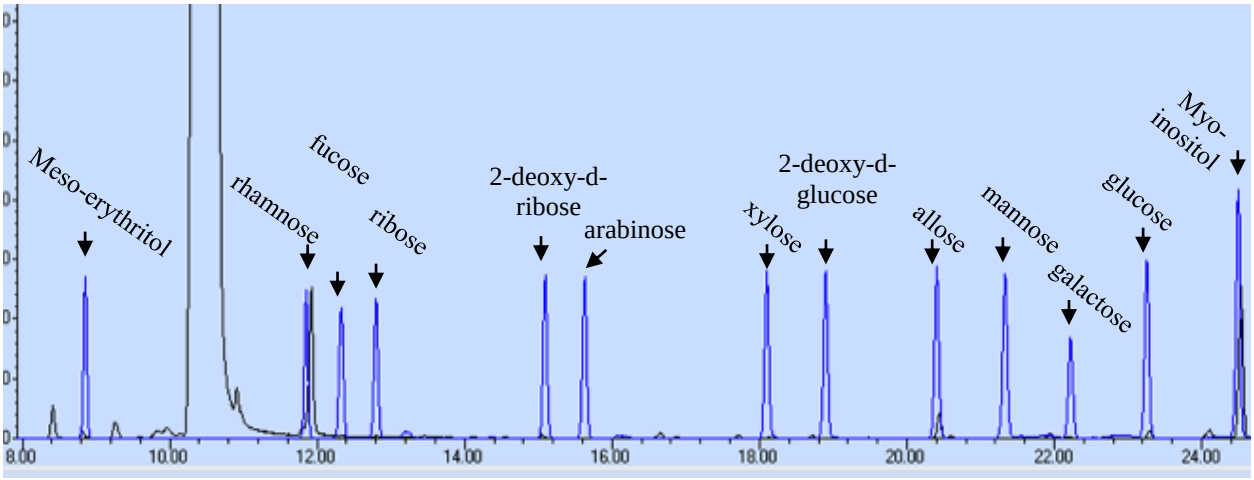

Figure 4.4. Chromatogram of the12 labeled sugar standards and internal standard.

If retention times of the sugar standards are unknown, independent monosaccharide reduction and acetylation (steps 42-55) of each sugar (12 sugar standards) may be needed to identify the retention times. Once the retention times are identified from each sugar standard, each of the independent chromatograms from the calibration curve will be quantitated. Open a sugar standard chromatogram in the MSD data analysis program. Then click on calibrate and then "update", this will allow the user to add each of the alditol acetates based on retention time. Once the first chromatogram has been calibrated, open the next sugar standard chromatogram and under calibrate, click on "edit compounds". This will allow the user to add sugar standard levels (one level will be denoted to each diluted sugar mix and each extended sugar mix, 7 levels will be used in total. Calibrate each diluted sugar standard (1:20, 1:15, 1:10, 1:5 and no dilution, 50 μL, 100 μL and 150 μL). A screen will open up in chemstation and it will allow for the concentration of each generated sugar standard to be input. Use the internal standard mode and set the concentration of the internal standard to 13.561 $\mu g \cdot mL^{-1}$. This is important as the calibration curve and all quantitated watermelon samples will be normalized against the internal standard. Once the calibration curves have been quantitated and the concentrations have been added, check the linearity of each independent sugar curve via their r^2 value, an $r^2 = 0.9999$ is preferred.

Alditol acetate concentration

Start with hydrolyzed D/D and D/H sister samples. Quantitate each sample, the concentration ($\mu g \cdot mL^{-1}$) of each neutral sugar in the samples will be calculated by chemstation from the calibration curves. All data will then be exported into excel. Calculate the relative retention time (rrt) of each sugar derivative to the internal standard. This is done by dividing the retention time of the sugar derivative by the retention time of the internal standard. Pettolino et al. (2012) suggests to calculate the mol% of each alditol acetate in the samples. This is done by using supplementary table 1 (Pettolino et al., 2012) as she identifies the formula weight of the derivatized monosaccharides. To calculate mol%, divide the peak area of the derivatized monosaccharide (alditol acetate) by the formula weight. Since the experiment was performed in a quantitative fashion, quantitative estimates of each alditol acetate can calculated. To calculate the concentration, further normalize against the spilt pellet weight of the samples using equation 4.1.

Equation 4.1.

$$\frac{(\mu g \cdot mL^{-1} \text{ of D/D or D/H alditol acetate}) \times (0.750 \text{ mL dichloromethane})}{\text{AIR pellet weight (mg)}} = \begin{matrix}\text{Alditol acetate} \\ \text{concentration} \\ (\mu g \cdot mg^{-1} \text{ AIR})\end{matrix}$$

The D/D and D/H sample concentrations will be averaged together and statistical analysis will be performed on the monosaccharide composition from hydrolyzed alditol acetates.

Degree of methylation and uronic acid concentration

The degree of methylation and uronic acid concentration will also be calculated from the hydrolyzed D/D and D/H sister samples. To calculate the degree of methylation use the peak area of D/D *m/z* = 117, galactose and D/H *m/z* = 117, galactose. Start by dividing the peak area of D/D *m/z* = 117, galactose by the pellet weight of the D/D sample. Then divide D/H *m/z* = 117, galactose by the pellet weight of the D/H sample. This normalizes both D/D and D/H peak areas against the internal standard and pellet weight. To calculate the degree of methylation both ratios of the D/H sample and D/D samples will be used following equation 4.2:

Equation 4.2.

$$\frac{\dfrac{\text{peak area } m/z = 117 \text{ D/H sample}}{\text{D/H AIR pellet weight (mg)}}}{\dfrac{\text{peak area } m/z = 117 \text{ D/D sample}}{\text{D/D AIR pellet weight (mg)}}} \times 100 = \text{Degree of methylation (\%)}$$

To calculate the galacturonic and glucuronic acid concentrations use the D/D data that has been normalized against the pellet weight. The uronic acid concentration will be calculated via the peak area *m/z* = 117, galactose normalized by pellet (see equation 4.2 on how to normalize against pellet weight. The same normalization will be with the peak area, *m/z* = 115, galactose. The ratio of D/D *m/z* = 117, galactose will be divide by the ratio of galactose D/D *m/z* = 115, galactose multiplied the concentration of galactose from equation 4.1. Use equation 4.3 to calculate galacturonic acid concentrations

Equation 4.3.

$$\frac{\dfrac{\text{Gal peak area } m/z = 117 \text{ D/D sample}}{\text{D/D AIR pellet weight (mg)}}}{\dfrac{\text{Gal peak area } m/z = 115 \text{ D/D sample}}{\text{D/D AIR pellet weight (mg)}}} \times \text{Gal conc. } (\mu g \cdot mg^{-1} \text{ AIR}) = \text{galacturonic acid conc. } (\mu g \cdot mg^{-1} \text{ AIR})$$

The same calculation will be used to find the concentration of glucuronic acid in the samples. Be sure to use the peak area of glucose at both *m/z* = 115 and *m/z* = 117 instead of galactose.

Partially methylated alditol acetate (linkage assembly) data processing (30-60 min per chromatogram)

Begin by opening the methylated D/D chromatograms from each of the designated experimental treatments (e.g., graft no HH, graft HH, non-graft no HH, non-graft HH). Integrate each of the chromatograms and export the data to excel. Calculate the relative retention time (rrt) of each partially methylated alditol acetate. Using Pettolino's supplementary table 1, compare each sample's rrt to supplementary table 1. Once the peaks have been identified based on rrt, assess the four treatments via "analyze multiple spectra" in chemstation data analysis. This allows the user to identify the peaks and spectral data in each treatment. The sample peaks and rrt(s) will be compared to the rrt(s) in supplementary table 1 and the spectral data from the Complex Carbohydrate Research Center (Georgia, USA) (http://www.ccrc.uga.edu/specdb/ms/pmaa/pframe.html).

To set up a cell wall polysaccharide linkage assembly method, calibrate and update the opened chromatograms by adding the peaks and compound names with the same tentative retention times and rrt(s) as supplementary table 1. Be sure to calibrate using internal standard mode and set the concentration to 13.561 $\mu g \cdot mL^{-1}$. Then to clean up the linkage assembly method, click on calibrate and then click on "edit compounds" via chemstation data analysis. First open the complex carbohydrate spectral data and compare each peak's spectral data and rrt to supplementary table 1 and then compare to complex carbohydrate spectral data. Edit peaks and compound names based on rrt and spectral data. Delete replicated peaks. Be sure to edit the target quant mass of each compound to the most abundant peak in the spectral data. Check the retention time window and shorten the window if peaks coelute at similar retention times. Some partially methylated alditol acetates can coelute at the same time (and some spectral data is not

available via complex carbohydrate research database); so it may be necessary to generate partially methylated alditol acetate standards to further assess the spectral data.

To obtain linkage assembly data, use MSD chemstation data analysis program. Go to quantitate and click on “custom reports”. A window will open, click on “update as part of method” and “create new database”. Using the database wizard, edit the contents in the database and add items (e.g., sample name and compound name, compound retention time and compound target response). Click okay and a new window will open allowing for samples to be processed. Select the methylated D/D experimental samples, click “okay” and save as a file name. A new window will open and click “edit database”, this will allow the user to see all linkage assembly data generated from the first batch. To analyze the rest of the experimental samples, click on “file” and then “multiple file select”. Browse the data files and select the appropriate methylated D/D chromatograms. Copy and paste all linkage assembly data into excel.

Linkage assembly compound calculations

Since all data is exported into excel, each methylated compound will be normalized against the internal standard. This is done by taking the peak area of the partially methylated alditol acetate (PMAA) divided by the peak area of the internal standard. Then to estimate the content of methylated derivatives, multiply by the concentration of the internal standard. Equation 4.4 is used to get the estimated content of methylated derivatives.

Equation 4.4.

$$\frac{\text{Peak area PMAA}}{\text{Peak area int. std.}} \quad X \quad 13.561\ \mu g \cdot mL^{-1} \quad = \quad \text{estimated content PMAA}$$

Now that the PMAA have been normalized against the internal standard. The concentration of the PMAA’s in each sample will be normalized against the pellet weight. To calculate the estimated concentration of each PMAA in the samples use equation 4.5.

Equation 4.5.

$$\frac{\text{Estimated content PMAA } (\mu g \cdot mL^{-1}) \text{ x } 0.750 \text{ mL dichloromethane}}{\text{AIR pellet weight (mg)}} \quad = \quad \text{PMAA } (\mu g \cdot mg^{-1}) \text{ AIR}$$

Once the concentrations of the PMAA have been calculated and the deduced linkages have been identified. Monosaccharide linkage composition can be done following Table 1 (Pettolino et al. 2012).

Anticipated results

Monosaccharide composition and monosaccharide linkage composition analysis are complementary techniques that provide information on watermelon cell wall polysaccharides and any glycan-containing material. Alditol acetates of the cell walls generated from Saeman hydrolysis can be used to cross-check total monosaccharide levels and to look for naturally occurring methyl sugars.

Monosaccharide linkage composition determined by methylation analysis is far more informative and with pre-reduction is used to determine, for both neutral and acidic sugars simultaneously, how each monosaccharide is linked, the positions of non-glycosyl substituents and possible polysaccharide structures. Pettolino et al. (2012) provides an example of monosaccharide linkage composition from *Arabidopsis* leaf cell walls. Taking into account the comments in Table 1 and anticipated structures in Table 2 (Pettolino et al., 2012), the monosaccharide linkage of watermelon can be used to estimate total cell wall polysaccharide composition.

Notes about modifications

Several changes were made when optimizing for watermelon cell wall analysis including particle size, quantitative transfer, hydrolysis and methylation.

The changes are listed below:

Particle Size: Particle size of the AIR is critical for carboxyl reduction, hydrolysis and methylation. To achieve smaller particle size regrinding of the AIR can be done. The grinding treatments were: 1) control, no grinding, 2) grinding for 30 sec, 3) grinding for 60 sec and 4) grinding for 90 sec. Three mg AIR with 6 x 2.8 mm steel beads were added and ground via bead bug homogenizer. Regrinding AIR for 60 sec achieved an average particle size of 55.3 ± 0.43 μm.

Carboxyl reduction I and II: AIR particles float on top of the $NABD_4$ or $NaBH_4$ - di-water solution. Solubilization of the AIR is done for 2.5 hours; reduction is complete when the ground AIR is fully solubilized and particles sink to the bottom of the test tube.

Centrifugal filters: Instead of dialysis, 3Kda centrifugal filters were used to filter out the small molecules decrease laboratory time.

Quantitative transfer: Performed during carboxyl reduction steps to properly quantify the monomeric building blocks and linkage residues instead of reporting on a %mol basis.

Speed vacuum: Samples were in initially tested on speed vacuum to try and speed up drying time. Issues arose with speed vacuuming as the samples did not fully dry and freeze drying is required.

Sulfuric acid hydrolysis: The standard hydrolysis method for cell wall AIR uses between 63 to 252 µl of 72% sulfuric acid for 3 to 5 mg AIR. Hydrolysis treatments consisting of 63, 126, 189, and 252 µL of 72% sulfuric acid were applied to 3-5 mg of watermelon AIR. Total sugar content was used as a measure of effectiveness. Total sugars were found to be similar between 126 and 252 µL sulfuric acid. At 252 µL, variability among replicates was high so 126 µL sulfuric acid is recommended for complete hydrolysis of 3 ± 0.21 mg watermelon.

Methylation: For Arabidopsis, 50 µL of dimelthyl sulfoxide was used to solubilize the AIR. Watermelon AIR did not fully solubilize in 50 µL of dimelthyl sulfoxide, instead required 200 µL of dimethyl sulfoxide. Watermelon AIR samples were solubilized overnight (~16 hours).
Visual distinguisher: watermelon samples are fully solubilized when the opaqueness of the AIR turned from a white pellet to translucent/clear.

- Still had some issues with our methylation and deduced linkages. Thoughts on this may be due to the amount of iodomethane applied to the pellet. For Arabidopsis when 50 µL of dimelthyl sulfoxide was applied to solubilize the pellet, 10 µL of iodomethane was applied and the sample was sonicated for 10 min. Then, 10 µL of iodomethane was applied and again sample was sonicated for 10 min. Finally, 20 µL iodomethane was applied and the sample was sonicated for 20 min.
- Since the amount of dimethyl sulfoxide increased from 50 µL to 200 µL increasing the amount of iodomethane applied from 10 µL to 40 µL for the first two applications plus increase sonicating time from 10 min to 40 min may better optimize this step.

Total pectin content in watermelon

Along with cell wall polysaccharide assays, total pectin extraction is important to better elucidate the nature of rootstock-mediated affects and HH disorder. Correlating cell wall polysaccharide data (e.g., neutral sugars, degree of methylation, uronic acid concentrations and linkage assembly) to total pectin sequential fraction. Pectin can be analyzed by extraction of total pectins or via intensive wet chemistry to characterize cell wall polysaccharides (Soteriou et al., 2017; Pettolino et al., 2012). Total pectin content is assessed via sequential fractions of total cell wall material. The fractions are water soluble (WSF), carbonate soluble (CSF), alkali soluble (ASF) and unextractable fractions.

Each fraction is known to have different types of pectic polysaccharide classes, which are useful when compared to cell wall polysaccharide analysis. Total pectin extraction is a more general approach while complete characterization is robust. The WSF yield pectins "freely bound" in the plant cell well and are also freely soluble in the apoplast (Panigua et al., 2014). CSF are considered to be enriched in de-esterified pectins covalently bound to the cell wall (Panigua et al., 2014). They are also found be enriched in homogalacturonan (Panigua et al., 2014; Soteriou et al., 2017). ASF are derived from matrix glycans tightly attached to the cell wall via hydrogen bonds and are generally the hardest to solubilize (Brummell and Harpster, 2001). ASF are also considered to have a low degree of methylesterification and high polyuronide (uronic acid) concentrations compared to WSF and CSF (Soteriou et al., 2017).

The implications of total pectins alongside cell wall polysaccharide characterization may better suggest how changes in fruit textural characteristic are associated with the cell wall. Soteriou et al. (2017) speculates that de-esterified pectins bound to the cell wall by covalent bonds and matrix glycans tightly attached to the cell wall by hydrogen bonds may be most responsible for changes in fruit textural characteristics. Determining qualitative differences of cell wall pectic polysaccharides and total pectin content may help to better understand the role of the cell wall and fruit textural differences.

Objective

Determine total pectin content in watermelon alongside cell wall polysaccharide linkage assembly data.

Approach

The method of Soteriou et al. (2017) was followed for total pectin extraction. Starting with extracted watermelon cell wall material, total pectin fractions were sequentially extracted from watermelon AIRs as follows: water soluble fraction (WSF), carbonate soluble fractions (CSF), alkali soluble fraction (ASF) and unextractable fraction (UNX) (Fig 4.4). Total neutral sugars and uronic acids of each fraction were quantified to assess differences in the pectic fractions in grafted and non-grafted fruit at varying levels of HH. Materials and equipment needed for the assays are provided in tables 4.10 and 4.11.

Materials lists

Table 4.11. List of chemicals required for total pectin extraction.

Chemical	Company	Cas no.	grade	Quantity
sodium bicarbonate,	Sigma-Aldrich	144-55-8	ACS reagent	25g
sodium carbonate	Sigma-Aldrich	497-19-8	anhydrous	500 g
Potassium hydroxide	Sigma-Aldrich	1310-58-3	ACS reagent	250 g
Ultrapure water	Sigma-Aldrich	TMS-006	Cell culture	1 L
Galacturonic acid (monohydrate)	Sigma-Aldrich	91510-62-2	Analytical, ≥99.9%	5 g
d-Glucose	Sigma-Aldrich	47829	Analytical	1 g
Sodium tetraborate	Sigma-Aldrich	1330-43-4	≥99.9%	100 g
3-phenylphenol	Sigma-Aldrich	580-51-8	ACS Reagent	5 g
Sulfuric acid	Sigma-Aldrich	7664-93-9	Airstar	1 L
Calcium carbonate	Sigma-Aldrich	471-34-1	≥ 99.0%	250 g
Methanol	Fisher	64-56-1	HPLC	16 L
Ethanol	Fisher	64-17-5	Analytical	16 L
Acetone	Sigma-Aldrich	67-64-1	HPLC	16 L
Liquid N	Airgas		t-tank	
Phenol	Sigma-Aldrich			

Table 4.12. List of equipment and instrumentation for total pectin extraction.

Equipment	Company	Headquarters
Amber glass vials, 40 mL	Glassvials.com	
Nylon mesh filters, 60 μm, 47 mm diam.	Millipore Sigma	
Nylon mesh filters, 20 μm, 47 mm diam.	Millipore Sigma	
Geno/Grinder 2010, Model SN 10592	Spex Sample Prep	USA, Metuchen, NJ
Steel beads, 6.5 mm, magnetic, high carbon (4RJH5)	Grainger	USA, Lake Forest, IL
Steel beads, 2.8 mm, magnetic, high carbon (4RJH5)	Grainger	USA, Lake Forest, IL
BeadBug Microtube Homogenizer, Model D1030	Sigma-Aldrich	Germany, Darmstadt
Benchtop Sorval Legend RT Centrifuge, Model D-37520 Osterode	Thermo Electron Corporation	Waltham, MA
Freeze dryer, Model 24DX48GPFD, 25 L, EL-85	Virtis	USA, Houston, TX
Erlenmeyer flasks with rubber tubing (filtration)	Labware	
Buchner funnel	Labware	
UV-2450 Spectrophotometer equipped with UVProbe 2.34 software	Shimadzu Corp.	Kyoto Japan
Microcentrifuge tubes with screw cap (PFSS 2800-50-20U)	OPS Diagnostics	USA, Lebanon, NJ
Hot plate		
Thermometer, alcohol, 0-100 ºC		
Incubator Shaker Series, Model I 24	New Brunswick Scientific	USA, Edison, NJ

Flow Chart of Methods

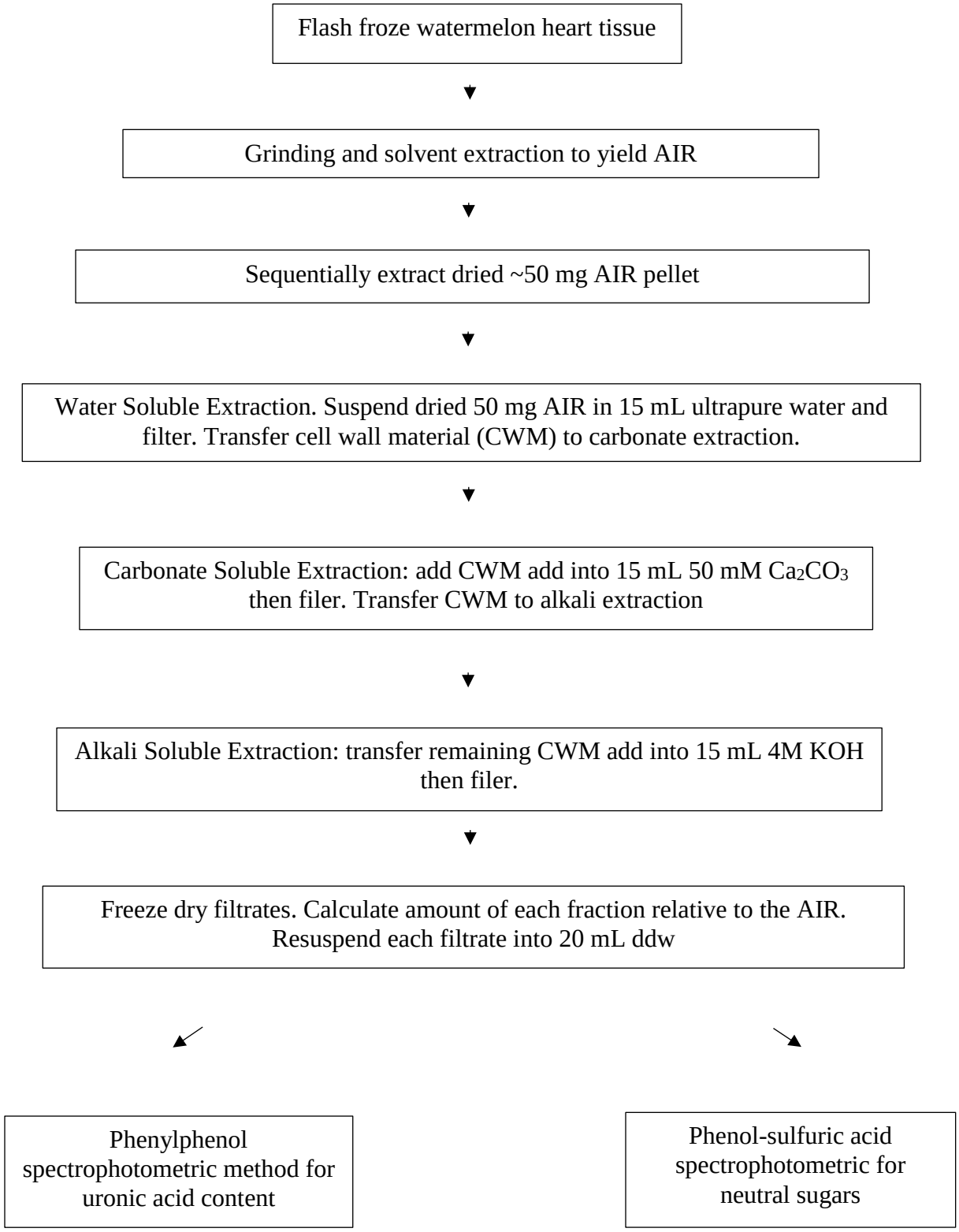

Figure 4.5. Schematic methods for total pectin extraction.

Table 4.13. Preparation and sampling of fresh watermelon fruit tissue for total pectin extraction.

Steps	Description
1	Clean the exterior of the fruit by wiping away any dirt or remining debris left on the fruit.
2	Rinse the fruit with tap water and then spray a 5% bleach solution on the fruit. Carefully wipe the exterior of the fruit.
3	Completely dry the fruit
4	Longitudinally cut the fruit (stem to blossom end) to expose watermelon flesh
5	Excise the heart tissue from the watermelon, free of locules, seed cavity and seed. Aim for ~100 grams.
6	Label a 4x6 sample bag with the sample name, place watermelon tissue in the bag and immediately place into a -80 ºC freeze (Fig 4.5)

Figure 4.6. Image showing total pectin sample extraction from the placental tissue, free of locules and seed traces.

Table 4.14. Comprehensive total pectin extraction methods and identification of total neutral sugars and uronic acids (6-8 hrs).

Steps	Description of methods
1	Start by recording the weight of the 50 mL test tube then pre-tare and add 10 g of pre-frozen watermelon into the test tube. Record the weight of watermelon to 4 decimals. Add 4 x 6.5 mm steel balls and 15 mL of 80% ethanol. Samples will be ground with a Geno/Grinder in ethanol. *Need 50 mg of watermelon cell wall material (CWM) after all extractions. Since size of test tubes are 50 mL, be sure to double each watermelon sample for the first ethanol rinse (will have two test tubes with 10 g fresh watermelon per one sample to achieve 50 mg AIR pellet)
2	Flash freeze samples by immersing tubes in liquid N 30-45 sec. Transfer the test tube to aluminum block, then transfer to Geno/Grinder and grind sample for 8 min at 20 Hz (1,200 rpm). Be sure to check temperature of matrix, keep below 4 ºC. Remove the steel beads
4	Place the samples for 30 min on ice. Centrifuge samples in centrifuge for 5 min at 4,000*g* at 4 ºC. Collect CWM on 60 µm nylon? mesh and discard the supernatant. Be extremely careful to keep all CWM for quantification purposes. The two ethanol residues will then be combined after the first extraction.
5	For the 2nd and 3rd ethanol extraction use 20 mL of 80% ethanol. Be sure to vortex all samples for 45-60 sec after each addition of ethanol. Centrifuge for 5 min at 4,000*g*. Collect CWM on 60 µm mesh and discard the supernatant. Repeat until a clean sample is obtained. Discard supernatant between washes. **Three ethanol washes are required in total.**
6	Add 20 ml of acetone at room temperature. Vortex sample for 45-60 seconds. Extract material for 10 min. Centrifuge (5 min 4,000*g*, room temperature) and discard the supernatant being sure to filter CWM through 60 µm mesh.
7	Add 20 mL of methanol. Vortex the sample for 45-60 seconds. Centrifuge (5 min 4,000*g*, room temperature) and discard the supernatant. Filter through 60 µm mesh and discard the supernatant.
8	Another acetone and methanol rinse is required: Add 20 mL of acetone at room temperature. Vortex sample for 45-60 seconds. Extract material for 10 min. Centrifuge for 5 min at 4,000*g* and discard the supernatant being sure to collect any CWM that isn't pelletized on 60 µm mesh.
9	Add 20 mL of methanol. Vortex the sample for 45-60 seconds. Centrifuge for 5 min at 4,200 rpm and discard the supernatant. Filter through 60 µm mesh and discard the supernatant.

Table 4.14. (continued)

10	Repeat acetone and methanol extraction steps. **Three total acetone and methanol extractions are required**.
11	Place samples in a fan forced oven at 37 ºC for 16 hours
12	Pull from oven and calculate weight of AIR compared to fresh weight: AIR (mg) / Fresh weight (mg) x 100 = %AIR from fresh watermelon
13	Store samples on desiccant until ready to preform sequential extraction.

Methods for sequential extractions of AIR from watermelon flesh tissue

Reagent set up

1. Sodium bicarbonate-carbonate ($NaCO_3$)
    a. Using a 1000 mL volumetric flask, add 1.05 g sodium bicarbonate and 9.275 g sodium carbonate (anhydrous) to the flask. Fill the flask half way and solubilize the pellets. Then fill to volume
    b. A 50 mM solution is required. Prepare by using the solution generated in part A: pipet 50 mL of 1 M sodium bicarbonate in part A into a 1,000 mL volumetric flask and fill the flask to volume

2. 4 M potassium hydroxide (KOH)
    a. Fill a 500 mL volumetric flask half full with di-water, add 112.0 g of KOH and solubilize the pellets, then fill to volume (final volume adjustment should be done when at ambient temperature)

Table 4.15. Water soluble fraction extraction (WSF) (3 hr).

Steps	Description of methods
1	Accurately weigh out ~50 mg of CWM from AIR and record the weight to 4 decimals.
2	Suspend the sample in 15 mL of ultrapure water in a 40 mL labeled, amber vial.
3	Place the vial with sample on an orbital shaker, set at 180 rpm (room temperature) for 2.5 hours
4	Remove from shaker and vacuum filter the sample through 20 µm nylon net filters.
5	Save the filtrate and collect the remaining CWM on the nylon net filters.
6	Record the weight of test tube without sample. Transfer the filtrate to 50 mL test tubes, label the test tube. Store in -80 ºC until ready to freeze dry all samples.
7	Sequentially transfer CWM to the Carbonate Soluble Steps.

Table 4.16. Carbonate soluble fraction extraction (CSF) (~3 hr).

Steps	Description of methods
1	Quantitatively transfer CWM from WSF. The CWM will be on the 20 µm nylon filters. To quantitively transfer use a metal spatula and remove all CWM and place into a cleaned amber vial. Rinse with 500 µL 3 times into the amber glass.
2	Suspend the CWM into 15 mL of prepared 50 mM Na_2CO_3 into a new 40 mL amber vial.
3	Place the vial on an orbital shaker, set at 180 rpm (room temperature) for 2.5 hours
4	Vacuum filter the sample through 20 micrometer nylon net filters: save filtrate and CWM.
5	Record the weight of 50 mL test tube without filtrate. Then save the filtrate by transferring to 50 mL test tubes, label the test tube. Store in -80 ºC until ready to freeze dry all samples.
6	Sequentially transfer CWM from carbonate soluble fractions to Alkali Soluble steps

Table 4.17. Alkali soluble fraction extraction (ASF) (~3 hr).

Steps	Description of methods
1	Quantitatively transfer CWM from CSF. The CWM will be on the 20 µm nylon filters. To quantitively transfer use a metal spatula and remove all CWM and place into a cleaned amber vial. Then using 500 µL of water rinse the filter 3 times into the amber glass.
2	Suspend the sample into 15 mL of prepared 4 M KOH in a new, labeled 40 mL amber vial.
3	Place the vial on an orbital shaker set at 180 rpm (room temperature) for 2.5 hours. Then Vacuum filter the sample through 20 micrometer nylon net filters.
4	Save the filtrate by transferring to pre-tared, labeled, 50 mL test tubes. Store in -80 ºC until ready to freeze dry all samples.
5	Transfer the filtrate to 50 mL test tubes, label the test tube. Store in -80 ºC until ready to freeze dry all samples.
6	Collect the remaining CWM fraction and label as “unextractable fraction”
7	Place unextractable fractions into a labeled weigh boat/container.
8	Oven dry unextractable fraction at 50 ºC for 4 days hours to obtain dry weight of fraction.

Freeze drying Filtrates

A. Remove the filtrates from -80 ºC
B. Place into a Freeze dryer for 10 days. Freeze dry shelf parameters were held at -25 ºC, for 240 mins and 50 mtorr, then -20 ºC for 500 mins at 200 mtorr, then -10 ºC for 1200 min at 190 mtorr, -5 ºC for 1200 min at 100 mtorr, 0 ºC, for 1,200 min at 50 mtorr, +10 ºC for 1,200 min at 50 mtorr, +20 ºC for 1,200 min at 50 mtorr then +26 ºC at 50 mtorr for the remaining time of freeze drying. The condenser was held at -60 during each freeze drying step. Samples were pulled from the freeze dryer
C. Record the weight of each freeze dried filtrate
D. Calculate pectins; mg fraction (WSF, CSF or ASF) / mg AIR x 100 = % pectic fractions from AIR
E. Suspend the freeze dried filtrates into 20 mL of ddw to dilute the amount of CWM in the sample (e.g., lower the concentration of total neutral sugars and uronic acids)
F. Follow spectrophotometric assays for uronic acids or phenol-sulfuric acid assay for neutral sugar concentrations

Phenylphenol spectrophotometric assay for total uronic acids

Galacturonic acid is used as the calibration standard; prepare solutions of galacturonic acid from 0 to 100 $mg \cdot mL^{-1}$. Store the calibration solutions in a -80 ºC freezer. Results will be expressed in galacturonic acid equivalents per g of CWM from each of the sequential extractions. This method does not account for rhamnose, galactose and arabinose components (Blumenkrantz and Asbore-Hansen, 1973)

Reagent set up

1. Galacturonic Acid Stock Solution (1000 $\mu g \cdot mL^{-1}$, store at -80 ºC for 12 months)
    a. Weigh 109.2 mg of D-Galacturonic acid monohydrate and dissolve into 100 mL of ddw
        i. Pipette 250 µL GA stock solution into a 25 mL volumetric flask. Bring to volume with ddw. The concentration of GalA in this sample will be 10 $\mu g \cdot mL^{-1}$
    b. Prepare the following concentrations:
        i. 250 µl stock solution into 25 mL-> 10 $\mu g \cdot mL^{-1}$
        ii. 500 µL stock solution into 25 mL -> 20 $\mu g \cdot mL^{-1}$
        iii. 1000 µL stock solution into 25 mL-> 40 $\mu g \cdot mL^{-1}$
        iv. 1500 µL stock solution into 25 mL -> 60 $\mu g \cdot mL^{-1}$
        v. 2000 µL stock solution into 25 mL -> 80 $\mu g \cdot mL^{-1}$
        vi. All solutions are stored in a labeled test tubes at -80 ºC for 12 months

2. Sodium tetraborate in sulfuric acid (0.0125 M Solution)
    a. Weigh 0.629 g anhydrous sodium tetraborate (Na_2BO_4) into a 250 mL volumetric flask. Add a small amount (0.5 mL) ddw to improve solubility. Carefully add 100-150 mL of concentrated sulfuric acid. Mix well. Leave overnight in a fume hood if sodium tetraborate is not solubilized. Bring to volume with concentrated sulfuric acid. Store in the fume hood at ambient temperature for 6 mo

3. M-Hydroxydiphenyl solution (0.15%) (Chromogenic Reagent)
    a. Weigh 15 mg m-hydroxydiphenyl into a 10 mL volumetric flask. Bring to volume with 0.5% sodium hydroxide solution. Separate into appropriately sized aliquots and cover with aluminum foil to protect from light. Store at ambient temperature for 6 mo.

Table 4.18. Phenylphenol colorimetric micro method for total uronic acids.

Steps	Protocol
1	Pipet 0.2 mL of the sequential cell wall extractions (WSF, CSF and ASF) and galacturonic standards into labeled microcentrifuge tubes. For every cell wall fraction sample, two tubes are required. One tube is considered the blank and no meta-hydroxydiphenol will be added, the second tube is the chromogenic sample with the addition of meta-hydroxydiphenol.
2	Place all labeled tubes in an ice bath and add 1.2 mL of sulfuric acid/tetraborate to all of the samples.
3	Keep samples on ice for 5 min
4	Place the tubes in a vortex mixer for 45-60 sec. and then into a heated water bath held at 100 ºC for 5 min
5	Cool the samples in a ice-water bath for 2-3 min. Then remove from ice bath and perform the next steps at room temperature.
6	To the reagent blank add 20 µL 0.5% sodium hydroxide and be sure to zero the spectrophotometer with the blank prior to sample readings. Take the absorbance of the reagent blank and blank samples at 520 nm.
7	To the "blank samples' add 20 µL 0.5% sodium hydroxide.
8	To the "chromogenic samples" and add 20 µL of meta-hydroxy-diphenyl to each of the tubes
9	Vortex/shake the tubes for 15-30 sec
10	Take absorbance measurements at 520 nm in a spectrophotometer within 5 min of adding meta-hydroxy-diphenyl. Carbohydrates produce a pinkish chromogen with sulfuric acid/tetraborate at 100 ºC and the addition of meta-hydroxy diphenyl
12	Be sure to take the absorbance of the blank sample and subtract from the total absorbance of the samples.
13	Plot a calibration curve of Absorbance (y-axis) against concentration of galacturonic acid (x-axis). Use this curve for standardization.

Phenol-sulfuric acid colorimetric assay for total sugars

Reagent set up follows Masuko et al., 2005

1. Make a stock solution of d-glucose (1000 $\mu g \cdot mL^{-1}$): accurately weigh 100 mg of dry D-glucose and dissolve into 100 mL of ddw. Store in a labeled test tube at -80 ºC for 12 months.

a. Pipette 250 µL glucose stock solution into a 25 mL volumetric flask. Bring to volume with ddw. The concentration of GA in this sample will be 10 $\mu g\ mL^{-1}$ Prepare the following concentrations:
b. 250 µl stock solution into 25 mL-> 10 $\mu g \cdot mL^{-1}$
c. 500 µL stock solution into 25 mL -> 20 $\mu g \cdot mL^{-1}$
d. 1000 µL stock solution into 25 mL-> 40 $\mu g \cdot mL^{-1}$
e. 1500 µL stock solution into 25 mL -> 60 $\mu g \cdot mL^{-1}$
f. 2000 µL stock solution into 25 mL -> 80 $\mu g \cdot mL^{-1}$
g. All solutions are stored in a labeled test tubes at -80 ºC for 12 months

2. 5% phenol solution (vol/vol%)
    a. Pipet 5 mL of phenol into 100 ml volumetric flask
    b. Bring up to volume with ddw
    c. Transfer to a glass storage container and shake well
    d. Store in a chemical cabinet at ambient temperature for 6 mo.

Table 4.19. Phenol-sulfuric acid colorimetric assay for total neutral sugars.

Steps	Protocol
1	Pipet 150 µL of diluted filtrates into and glucose standards into a microcentrifuge tube
2	Add 450 µL of concentrated sulfuric acid to each sample
3	Immediately pipet 90 µL of 5% phenol into the same sample
4	Heat samples for 5 min at 90ºC
5	Cool in a room temperature water bath for 5 min.
6	Run a blank di-water sample to zero the spectrophotometer
7	Transfer sample from microcentrifuge tube to glass cuvette and read absorbance at 490 nm
8	Generally the calibration curve will be done and run first to ensure linearity in the standards. Then the samples will be prepared
9	Plot a calibration curve of absorbance (y-axis) against concentration of D-glucose (x-axis). Use this curve for standardization

References

1. Argawal, U., J.Y. Zhu and S.A. Ralph. 2011. Hydrolysis of biomass: Effects of crystallinity, particle size and lignin removal. Proceedings of ISFWPC 1:910-914.

2. Al-Dulaimi, A., R. Rohaizu, and W.D. Wanrosli. 2015. Production of nanocrystalline cellulose from empty fruit bunches using sulfuric acid hydrolysis: Effect of reaction time on the molecular characteristics. J. Physics 622:1-6.

3. Blankenly. A., P.J. Harris, R. Henry, and B. Stone. 1983. A simple and rapid preparation of alditol acetates for monosaccharide analysis. Carbohydrate Res. 113:291-299.

4. Blumenkrantz, N and G. Asboe-Hansen. 1973. New Method for Quantitative Determination of Uronic Acids. Anal. Biochem. 54:484-489.

5. Broxterman, S. and H. Schols. 2018. Interactions between pectin and cellulose in plant cell walls. ScienceDirect 192:263-272.

6. Brummel, D.A. 2006. Cell wall disassembly in ripening fruit. Funct. Plant Biol. 33:103-119.

7. Brummell, D.A. and M.H. Harpster. 2001. Cell wall metabolism in fruit softening and its manipulation in transgenic plants. Plant Mol. Biol. 47:311-340.

8. Caffall, K.H. and D. Mohnen. 2009. The structure, function and biosynthesis of plant cell wall pectic polysaccharides. Carbohydrate Res. 14:1879-1900.

9. Ciucanu, I. and F. Kerek. 1984. A simple and rapid method for the permethylation of carbohydrates. Carbohydrate Res.131:209–217.

10. Cosgrove, D. J. 2005. Growth of the plant cell wall. Nature Reviews Mol. Cell Biol. 6:850–861.

11. Gates, P.D. 2008. Gas chromatography mass spectrometry. University of Bristol. [Online]. http://www.bris.ac.uk/nerclsmsf/techniques/gcms.html

12. Harazono, A., T. Kobayashi, N. Kawasaki, S. Itoh, M. Tada, and N. Hashii, N. 2011. A comparative study of monosaccharide composition analysis as a carbohydrate test for biopharmaceuticals. Biol. 39:171–180.

13. Hofte, H., A. Peaucelle and S. Braybrook. 2012. Cell wall mechanics and growth control in plants: the role of pectins revisited. Front. Plant Sci. 3:121-130.

14. Houben, K., R.P. Jollie, I. Fraeye, A.M. Van Loey, and M. Hendrick. 2011. Comparative study of the cell wall composition of broccoli, carrot, and tomato: Structural

characterization of the extractable pectins and hemicelluloses. ScienceDirect 346:1105-1111.

15. Hu, R., L. Lin, T. Liu and S. Liu. 2010. Dilute sulfuric acid hydrolysis of sugar maple wood extract at atmospheric pressure. Bioresearch Tech. 101:3586-3594.

16. Jung, H.J. and R. Bernardo. 2012. Comparison of Polysaccharide Hydrolysis by a Dilute Acid/Enzymatic Saccarification Process and Rumen Organisms. BioEnergy 5:319-329.

17. Karakurt, Y. and D.J. Huber. 2008. Cloning and characterization of differentially expressed genes in ethylene-treated watermelon fruit. Postharvest Biol. Tech. 48:372-377.

18. Karakurt, Y., N. Muramatsu, J. Jeong, B. Hurr and D. Huber. 2008. Matrix glycan depolymerization and xyloglucan endohydrase activity in ethylene-treated watermelon fruit. J. Sci. Food Agric. 88:684-689.

19. Kim, J.B. and N.C. Carpita. 1992. Changes in esterification of the uronic acid groups of cell wall polysaccharides during elongation of maize coleoptiles. Plant Physiol. 98:646–653.

20. Lareo, C., M. Ferrari, M. Guigou, L. Fajardo, V. Larnaudie, M. Ramierez and J. Martinez-Garrerio. 2013. Evaluation of sweet potato for fuel bioethanol production: hydrolysis and fermentation. Springer Plus 2:2-11.

21. Li, Y. R. Mehta and J. Messing. 2018. A new high-throughput assay for determining soluble sugar in sorghum internode-extracted juice. Planta 248:785-793.

22. Masuko, T., A. Minami, N. Iwasaki, T. Majima, S-I Nishimura and Y.C. Lee. 2005. Carbohydrate analysis by a phenol-sulfuric acid method in microplate format. Anal. BioChem. 339:69-72.

23. McFeeters, R.F., H.P. Flemming and M.A. Daeschel. 1984. Maleic acid degradation and brinded cucumber bloating. J. Food Sci. 49:999-1002.

24. Mohnen, D. 2008. Pectin structure and biosynthesis. Curr. Opinion Plant Biol. 11:266–277.

25. Paniagua, C., N. Santiago-Domenech, A.R. Kirby, A.P. Gunning, V.J Morris, M.A. Quesada, A.J. Matas and J.A. Mercado. 2017. Structural changes in cell wall pectins during strawberry fruit development. Plant Physiol. Biochem. 118:55-63.

26. Pettolino, F.A., C. Walsh, G.B. Fincher and A. Bacic. 2012. Determining the polysaccharide composition of plant cell walls. Nature Protoc. 9:1590-1607.

27. Petkowicz, C.L.O, L.C. Vriesmann, and P.A. Williams. 2016. Pectins from food waste: Extraction, characterization and properties of watermelon rind pectin. Food Hydrocolloids 65:57-67.

28. Saeman, J.F. W. Moore, R.L. Mitchell and M.A. Millet. 1954. Techniques for the Determination of Pulp Constituents by Quantitative Paper Chromatography. TAPPI, 37(8):336-343.

29. Soteriou, G.A., A.S. Simons, D. Gerasopoulos, Y. Rouphael, S. Georgiadou and M.C. Kyriacou. 2017. Biochemical and histological contributions to textural changes in watermelon fruit modulated by grafting. Food Chem. 237:133-140.

30. Taylor, N. G. 2006. Cellulose biosynthesis and deposition in higher plants. New Phytol. 178:239–252.

31. Wang, D. T.H. Yeats, S. Uluisik, J.K.C. Rose and G.B. Seymour. 2018. Fruit Softening: Revisiting the role of pectin. Trends Plant Sci. 23:302-310.

32. Willfor, S., A. Pranovich, T. Tamminen, J. Puls, C. Laine, A. Suurnakki, B. Saake, K. Uotila, H. Simolin, J. Hemming, and B. Holmbom. 2009. Carbohydrate analysis of plant materials with uronic acid containing polysaccharides- A comparison between different hydrolysis and subsequent analytical techniques. Carbohydrate Poly. 29:571-580.

33. Worrall, K. and A. Newton. 2004. The advantages of using GC-MS for the analysis of trace components in complex matrices. Waters Corporation, pp 1-3.

CHAPTER 5

THE BACKBONE OF FRUIT: EXPLORING CELL WALL POLYSACCHARIDES IN GRAFTED AND NON-GRAFTED WATERMELON WITH AND WITHOUT HOLLOW HEART

Abstract

Triploid (seedless) watermelon cultivars are susceptible to hollow heart (HH), an internal fruit disorder. HH was induced in a high percentage of 'Liberty' fruit by reducing pollen availability. Grafting scions to 'Carnivor', an interspecific hybrid rootstock (*C. moschata* x *C. maxima)*, reduced HH by 34% and increased tissue firmness by 3 N. Cell wall pectins were explored in watermelon fruit with or without HH from grafted or not grafted plants. Alcohol insoluble residues (AIR) were sequentially extracted to yield water soluble (WSF), carbonate soluble (CSF), alkali soluble (ASF) and unextractable (UNX) fractions. Total neutral sugars and uronic acids were quantified in the sequential fractions. A second set of AIRs were reduced, hydrolyzed, methylated for linkage assembly, derivatized then acetylated and analyzed by GC-MS for compositional analysis of monosaccharide building blocks and partially methylated alditol acetates. The CSF residue was less abundant in fruit with HH (24.5 % AIR) compared to those without HH (27.1 % AIR). No differences were found in total neutral sugars or total uronic acids content among watermelon from the various HH or grafting combinations. Twelve monosaccharide building blocks were detected in watermelon cell wall material. Glucose and galactose were in highest amounts followed by xylose and arabinose. No differences were found in degree of methylation of galacturonic and glucuronic acids due to grafting treatment or HH phenotype. In fruit with HH, meso-erythritol (0.032 $\mu g \cdot mg^{-1}$), fucose (2.36 $\mu g \cdot mg^{-1}$), rhamnose (3.38 $\mu g \cdot mg^{-1}$) and arabinose (21.29 $\mu g \cdot mg^{-1}$) were higher compared to fruit without HH. Conversely, fruit without HH had the highest concentration of 2-deoxy-d-glucose (0.42 $\mu g \cdot mg^{-1}$). In watermelon cell walls, 32 polysaccharide linkages were found and 3 linkages, 4-Glc(p), 3-Glc(p) and 2,4-Glc(p), were highest in grafted fruit without HH ($p < 0.05$). Although fruit textural characteristics were different between grafting treatments, no clear trends were identified in cell wall composition and the current analyses could not fully explain the increased fruit tissue firmness. In future watermelon research, exploring the relationships among fruit tissue microstructure, middle lamella separation, degree of polymerization and enzyme activity may help link textural differences to cell wall composition.

Introduction

In the U.S., seedless (triploid) watermelon now make up 90-95% of the U.S. market (Levi et al., 2014). Triploid watermelon are prone to an internal fruit disorder known as hollow heart (HH), characterized by a cavity or void air space in the center of the fruit (Johnson 2014; 2015). Watermelon pollination plays a role in the onset of HH because triploid fruit do not produce viable pollen, they require diploid (seeded) pollenizer plants (Freeman et al., 2007). Inadequate pollination from reduced bee visits or limited pollen release due to cold or wet weather is also thought to be one of the leading causes of HH in watermelon (Johnson, 2015). Hollow heart disorder may also be induced by reducing the ratio of diploid to triploid plants during production (Trandel et al., 2020a).

Grafting watermelon onto *Cucurbita* rootstocks has been used as a means to reduce damage caused by soil-borne diseases (Mohamed et al., 2012). Additionally, grafting onto interspecific hybrid rootstocks (*Cucurbita maxima* x *C. moschata*) has been reported to increase tissue firmness (e.g., tissue density), rind thickness, lycopene content, and postharvest shelf life (Soteriou et al., 2014; 2017). Triploid fruit with lower tissue firmness tend to have a higher incidence of HH (Trandel et al., 2020b). Hollow heart is thought to develop as a result of unequal expansion of placental and rind tissues (Kano, 1993). Additionally, the morphological characteristics of fruit cells can affect cell wall strength, firmness of fruit, and pectin content in the cell wall (Ng et al., 2013). It may be possible to decrease HH incidence by grafting watermelon to interspecific hybrid rootstocks.

The plant cell wall is critical to internal flesh quality of many crops, including watermelon. The cell wall maintains fruit structural integrity as cell size expands and associated extracellular air spaces develop during fruit growth and maturation (Ng et al., 2013). A primary cell wall is ubiquitous among all plant tissues and serves a variety of functions, including cell wall strength, integrity, and protection of intracellular contents (Rose et al., 2003; Brummell, 2006). In general, plant cell walls are composed of polysaccharides (90% of dry weight), structural glycoproteins (2-5%), phenolic esters (< 2%) and minerals (5%) (Rose et al., 2003). Cell wall polysaccharides commonly include cellulose, hemicellulose and pectins.

During fruit growth and development, the cell wall undergoes protoplast-controlled modification in both morphology and composition (Tanner and Loewus, 2012). Pectic polysaccharides are deposited during the formation of new cell walls in the process of cell plate

formation (Amos and Mohnen, 2019). The plate persists during deposition of the primary cell wall and layers of pectic polysaccharides are secreted then pushed outward via internal cell pressure (Tanner and Loewus, 2012), resulting in a pectin-rich middle lamella (Amos and Mohnen, 2019). Crosslinking of pectin within the middle lamella strongly controls intercellular junction and cellular adhesion (Ng et al., 2013; Daher and Braybrok, 2015; Amos and Mohnen, 2019). As a fruit matures, pectin depolymerization and de-esterification occurs (e.g., breakdown of pectin) and changes crosslinking within the middle lamella, loosening cell to cell adhesion that leads to lower tissue firmness (Amos and Mohnen, 2019; Ng et al., 2013). Pectin breakdown can affect the strength of the cell wall along with other ripening changes (Daher and Braybrok, 2015) and researchers propose pectin may be most responsible for decreasing tissue firmness and diminishing flesh quality (Brummell, 2006; Amos and Mohnen, 2019).

Cell wall structure has been linked to changes in fruit quality and firmness (Brummell, 2006). Ways to explore this relationship generally involve assays of pectin and hemicellulose and may include broad categorization of total pectin and pectic fractions or specific polysaccharide quantification and determination of linkage resides. Total pectin content can be assessed via sequential fractions of total cell wall material. The sequential fractions are water soluble (WSF), carbonate soluble (CSF), alkali soluble (ASF) and unextractable fractions. The water soluble fraction yields pectins “freely bound” in the plant cell well and are also freely soluble in the apoplast (Paniagua et al., 2014). The carbonate soluble fraction is considered to be enriched in de-esterified pectins covalently bound to the cell wall enriched in homogalacturonan (Paniagua et al., 2014; Soteriou et al., 2017). The alkali soluble fraction is derived from matrix glycans that are tightly attached to the cell wall via hydrogen bonds, and this fraction is generally the hardest to solubilize (Brummell and Harpster, 2001). The alkali soluble fraction is also considered to have a low degree of methylesterification (Gawkowska et al., 2019) and high polyuronide (uronic acid) concentrations compared to the WSF and CSF (Soteriou et al., 2017).

Total pectin and sequential fractions have been identified in watermelon fruit. Watermelon has a low degree of pectin solubilization, meaning it is difficult to extract pectin from the cell wall and place it into solution; (Brummell, 2006). Highest fractions of total cell wall material were found for ASF (40%), CSF (37%) and lowest was WSF (23.0%). Soteriou et al. (2017) performed total pectin extraction on placental tissue to explore watermelon textural differences in non-grafted watermelon (lower heart firmness) and watermelon grafted onto

interspecific hybrid rootstocks (higher tissue firmness). Pectin solubilization of the total cell wall material was very low at around 0.65%. No differences were found among the sequential pectic fractions, implying that the firmness differences identified between grafted and non-grafted watermelon could not be explained by WSF (Soteriou et al., 2017). However, a positive correlation was seen between tissue firmness and the sum of insoluble pectic fractions (e.g., %CSF + %ASF). This relationship suggests that changes in watermelon fruit textural characteristics may be associated with fractions containing de-esterified pectins bound to the cell wall by covalent bonds, and matrix glycans tightly attached to the cell wall by hydrogen bonds (Brummell and Harpster, 2001).

Cell wall composition (polysaccharide assays) entails quantification of cellulose, hemicellulose and pectin (Pettolino et al., 2012). These assays can be used to deduce the various pectic classes through identification of monosaccharides and associated linkage assembly. This provides more robust information than total pectin extractions as the various pectic classes can be deduced by combining monosaccharide composition with linkage assembly. Cell wall composition was used to determine changes in watermelon tissue firmness induced by ethylene. Ethylene stimulates polygalacturonase activity in watermelon, which depolymerizes cell wall pectins and softens fruit texture (Karakurt et al., 2008; Mort et al., 2008). Watermelon were treated with 50 $\mu L \cdot L^{-1}$ of ethylene or air-treated (ambient control) and then were stored for 6 d. Placental tissue was excised from the watermelon and prepared into alkali soluble fractions. Cell walls were depolymerized using enzymatic hydrolysis (endo-polygalacturonase) prior to pectin fraction extraction, followed by quantification of the monosaccharides glucose, xylose, galactose, arabinose, galacturonic acid and glucuronic acid as a %mol in the fractions. Despite decreased fruit firmness in ethylene- treated watermelon, no change in matrix glycans were found (Karakurt et al., 2008; Mort et al., 2008). Approximately 95% of the watermelon matrix glycans consisted of 40% glucose, 30% xylose, 15% arabinose and 14% galactose (Karakurt et al., 2008).

Differences in xyloglucan and xylogalacturonan monomers were also followed on cell walls depolymerized and hydrolyzed with endo-polygalacturonase (Karakurt et al., 2008; Mort et al., 2008). Xylosyl-linked residues were followed by studying their hydrogen and carbon (^{1}H and ^{13}C) shifts (Mort et al., 2008). Nine linkage residues were identified in matrix glycan oligomers consisting of xylose (1-Xyl(p) and galacturonic acid (3-GalA(p), 4-GalA(p) and 3,4-GalA(p))

linkages. Karakurt and Huber (2009) further studied ethylene treated watermelon and focused on xyloglucan fractions to characterize various xylosyl enzymes known to have hydrolytic activity in the cell wall. Five enzymatic substrates (P1S1, P2S2, P3S1, P3S2 and P3S3) were found in watermelon matrix glycans and xylogalacturonan, with highest enzymatic activity in the glycans ranging from 7.6 to 17.6 units·mg^{-1}. This suggests depolymerization occurs via non-specific xylosyl enzymes and they likely contribute to cell wall hydrolysis during ripening and ethylene-induced breakdown of watermelon fruit.

The objectives of this study were to explore changes in watermelon cell walls relative to HH and grafting, using fruit from a large field study where HH was induced via reduced pollinizer plants. Polysaccharide characterization was done through assessment of total pectin content, neutral sugars and uronic acids of pectic fractions. Determination of neutral sugar composition and linkage assembly was followed using cell walls hydrolyzed with acid rather than polygalacturonase.

Materials and Methods

Plant material

Triploid and diploid watermelon were grown as transplants. 'Liberty' triploid watermelon (Nunhems USA Inc, Parma ID) was used as the scion and not grafted or grafted onto the interspecific hybrid RS (*Cucurbita maxima x C. moschata*) 'Carnivor' (Syngenta AG, Basal Switzerland). 'Liberty' seed was sown on 29 April 2019, 7 d prior to 'Carnivor'. The diploid pollenizer 'SP-7' (Syngenta AG, Basal Switzerland) was sown on 16 April 2019.

A one-cotyledon graft method was utilized on 11 May 2019 following the method of Hassell et al. (2008). Grafted plants were placed into a healing chamber at a constant 27^{o}C, with 100% humidity provided by a Trion Comfortbreeze CB777 Atomizing Hurmidifier (Trion, Sanford NC). Following a 6 day graft union healing interval, the plants were held in an open wall greenhouse to harden off for 2 to 3 d prior to field plantings.

Experimental design and field establishment

The experiment was planted at the Cunningham Research Center (35.8942 ^{o}N, 77.6801 ^{o}W) in Kinston, NC. Six watermelon beds (rows) were used and were split evenly into two blocks via a 7 m drive row. The experimental design was a two factor, full factorial design with grafting treatments and HH incidence as the main effects. One block (3 rows) was planted with non-grafted plants and the second block (3 rows) was planted with grafted transplants. Rows

were 100 m long, with 3.1 m between row spacing and 0.8 m in-row spacing for graft and non-graft watermelon plants. The diploid pollenizer 'SP-7' was transplanted every 12 m in each of the rows and held at 8% of the total plant population. Crop production and fertigation followed conventional watermelon production (Schultheis and Starke, 2019). Fruit were harvested between 71 and 77 days from transplant, utilizing fruit selection by dead tendril.

Quality Evaluation

Fruit were weighed and stem to blossom end length (cm) and maximum fruit diameter (cm) were determined by caliper (Precise Heavy Large Vernier Caliper 40/1000MM-LC-040, Penn Tool Co., Maplewoood, NJ. Fruit were cut longitudinally from stem to blossom end and rated for the incidence and severity of HH with a 1-5 scale (1= no HH to minor crack and 5= severe cavity) following USDA grading standards (2006). Fruit were subjectively rated for ripeness based on color development and tissue breakdown in the seed trace cavity areas. One fruit half was saved for cell wall polysaccharide and total pectin sample extraction. Rind firmness and tissue firmness (N) were assessed as maximum resistance to puncture (5 mm depth) at two locations near or in heart tissue using a stationary firmness tester equipped with a Force One FDIX Digital Force Gauge (Wagner Instruments, Greenwich, CT) and a 0.8 cm diameter flat tip probe (Perkins-Veazie et al., 2016). Following flesh firmness readings, the fruit half was inverted and rind firmness determined using a needle style probe with 0.3 cm diameter. Total number of grafted fruit samples was 102 and 19 had hollow heart. Total number of non-grafted fruit samples was 138 and 73 had hollow heart.

A central core of tissue (about 10 g) was cut from the placental tissue of the fruit half, squeezed onto a digital refractometer (Atago Pal-1, Bellevue WA) and soluble solids (°Brix) content determined. Another sample (50 g) was removed from the heart area, weighed, frozen, freeze dried, and mineral analysis determined by A&L Great Lakes Laboratory, Fort Wayne, IN. A second set of tissue samples (100 g) were taken from the heart area, frozen, thawed, and pureed for determination of pH, soluble sugars (sucrose, fructose and glucose), free citrulline, free arginine and total lycopene following the methods of Fall et al. (2019).

Experimental design for cell wall analysis

Cell wall analysis was set up as a randomized complete block design (RCBD) to assess the cell wall architecture of watermelon fruits with and without HH from grafted and non-grafted plants. Samples with or without severe HH and of similar ripeness as determined by SSC and pH

were selected for cell wall analysis. Two fruit replicates were used in each batch. A total of three batches (24 fruit samples) were analyzed for total pectin and cell wall polysaccharides. Samples were blocked by analysis batch. Each batch was comprised of a randomized sampling of watermelon AIRs that included 2 watermelon fruit for each of the four treatment combinations per batch.

Total pectin content

Samples for total pectin content (50 g) were cut with a sharp knife from the center portion of each watermelon heart, and frozen at -80 ºC. About 20 fruit per graft and HH combination were used to collect samples. Samples with no HH and severe HH ratings (4-5) were selected for analysis. About 20 g of frozen tissue were weighed into 50 mL disposable test tubes for total pectin analysis. These samples were ground in 80% ethanol and further extracted with acetone and methanol to yield alcohol insoluble residues AIR (prepared with methods provided in chapter 4 following Pettolino et al. (2012).

AIR yields were ~40-50 mg and were then sequentially extracted with ultrapure water, 50 mM calcium carbonate and 4 M potassium hydroxide to create water-soluble (WSF), carbonate soluble (CSF), and alkali soluble pectic fractions (ASF). The cell wall material was filtered and filtrates were saved between sequential extractions. The sequential fraction filtrates were freeze dried and the weight of the fraction was obtained to calculate the percentage of each fraction relative to the starting AIR. Then the freeze dried fractions were diluted with 20 mL of di-water and total neutral sugars (Masuko et al., 2005) and uronic acids (Blumenkrantz and Asboe-Hansen, 1973) were determined on all sequential fractions. Galactose was used as the calibration standard for total neutral sugars and galacturonic acid was used as the calibration standard for total uronic acids. Results were expressed in galacturonic acid and/or galactose equivalents per g of cell wall material from each of the sequential extractions.

Cell wall polysaccharide characterization

Samples for cell wall characterization (10 g) were cut from the placental tissue of the watermelon heart, immediately frozen with liquid nitrogen, packed into 50 mL disposable test tubes and stored at -80 ºC. In watermelon with severe HH, samples were taken directly from the cavity. To prepare the AIRs, 10 g samples were ground in 80% ethanol, then extracted in acetone and methanol (prepared with methods provided in chapter 4). AIRs (~20-30 mg) were stored in the presence of desiccant until ready for cell wall characterization.

Prior to starting carboxyl reduction, the sample/batch of choice was selected and ~ 5 mg of AIR was weighed. The AIRs were further ground with a bead homogenizer (Bead Bug, Model D1030, Sigma Aldrich, Darmstadt, Germany). Cell wall characterization using Arabidopsis and the methods of Pettolino et al. (2012) was then optimized for watermelon cell walls. In short, carboxyl reductions (I and II) were performed on the ground AIR. Instead of dialysis, Vivaspin turbo 15 mL Centrifugal Ultrafiltration Filters (3Kda, Millipore/Sigma, Darmstadt, Germany) were used to filter out the small molecules and the retentate was saved. After carboxyl reduction I, the retentates were quantitatively split and reduced with either sodium borodeuteride or sodium borohydride to yield a doubly-deuterated (D/D) and singly-deuterated (D/H) sister sample. The samples were freeze dried and then were methylated and hydrolyzed with trifluoracetic acid (TFA) for linkage analysis or hydrolyzed via Saemen hydrolysis for monosaccharide composition. All samples were further reduced and acetylated to generate volatile alditol acetates. Samples were packed into vials (2 mL, screw, clr, WrtOn, cert, part no. 5182-0715, Agilent, Santa Clara, CA) and stored at -80 ºC until ready for GC-MS analysis.

GC-MS analysis of neutral sugars and partially methylated alditol acetates

An Agilent GC 7098A system with MSD VL 5975C system (Agilent, Santa Clara, CA) was used for GC-MS analysis of alditol acetates with methodology adapted from Pettolino et al. (2012). Helium was used as the carrier gas with a flow rate of 1 $mL \cdot min^{-1}$. Samples (1 μL) were injected into a 240 ºC inlet with a split (1/10) injection using an Agilent autosampler (Model N10149, 0-50 vials, Agilent, Santa Clara, CA). Five syringe washes with dichloromethane were preformed between each sample. The oven conditions were set to an initial temperature of 170 ºC, held for 2 min, and then ramped at 3 ºC min^{-1} to 260 ºC, and held for 3 min. The mass selective detector (MSD) transfer line was held at 260 ºC.

The MS quad was maintained at 106 ºC and MS source at 230 ºC, 70 eV electron impact ionization was used and data were acquired in scan mode from 100 to 350 m/z at 2.14 scans per s with a solvent delay of 3 min. A BPX 70 column with 70% cyanopropyl polysilphenylene siloxane as the station phase (25 m x 0.22 mm inner diameter, film = 0.25 μm, SGE Analytical Science, Australia) was used, trimmed and purged before starting sample injections. Injector syringe, septa (premium inlet septa, part no. 5183-4757, Agilent, Santa Clara, CA) and inlet liners (liner 4 mm, part no. 5181-3316, Agilent, Santa Clara, CA) were changed every 50 injections.

Quantification of neutral sugars, degree of methylation and uronic acids in watermelon

Alditol acetate data were integrated and quantitated based off of the calibration curve containing the 12 neutral sugars. The relative retention time (rrt) of each sugar derivative was calculated relative to the myo-inositol internal standard. This was done by dividing the retention time of the sugar derivative by the retention time of the internal standard. The 12 alditol acetates were normalized against the AIR pellet weight (mg) and quantitative estimates of each alditol acetate in the samples are reported in $\mu g \cdot mg^{-1}$ AIR.

The degree of methylation was calculated by taking the ratio of the peak area of galactose in the D/H sample at *m/z* = 117 divided by the peak area of galactose in the D/D sample at *m/z* = 117 and are reported as percent (%). The uronic acid (galacturonic and glucuronic acid) concentrations were normalized against the pellet weight. Galacturonic acid concentration was calculated via the peak area of galactose in the D/D sample at *m/z* = 117 divided by the peak area of galactose in the D/D sample at *m/z* = 115. That ratio was then multiplied by the concentration of galactose to yield the galacturonic acid concentration. Glucuronic acid concentrations were calculated using the same methods and both uronic acids are reported in $\mu g \cdot mg^{-1}$ AIR.

Linkage analysis of watermelon cell wall polysaccharides

Partially methylated alditol acetates (PMAA) were tentatively identified based on their rrt to the myo-inositol internal standard. Sample peak rrts were compared to the rrts in supplementary Table 1 of Pettolino et al (2012). The sample peaks and rrt(s) were then compared to the mass spectral data from the Complex Carbohydrate Research Center (Georgia, USA) (http://www.ccrc.uga.edu/specdb/ms/pmaa/pframe.html). Identified linkages are deemed 'tentative' as partially methylated sugar standards were not generated for confirmation.

Once the tentative linkages were identified, the methylated compounds were normalized against the internal standard by dividing the peak area of the PMAA by the peak area of the internal standard. Then the content of each methylated derivative was estimated from the concentration of the internal standard. The 'tentative' linkages are reported in PMAA $\mu g \cdot mg^{-1}$ of starting AIR.

Statistical analysis

All fruit quality data were subjected to analysis using R 3.5.3 (Revolution Analytics, Mountain View, CA). A one-way ANOVA was run on the incidence of hollow heart (%) between grafting treatments. A two-way ANOVA was run on heart firmness (N), rind firmness

(N), soluble solids content and pH modeled on grafting treatment and hollow heart phenotype. Data were subjected to Bonferroni correction for mean separation ($p \leq 0.05$).

Compositional data were subjected to analysis using SAS 9.4 (SAS Institute, Cary, NC). A two-way ANOVA, was run to determine whether lycopene, arginine, citrulline, total sugars, fructose, glucose, sucrose and mineral contents differ among watermelon from grafting treatment or hollow heart phenotype. Students T-test was done on the significant main effects for mean separation ($p \leq 0.05$). Tukey's honest significant difference test was conducted on any significant interaction between graft and hollow heart, $p \leq 0.05$. Pearson's correlation was done with mineral analysis, flesh tissue firmness, soluble solids, pH, lycopene, arginine and citrulline to detect possible relationships among the fruit.

All cell wall polysaccharide data (neutral sugar concentrations, degree of methylation, uronic acid concentration and individual polysaccharide linkages) and total pectin data were analyzed using JMP, Version 15 (SAS Institute, Cary, NC). A two-way ANOVA determined the significance of graft treatment and hollow heart phenotype on total cell wall material, water soluble, alkali soluble, carbonate soluble, and unextractable pectic fractions, total neutral sugars ($nmole \cdot mg^{-1}$), total uronic acids ($nmole \cdot mg^{-1}$), each of the 12 neutral sugars, degree of methylation, galacturonic and glucuronic acids. Finally, a two-way ANOVA determined if graft treatment and hollow heart phenotype were associated with specific differences in the 34 polysaccharide linkages detected in watermelon cell walls. Where significance was found, a Student's T-test was used for mean separation between the main effects $p \leq 0.05$. Tukey's honest significance test was done for mean separation where there was significant interaction of graft x hollow heart ($p \leq 0.05$).

Results

Fruit quality attributes

The total number of fruit from grafted plants was 102, and 19% had HH. A total of 138 fruit from non-grafted plants were collected with 53% of these having HH (Fig. 5.1). Fruit weight (kg) did not differ significantly in fruit from grafted (8.1 kg) or non-grafted plants (8.0 kg) ($p < 0.732$) and did not differ in fruit with (7.7 kg) and without HH (8.1 kg) ($p > 0.38$). Heart tissue firmness was higher in fruit from grafted plants compared to fruit from non-grafted plants ($p < 0.0001$) no differences were seen in fruit from grafted or non-grafted plants with and without HH ($p < 0.1003$) (Fig. 5.2 A and C). Rind firmness was higher in fruit from grafted

plants than those from not grafted (45.1 and 38.4 N, $p < 0.0001$). Fruit from grafted plants with and without HH indicated no differences in rind firmness ($p < 0.06311$) (Fig. 5.2 B and D). Differences were not found the soluble solids content of fruit from grafted plants (12.2 ºBrix) compared to those from non-grafted plants (11.9 ºBrix) (Fig. 5.3 A). Soluble solids content did not differ in fruit from grafted and non-grafted plants with and without HH $p > 0.3321$) (Fig 5.3 B). The pH of fruit from grafted or not grafted fruit was similar (5.38 and 5.40, respectively) ($p < 0.694$) and pH was not different in fruit from grafted and non-grafted plants with and without HH ($p > 0.0776$) (data not shown).

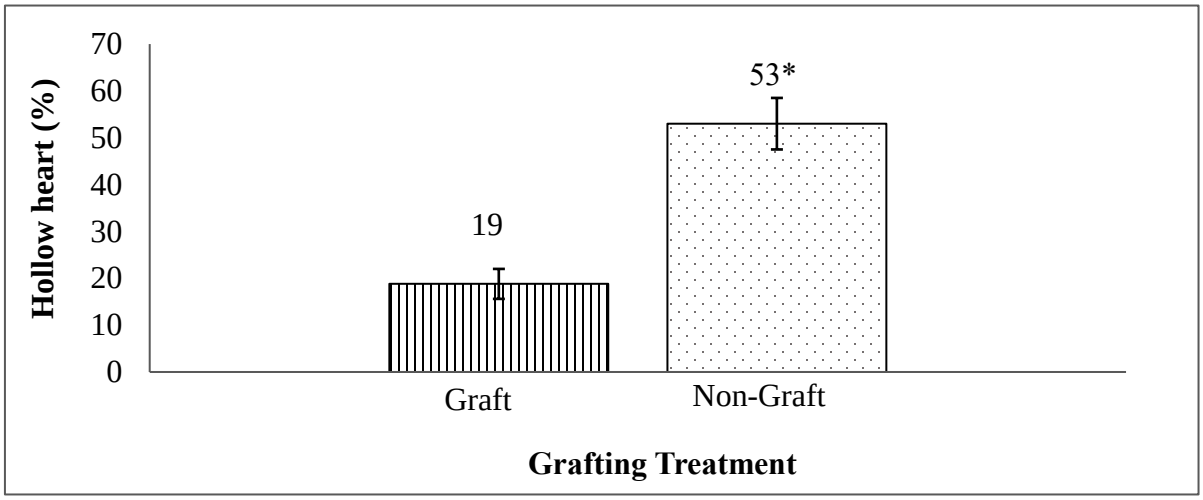

Figure 5.1. Incidence of hollow heart (%) in fruit from grafted and non-grafted plants. Means were separated using Bonferonni correction ($p \leq 0.05$).

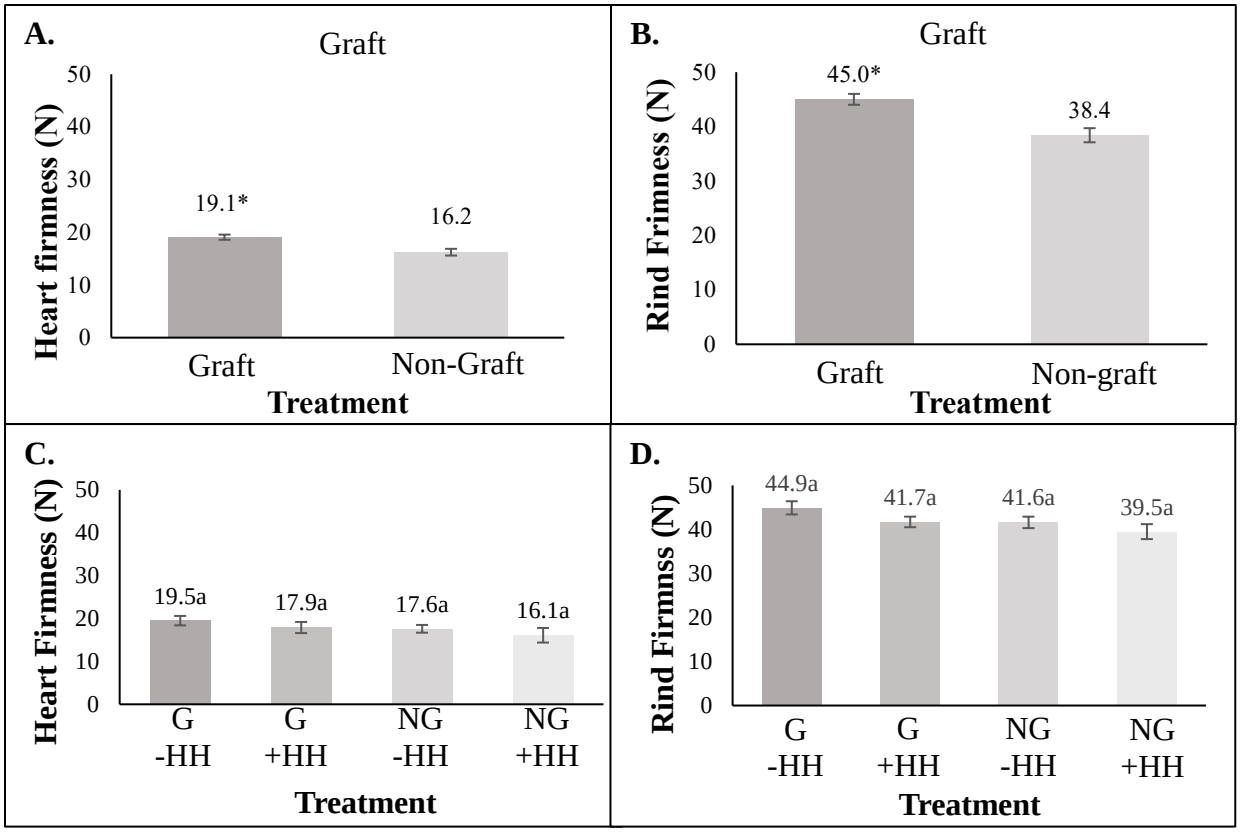

Figure 5.2. Heart tissue firmness (A) and rind firmness (B) in fruit from grafted (G) and non-grafted (NG) plants and with (+HH) and without hollow heart (-HH) (C, D), with standard error bars. Mean separation of values from graft and non-graft was done using Bonferroni correction ($p \leq 0.05$), with differences indicated by *. The significance of graft and HH interactions were determined using Tukey's honest significant difference effects where different letters indicate significance ($p \leq 0.05$).

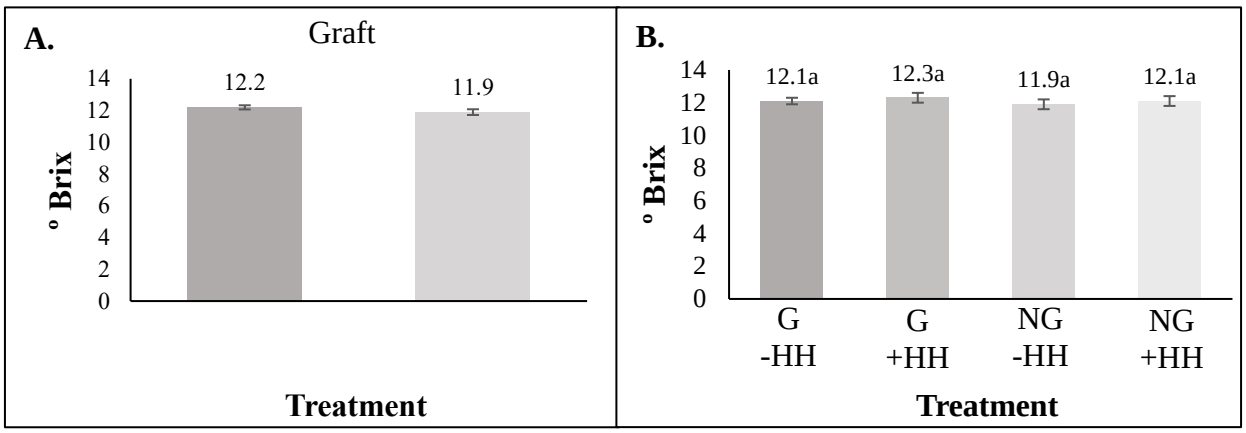

Figure 5.3. Soluble solids content with standard error bars in fruit from grafted and non-grafted plants (A) and from grafted and non-grafted fruit with (+HH) and without hollow heart (-HH) (B). Mean separation of values from graft and non-graft was done using Bonferroni correction ($p \leq 0.05$), with differences indicated by *. The significance of graft and HH interactions were determined using Tukey's honest significant difference effects where different letters indicate significance ($p \leq 0.05$).

Fruit composition in relation to grafting and hollow heart phenotype

Phytonutrient data with graft and HH are reported in Table 5.1. Total lycopene, free arginine and free citrulline contents were similar in tissues regardless of grafting treatment or presence of HH. Total lycopene across treatments was 61.2 ± 0.9 $mg \cdot kg^{-1}$, arginine was 1.2 ± 0.2 $g \cdot kg^{-1}$ and citrulline was 3.9 ± 0.7 $g \cdot kg^{-1}$, respectively. Watermelon sugar data for graft and HH are reported in Table 5.2. Total sugars, glucose and fructose did not differ with grafting treatment or incidence of HH ($p > 0.05$). Total soluble sugars averaged across treatments was 95.3 ± 2.7 $mg \cdot g^{-1}$. Total sucrose content in watermelon flesh was higher than fructose and glucose, but did not differ with HH or graft. When expressed as percent of total sugars, glucose and fructose averaged 17.5 ± 1.0 and 31.3 ± 0.7, respectively and were not different with treatment (data not reported) ($p > 0.05$). Sucrose (%) was higher in fruit with HH (52.2%) compared to fruit with no HH (43.4%) ($p < 0.0092$) but did not differ with grafting ($p < 0.5787$).

Table 5.1. Phytonutrient content in watermelon fruit from grafted and non-grafted plants and in fruit with or without hollow heart.

Variable	Lycopene (mg·kg^{-1})	Arginine (g·kg^{-1})	Citrulline (g·kg^{-1})
Graft	63.0 ± 0.5	1.1 ± 0.2	3.4 ± 0.6
Non-graft	59.7 ± 1.1	1.3 ± 0.2	3.4 ± 0.7
Hollow heart			
HH	63.1 ± 0.9	1.3 ± 0.2	3.5 ± 0.6
No HH	58.9 ± 0.8	1.1 ± 0.2	5.4 ± 0.7

Phytonutrients are reported as LS-means ± standard errors, and means separated within the main effects of graft or HH using Students T-test ($p \leq 0.05$). Significant differences within column and variable are indicated by *.

Table 5.2. Total sugars, sucrose, glucose, fructose and percentage of sucrose in watermelon fruit from grafted and non-grafted plants and in fruit with or without hollow heart.

Variable	Total sugars (g·kg^{-1})	Sucrose (g·kg^{-1})	Glucose (g·kg^{-1})	Fructose (g·kg^{-1})	Sucrose (%)
Graft	94.6 ± 2.3	42.4 ± 3.3	18.7 ± 2.4	33.4 ± 6.6	44.8 ± 7.6
Non-graft	95.8 ± 3.6	44.5 ± 2.5	18.5 ± 2.2	32.4 ± 1.7	46.2 ± 2.5
Hollow heart					
HH	98.6 ± 2.7	51.8 ± 9.2	18.6 ± 0.9	32.9 ± 2.3	52.2 ± 1.2*
No HH	95.2 ± 3.1	43.5 ± 7.3	16.4 ± 2.3	29.7 ± 3.1	44.8 ± 3.3

Sugars are reported as LS-means ± standard errors, and means separated within the main effects of graft or HH using Students T-test ($p \leq 0.05$). Significant differences within column and variable are indicated by *.

Mineral analysis of watermelon flesh

Total nitrogen, magnesium, sulfur and calcium did not differ in fruit from grafted or non-grafted plants or in fruit with and without HH (data not shown). Watermelon fruit tissue had a mean content of 12.5 ± 0.7, 14.4 ± 0.3, 7.5 ± 0.1, 1.1 ± 0.5 and 6.5 ± 0.2 x 10^3 ppm total nitrogen, potassium, magnesium, sulfur and calcium, respectively. Other minerals that differed in fruit from grafted or non-grafted plants and with and without HH are reported in Table 5.3. Phosphorus did not differ with grafting treatment, but was highest in fruit with HH (13.1 x 10^3 ppm) compared to fruit without HH (2.8 x 10^3 ppm). Fruit with HH (3.5 ppm) had higher amounts of boron compared to fruit without HH (12.8 ppm). Copper was higher in fruit from grafted plants (7.1 ppm) compared to those from non-grafted plants (5.6 ppm). Zinc and manganese were higher in fruit from grafted plants at 20.7 and 8.6 ppm, respectively, compared

to non-grafted plants (18.2 ad 6.8 ppm). Fruit with HH had higher amounts of copper, zinc, and manganese (6.8, 20.6 and 8.1 ppm) compared to those with no HH plants (6.2, 18.1 and 7.1 ppm). No differences were seen in relative amounts of iron (21.4 ± 2.5 ppm) (data not shown).

Table 5.3. Minerals in watermelon fruit tissue that were significantly different with graft or hollow heart.

Variable	Phosphorus (ppm x 10^3)	Copper (ppm)	Boron (ppm)	Zinc (ppm)	Manganese (ppm)
Graft	4.6 ± 0.1	7.1 ± 0.9*	12.9 ± 1.2	20.7 ± 0.7*	8.6 ± 2.4*
Non-graft	4.1 ± 0.6	5.6 ± 1.1	13.2 ± 1.3	18.2 ± 0.9	6.8 ± 1.0
Hollow heart					
No HH	2.8 ± 0.2	6.2 ± 0.1	12.8 ± 0.3	18.1 ± 3.8	7.1 ± 0.4
HH	3.1 ± 0.2*	6.8 ± 0.3*	13.5 ± 0.3*	20.6 ± 1.5*	8.1 ± 0.7*

Minerals are reported as LS-means ± standard errors. Significant differences within column and variable are indicated by *, Students T-test ($p \leq 0.05$).

Total Pectin Content

Total cell wall material, reported as AIR, was calculated as a percentage of fresh watermelon tissue weight and was not different due to grafting treatment ($p > 0.3143$) or HH phenotype treatment ($p > 0.9806$). Sequential fractions are reported as a percentage of that extracted from AIR. The WSF was the least abundant of the pectic fractions (Table 5.4). Of the pectic fractions, the carbonate soluble fraction was lower in fruit with HH than fruit without HH ($p < 0.0428$). No other differences were found among the pectic fractions (%) ($p > 0.05$). Total neutral sugars and uronic acids of the pectic fractions were not different with graft or HH ($p > 0.05$) (Table 5.5).

Table 5.4. Total cell wall material and sequential fractions (% of total cell wall material) among graft and incidence of hollow heart.

		% sequential fraction			
Variable	**TCWM**	**WSF**	**CSF**	**ASF**	**UNX**
Graft	0.39 ± 0.02	12.56 ± 0.8	25.77 ± 1.0	34.02 ± 1.0	27.29 ± 1.2
Non-graft	0.36 ± 0.02	13.09 ± 0.9	26.21 ± 1.2	35.13 ± 1.0	25.49 ± 1.3
Hollow heart					
No HH	0.37 ± 0.02	12.60 ± 0.9	27.11 ± 1.8*	33.91 ± 1.0	25.78 ± 1.2
Severe HH	0.36 ± 0.02	13.05 ± 0.9	24.79 ± 1.5	35.24 ± 1.0	26.98 ± 1.2

Values represent LS-means ± standard errors. Means are separated within column and variable using Students T-test and significance ($p \leq 0.05$) is indicated by *. TCWM = total cell wall material, WSF = water soluble fraction, CSF = carbonate soluble fraction, ASF = alcohol insoluble fraction, and UNX = unextractable fraction.

Table 5.5. Total neutral sugars and uronic acids among the sequential fraction between grafting treatments and incidence of hollow heart.

Variable	**WSF**	**CSF**	**ASF**
	Total neutral sugars (nmole·mg^{-1})		
Graft	18.36 ± 1.0	8.91 ± 0.2	12.31 ± 0.7
Non-graft	19.17 ± 1.0	8.61 ± 0.2	12.11 ± 0.9
No HH	19.41 ± 1.0	8.54 ± 0.2	12.02 ± 0.9
Severe HH	18.12 ± 1.1	8.98 ± 0.2	12.40 ± 0.9
	Total uronic acids (nmole·mg^{-1})		
Graft	8.86 ± 0.5	5.08 ± 0.1	6.10 ± 0.3
Non-graft	9.35 ± 0.5	5.18 ± 0.2	6.24 ± 0.3
No HH	9.39 ± 0.5	4.98 ± 0.1	6.12 ± 0.3
Severe HH	8.82 ± 0.5	5.28 ± 0.1	6.22 ± 0.3

Values represent LS-means ± standard errors. Means are separated within column and variable using Students T-test and * indicates significance at $p \leq 0.05$. WSF = water soluble fraction, CSF = carbonate soluble fraction, and ASF = alcohol insoluble fraction.

Cell wall polysaccharide composition

The average concentration of monomers (alditol acetates) and the degree of methylation (%) for watermelon cell wall polysaccharides are reported in Table 5.6. In watermelon fruit, the major monosaccharides consisted of glucose (78.22 μg·mg^{-1}), galactose (48.94 μg·mg^{-1}), xylose (27.65 μg·mg^{-1}) and arabinose (19.72 μg·mg^{-1}), respectively. Galacturonic acid was found to be the highest in concentration at 26.28 μg·mg^{-1} compared to glucuronic acid at 10.15 μg·mg^{-1}, respectively. No 2-deoxy-d-ribose was detected in watermelon cell walls. No differences ($p >$

0.05) were found in xylose, glucose and galactose concentrations in relation to grafting treatment, hollow heart phenotype or the interaction.

Fucose, rhamnose, arabinose, and meso-erythritol contents were higher in fruit with HH but no differences were found in fruit from grafted or non-grafted plants (Fig 5.4 A-E). Arabinose was highest in fruit with HH (21.29 $\mu g \cdot mg^{-1}$) compared to those without HH (19.82 $\mu g \cdot mg^{-1}$) ($p < 0.0309$) (Fig 5.5 A). Rhamnose was higher in fruit with HH (3.38 $\mu g \cdot mg^{-1}$) compared to no HH (3.09 $\mu g \cdot mg^{-1}$) ($p < 0.0396$) (Fig 5.5 B). Fucose concentration was higher in fruit with HH (2.36 $\mu g \cdot mg^{-1}$) than no HH (1.92 $\mu g \cdot mg^{-1}$) ($p < 0.0005$) (Fig. 5.5 C). Meso-erythritol was 0.032 and 0.00 $\mu g \cdot mg^{-1}$ for fruit with or without HH, respectively ($p < 0.0422$) (Fig 5.5 E). In contrast, 2-deoxy-d-glucose was highest in fruit without HH (0.55 $\mu g \cdot mg^{-1}$) compared to fruit with HH (0.21 $\mu g \cdot mg^{-1}$) ($p < 0.0008$) (Fig 5.5 D).

A significant interaction between grafting treatment and HH phenotype was found for ribose and allose (Fig 5.6 A, B). Ribose concentration was highest in fruit without HH from grafted plants (1.27 $\mu g \cdot mg^{-1}$) compared to other treatments ($p < 0.0199$), but was similar to that of watermelon with HH from non-grafted plants (Fig 5.6 A). Allose was highest in fruit from grafted plants without HH (0.80 $\mu g \cdot mg^{-1}$) compared to other treatments ($p < 0.0250$) (Fig. 5.6 B).

No significant differences were seen in galacturonic or glucuronic acid concentrations ($p > 0.05$) or the degree of methylation ($p > 0.05$) with graft or HH (Table 5.6)

Table 5.6. Average concentration of monomeric building blocks, degree of methylation and uronic acids in watermelon cell walls.

Monosaccharide	**Concentration (μg·mg^{-1} AIR)**
Glucose	78.22 ± 3.26
Galactose	48.94 ± 1.89
Xylose	27.65 ± 1.14
Arabinose	19.72 ± 1.11
Rhamnose	3.26 ± 0.12
Fucose	2.21 ± 0.10
Mannose	2.03 ± 0.10
Ribose	1.15 ± 0.05
Allose	0.48 ± 0.08
2-deoxy-d-Glucose	0.38 ± 0.06
Meso-Erythritol	0.015 ± 0.01
2-deoxy-d-Ribose	-
Galacturonic acid	26.28 ± 2.14
Glucuronic acid	10.15 ± 0.84

Degree of Methylation	%
Methylation	72.11 ± 5.87

- = no 2-deoxy-d-ribose detected in watermelon cell wall samples. Values represent LS-means ± standard error, N=24.

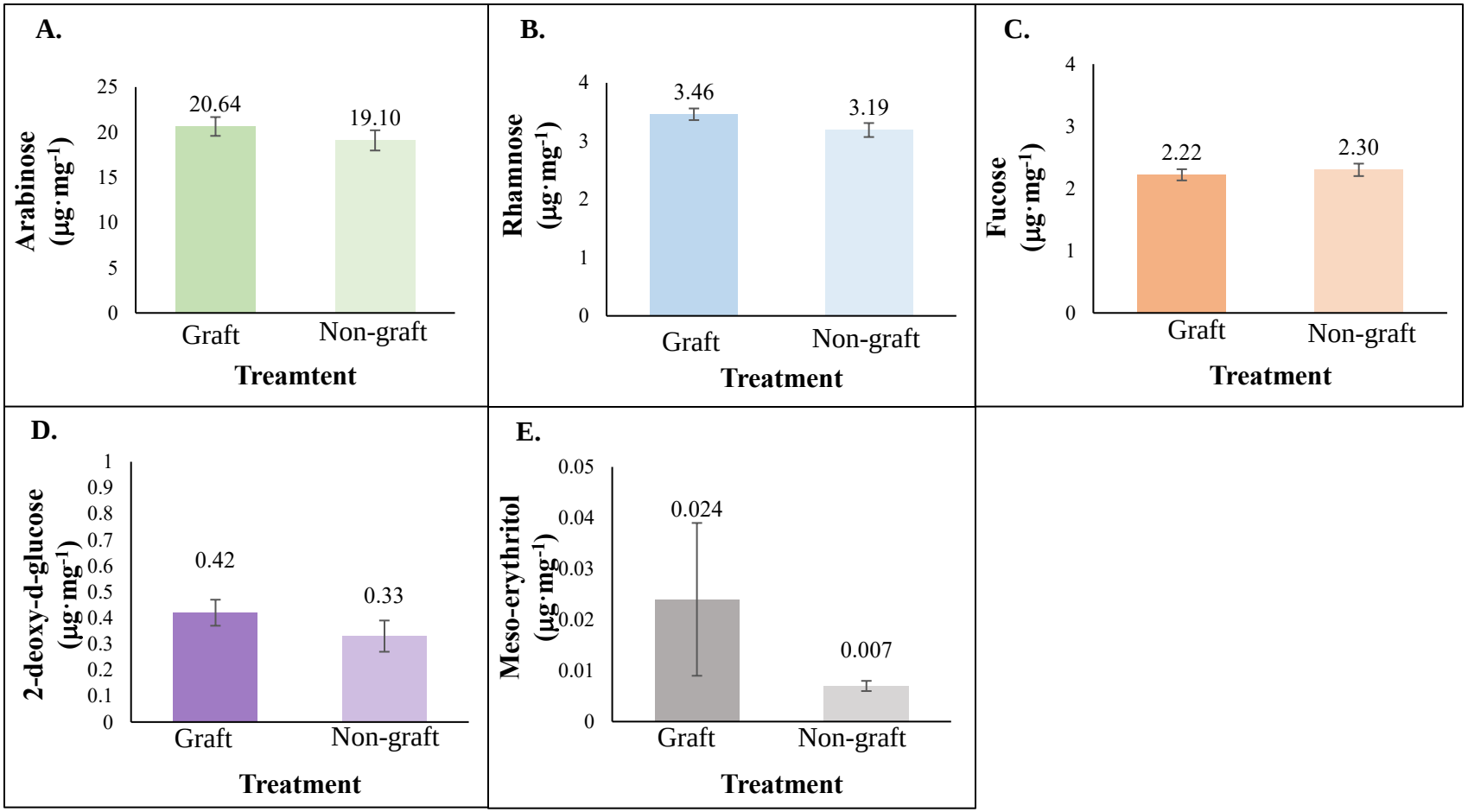

Figure 5.4. Monomers of the alditol acetates (µg·mg^{-1}) ± standard error in watermelon fruit tissue from grafted and non-grafted plants. Arabinose (A), rhamnose (B), fucose (C), 2-deoxy-d-glucose (D) and meso-erythritol (E). Student T-test used for mean separation ($p \leq 0.05$).

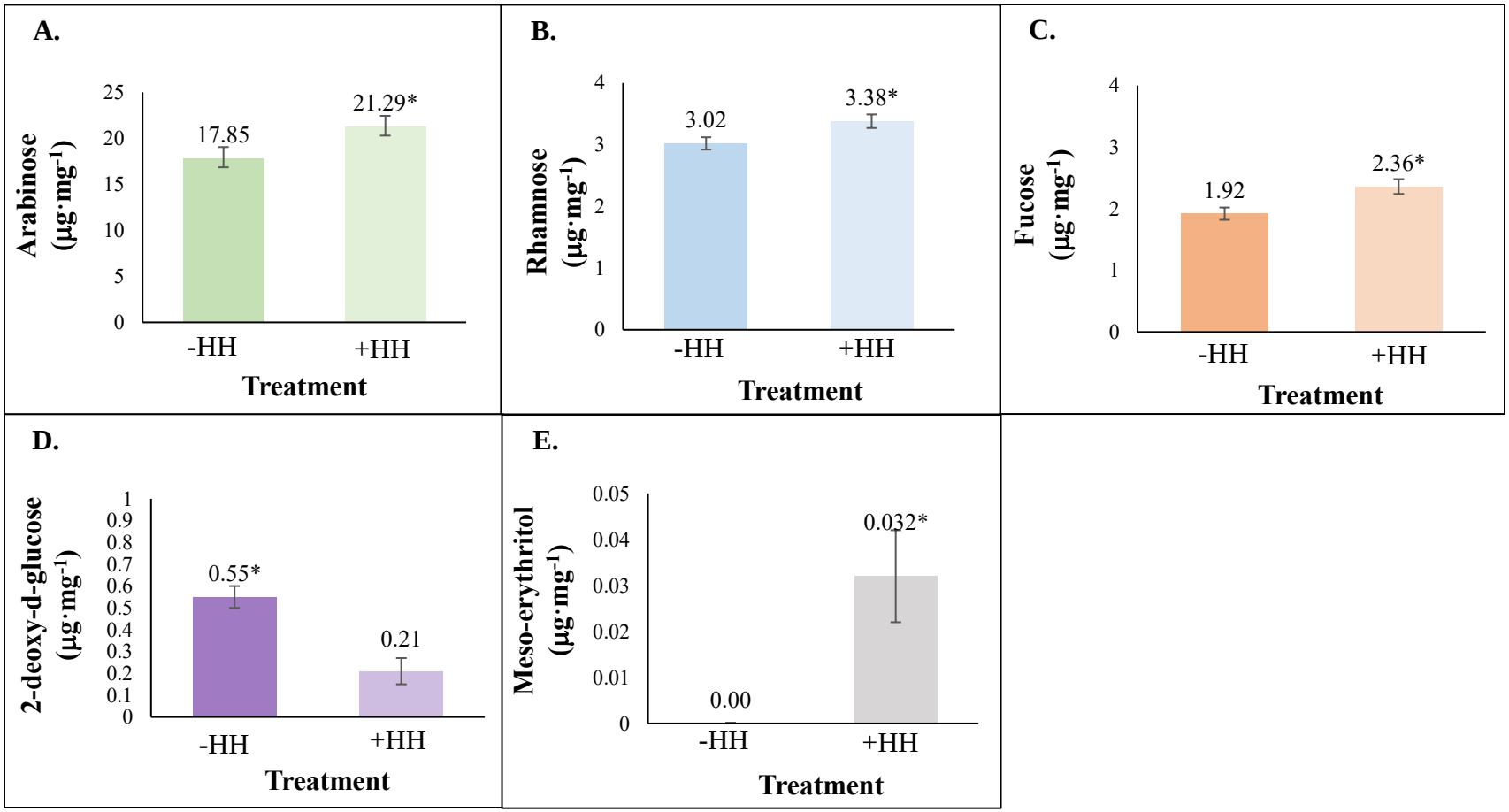

Figure 5.5. Monomers of the alditol acetates (µg·mg^{-1}) ± standard error in watermelon fruit tissue from grafted and non-grafted plants. Arabinose (A), rhamnose (B), fucose (C), 2-deoxy-d-glucose (D) and meso-erythritol (E). Student T-test used for mean separation ($p \leq 0.05$), and significant differences indicated by *.

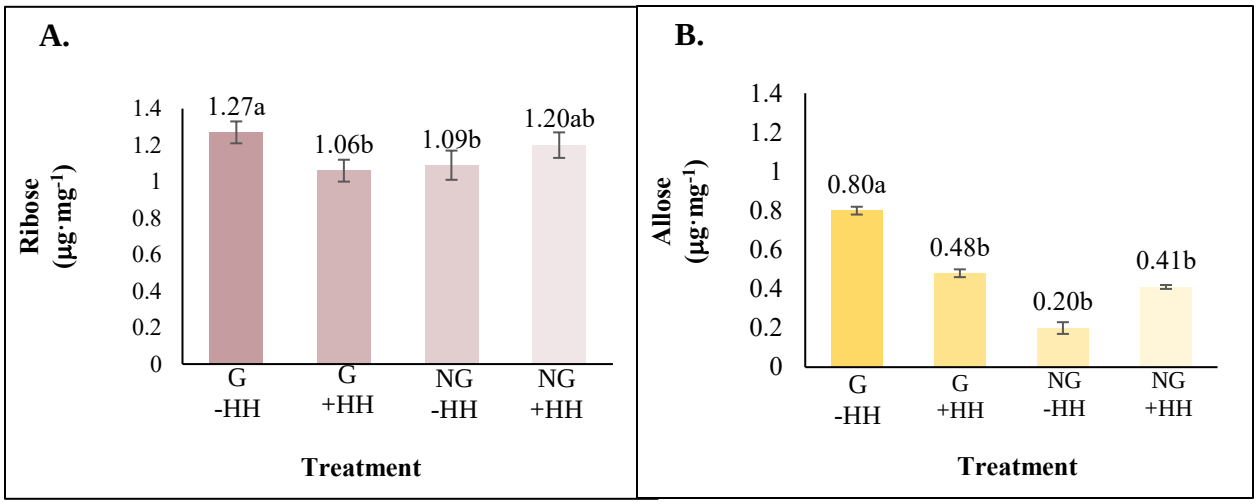

Figure 5.6. Ribose (A) and allose (B) monomers of the alditol acetates (µg·mg^{-1}) ± SE in fruit tissue from watermelon from grafted (G) or not grafted (NG) plants and with no (-HH) or severe (+HH) hollow heart. Means separated using Tukey's honest significant difference, with different letters indicating significance ($p \leq 0.05$).

Partially methylated alditol acetate linkage assembly

Comprehensive linkage assembly data is reported as averages in Table 5.7. In watermelon cell wall polysaccharides, 32 partially methylated alditol acetates (PMAA) were detected, including 7 unknowns. Five linkages, t-Ara(p)/t-Xyl(p), 3,4-Rha(p)/2-Ara(f), 4-Fuc(p)/t-Gal(p)/3-Ara(f), 3,4-Fuc(p)/2-Xyl(p) and 2,3,6-Gal(p)/2,4,6-Gal(p) had similar mass spectra and rrt and could not be distinguished. In this study 4-Glc(p) (14.48 µg·mg^{-1}), 3-Glc(p) (4.17 µg·mg^{-1}), 2-Ara(f) (3.52 µg·mg^{-1}), t-Rha(p) (2.31 µg·mg^{-1}), 3,4,6-Glc(p) (2.08 µg·mg^{-1}), and 3,6-Gal(p) (1.17 µg·mg^{-1}) were found to be the linkages in highest abundance in watermelon cell walls.

Differences were found in only three linkages for the interaction of GXHH. Fruit from grafted plants without HH had the highest concentrations of the linkages, 2,4-Fuc(p), 3-Glc(p) and 4-Glc(p) (Fig. 5.7 A,B,C). No other differences in PMAAs were found relative to grafting treatment or HH phenotype.

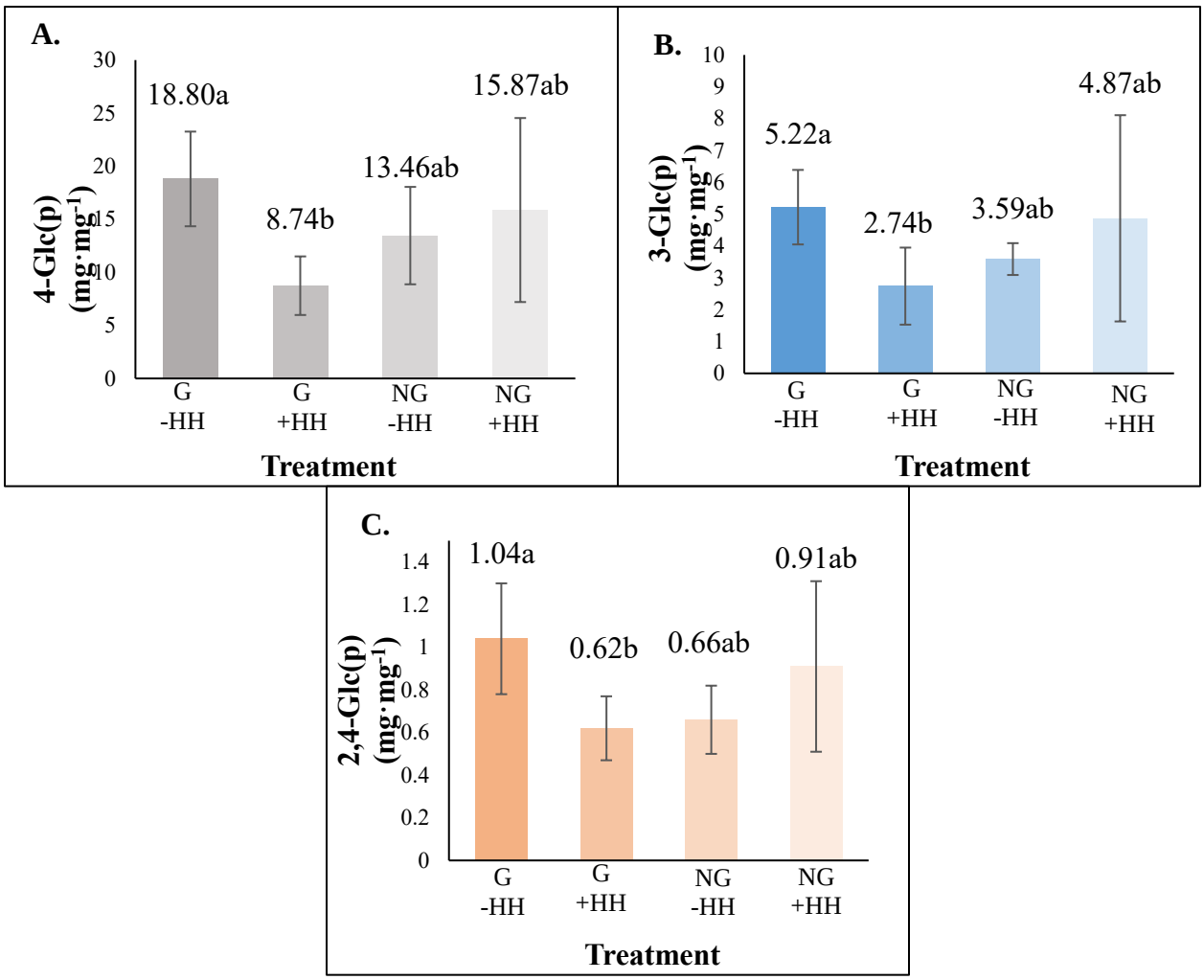

Figure 5.7. Linkage analysis of the partially methylated alditol acetates (μg·mg^{-1}) ± SE in fruit tissue from watermelon from grafted (G) or not grafted (NG) plants and without (-HH) or severe (+HH) hollow heart. Means separated using Tukey's honest significant difference, with different letters indicating significance ($p \leq 0.05$).

Table 5.7. Linkage assembly of watermelon cell wall polysaccharides and estimated concentration of each linkage.

Linkage	Average concentration ($\mu g \cdot mg^{-1}$ AIR)	Tentative Polysaccharide class
3-Fuc(p)	0.61 ± 0.19	AG, AG Proteins
2,4-Fuc(p)	0.81 ± 0.35	
4-Fuc(p), t-Gal(p) or 3-Ara(f)	0.63 ± 0.33	RG I, II, AG or AG proteins
3-Gal(p)	0.17 ± 0.08	AG II and RG I, II
6-Gal(p)	0.30 ± 0.24	
t-Ara(f)	0.11 ± 0.13	AG I or II, HX, XG or RG II
2-Ara(f)	3.52 ± 2.20	AG I or II
t-Ara(p) or t-Xyl(p)	0.65 ± 0.31	
3,4-Fuc(p) or 2-Xyl(p)	0.02 ± 0.04	XG
3,4-Rha(p) or 2-Ara(f)	1.14 ± 0.38	RG I
t-Rha(p)	2.32 ± 0.78	AG II or RG II
2,4-Xyl(p)	0.15 ± 0.02	HX
4-Glc(p)	14.5 ± 5.12	XG, HM or cellulose
3,6-Gal(p)	1.17 ± 0.44	Galactan chains
2,4,6- or 3,4,6-Gal(p)	0.38 ± 0.23	
3-Glc(p)	4.17 ± 1.63	Glycosidic backbone of hemicellulose
2,4-Glc(p)	0.09 ± 0.05	Glycosyl linkage
3,4-Glc(p)	3.48 ± 1.64	
3-Ara(f)	0.54 ± 0.26	Unknown components
3-Ara(p)	0.61 ± 0.36	of the cell wall
3,6-Glc(p)	0.11 ± 0.08	
2,4,6-Glc(p)	0.49 ± 0.43	
3,4,6-Glc(p)	2.08 ± 1.23	
2,3-Gal(p)	0.20 ± 0.13	
3,6-Man(p)	0.46 ± 0.44	
Unknown 1	0.84 ± 0.29	Unknown linkages
Unknown 2	1.31 ± 0.42	
Unknown 3	0.91 ± 0.66	
Unknown 4	0.22 ± 0.13	
Unknown 5	1.86 ± 0.44	
Unknown 6	0.71 ± 0.35	
Unknown 7	0.30 ± 0.13	

Values represent LS-means of partially methylated alditol acetates ± standard error, N=24.
AG = arabinogalacturonan, RG = rhamnogalacturonan, HX = heteroxylan, HM = heteromannan, XG = xylogalacturonan

Discussion

Grafting and hollow heart

Fruit from 'Liberty' grafted onto the interspecific hybrid rootstock had 34% less HH (Fig. 5.1) and placental tissue firmness was 3 N higher compared to fruit from non-grafted plants (Fig. 5.2 A). Soteriou et al. (2017) reported that watermelon flesh firmness increased in fruit from plants grafted onto interspecific hybrid rootstock. Researchers have hypothesized that fruit with lower tissue firmness are often more affected by internal fruit disorders compared to dense fruit types (Guan, 2018). During watermelon fruit growth, tension can be imposed on the placental cells (Kano, 1993) and may cause separation along the middle lamella (Ng et al., 2013). Increases in watermelon firmness have been related to more cells/unit area in the placental tissue (Kano, 1993). Increased fruit tissue firmness may decrease the tension imposed on the placental tissue ultimately decreasing middle lamella separation leading to smaller intracellular air spaces.

Resistance to probe penetration through rind and peel was higher in fruit from grafted plants and but no differences were seen in fruit with and without HH regardless of graft treatment (Fig. 5.2 B, D). Fredes et al. (2016) found grafting onto interspecific hybrid rootstocks increased rind thickness by 2 mm compared to fruit from non-grafted plants. Increased rind thickness and firmness are also associated with increased flesh tissue firmness (Fredes et al., 2016), which was found in this experiment for fruit grafted to the interspecific hybrid rootstock (Fig. 5.2 A, B).

Fruit quality of grafted watermelon with and without hollow heart

No differences were found in fruit weight, pH, lycopene, arginine and citrulline with graft or HH (Table 5.1). Soluble solids content did not differ between grafting treatments (Fig 5.3 A), and was not different in fruit with and without HH from grafted or non-grafted plants (Fig 5.3 B.). Sweetness is a very important aspect of watermelon fruit quality as consumers relate high soluble solids content to high quality fruit (Liu et al., 2017), and a 10 ºBrix is needed to meet USDA grading standards (USDA, 2006). Although HH is a visual defect for marketability and consumer acceptability (USDA, 2006), the disorder does not compromise the soluble solids content.

Watermelon phytonutrients (e.g., lycopene, arginine and citrulline) strongly depend on fruit maturation (Liu et al, 2017). Generally, in ripening watermelon, fruit pH tends to increase after soluble solids content and lycopene increase (Corey and Schlimme, 1988). Soteriou et al.

(2014) found that grafting did not affect lycopene content. However, grafting to an interspecific hybrid RS has been shown to slow ripening (Fallik et al., 2014), and it is possible that fruit with HH also have slightly delayed ripening. Fruit pH is a strong indicator of ripeness and watermelon are considered ripe between pH values of 5.0 to 5.5 (Soteriou et al., 2014; Kyriacou et al., 2016). Since watermelon pH was near 5.5, this suggests all the fruit were fully ripe and would explain the lack of differences seen in phytonutrient concentrations.

In watermelon fruit, the soluble sugars are sucrose, glucose and fructose (Fall et al. 2019). Total sugars, glucose, sucrose, and fructose did not differ with HH or graft (Table 5.2). Previous research has found that significant differences in total sucrose were not necessarily associated with differences in the level of total sugars (Aslam et al., 2020; Yativ et al., , 2010). However, the percentage of sucrose is expressed as a percent of total sugars (e.g., sucrose / sucrose + glucose + fructose). Percentage sucrose did not differ with graft but was higher in fruit with HH compared to fruit with no HH (Table 5.2). Sucrose is the product of fructose and glucose being reduced during fruit ripening (Yativ et al., 2010). Slight changes in sucrose enzymatic activity, specifically the enzyme *SPS,* have been linked to high or low sucrose content in watermelon and fruit with higher sucrose content indicated higher *SPS* activity (Yativ et al., 2010). Since total glucose and fructose were decreased in comparison to total sucrose, an increase in enzyme activity may be occurring with the onset of HH leading to increases of %sucrose.

Graft and hollow heart effects on fruit minerals

The mineral content of watermelon fruit was generally similar for graft or HH. However, copper, manganese and zinc were higher in fruit from grafted plants compared to those from non-grafted plants (Table 5.3). When watermelon is grafted with a compatible rootstock and a vigorous root system is created, plants absorb and shuttle mineral nutrients more efficiently than those of non-grafted watermelon (Martinez-Ballesta et al., 2010). Martinez-Ballesta et al. (2010) also reported that grafting to hybrid rootstocks shuttles minerals more efficiently and increases water uptake. Grafted plants form a callus at the graft interface, enabling water flow from the rootstock to the scion (Ruiz et al., 1997). The increase in copper, manganese and zinc in fruit from grafted plants may be indicative of increased nutrient shuttling and waterflow from the soil into plant roots (Martinez-Ballesta et al., 2010). The cell wall can also play a role in mineral shuttling and is responsible for the movement of metal cations into cellular organelles (Yang et

al. 2018). Due to increased waterflow and nutrient uptake from watermelon grafting, the cell wall may readily transport copper, manganese and zinc through the cell wall into storage organelles, further accounting for the significant increase of these minerals.

Fruit with HH had higher amounts of copper, manganese, zinc, phosphorus and boron compared to fruit without HH (Table 5.3). Phosphorus aids plant growth and is affected by sink to source relationships in the plant. Phosphorus content can influence fruit quality attributes, as found for increased soluble solids content in strawberries (Cao et al., 2015). Strawberry fruit are a strong sink organ and fruit with higher P have enhanced sugar transport from leaf to fruit (Cae et al., 2015). Higher P content in watermelon fruit with HH may indicate higher sugar enzyme activity, resulting in the observed higher soluble solids content (Fig 5.3 B).

As previously mentioned, the cell wall is the first barrier to cellular cation uptake and retention is thought to be controlled by cell wall (Chormova and Fry, 2016; Penaloza and Toloza, 2018; Yang et al. 2018). Boron is essential throughout the plant and is responsible for boron-bridging and dimerization of rhamnogalacturonan II, an important structural pectin in the plant cell wall (Chormova and Fry, 2016). Boron generates a covalent bridge between pectin molecules and decreases cell wall porosity by modifying biochemical properties of the cell wall (Chromova and Fry, 2016). The major sites of mineral accumulation like copper, manganese and zinc are in the chloroplast, vacuole and cytoplasm, and the cell wall controls heavy metal uptake and storage (Printz et al., 2016). A hypothesis is that the increased boron, copper, manganese and zinc in fruit with HH may be from storage in fruit cells, a change in metal transport mechanisms in the cell wall (Printz et al., 2016), and/or use of the minerals to aid pectin bridging (Chormova and Fry, 2016) and decrease the onset of the internal fruit disorder.

Total pectin content and fruit textural characteristics

Watermelon tissue firmness is attributed to the strength and intercellular connections of the primary cell wall (Brummell, 2006). Pectin is the most abundant polymer in the middle lamella and it is known to regulate intercellular adhesion (Paniagua et al., 2014). The solubilization of pectin (e.g., ability to move pectins from the cell wall into solution) varies greatly among fruit species. Fruit with a crisp texture, like watermelon, have a low degree of pectin depolymerization and solubilization when ripe (Brummell, 2006; Soteriou et al., 2017). Watermelon placental tissue firmness increased in fruit from plants grafted to interspecific hybrid rootstocks (Fig. 5.2 A), yet no differences were seen in total cell wall material or

sequential fractions (%) with respect to grafting treatments. Hollow heart phenotype indicated differences only in CSF and fruit without HH had higher amounts of this fraction (Table 5.4). Total cell wall material (AIR) did not differ in fruit from grafted and non-grafted plants with and without HH. In general, previous researchers have found pectin solubilization in solvents (e.g., ethanol, methanol and acetone) range from 0.60-0.77% in watermelon (Soteriou et al., 2017). Pectin solubilization averaged around 0.39% in this experiment and is similar to that of cactus pear fruit (Soteriou et al., 2017). The low amount of total cell wall material found in watermelon supports the low degree of pectin solubilization reported by Brummell (2006). Soteriou et al. (2017) speculated that increased watermelon fruit tissue firmness could be elicited by an increase in cytokinin production from the grafting rootstock. Grafting is known to promote plant growth through increased synthesis and translocation of both cytokinin and gibberellin. Cytokinin is generally synthesized in the roots and mediates local and long-distant signaling that influence fruit qualities by increasing cell division (Srivastava and Handa, 2005). Increases in cell division are related to an increased number of cells/unit area (Kano, 1993). Unfortunately little is known about the influence of cytokinin on cell wall pectins.

Total cell wall material recovered from watermelon in this experiment was lower compared to Soteriou et al. (2017) (0.39% vs. 0.64%). Correspondingly, the average WSF, CSF and ASF were also lower, at 12.82%, 25.97%, and 24.58%, respectively, (Table 5.4). These fractions were lower than the 23.3%, 39.9% and 36.8%, respectively, reported by Soteriou et al., (2017). The differences in the amount of total cell wall material and subsequent fractions could be due to the use of different triploid cultivars. Soteriou et al. (2017) used the triploid 'Pegasus', while in this experiment 'Liberty' was used as the triploid. In contrast, total neutral sugars were comparable between the studies. In our study, neutral sugars were 18.76 nmole mg^{-1} in the WSF, 8.78 nmole mg^{-1} in the CSF and 12.21 nmole mg^{-1} in ASF, respectively. Souterio et al. (2017) found the WSF, CSF and ASF total neutral sugars to be 76.2 mol%, 6.5 mol% and 17.3%, respectively. In both experiments, the WSF had the highest amount of total neutral sugars and CSF had the lowest. Research on neutral sugars in sequential fractions were previously reported as mol% (Soteriou et al., 2017), however, in this experiment sugars were measured on a quantitative basis. The total uronic acids were found to be 9.11 nmole·mg^{-1} in WSF, 5.13 nmole·mg^{-1} in CSF and 6.17 nmole·mg^{-1} in ASF, respectively (Table 5.5).

The %WSF was lowest compared to the %CSF and %ASF of total cell wall material (Table 5.4). WSF yields pectins in the plant cell well that are both freely bound and soluble in the apoplast (Panigua et al., 2014). Soteriou et al. (2017) found no differences in the %WSF in fruit from homeografted, non-grafted and heterografted plants suggesting a limited association between WSF and tissue firmness. Similarly, in this experiment the %WSF was not different with graft or HH fruit further eliciting that the WSF does not play a significant role in tissue firmness. Total neutral sugars were highest in the WSF compared to all other pectic fractions and neutral sugars were higher compared to total uronic acids (Table 5.5). Polysaccarhides such as xylogalacturonan and rhamnogalacturon I and II have neutral sugar side chains and thus increase in neutral sugars may be due to the pectic sidechains solubilizing in the apoplast of intact cell walls (Redgwell et al., 1992).

Carbonate soluble fractions are considered to be enriched in de-esterified pectins covalently bound to the cell wall (Panigua et al., 2014). They are also found to be enriched in homogalacturonan (Panigua et al., 2014; Soteriou et al., 2017), the most abundant pectic polysaccharide in the plant cell wall (Mohnen, 2008). Carbonate soluble fractions extracted with calcium or sodium carbonate have previously been found to have higher total neutral sugar concentrations compared to total uronic acids. This suggests CSF also has higher amounts of rhamnogalacturonan I (Paniguia et al., 2014; Soteriou et al., 2017). The CSF was found to differ only in watermelon with the HH disorder (Table 5.4) and was higher in fruit without HH (27.0%) compared to those with HH (24.8%). Although total neutral sugars did not differ with respect to HH, total neutral sugars coming from CSF were higher compared to total uronic acids. This suggests fruit with HH have lower enrichments of rhamnogalacturonan I and homogalacturonan. Furthermore, loss of arabinan and galactan side chains from rhamnogalacturonan I could contribute to increased solubilization of CSF in fruit without HH (Zywinska et al., 2005).

Alkali soluble fractions are derived from matrix glycans tightly attached to the cell wall via hydrogen bonds and are generally the hardest to solubilize (Brummell and Harpster, 2001). ASF are also considered to have a low degree of methylesterification (Gawkowska et al., 2019) and high polyuronide (uronic acid) concentrations compared to WSF and CSF (Soteriou et al., 2017). In this experiment, ASF were highest compared to all other pectic fractions extracted from watermelon tissue but had no discernable treatment differences (Table 5.4). ASF also had higher total neutral sugars compared to total uronic acids. Gawkowska et al. (2019) found in

apple peal high relative amounts of arabinose and galactose and high uronic acid amount in ASF. Arabinose and galactose are important neutral sugars and are generally found in higher concentrations in watermelon (Brummell, 2006; Soteriou et al., 2017) and account for the higher abundance of total neutral sugars compared to uronic acids.

Role of neutral sugar composition in watermelon

Neutral sugars and galacturonic and glucuronic acids are the monomeric building blocks that form complex polysaccharide networks. Understanding the composition of cell wall monosaccharides and subsequent changes can better elucidate watermelon cell wall polysaccharides and the onset of internal fruit disorders. The net change or loss of specific monosaccharides have been linked to fruit ripening characteristics in strawberry, beet, tomato, stonefruit (apple and pear), melon, starfruit and watermelon (Brummell, 2006; Karakurt et al., 2008; Broxterman and Schols, 2018; Petkowicz et al., 2016).

In this experiment, 12 neutral sugars were analyzed in fruit from grafted and non-grafted plants with and without HH (Table 5.6). Previous research on watermelon focused on the mol% of only the major monosaccharide building blocks (e.g., galactose, glucose, arabinose, xylose, rhamnose, galacturonic and glucuronic acid) (Yu and Mort, 1996; Brummell, 2006). Furthermore, past watermelon research concentrated on the composition of crude AIR samples and ASD after fruit were treated with or without ethylene and then were hydrolyzed with endo-polygalacturonase (Yu and Mort, 1996; Karakurt et al., 2008; Mort et al., 2008). Similarly to other watermelon research, monosaccharides in highest content in this study were glucose (78.22 $\mu g \cdot mg^{-1}$), galactose (48.49 $\mu g \cdot mg^{-1}$), xylose (27.65 $\mu g \cdot mg^{-1}$) and arabinose (19.76 $\mu g \cdot mg^{-1}$), respectively (Table 5.6).

Among the major monosaccharides identified in watermelon cell wall materials, galactose plays a role in the backbone of plant cell wall pectins and is also a major constituent in arabinogalacto-proteins and rhamnogalacturonan I and II (Jimenez et al., 2001; Kruger et al., 2008; Pogosyn et al., 2018). Due to the presence of galactose in many of the pectic polysaccharides, high concentrations of galactose are expected in watermelon and data in Table 5.6 supports this. Glucose is known to increase in the cell wall as plant and fruit parts ripen (Jimenez et al., 2001), and is a monomeric building block in cellulose, hemicellulose and pectic polysaccarhides of rhamnogalacturonan II (Pettolino et al., 2012; Chormova and Fry, 2015). Research on olive fruits suggests increases in glucose are related to increases in

rhamnogalacturonan II (Jimenez et al., 2001). Xylose is major monosaccharide in the formation of xylogalacturonan, encompassing about 10% of plant cell wall pectins (Kruger et a., 2008). Xylose also plays a role in rhamnogalacturonan II side branches and high amounts of xylose are expected in the plant cell wall (Brummel, 2006; Karakurt, 2008; Kruger et al., 2008). Arabinose is known primarily to be a pectic sugar and is dominant in building type I and II arabinogalacturonan which attach to rhamnogalacturonan I and xylogalacturonan (Pogosyn et al., 2013; Yang et al., 2018).

In the watermelon fruit AIR, no 2-deoxy-d-ribose was detected and no differences were found in galactose, glucose, mannose, xylose, and galacturonic and glucuronic acids in fruits from grafted and non-grafted plants. Higher amounts of galacturonic acid (26.28 $\mu g \cdot mg^{-1}$) were found compared to glucuronic acid (10.15). Since galacturonic acid (GalA) is the most common uronic acid backbone in the pectic polysaccharides, high amounts of GalA are expected in watermelon cell walls (Pogosyn et al., 2013; Yang et al., 2018). Coenen et al. (2007) identified a model for the pectic backbone which is made up of alternating homogalacturonan and rhamnogalacturonan I with xylose as side chains. It has been shown that homogalacturonan elements are built up 81-117 GalA residues (Coenen et al., 2007), while rhamnogalacturonan I is built of ~20 GalA residues (Amos and Mohnen, 2019), which further relates to the high amounts of GalA found in watermelon cell walls. Glucuronic acid (GlcA) is expected to be found in lower amounts compared to GalA. Glucuronic acid is found only in xylans (made up of 12 GlcA residues), arbinogalacturonan backbones (1-8 GlcA residues) and rhamnogalacturonan II side chains (8-27 GlcA residues) (Chormova and Fry, 2015; Amos and Mohnen, 2019). Since GalA builds the pectic backbones of homogalacturonan and rhamnogalacturonan I, while GlcA is found in the side chains, this is the probable cause for lower amounts of GlcA compared to GalA in watermelon flesh tissue.

Monosaccharide concentrations in fruit were similar with grafting (Fig. 5.4 A-E) but differed with and without HH (Fig. 5.5 A-E). Arabinose (21.29 $\mu g \cdot mg^{-1}$) (Fig 5.5 A), rhamnose (3.38 $\mu g \cdot mg^{-1}$) (Fig 5.5 B), fucose (2.28 $\mu g \cdot mg^{-1}$) (Fig 5.5 C), and meso-erythritol (0.0333 $\mu g \cdot mg^{-1}$) (Fig. 5.5 E) were higher in fruit with HH. Arabinose is an important monosaccharide known to build arabinose-rich polymers in the cell wall (e.g., pectin arabinans, arabinogalacuturonans and arbionogalacto-proteins) (Verhertbruggen et al., 2009). The increase in arabinose in fruit with HH suggests that there is an increase in arabino-xylan interactions

which aid plasticity in the cell wall and interact the hemicellulose-cellulose network with the pectic network (Moore et al., 2013). Rhamnose monomers (1,4-L-Rha(p)) are present on the side branches of rhamnogalacturonan I (Pogosyan et al., 2013). Pogosyan et al. (2013) found that 1,4-Rha(p) linkages are stereoselective in their binding and either link to 1,4-d-galacturonate or accept a-1,2-L-galacturonate. To date there is no information regarding rhamnose in watermelon fruit with HH. However, increases of rhamnose may change the stereoselectivity of rhamnogalacturonan I binding (Pogosyan et al., 2013), ultimately changing the side branch configuration and the interaction of rhamnogalacturonan I with other pectins and the hemicellulose-cellulose network.

Fucose was also higher in fruit with HH compared to fruit without HH. Although fucose is a considered a minor cell wall constituent, it plays a role in the formation of several cell wall polymers. Fucose is found in rhamnogalacturonan II side branches and also in arabinogalacturonan I and II side branches along with arabinogalacto-proteins (Chormova and Fry, 2015; Yang et al., 2018). Increases in fucose are often specifically related to increases in rhamnogalacturonan II, which aids cell wall strength and integrity due to its interaction with homogalacturonan (Verhertbruggen et al., 2009; Leivas et al., 2015), since rhamnogalacturonan II is thought to be covalently linked to homogalacturonan (Cardosa et al., 2007). Meso-erythritol was also higher in fruit with HH and is denoted as a sugar alcohol found in the lipid membrane (Morita et al., 2007). Meso-erythritol serves in the formation of glycolipids which are lipids with a carbohydrate attached by a glycosidic bond; their role is to maintain stability in the cell membrane (Morita et al., 2007). It important to note that the methodology optimized for cell wall polysaccharide composition in watermelon did not take into account cell wall polysaccharide interactions with glycolipids.

The neutral sugar, 2-deoxy-d-glcose was highest in fruit without HH (Fig 5.4 D). Currently, very little information on 2-deoxy-d-glcose is present with respect to its importance in the plant cell wall. Researchers have identified that 2-deoxy-d-glucose, stored in plant cytosol and vacuoles, is an analog of glucose, known to inhibit glycolysis and protein synthesis (Kunz et al., 2001). Gale et al. (1984) studied *Candida albicans,* and found that 2-deoxy-d-glucose can be incorporated into glucan chains. Glucose residues are incorporated into glucan chains when the cell wall is damaged or disassembled as 1,3-β-glucan. In cases where plant cells store 2-d-Glc, it will be incorporated into the β-glucan chains. 2-deoxy-d-glucose residue is generally added at

the terminal (growing) end of the 1,3-β-glucan chain; however, it does not out compete the addition of Glc residues into the chain, instead it alters cell wall properties and interactions pectic polysaccharides with eachother and other cell wall constituents (Harholt et al., 2010). A similar phenomena may be occurring in watermelon due to changes in cell wall metabolism in watermelon fruit from grafted plants without HH.

Ribose was highest in fruit from grafted plants without HH compared to all other treatments (Fig. 5.6 A). Ribose is a monosaccharide also found in rhamnogalacturonan II. In olive research, increased ribose was suspected to increase rhamnogalacturonan I and II (Verhertbruggen et al., 2009). Since fruit from grafted plants without HH had higher amounts of fucose, a similar situation may be occurring in watermelon. Allose was also highest in fruit from grafted plants without HH (Fig 5.6 B). Research on bitter melon indicated allose was a contributor to plant glycosides (Nhiem et al., 2010), which are known as secondary metabolites generally used for plant defense mechanisms. Allose was found in very low concentrations in watermelon cell wall. The hydroxyl groups on allose were previously found to form hydrogen bonds with protein (Ser147 and Arg151) side branches in *E. coli*. (Chaudhuri et al., 1999) and may have a similar role in watermelon cell walls.

The degree of methylation has been associated with the rate of cell wall degradation in that higher rates of methylation are related to increases of cell wall disassembly (Krall and McFeeters, 1998; Lurie et al, 2003). Pectin can be demethylated and depolymerized both by enzymatic and non-enzymatic reactions in fruit and vegetables (Krall and McFeeters, 1998). During fruit ripening there is extensive depolymerization of pectin and removal of neutral sugar side chains (Brummell and Harpster, 2001). No significant differences in the degree of methylation were found with watermelon grafting treatment or HH phenotype. The degree of methylation was highly variable and may explain the lack of significance found in the watermelon treatments.

Linkage assembly of cell wall constituents

Methylation analysis is an important tool used to elucidate polysaccharide structure and investigate cell wall architecture (Pettolino et al., 2012). Complex polysaccharide classes are partially methylated to yield partially methylated alditol acetates (PMAA) after subsequent hydrolysis and acetylation. PMAAs can be separated, quantified and identified with linkage positions via GC-MS. T-Rha(p), 4-Glc(p), 3-Glc(p) and 3,4-Glc(p) were found to be in highest

abundance in watermelon cell wall materials at 41.51 μg·mg^{-1}, 14.50 μg·mg^{-1}, 4.17 μg·mg^{-1} and 3.48 μg·mg^{-1}, respectively (Table 5.7). Pettolino et al. (2012) identified the linkage assembly of Arabidopsis and listed the plausible polysaccharides responsible for each linkage in her protocol. T-Rha(p) is commonly found in type II arbinogalacturonan and small amounts are present in rhamnogalacturonan II (Pettolino et al., 2012). In olive fruit, t-Rha(p) was also found to be dominate in linkages with t-Ara(f), commonly found in arabinan-rich polysaccharides like type I and II arabinogalacturonan (Cardoso et al., 2007). Since t-Rha(p) was the linkage in highest concentration in this study, type II arabinogalacturonan may be a dominant pectic polysaccharide (Cardoso et al., 2007) in watermelon.

Another linkage found in high concentration in watermelon tissue was 4-Glc(p) at 14.50 μg·mg^{-1}. This PMAA is commonly derived from cellulose, homogalacturonan or xylogalacturonan (Pettolino et al., 2012). However, 4,6-Man(p) is required to link to 4-Glc(p) for homogalacturonan and 4,6-Glc(p) is required for xylogalacturonan (Pettolino et al., 2012; Jensen et al., 2008). Since 4,6-Man(p) or 4,6-Glc(p) were not identified in this experiment, this linkage may not be related to xylogalacturonan or homogalacturonan. Further confirmation of the absence of these linkages is needed to fully rule out the presence of these polysaccharides. Cellulose is another dominant polysaccharide with 4-Glc(p) linkages (Pettolino et al., 2012), indicating watermelon cell walls may have relatively high amounts of cellulose.

The linkage residue of 3-Glc(p) is quite common in the glycosidic backbone of hemicellulose (Berglund et al., 2016). Pectic polysaccharides are known to embed in the hemicellulosic network, aiding in cell wall strength and integrity (Hofte et al., 2012; Broxterman and Schols, 2018). Due to 3-Glc(p) being in high abundance, interactions between pectin and hemicellulose may be prevalent in watermelon cell walls. In celery, 3,4-Glc(p) was identified in the collenchyma cells and is known to be a glycosyl linkage that plays a role in cell wall growth and elongation (Chen et al., 2017). Researchers have found that glycosidic bonds (e.g., covalent bonds) join a carbohydrate to another functional group or cell wall carbohydrate, aiding cell wall growth and elongation.

Three of the identified linkages, 4-Glc(p), 3-Glc(p) and 2,4-Glc(p), were highest in fruit without HH from grafted plants (Fig. 5.4 A, B and C). The linkage residue of 4-Glc(p) is commonly found in cellulose, homogalacturonan or xylogalacturonan. Since no 4,6-Man(p) or 4,6-Glc(p) were found in this experiment, higher amounts of 4-Glc(p) may be associated to

increased rates of cellulose. As mentioned, 3-Glc(p), is important to the glycosidic backbone of hemicellulose. Increases in this linkage in fruit from grafted plants without hollow heart suggest structural changes in network interactions may be prevalent in these fruit (Verhertbruggen et al., 2009). The PMAA, 2,4-Glc(p) is currently unassigned to specific polysaccharide classes and instead is considered 'other' or an unclassified component of polysaccharides (Pettolino et al., 2012; Chen et al., 2017).

Linkage assembly of cell wall constituents

Methylation analysis is an important tool used to elucidate polysaccharide structure and investigate cell wall architecture (Pettolino et al., 2012). Complex polysaccharide classes are partially methylated to yield partially methylated alditol acetates (PMAA). PMAAs can be separated, quantified and identified with linkage positions via GC-MS. The linkages 4-Glc(p), 3-Glc(p), 3,4-Glc(p) and t-Rha(p) were found to be in highest concentration at 14.50 $\mu g \cdot mg^{-1}$, 4.17 $\mu g \cdot mg^{-1}$, 3.48 $\mu g \cdot mg^{-1}$ and 2.31 $\mu g \cdot mg^{-1}$, respectively (Table 5.7). Pettolino et al. (2012) identified the linkage assembly of Arabidopsis and lists the plausible polysaccharides responsible for each linkage in her protocol. T-Rha(p) is commonly found in type II arbinogalacturonan and small amounts are present in rhamnogalacturonan II (Pettolino et al., 2012). In olive fruit, t-Rha(p) was also found to be dominate in linkages with t-Ara(f), commonly found in arabinan-rich polysaccharides like type I and II arabinogalacturonan (Cardoso et al., 2007). Since t-Rha(p) is the linkage in highest concentration, type II arabinogalacturonan may be a dominant pectic polysaccharide (Cardoso et al., 2007) in watermelon.

Another linkage found in high concentration in watermelon tissue was 4-Glc(P) at 14.50 $\mu g \cdot mg^{-1}$. This PMAA is commonly found in cellulose, homogalacturonan or xylogalacturonan (Pettolino et al., 2012). However, 4,6-Man(p) is required to link to 4-Glc(p) for homogalacturonan and 4,6-Glc(p) is required for xylogalacturonan (Pettolino et al., 2012; Jensen et al., 2008). Unfortunately, 4,6-Man(p) or 4,6-Glc(p) and were not identified in this experiment, thus watermelon from this experiment could not be related to xylogalacturonan or heteromanan. Although, cellulose is another dominant polysaccharide with 4-Glc(p) (Pettolino et al., 2012), indicating watermelon cell walls may have high amounts of cellulose.

Two other glucose linkages, 3-Glc(p) and 3,4-Glc(p) were found in high abundance in watermelon, 3-Glc(p) and 3,4-Glc(p). The linkage residue of 3-Glc(p) is quite common in the glycosidic backbone of hemicellulose (Berglund et al., 2016). Pectic polysaccharides are known

to embed in the hemicellulosic network, aiding in cell wall strength and integrity (Hofte et al., 2012; Broxterman and Schols, 2018). Due to 3-Glc(p) being in high abundance, interactions between pectin and hemicellulose may be prevalent in watermelon cell walls. In celery, 3,4-Glc(p) was identified in the collenchyma cells and is known to be a glycosyl linkage that plays a role in cell wall growth and elongation (Chen et al., 2017). Researchers have found that glycosidic bonds (e.g., covalent bonds) join a carbohydrate to another functional group or cell wall carbohydrate, aiding cell wall growth and elongation.

Three various linkages, 4-Glc(p), 3-Glc(p) and 2,4-Glc(p), were found to be different only in the interaction of graft and hollow heart, and were highest in fruit from grafted plants without HH (Fig. 5.4 A, B and C). The linkage residue of 4-Glc(p) is commonly found in cellulose, homogalacturonan or xylogalacturonan. Since data from this experiment did not identify critical linkages (e.g., 4,6-Man(p) or 4,6-Glc(p)) that play a role in homogalacturonan and xylogalacturonan, this suggests that fruit with higher amounts of 4-Glc(p) have no association to these two polysaccharide classes. Instead, fruit from grafted plants without HH may have increased amounts of cellulose (Pettolino et al., 2012). As mentioned, 3-Glc(p), is important to the glycosidic backbone of hemicellulose. Increases of this linkage in fruit from grafted plants without hollow heart suggest structural changes in network interactions may be prevalent in these fruit (Verhertbruggen et al., 2009). The PMAA, 2,4-Glc(p) is currently unassigned to specific polysaccharide classes and instead is considered ‘other’ or unknown components of polysaccharides (Pettolino et al., 2012; Chen et al., 2017). Researchers have found that glycosidic bonds (e.g., covalent bonds) join a carbohydrate to another functional group or cell wall carbohydrate. Since 2,4-Glc(p) is a glycosidic bond, grafted fruit without HH potentially have increases in glycosidic linkages.

The cell wall data had several unknown methylated sugars and/or sugars with the same relative retention times and mass spectra. Due to this missing data, calculating tentative classes of polysaccharides is very difficult and additional verification is needed. There are several unknown mass spectra for partially methylated xylose, glucose and galactose (Complex Carbohydrate Researcher Center, 2020). Pettolino et al. (2012) suggests that partially methylating sugar standards can help with verifying of this unknown data, and is a necessary step to complete watermelon polysaccharide linkage assembly. Additionally, some peaks coeluted at the same time or were of very low intensities. These issues may be due to low abundance of

these linkages, low amounts of starting AIR pellet, or improper solubilization in dimethyl sulfoxide (Pettolino et al., 2012) Solubilization of the plant cell wall is critical in methylation analysis (Pettolino et al., 2012). Thus, future work on watermelon may need to address this problem by increasing the amount of AIR to potentially increase peak intensity. Optimization of AIR solubility in dimethyl sulfoxide may also be needed; this can be done by increasing freeze drying time to eliminate trace amounts of water and improve dimethyl sulfoxide solubility (Pettolino et al., 2012). Increasing freeze drying time may help with complete AIR solubilization allowing for researchers to identify PMAA mass spectra with known linkages.

Cell wall analysis and fruit quality

Data showed interesting and unexpected trends with respect to linkage analysis and monosaccharide composition. However, total pectin and cell wall composition data could not be linked directly to differences in fruit textural characteristics. Heart tissue firmness in fruit from grafted plants was 3 N higher compared to fruit from non-grafted plants (Fig 5.1 A). Since no direct changes in monosaccharides or monosaccharide linkages (PMAAs) were directly related, there may be other factors playing a role in watermelon textural characteristics.

By using a combination of different techniques, a stronger investigation of the plant cell wall and its association to fruit textural qualities can be done (Ng et al., 2013). In apple, the degree of polymerization, enzymatic activity (endo-polygalacturonase and pectin methylesterase), tissue microstructure/middle lamella separation and molecular weight of pectin were related to changes in fruit texture relative to the cell wall (Ng et al., 2013). Size exclusion chromatography assesses the molecular weight of pectins in the cell wall and can indicate how polysaccharides were cleaved (Uliyanchenko, 2014). Larger pectin molecules were associated with increased tissue firmness in apple (Ng et al., 2013). Utilizing pectin immunolabeling, L19 antibody labelled lowly-esterified homogalacturonan and L20 antibody labelled highly-esterified homogalacturonan in apple middle lamella (Ng et al., 2013). The intensity of the antibodies along with microscopy images of labeled cells gave insight on cell adhesion, cell-to-cell loosening and middle lamella separation (Ng et al., 2013; Pose et al., 2015). Immunolabeling also indicated the type of homogalacturonan within the middle lamella, which was most responsible for cell-to-cell communication (Ng et al., 2013).

The degree of polymerization is similar to molecular weight analysis, and can give insight on the number of residues within a polysaccharide chain (Pose et al., 2015). In

strawberry, decreases in the degree of polymerization were found as fruit matured and fruit firmness decreased (Pose et al., 2015). Enzymes of pectin methylesterase (PME) and endo-polygalacturonase (PG) are known to play a role in the adhesion properties of cells. (Ng et al., 2013). Endo-polygalacturonse is thought to depolymerize homogalacturonan within streachtches of unesterified galacturonic acid residues that are created by PME (Ng et al., 2013; Brummell and Harpster, 2001). Analyzing PME in apple indicated higher enzyme activity was related to decreases in highly-esterified homogalacturonan while increases in PG were found to depolymerize pectins in the cell wall leading to softer fruit (Ng et al., 2013). Enzymes (PG and PME) have been previously followed in ethylene and air treated watermelon to follow tissue softening, yet no differences were found in enzyme activity (Brummell, 2006; Karakurt et al., 2009; Karakurt and Huber, 2009).

Finally, assessing microRNA in fruit from grafted and non-grafted plants with and without HH can give information on expression patterns of the genome (Luo et al., 2018), difference in textural properties and cell wall characteristics by up or downregulating genes. Genes that determine important traits are usually negatively regulated by microRNA, which participate in numerous biological properties in plants (Luo et al., 2018). Pomegranate seed hardness was linked to different fruit stages and differentially expressed microRNA (Luo et al., 2018). Cell wall biosynthesis and microRNA in *Acacia mangium* indicated that presence of certain microRNA affected the role of cell wall formation (Ong and Wichneswari, 2012). By analyzing microRNA in grafted and non-grafted plants, information about root-stock scion interaction will be gained, which may give better insight as to the role of the rootstock and differences in textural properties between fruit from grafted or non-grafted plants.

Summary

Hollow heart is a serious internal defect found predominantly in triploid watermelon types, and cannot be visually distinguished from normal fruit unless cut. The incidence of hollow heart varies tremendously between growing seasons, making it difficult for breeders to develop screening strategies for the disorder. Grafting a susceptible triploid cultivar to an interspecific hybrid rootstock increased tissue firmness and decreased the incidence of HH, which was induced under conditions of limited pollen. Although the presence of HH can cause load rejection, HH did not compromise fruit quality (e.g., firmness, pH, ^{o}Brix and total sugar) or phytonutrient content.

Tissue firmness has been related to tissue density in watermelon (Kano, 1993) and changes in tissue firmness affect morphological characteristics of fruit cells. In this study, differences in fruit firmness with respect to grafting were not related to cell wall composition. Total pectins from CSF were lowest in fruit with HH. These fractions are found be enriched in homogalacturonan (Panigua et al., 2014; Soteriou et al., 2017) and suggests fruit with HH have lower enrichments of RG I and HG. Unexpected trends were found in monosaccharide composition and linkage analysis. Grafting may protect pectic polysaccharides from cell wall degradation thus increasing tissue firmness. However, other cell wall attributes like tissue microstructure, pectin immunolabelling, enzymatic activity, degree of polymerization and molecular weight may help delineate the relationship of cell wall polysaccharides to fruit textural characteristics.

References

1. Amos, R.A and D. Mohnen. 2019. Critical review of plant cell wall matrix polysaccharide glycosyltransferase activities verified by heterologous protein expression. Frontiers Plant Sci. 10:1-2.

2. Aslam, A. S. Zhao, M. Azam, X. Lu and N. He. 2020. Comparative analysis of primary metabolites and transcriptome changes between ungrafted and pumpkin grafted watermelon. Peer J. 82:1-30l

3. Berglund, J. T.A. d'Ortoli, F. Vilaplana, G. Widmalm, M. Bergenstrahle-Wohler, M. Lawoko, G. Heriksson, M. Lindstrom and J. Wohlert. 2016. A molecular dynamic study of the effect of glycosidic linkage type in the hemicellulose backbone on the molecular chain flexibility. Plant J. 88:56-70.

4. Blumenkrantz, N and G. Asboe-Hansen. 1973. New Method for Quantitative Determination of Uronic Acids. Anal. Biochem. 54:484-489.

5. Broxterman, S. and H. Schols. 2018. Interactions between pectin and cellulose in plant cell walls. Carbohyd. Polymers 192:263-272.

6. Brummell, D.A. 2006. Cell wall disassembly in ripening. Funct. Plant Biol. 33:103-119.

7. Brummell, D.A. and M.H. Harpster. 2001. Cell wall metabolism in fruit softening and quality and its manipulation in transgenic plants. Plant Molec. Biol. 47:311-340.

8. Cao. F., C. Guan, H. Dai, X. Li and Z. Zhang. 2015. Soluble solids content is positively correlated with phosphorus content in ripening strawberry fruits. Scientia Hort. 195:183-187.

9. Cardosa, S. J.A. Ferreira, I. Mafra. A.M.S. Silva and M.A. Combra. 2007. Structural ripening-related changes of the arabinan rich pectic polysaccharides from olive pulp cell walls. J. Agric. Food Chem. 55:7125-7130.

10. Chaudhri, B.N., J. Ko, C. Park, T.A. Jones and S.L. Mowbray. 1999. Structure of d-allose binding protein in *Escherichia Coli* bound to d-allose at 1.8 A resolution. J. Mol. Bio 12:1519-1531.

11. Chen, D. P. J. Harris, I.M. Sims, Z. Zujovic and L.D. Melton. 2017. Polysaccharide compositions of collenchyma cell wall form celery (*Apium graveolens* L.) petioles. BMC Plant Biol. 104:2-13.

12. Chormova, D. and S.C. Fry. 2015. Boron bridging of rhamnogalacturonan II is promoted in vitro by cationic chaperones, including polyhistidine and wall glycoproteins. New Phytol. 209:241-251.

13. Coenen, G.J., E.J. Bakx, R.P. Verhoef, H.A. Schols and A.G.J. Voragen. 2007. Identification of the connecting linkage between homo- or xylogalacturonan and rhamnogalacturonan type 1. Carbohydrate Polymers 70:224-235.

14. Corey, K.A. and D.V. Schlimme. 1988. Relationship of rind gloss and groundspot color to flesh quality of watermelon fruits during maturation. Sci. Hortic. 34:211-214.

15. Daher, F.B and S.A. Braybrook. 2015. How to let go: pectin and plant cell adhesion. Front Plant Sci. 6:523-540.

16. Fall, L.A., P. Perkins-Veazie, G. Ma and C. McGregor. 2019. QTLs associated with flesh quality traits in an elite x elite watermelon population. Euphytica 215:xx-xx.

17. Fallik, E. and Z. Ilic. 2014. Grafted vegetables – The influence of rootstock and scion on postharvest quality. Folia Hortic. 26:79-90.

18. Fredes, A., S. Rosello, J. Beltran, J. Cobella-Cornejo, A.P. De-Castro, C. Gisbert and M. Belen-Pico. 2016. Fruit quality assessment of watermleon grafted to citron melon J. Sci. Food Agric. 97:1646-1655.

19. Freeman, J., G.A. Miller, S.M. Olson and W.M. Stall. 2007. Diploid watermelon pollenizer cultivars differ with respect to triploid watermelon yield. HortTechnology 17:518-523.

20. Gale, E.F., F. Wayman and P.A. Orlean. 1984. The action of 2-deoxy-D-gluose on the incorporation of glucose into (1-3)-β-glucan in station phase cultures of *Candida albicans*. Microbiology 130:3303-3311.

21. Gawkowska, D., J. Ciesla, A. Zedunek and J. Cybulska. 2019. Cross-linking of diluted alkali-soluble pectin from apple (Malus domestica fruit) in different acid-base conditions. Food Hydrocolloids 92:285-292.

22. Guan, W. 2018. Hallowheart of watermelons. Purdue Agriculture. [Online]. https://ag.purdue.edu/btny/ppdl/Pages/POTW2018/POTW09042018.aspx

23. Harholt, J., A. Suttankakul and H.V. Scheller. 2010. Biosynthesis of Pectin. Plant Physiol. 153:384-395.

24. Hassell, R., F. Memmott, and D.G. Liere. 2008. Grafting methods for watermelon production. HortScience 43:1677-1679.

25. Hofte, H., A. Peaucelle and S. Braybrook. 2012. Cell wall mechanics and growth control in plants: the role of pectins revisited. Front. Plant Sci. 3:121-130.

26. Jensen, J.K., S.O. Sorensen, J. Harholt, N. Geshi, Y. Sakuragi, I. Moller, J. Zandleven, A.J. Bernal, N.B. Jensen, C. Sorensen, M. Pauly, G. Beldman, W.G.T. Willats and H.V. Scheller. 2018. Plant Cell 120:1289-1302.

27. Jimenez, V.A.O., G. Berumen-Varela, R.F.V. Tiznado-Hernandez. 2001. Rhamnogalacturonan lyase: a pectin modification enzyme of higher plants. J. Food Agric. 30:910-917.

28. Johnson, G. 2014. These beautiful watermelon patterns are driving everyone crazy. [Online]. https://www.boredpanda.com/weird-watermelons-beautiful-hollow-heart/

29. Johnson, G. 2015. Research finds potential cause of hollow heart disorder in watermelon. PhysOrg. [Online]. https://phys.org/news/2015-06-potential-hollow-heart-disorder-watermelons.html

30. Kano, Y. 1993. Relationship between the occurrence of hollowing in watermelon and the size and the number of fruit cells and intercellular air space. J. Japan Soc. Hortic. Sci. 62:103-112.

31. Karakurt, Y. and D.J. Huber. 2009. Purification and partial characterization of xyloglucan-hydrolyzing enzymes from watermelon placental tissue. J Sci. Food Agric. 89:645-652.

32. Karakurt, Y., N. Muramatsu, J. Jeong, B. Hurr and D. Huber. 2008. Matrix glycan depolymerization and xyloglucan endohydrase activity in ethylene-treated watermelon fruit. J Sci. Food Agric. 88:684-689.

33. Krall, S.M and R.F. McFeeters. 1998. Pectin hydrolysis: Effect of temperature, degree of methylation and calcium on hydrolysis rates. J. Agric Food Chem. 46:1311-1315.

34. Kruger, J., S.A. Sorensen, J. Harholt, N. Geshi, Y. Sakuragi, J. Moller, J. Zandleven, A.J. Bernal, N.B. Jensen, C. Sorensen, M. Pauly, G. Beldman, W.G.T. Williats and H.V Scheller. 2008. Identification of xylogalacturonan xylosyltransferase involved in pectin biosynthesis in Arabidopsis. Plant Cell 20:1289-1302.

35. Kunze, I., M. Ebneth, U. Heim, M. Geiger, U. Sonnewald and K Herbers. 2001. 2-Deoxyglucose resistance: a novel selection marker for plant transformation. Molec. Breeding 7:221-227.

36. Kyriacou, M.C. G.A. Soteriou, Y Rouphal, A.S. Siomos and D. Gerasopoulos. 2016. Configuration of watermelon fruit quality in response to rootstock-mediated harvest maturity and postharvest storage. J. Sci. Food Agric. 96:2400-2409.

37. Leivas, C.L. M. Lacomini. And L.M.C. Cordeiro. 2013. Structural characterization of rhamnogalacturonan I-arabinan-type-I arabinogalactan macromolecule from starfruit (*Averrhoa carambola* L.). Carbohydrate Polymers 121:224-230.

38. Levi, A., J.A. Thies, P.W. Wechter and M. Farnham. 2014. USVL-360, a novel watermelon tetraploid germplasm line. HortScience 49:354-357.

39. Liu, Q. X. Zhao, J. Brecht, C.A. Sims, T. Sanchez and N. Dufault. 2017. Fruit quality of seedless watermelon grafted onto squash rootstocks under different production systems. J. Sci. Food Agri. 97:4704-4711.

40. Luo, X., D. Cao, J. Zhang, L. Chen, X. Xia, H. Li, D. Zhao, F. Zhang, H. Xue, L Chen, Y. Li and S. Cao. 2018. Integrated microRNA and mRNA expression profiling reewals a complex network regulating pomegranate (*Punica granatum* L.) seed hardness. Scientific Reports 8:9292-9306.

41. Lurie, S., H.W. Zhou, A. Lers, L. Sonego. S. Alexandrov and I. Shomer. 2003. Study of pectin esterase and changes in pectin methylation and abnormal peach ripening. Plant Physiol. 119:287-293.

42. Martinez-Ballesta, M.C., C. Alcaraz-Lopez, B. Muries, C. Mota-Cadenas and M. Carvajal. 2020 Physiological aspects of rootstock-scion interactions. Sci. Hortic 127:112-118.

43. Masuko, T., A. Minami, N. Iwasaki, T. Majima, S-I Nishimura and Y.C. Lee. 2005. Carbohydrate analysis by a phenol-sulfuric acid method in microplate format. Anal. BioChem. 339:69-72.

44. Mohamed, F.H., E. Khalid, A. El-Hamed, M.W.M. Elwan and N.E. Hussien. 2012. Impact of grafting on watermelon growth, fruit yield and quality. Veg. Crops Res. Bull 76:99-118.

45. Mohnen, D. 2008. Pectin structure and biosynthesis. Curr. Opin. Plant Biol. 11:266–277.

46. Moore, J.P., E.E. Nguema-Ona, M. Vicre-Gibouin, E. Sorensen, W.G.T. Willats, A. Driouich and J.M Farrant. 2013. Arabinose-rich polymers as an evolutionary strategy to plasticize resurrection plant cell walls against desiccation. Planta 237:739-754.

47. Morita, T. M. Konishi, T. Fukuoka, T. Imura, H.K. Kitamoto and D. Kitamoto. 2006. Characterization of the genus *Pseudozyma* by the formation of glycolipid biosurfactants, mannosylerythritol lipids. FEMS Yeast Res. 7:286-292.

48. Mort, A., Y. Zeng, F. Qiu, M. Nimtz, and G. Bell-Eunice. 2008. Structure of xylogalacturonic fragments from watermelon cell-wall pectin. Endopolygalacturonase can accommodate a xylosyl residue on the galacturonic acid just following the hydrolysis sight. Carbohyd. Res. 434:1212-1221. Magn. Reson. Chem. 48:392-396.

49. Ng, J.K.T., R. Schroder, P. Sutherland, I. Hallett, M. Hall, R. Prakash, B. Smith, L. Melton and J. Johnston. 2013. Cell wall structures leading to cultivar differences in

softening rates develop early during apple (*Malus* x *domestica*) fruit growth. BMC Plant Biol. 13:183-196.

50. Nhiem, N.X., P.V. Kiem, C.V. Mink, N.K. Ban, N.X. Cuong, L.M. Ha, B.H. Tai, T.H. Quang, N.H Tung and Y.H Kim. 2010. Cucurbitane-type triterpene glycosides from the fruits *Momordic charantia*.Chem. Pharm. Bull. 58:720-724.

51. Ong, S.S. and R. Wichneswari. 2012. Characterization of microRNAs expressed during secondary wall biosynthesis in *Acacia mangium*. PLOS ONE 7:49662-49675.

52. Paniagua, C., N. Santiago-Domenech, A.R. Kirby, A.P. Gunning, V.J Morris, M.A. Quesada, A.J. Matas and J.A. Mercado. 2017. Structural changes in cell wall pectins during strawberry fruit development. Plant Physiol. Biochem. 118:55-63.

53. Penaloza, P and P. Toloza. 2018. Boron increases pollen quality, pollination and fertility of different genetic lines of pepper. J Plant Nutrition 41:969-979.

54. Petkowicz, C.L.O, L.C. Vriesmann, and P.A. Williams. 2016. Pectins from food waste: Extraction, characterization and properties of watermelon rind pectin. Food Hydrocolloids, 65:57-67.

55. Perkins-Veazie, P. J. Lotito and R. Hassell. 2016. Development of a firmness tester designed for large watermelon. HortScience Poster board 51:S250.

56. Pettolino, F.A., C. Walsh, G.B. Fincher and A. Bacic. 2012. Determining the polysaccharide composition of plant cell walls. Nat. Protoc. 9:1590-1607.

57. Pogosyn, A. A. Gottwalk, D. Michalik, H.U. Endress and C. Vogel. 2013. Efficient synthesis of building blocks for branched rhamnogalacturonan I fragments. Carbohydrate Res. 380:9-15.

58. Pose, S., A.R. Kirby, C. Paniagua, K.W. Waldron, V.J Morris, M. Quesada and J.A. Mercado. 2015. The nanostructural characterization of strawberry pectins in pectic lyase or polygalacturonase silenced fruits elucidates their role in softening. Carbohydrate Polymers 132:134-145.

59. Printz, B., L. Stanley, J.F. Hausman and K. Sergeant. 2016. Copper trafficking in plants and its implication on cell wall dynamics. Frontiers Plant Sci. 7:601-617.

60. Redgwell, R.J., L.D. Melton and D.J. Brash. 1992. Cell wall dissolution in ripening kiwifruit. Plant Physiol. 98:71-81.

61. Rose, J.K. 2003. The Plant Cell Wall. © Blackwell publishing LTD.

62. Ruiz, J.M. A. Belakbir, I. Lopez-Cantarero and L. Romero. 1997. Leaf macronutrient content and yield in grafted melon plants: a model to evaluate the influence of rootstock genotype. Sci. Hortic. 71:227-234.

63. Schultheis, J.R. and K. Starke. 2019. North Carolina triploid standard and mini-size watermelon cultigen studies. No. 233. Pp 1-39. [Online]. https://cucurbits.ces.ncsu.edu/growing-cucurbits/variety-trials/2019-north-carolina-triploid-standard-mini-size-watermelon-cultigen-evaluation-studies/

64. Soteriou, G.A., Kyriacou, M.C., Simons, A.S., and Gerasopoulos, D. 2014. Evolution of watermelon fruit physicochemical and phytochemical composition during ripening as affected by grafting. J. Food Chem.165:282-289.

65. Soteriou, G.A., A.S. Siomos, D. Gerasopoulous, Y. Rouphael, S. Georgiadou, S. and M.K. Kyriacou. 2017. Biochemical and histological contributions to textural changes in watermelon fruit modulated by grafting. J. Food Chem. 237:133-140.

66. Srivastava, A. and A.K. Handa. 2005. Hormonal regulation of tomato fruit development: A molecular perspective. J Plant Growth Reg. 24:67-82.

67. Tanner, W. and F.A. Loewus. 2012. Plant Carbohydrates II. Cell wall in higher plants. Springer-Verlag Berlin Heidleberg, New York. © 2012.

68. Trandel, M., P. Perkins-Veazie, J. Schultheis, C. Gunter and E. Johannes. 2020a. Grafting watermelon onto interspecific hybrid rootstock reduces hollow heart. ActaHortic. Xx:xx-xx. (in review).

69. Trandel, M., P. Perkins-Veazie and J. Schultheis. 2020b. Predicting hollow heart incidence in triploid watermelon (*Citrullus lanatas*). HortScience Xx:xx-xx. (in press).

70. Uliyanchenko, E. 2014. Size-exclusion chromatography-from high performance to ultra-performance. Anal. Bioanal. Chem. 406:6087-6094.

71. USDA. 2006. US Standards for Grades of Watermelon. Agricultural Marketing Services, Fruit and Vegetable Program, pp. 1-11.

72. Verhertbruggen, Y., S.E. Marcus, A. Haeger, R. Verhoef, H.A. Schols, B.V. McCleary, L. McKee, H.J. Gilbert and J.P. Knox. 2009. Developmental complexity of arabinan polysaccharides and their processing in plant cell walls. Plant J. 59:413-425.

73. Yang, J., L. Wen, Y. Zhao, Y. Jian, M. Tian, H. Liu, J. Liu and B. Yang. 2018. Structure and identification of an arabinogalacturonan in *Citrus reticulata* Blanco 'Chachiensis' peel. Food hydrocolloids 84:481-488.

74. Yativ, M, I. Haray and S. Wolf. 2010. Sucrose accumulation in watermelon fruits: Genetic variation and biochemical analysis. J. Plant Physiol. 167:589-596.

75. Yu, L. and A.J. Mort. 1996. Partial characterization of xylogalacturonans from cell walls of ripe watermelon fruit: inhibition of endo-polygalacturonase activity by xylosylation. Progress Biotech. 14:79-88.

76. Zywinska, A.W., M.C.J. Ralet, C.D. Gernier and J.F.J Thibault. 2005. Evidence for in vitro binding pectin side chains to cellulose. Plant Physio. 139:397-407.

APPENDICES

Appendix A

Quality Measurements for the 2019 Field Trial: Cell Wall Polysaccharides in Grafted and Non-Grafted Watermelon

Table A.1. LS-means of quality and composition of fruit with or without hollow heart (HH) from grafted or not grafted plants.

Quality measurement	Graft		Hollow Heart		Interaction			
	Graft	Non-Graft	- HH	+ HH	Graft -HH	Graft +HH	Non-Graft -HH	Non-graft +HH
Fruit Quality								
Weight (kg)	8.1± 1.7	8.0 ± 1.6	7.6 ± 1.7	8.4 ± 1.6	8.0 ± 1.6a	8.3 ± 1.6a	8.6 ± 2.0a	7.3 ± 1.7a
SSC (ºBrix)	12.3 ± 1.0	12.1 ± 1.5	12.1 ± 1.4	12.4 ± 1.3	12.2 ± 1.5a	12.7± 1.0a	12.0 ± 1.0a	12.1 ± 1.8a
pH	5.4 ± 0.2	5.5 ± 0.3	5.4 ± 0.2	5.6 ± 0.2	5.4 ± 0.2a	5.5 ± 0.2a	5.4 ± 0.2a	5.5 ± 0.2a
Fruit Composition								
Total Sugars ($mg \cdot g^{-1}$)	94.2 ± 2.4	98.2 ± 3.6	95.2 ± 3.1	98.6 ± 2.7	94.7± 2.9a	96.7± 1.4a	98.4 ± 3.0a	96.7 ± 1.7a
%Sucrose	49.6 ± 3.1	46.0 ± 2.5	43.4 ± 3.3	52.2 ± 1.2*	46.4 ± 3.2a	50.9 ± 2.2a	44.7 ± 3.1a	49.1± 3.1a
%Glucose	17.5 ±0.4	17.4 ± 0.2	16.4 ± 2.3	18.6 ± 0.9	17.0 ± 1.9a	18.1 ± 1.2a	16.9 ± 1.0a	18.0 ± 1.2a
%Fructose	31.3 ± 0.1	31.2 ± 0.7	32.9 ± 3.1	29.7 ± 2.3	32.1 ± 1.8a	30.5 ± 2.1a	32.1 ± 1.9a	0.4 ± 2.2a
Phytonutrients								
Lycopene ($mg \cdot kg^{-1}$)	63.1 ± 0.5	60.0 ± 1.1	59.7 ± 0.8	63.2 ± 0.9	61.0 ± 0.8a	66.1 ± 0.5a	56.4 ± 0.8a	59.0 ± 1.3a
Citrulline ($g \cdot kg^{-1}$)	3.4 ± 0.6	3.4 ± 0.7	5.4 ± 0.7	3.5 ± 0.6	3.3 ± 0.6a	3.5 ± 0.6a	3.4 ± 0.8a	3.4 ± 0.7a
Arginine ($g \cdot kg^{-1}$)	1.1 ± 0.2	1.3 ± 0.2	1.1 ± 0.2	1.3 ± 0.2	1.2 ± 0.1a	1.0 ± 0.2a	1.0 ± 0.1a	1.5 ± 0.2a

All quality measures are reported as LS means ± standard errors are separated within row. Tukey's honest significance test done for mean separation ($p \leq 0.05$). Dissimilar means are reported with different letters. * = differences within graft or hollow heart effect. Dissimilar means are reported with different letters in the interaction. -HH = no hollow heart, and +HH = with hollow heart.

Appendix B

Mineral Analysis for the 2019 Field Trial: Cell Wall Polysaccharides in Grafted and Non-Grafted Watermelon

Table A.2. Mineral analysis content of fruit with or without hollow heart (HH) from grafted or not grafted plants.

Mineral	Graft		Hollow Heart		Interaction			
	Graft	Non-Graft	- HH	+ HH	Graft -HH	Graft +HH	Non-Graft -HH	Non-graft +HH
				Macro nutrients (ppm x 10^3)				
Nitrogen	12.8 ± 0.9	12.4 ± 0.9	12.7 ± 0.9	12.4 ± 0.4	12.9 ± 0.9a	12.7 ± 0.8a	12.5 ± 0.9a	12.3 ± 0.9a
Potassium	14.1 ± 0.1	14.6 ± 0.3	14.1 ± 0.1	14.4 ± 0.1	13.9 ± 0.9a	14.5 ± 0.9a	14.3 ± 0.9a	14.9 ± 0.3a
Phosphorus	4.6 ± 0.3	4.1 ± 0.3	2.8 ± 0.3	3.0 ± 0.3*	2.8 ± 0.2a	3.0 ± 0.4a	2.7 ± 0.3a	3.1 ± 0.4a
Magnesium	1.5 ± 0.2	1.4 ± 0.2	1.4 ± 0.1	1.5 ± 0.1	1.5 ± 1.1a	1.5 ± 1.3a	1.5 ± 1.0a	1.5 ± 1.3a
Sulfur	1.1 ± 0.9	1.0 ± 0.7	1.0 ± 0.1	1.0 ± 0.1	1.1 ± 0.1a	1.1 ± 0.2a	0.9 ± 0.1a	1.0 ± 0.2a
Calcium	6.4 ± 0.1	6.5 ± 0.2	6.7 ± 0.1	6.3 ± 0.1	6.7 ± 0.1a	6.1 ± 0.7a	6.6 ± 0.9a	6.5 ± 0.4a
				Micro nutrients (ppm)				
Boron	12.9 ± 1.2	13.2 ± 1.3	12.8 ± 0.3	13.5 ± 0.3*	12.4 ± 1.4a	13.5 ± 1.0a	13.1 ± 1.2a	13.5 ± 1.5a
Zinc	20.7 ± 0.7*	18.2 ± 0.9	18.1 ± 1.6	20.6 ± 1.5*	19.8 ± 3.8a	21.9 ± 3.3a	16.4 ± 3.0a	19.7 ± 1.4a
Manganese	8.6 ± 2.4*	6.8 ± 1.0	7.1 ± 0.4	8.1 ± 0.7*	8.4 ± 2.8a	8.8 ± 2.2a	5.8 ± 0.9a	7.6 ± 1.4a
Iron	21.6 ± 2.8	21.2 ± 2.3	21.8 ± 2.3	21.1 ± 2.1	22.1 ± 2.5a	21.2 ± 3.1a	21.4 ± 2.2a	21.0 ± 2.4a
Copper	7.1 ± 0.9*	5.6 ± 1.1	6.2 ± 0.3	6.8 ± 0.3*	7.0 ± 0.8a	7.2 ± 1.1a	5.3 ± 1.2a	5.8 ± 0.9a

LS means ± standard errors reported within rows. Tukey's honest significance test used for mean separation ($p \leq 0.05$) within row, separately for main effects and interaction effects. Dissimilar means are reported with different letters. -HH = no hollow heart, and +HH = with hollow heart.

Appendix C

Total Cell Wall Material and Sequential for the 2019 Field Trial: Cell Wall Polysaccharides in Grafted and Non-Grafted Watermelon

Table A.3. Total cell wall material and sequential fractions, total neutral sugars and total uronic acids among graft, incidence of hollow heart and the interaction of graft*hollow heart.

	Graft		Hollow Heart		Interaction			
Pectic fractions	**Graft**	**Non-Graft**	**- HH**	**+ HH**	**Graft -HH**	**Graft +HH**	**Non-Graft -HH**	**Non-graft +HH**
				% Fraction				
AIR	0.39 ± 0.02	0.36 ± 0.02	0.37 ± 0.02	0.36 ± 0.02	0.39 ± 0.03a	0.38 ± 0.3a	0.35 ± 0.03a	0.37 ± 0.03a
WSF	12.56 ± 0.8	13.09 ± 0.9	12.60 ± 0.9	13.05 ± 0.9	12.94 ± 1.2a	12.18 ± 1.3a	12.27 ± 1.3a	13.92 ± 1.3a
CSF	25.76 ± 0.7	26.15 ± 0.8	27.08 ± 0.7*	24.83 ± 0.8	27.47 ± 1.0a	24.82 ± 1.1a	27.46 ± 1.1a	24.83 ± 1.1a
ASF	34.02 ± 1.0	35.13 ± 1.0	33.91 ± 1.0	35.24 ± 1.0	33.29 ± 1.3a	34.75 ± 1.4a	33.28 ± 1.3a	35.74 ± 1.5a
UNX	27.29 ± 1.2	25.49 ± 1.3	25.78 ± 1.2	26.98 ± 1.2	26.45 ± 1.5a	28.13 ± 1.7a	25.12 ± 1.8a	25.83 ± 1.8a
				Total Neutral Sugars (nmole·mg^{-1})				
WSF	18.36 ± 1.0	19.17 ± 1.0	19.41 ± 1.0	18.12 ± 1.1	17.81 ± 1.4a	18.88 ± 1.4a	20.97 ± 1.5a	17.37 ± 1.5a
CSF	8.91 ± 0.2	8.61 ± 0.2	8.54 ± 0.2	8.98 ± 0.2	8.25 ± 0.3a	8.97 ± 0.3a	8.82 ± 0.2a	8.99 ± 0.2a
ASF	12.31 ± 0.7	12.11 ± 0.9	12.02 ± 0.9	12.40 ± 0.9	11.96 ± 1.2a	12.66 ± 1.2a	12.08 ± 1.2a	12.14 ± 1.2a
				Total Uronic Acids (nmole·mg^{-1})				
WSF	8.86 ± 0.5	9.35 ± 0.5	9.39 ± 0.5	8.82 ± 0.5	8.59 ± 0.6a	9.14 ± 0.6a	10.18 ± 0.7a	8.52 ± 0.7a
CSF	5.08 ± 0.1	5.18 ± 0.2	4.98 ± 0.1	5.28 ± 0.1	4.82 ± 0.2a	5.34 ± 0.2a	5.15 ± 0.2a	5.21 ± 0.2a
ASF	6.10 ± 0.3	6.24 ± 0.3	6.12 ± 0.3	6.22 ± 0.3	5.88 ± 0.5a	6.12 ± 0.4a	6.36 ± 0.5a	6.13 ± 0.5a

Fractions are reported as LS means ± standard deviation. Total neutral sugars and uronic acids are reported as LS means ± standard deviation. Tukey's honest significance test used for mean separation ($p \leq 0.05$) within row, separately for main effects and interaction effects. Dissimilar means are reported with different letters.

AIR = alcohol insoluble residue, WSF = water soluble fraction, CSF = carbonate soluble fraction, ASF = alkali soluble fraction, UNX = unextractable fraction, -HH = no hollow heart, and +HH = with hollow heart.

Appendix D

Monomers Quantified in Fruit from the 2019 Field Trial: Cell Wall Polysaccharides in Grafted and Non-Grafted Watermelon

Table A.4. LS-means of the neutral sugars hydrolyzed from watermelon cell wall among graft, incidence of hollow and graft * hollow heart interaction.

	Graft		Hollow Heart		Interaction			
Monomer ($\mu g \cdot mg^{-1}$)	**Graft**	**Non-Graft**	**- HH**	**+ HH**	**Graft -HH**	**Graft +HH**	**Non-Graft -HH**	**Non-graft +HH**
				Alditol acetate concentration				
Meso-Ery	0.024 ± 0.01	0.007 ± 0.01	0.000 ± 0.01	0.032 ± 0.01*	0.044 ± 0.03a	0.004 ± 0.01a	0.000 ± 0.01a	0.020 ± 0.01a
2-d-Rib	-	-	-	-	-	-	-	-
Rha	3.46 ± 0.10	3.19 ± 0.12	3.02 ± 0.13	3.38 ± 0.12*	3.20 ± 0.16a	3.31 ± 0.15a	2.83 ± 0.18a	3.55 ± 0.17a
Fuc	2.22 ± 0.09	2.30 ± 0.10	1.92 ± 0.11	2.36 ± 0.11*	2.01 ± 0.15a	2.43 ± 0.14a	1.84 ± 0.17a	2.76 ± 0.16a
Rib	1.17 ± 0.05	1.15 ± 0.05	1.18 ± 0.04	1.13 ± 0.05	1.27 ± 0.06a	1.06 ± 0.06b	1.09 ± 0.08b	1.20 ± 0.07a
Ara	20.64 ± 1.04	19.10 ± 1.12	17.85 ± 1.20	21.29 ± 1.15*	19.31 ± 1.55a	21.98 ± 1.45a	16.32 ± 1.76a	21.95 ± 1.65a
Xyl	27.51 ± 1.14	27.79 ± 1.01	27.18 ± 1.23	28.13 ± 1.18	28.60 ± 1.59a	26.98 ± 1.48a	25.75 ± 1.79a	29.28 ± 1.69a
2-d-Glu	0.42 ± 0.05	0.33 ± 0.06	0.55 ± 0.05*	0.21 ± 0.06	0.58 ± 0.08a	0.28 ± 0.07a	0.52 ± 0.09a	0.15 ± 0.08a
All	0.64 ± 0.07*	0.31 ± 0.07	0.45 ± 0.08	0.50 ± 0.08	0.80 ± 0.11a	0.48 ± 0.11b	0.20 ± 0.12b	0.41 ± 0.12b
Man	1.98 ± 0.09	2.09 ± 0.11	2.11 ± 0.12	1.95 ± 0.11	2.12 ± 0.15a	1.82 ± 0.14a	2.10 ± 0.17a	2.09 ± 0.16a
Gal	51.29 ± 1.88	46.81 ± 1.67	48.27 ± 2.02	49.83 ± 1.94	46.83 ± 2.62a	46.79 ± 2.43a	49.79 ± 2.96a	52.87 ± 2.78a
Glc	75.89 ± 2.89	80.56 ± 3.25	78.07 ± 3.51	78.37 ± 3.37	77.37 ± 4.54a	74.41 ± 4.22a	78.77 ± 5.12a	82.35 ± 4.82a
GalA	24.77 ± 1.81	27.67 ± 2.21	27.67 ± 2.34	25.01 ± 2.18	27.05 ± 2.85a	22.48 ± 2.63a	28.30 ± 3.54a	27.54 ± 3.27a
GlcA	9.87 ± 0.71	10.48 ± 0.87	10.48 ± 0.92	9.76 ± 0.86	10.49 ± 1.12a	9.24 ± 1.03a	10.47 ± 1.39a	10.30 ± 1.28a
				Degree of methylation (%)				
Methylation	71.27 ± 5.96	72.95 ± 4.90	75.01 ± 6.32	69.22 ± 6.32	66.54 ± 7.68a	76.01 ± 7.12a	83.47 ± 9.56a	62.43 ± 8.83a

LSmeans ± standard deviation of the alditol acetates ($\mu g \cdot mg^{-1}$) and degree of methylation Tukey's honest significance test used for mean separation.

-HH = no hollow heart, and +HH = with hollow heart.

Appendix E

Linkage Residues Identified in Fruit from the 2019 Field Trial: Cell Wall Polysaccharides in Grafted and Non-Grafted Watermelon

Table A.5. Monosaccharide linkage assembly of watermelon cell wall polysaccharides in fruit from graft or not grafted fruit with or without hollow heart.

Monosaccharide	Treatment	Estimated concentration ($\mu g \cdot mg^{-1}$)	p-value	Common polysaccharide class
t-Rha(p)	G	40.91 ± 10.91	0.3833	RG II, Type II
	NG	42.00 ± 13.03		and AG
	-HH	44.63 ± 9.81	0.8516	
	+HH	38.51 ± 12.93		
	G -HH	44.45 ± 4.51a	0.9526	
	G +HH	36.64 ± 15.3a		
	NG -HH	44.88 ± 16.0a		
	NG +HH	40.06 ± 11.8a		
3,4-Rha(p)	G	1.11 ± 0.40	0.9829	RG I
	NG	1.17 ± 0.36		
	-HH	1.21 ± 0.41		
	+HH	1.08 ± 0.35		
	G -HH	1.24 ± 0.02a	0.2328	
	G +HH	0.95 ± 0.01a		
	NG -HH	1.15 ± 0.02a		
	NG +HH	1.18 ± 0.01a		
3-Fuc(p)	G	0.59 ± 0.19	0.6561	AG proteins
	NG	0.65 ± 0. 22		
	-HH	0.66 ± 0.19	0.7703	
	+HH	0.58 ± 0.25		
	G -HH	0.70 ± 0.18a	**0.0257**	
	G +HH	0.45 ± 0.09b		
	NG -HH	0.60 ± 0.19c		
4-Fuc(p)	NG +HH	0.68 ± 0.30a		RG I, II and XG
or t-Gal(p)	G	0.59 ± 0.27	0.8715	AG proteins
	NG	0.66 ± 0.40		
	+HH	0.63 ± 0.24	0.8341	
	-HH	0.62 ± 0.41		
	G -HH	0.69 ± 0.26a	0.0618	
	G +HH	0.46 ± 0.24a		
	NG -HH	0.53 ± 0.18a		
	NG +HH	0.74 ± 0.49a		
2,4-Fuc(p)	G	0.89 ± 0.43	0.2628	AG and AG proteins
	NG	0.81 ± 0.37		
	-HH	0.89 ± 0.43	0.4765	
	+HH	0.79 ± 0.37		
	G -HH	1.04 ± 0.46a	**0.0367**	
	G +HH	0.62 ± 0.26c		
	NG -HH	0.66 ± 0.28c		
	NG +HH	0.91 ± 0.40b		

Table A.5. (continued)

3,4-Fuc(p)	G	0.02 ± 0.02	0.8875	XG
	NG	0.02 ± 0.02		
	-HH	0.02 ± 0.02	0.336	
	+HH	0.02 ± 0.02		
	G -HH	0.02 ± 0.04a	**0.0447**	
	G +HH	0.01 ± 0.04b		
	NG -HH	0.01 ± 0.02b		
	NG +HH	0.02 ± 0.05a		
t-Ara(f)	G	0.07 ± 0.06	0.5991	Type I and II AG
	NG	0.16 ± 0.16		XG, arabinan and
	-HH	0.11 ± 0.12	0.2193	XH
	+HH	0.11 ± 0.11		
	G -HH	0.09 ± 0.07a	0.5665	
	G +HH	0.04 ± 0.02a		
	NG -HH	0.16 ± 0.17a		
	NG +HH	0.16 ± 0.15a		
2-Ara(f)	G	3.53 ± 2.11	0.8879	Type I and II AG
	NG	3.53 ± 2.25		HX and RGII
	-HH	2.88 ± 2.56	0.5848	
	+HH	4.13 ± 1.89		
	G -HH	3.81 ± 2.87a	0.0623	
	G +HH	3.21 ± 2.00a		
	NG -HH	1.48 ± 1.38a		
	NG +HH	4.89 ± 1.56a		
3-Ara(f)	G	0.42 ± 0.22	0.1243	
	NG	0.67 ± 0.25		
	-HH	0.53 ± 0.31	0.5664	
	+HH	0.57 ± 0.23		
	G -HH	0.61 ± 0.21a	0.0543	
	G +HH	0.37 ± 0.17a		
	NG -HH	0.57 ± 0.24a		
	NG +HH	0.82 ± 0.33a		
5-Ara(f)	G	0.60 ± 0.16	0.9849	
	NG	0.61 ± 0.30		
	-HH	0.66 ± 0.21	0.6754	
	+HH	0.55 ± 0.24		
	G -HH	0.64 ± 0.15	0.9889	
	G +HH	0.55 ± 0.16		
	NG -HH	0.68 ± 0.30		
	NG +HH	0.57 ± 0.31		
t-Ara(p) or	G	0.64 ± 0.32	0.8189	Type II AG;
t-Xyl(p)	NG	0.72 ± 0.35		XG
	-HH	0.69 ± 0.34	0.6639	
	+HH	0.67 ± 0.34		
	G -HH	0.76 ± 0.36a	**0.0205**	
	G +HH	0.45 ± 0.22b		
	NG -HH	0.59 ± 0.31b		
	NG +HH	0.81 ± 0.37a		
3-Ara(p)	G	0.50 ± 0.26	0.4985	Arabinan, Type II

Table A.5. (continued)

	NG	0.72 ± 0.45		AG and HX
	-HH	0.59 ± 0.25	0.9256	
	+HH	0.62 ± 0.47		
	G -HH	0.61 ± 0.26	0.0813	
	G +HH	0.37 ± 0.22		
	NG -HH	0.57 ± 0.28		
	NG +HH	0.82 ± 0.54		
2,4-Xyl(p)	G	0.15 ± 0.02	0.2707	HX
	NG	0.15 ± 0.03		
	-HH	0.16 ± 0.03	0.1342	
	+HH	0.14 ± 0.02		
	G -HH	0.16 ± 0.04a	0.8837	
	G +HH	0.14 ± 0.04a		
	NG -HH	0.16 ± 0.02a		
	NG +HH	0.14 ± 0.06a		
3,6-Man(p)	G	0.31 ± 0.30	0.1782	
	NG	0.61 ± 0.55		
	-HH	0.51 ± 0.47	0.5878	
	+HH	0.40 ± 0.44		
	G -HH	0.40 ± 0.37a	0.6961	
	G +HH	0.21 ± 0.18a		
	NG -HH	0.68 ± 0.61a		
	NG +HH	0.56 ± 0.55a		
3-Glc(p)	G	4.09 ± 1.78	0.6832	
	NG	4.35 ± 2.53		
	-HH	4.57 ± 1.33	0.5402	
	+HH	3.89 ± 2.68		
	G -HH	5.22 ± 1.27a	**0.0157**	
	G +HH	2.74 ± 1.31b		
	NG -HH	3.59 ± 0.69b		
	NG +HH	4.87 ± 3.24ab		
4-Glc(p)	G	14.2 ± 6.72	0.7356	
	NG	14.92 ± 7.10		
	-HH	16.68 ± 5.06	0.3598	
	+HH	12.63 ± 7.38		
	G -HH	18.80 ± 4.47a	**0.0149**	
	G +HH	8.74 ± 2.76c		
	NG -HH	13.46 ± 4.59b		
	NG +HH	15.87 ± 8.67ab		
2,4-Glc(p)	G	0.09 ± 0.05	0.3653	
	NG	0.09 ± 0.07		
	-HH	0.10 ± 0.05	0.6077	
	+HH	0.09 ± 0.07		
	G -HH	0.13 ± 0.05a	**0.0021**	
	G +HH	0.06 ± 0.04b		
	NG -HH	0.05 ± 0.02b		
	NG +HH	0.12 ± 0.08a		
3,4-Glc(p)	G	3.50 ± 2.06	0.6789	
	NG	3.66 ± 1.93		

Table A.5. (continued)

	-HH	4.12 ± 1.75	0.9819	
	+HH	3.09 ± 2.07		
	G -HH	4.73 ± 1.89a	**0.0175**	
	G +HH	2.03 ± 1.10b		
	NG -HH	3.20 ± 1.21b		
	NG +HH	3.96 ± 2.36ab		
3,6-Glc(p)	G	0.09 ± 0.05	0.9707	
	NG	0.12 ± 0.12		
	-HH	0.09 ± 0.04	0.5542	
	+HH	0.12 ± 0.11		
	G -HH	0.10 ± 0.04	0.1111	
	G +HH	0.08 ± 0.05		
	NG -HH	0.08 ± 0.03		
	NG +HH	0.15 ± 0.14		
2,4,6-Glc(p)	G	0.56 ± 0.23	0.1538	
	NG	0.41 ± 0.44		
	-HH	0.52 ± 0.45	0.8898	
	+HH	0.46 ± 0.60		
	G -HH	0.63 ± 0.53	0.3771	
	G +HH	0.47 ± 0.66		
	NG -HH	0.36 ± 0.29		
	NG +HH	0.45 ± 0.61		
3,4,6-Glc(p)	G	2.26 ± 1.61	0.1029	
	NG	1.97 ± 1.14		
	-HH	2.69 ± 1.38	0.4993	
	+HH	1.60 ± 1.22		
	G -HH	3.10 ± 1.55a	**0.0556**	
	G +HH	1.24 ± 1.08b		
	NG -HH	2.08 ± 0.95b		
	NG +HH	1.90 ± 1.33b		
3-Gal(p)	G	0.16 ± 0.07	0.8837	Type II AG
	NG	0.18 ± 0.09		
	-HH	0.17 ± 0.07	0.5898	
	+HH	0.17 ± 0.08		
	G -HH	0.19 ± 0.07a	0.0679	
	G +HH	0.13 ± 0.04a		
	NG -HH	0.15 ± 0.07a		
	NG +HH	0.20 ± 0.09a		
6-Gal(p)	G	0.33 ± 0.24	0.5076	Type II AG, RG I and RG II
	NG	0.27 ± 0.23		
	-HH	0.34 ± 0.27	0.4740	
	+HH	0.25 ± 0.20		
	G -HH	0.38 ± 0.27a	0.4213	
	G +HH	0.28 ± 0.23a		
	NG -HH	0.32 ± 0.31a		
	NG +HH	0.23 ± 0.20a		
2,3-Gal(p)	G	0.18 ± 0.10	0.8230	
	NG	0.20 ± 0.14		

Table A.5. (continued)

	-HH	0.20 ± 0.11	0.9297	
	+HH	0.17 ± 0.14		
	G -HH	0.21 ± 0.12a	0.1784	
	G +HH	0.13 ± 0.81a		
	NG -HH	0.17 ± 0.10a		
	NG +HH	0.21 ± 0.18a		
3,6-Gal(p)	G	1.09 ± 0.47	0.8388	Type II AG, RG I
	NG	1.18 ± 0.56		
	-HH	1.27 ± 0.40	0.4190	
	+HH	1.01 ± 0.58		
	G -HH	1.36 ± 0.38a	0.1561	
	G +HH	0.76 ± 0.35a		
	NG -HH	1.14 ± 0.42a		
	NG +HH	1.21 ± 0.68a		
2,3,6-Gal(p) or 2,4,6-Gal(p)	G	0.47 ± 0.57	0.6547	
	NG	0.37 ± 0.62		
	-HH	0.46 ± 1.38	0.1244	
	+HH	0.39 ± 1.21		
	G -HH	0.75 ± 0.65a	**0.0345**	
	G +HH	0.14 ± 0.21b		
	NG -HH	0.04 ± 0.01b		
	NG +HH	0.59 ± 0.08a		
Unknown 1	G	0.81 ± 0.23	0.9842	
	NG	0.87 ± 0.33		
	-HH	0.86 ± 0.30	0.7730	
	+HH	0.82 ± 0.27		
	G -HH	0.87 ± 0.24a	0.2878	
	G +HH	0.73 ± 0.22a		
	NG -HH	0.84 ± 0.41a		
	NG +HH	0.89 ± 0.29a		
Unknown 2	G	1.20 ± 0.35	0.3184	
	NG	1.41 ± 0.53		
	-HH	1.46 ± 0.29	0.3491	
	+HH	1.16 ± 0.52		
	G -HH	1.41 ± 0.44a	0.3697	
	G +HH	0.92 ± 0.32a		
	NG -HH	1.49 ± 0.56a		
	NG +HH	1.35 ± 0.39a		
Unknown 2	G	0.90 ± 0.67	0.1356	
	NG	0.90 ± 0.65		
	-HH	0.97 ± 0.72	0.9324	
	+HH	0.84 ± 0.59		
	G -HH	1.09 ± 0.82	0.1150	
	G +HH	0.67 ± 0.40		
	NG -HH	0.78 ± 0.61		
	NG +HH	0.98 ± 0.71		
Unknown 3	G	0.20 ± 0.14	0.8650	
	NG	0.27 ± 0.12		
	-HH	0.23 ± 0.14	0.6671	

Table A.5. (continued)

	+HH	0.24 ± 0.22	
	G -HH	0.27 ± 0.14a	**0.0054**
	G +HH	0.11 ± 0.06b	
	NG -HH	0.17 ± 0.10b	
	NG +HH	0.34 ± 0.25a	
Unknown 6	G	1.82 ± 0.43	0.8678
	NG	1.90 ± 0.48	
	-HH	1.97 ± 0.40	0.4405
	+HH	1.76 ± 0.48	
	G -HH	1.94 ± 0.05a	0.6070
	G +HH	1.61 ± 0.04a	
	NG -HH	2.01 ± 0.02a	
	NG +HH	1.82 ± 0.08a	
Unknown 7	G	0.69 ± 0.46	0.8667
	NG	0.74 ± 0.11	
	-HH	0.78 ± 0.37	0.6345
	+HH	0.66 ± 0.47	
	G -HH	0.83 ± 0.46a	0.1177
	G +HH	0.53 ± 0.47a	
	NG -HH	0.70 ± 0.20a	
	NG +HH	0.76 ± 0.48a	
Unknown 8	G	0.29 ± 0.14	0.6326
	NG	0.29 ± 0.12	
	-HH	0.34 ± 0.11	0.1907
	+HH	0.25 ± 0.13	
	G -HH	0.36 ± 0.13a	0.1416
	G +HH	0.20 ± 0.07a	
	NG -HH	0.30 ± 0.10a	
	NG +HH	0.29 ± 0.15a	

The 34 partially methylated alditol acetates (PMAA) reported as $\mu g \cdot mg^{-1}$ AIR found in watermelon cell wall polysaccharides. The deduced linkages are reported along with the known polysaccharide class. All PMAA data are reported as LS means ± standard deviation. Any bolded p-value is for significant interaction differences, $\alpha = 0.05$.
AG = arabinogalacturonan, RG = rhamnogalacturonan, HX = heteroxylan, HM = heteromannan, XG = xylogalacturonan, G = graft, NG = non-graft, -HH = no hollow heart, and + HH = with hollow heart.

Appendix F

2017 GOLDSBORO NORTH CAROLINA NON-GRAFTED WATERMLEON REGRESION TRIAL: CAN WE INDUCE HOLLOW HEART?

Abstract

Triploid (seedless) watermelon encompass 95% of the fresh market and require diploid (seeded) counter parts for viable pollen and fruit set. Hollow heart (HH), a defect that causes an internal void in the placental tissue of the fruit, is found predominantly in seedless (triploid) watermelon types, and cannot be visually distinguished from normal fruit unless cut. Proper pollination is thought to be one the most important factors involved with the onset of HH. Researchers have speculated that increasing triploid distance from diploid pollinizer plants will induce HH. In this study, non-grafted triploid 'Liberty' watermelon was planted into two 100 m blocks subdivided into two replicates. Diploid pollenizers 'SP-6' and 'Ace-Plus', were placed at the center of each replicate to limit pollen. Distance of fruit set from pollinizer plants were measured at harvest. Fruit weight, length, and diameter were measured. Fruit were longitudinally cut from stem to blossom end to rate for the incidence and severity of HH. Fruit with HH were larger than fruit without HH. Soluble solids content increased in fruit with HH compared to no HH. No clear influence of pollinizer distance with HH incidence was found. No other differences were found in fruit composition (lycopene, pH, arginine and citrulline) between the incidence or severity of HH. Although distance from pollinizer plants did not appear to affect the incidence or severity of HH, a non related watermelon study was planted unexpectedly close to the pollinizer study. Bee activity may have compromised attempts to limit pollen availability.

Introduction

Hollow heart, also known as internal cracking, is a physiological disorder most commonly found in seedless watermelon. This internal split or void that develops in the placental tissue is caused by the separation of three internal fruit compartments; ovule, locule and septum (Johnson, 2015). Although the cause of hollow heart has not been definitively determined, watermelon genetics, lack of adequate pollination and environment and water stress appear to play definitive roles (Johnson, 2014; 2015). However, researchers have speculated that inadequate pollination is thought to be one of the leading causes of HH in watermelon (Johnson, 2014; 2015).

Seedless (triploid) watermelon require diploid (seeded) watermelon as pollenizers for fruit set. The general ratio of diploid:triploid in a field is recommended at 1:4 (20 to 33% of field in diploid) (Freeman et al., 2007). Researchers speculate the further that a triploid is planted from the pollen source, the more HH severity will increase. Inadequate pollination can be caused from a number of things including reduced bee visits, poor pollen release, or unfavorable weather conditions that can affect bee activity and pollen release.

The objective of this study was to determine if HH would increase in incidence and/or severity as distance between triploid and diploid plants is increased.

Materials and methods

Plant material. Triploid and diploid watermelon were grown as transplants. 'Liberty' triploid watermelon (Nunhems USA Inc, Parma ID) was sown on 20 April 2017. Seed were placed into polytransplant trays (Hummert Int.; Earth City, MO) filled with commercial soilless mix (Fine Germinating Mix, Carolina Greenhouse and Soil Company, Kinston, NC) and held under greenhouse conditions (ranging from 24 to 30 °C). About 3 weeks after seeding, watermelon transplants were placed either in a cold frame or high tunnel to harden off. Transplants were field planted 13 May 2017.

Experimental design and field establishment. The experiment was planted at the Cherry Research Farm in Goldsboro, NC. Two blocks were used with six watermelon beds (rows) per block. The blocks were split evenly into two replicates for a total of 4 reps, each at 50 m long. Rows were 100 m long with 3.1 m between row spacing and 0.8 m in-row spacing for graft and non-graft watermelon plants. Non-grafted 'Liberty' watermelon, susceptible to hollow heart, were planted at 0.8 m in row. The diploid pollenizers 'SP-6' and 'Ace-Plus' were transplanted directly in the center of each plot. 'SP-6' was planted in the center of row 3 and 'Ace-Plus' was planted in the center of row 4.

Any rows with missing transplants were replanted about 7 d after planting to achieve 100% stand count. Trickle irrigation (NETAFIM, 197 ml, 0.24 gph; NETAFIM, Tel Aviv, Israel) was utilized over the course of the growing season. Fertigation started two weeks after planting and was applied weekly using a 4.5-0-9 $kg \cdot ha^{-1}$ liquid fertilizer (Harrell's Max® Potassium plus Calcium, Lakeland, FL). Crop production followed a conventional spray program (Schultheis et al., 2014) to decrease pest and weed pressure.

Measuring distance from pollenizer. The distance (m) of fruit set from the pollenizer plants were measured at harvest. Pollenizers were set at 25 m (mid point of the 50 m block). Fruit were harvested on 17 July, 27 July and 3 Aug. 2017.

Quality Evaluation. Fruit were taken to the laboratory and fruit weight (kg) was determined with an electronic scale (Ohaus RC31P6 Counting Scale, Parsippany, NJ). Fruit length (cm) from stem to blossom end and maximum fruit diameter (cm) were determined by caliper (Precise Heavy Large Vernier Caliper 40/1000MM-LC-040, Penn Tool Co., Maplewoood, NJ.

Fruit were then cut longitudinally from stem to blossom end and rated for the incidence and severity of HH. Hollow heart was rated on a 1-5 scale (1= no HH to minor crack and 5= severe cavity) following USDA grading standards (2006). Tissue firmness (N) were assessed as maximum resistance to puncture (5 mm depth) at two locations near or in heart and locular tissue using a stationary firmness tester equipped with a Force One FDIX Digital Force Gauge (Wagner Instruments, Greenwich, CT) and a 0.8 cm diameter flat tip (Perkins-Veazie et al., 2016).

A central core of tissue (about 10 g) was cut from the half, squeezed onto a digital refractometer (Atago Pal-1, Bellevue WA) and soluble solids (°Brix) content determined. A tissue sample (100 g) was taken from the heart area, frozen, thawed, and pureed for determination of pH, citrulline, arginine and lycopene following methods of Fall et al. (2019).

Data analysis. Data set started with all entries, then separated out those that did not had a problems (e.g., cull, bruise, rot, dropped). All data were analyzed using SAS 9.4 (SAS Institute, Cary, NC, USA). A simple linear regression was used to determine if increased distance from pollinizer plant increased HH incidence and severity. A one-way ANOVA was run to determine significance of fruit weight, tissue firmness, soluble solids, pH, lycopene, and citrulline. Interactions of HH*group (distance from pollenizer) and HH*block were run via a one-way ANOVA. Where significance was found, separation of means was done using Tukey's honestly significant difference (HSD) test at $p \leq 0.05$.

Results and discussion

Data for distance from pollenizer are reported in Table A.1. Distance from pollinizer plants was broken into four groups where 1 = 5 m from pollinizer, 2 = 10 m from pollinizer, 3 = 15 m from pollenizer and 4 = 20 m from pollenizer. There almost no watermelons after 20 m.

HH incidence did not increase at increasing distance from pollenizer (Table A.1). HH severity did not increase at increasing distance from diploid plant ($p > 0.05$) (Fig. A.2).

Fruit size was bigger with HH compared to no hollow heart ($p<0.05$) (Table A.2). Fruit from 5-10 m and 15-20 m had the smallest diameter (Table A.3). Fruit size decreased with increasing harvest data (Table A.4.). No differences were seen in heart or locular firmness in fruit with and without HH (Table A.2). No differences were seen in fruit firmness (heart and locular) when compared to distance from pollinizer plants (Table A.3). No differences were seen in heart firmness but differences were seen in locular firmness in harvest date ($p>0.05$) (Table A.4). Soluble solids content was highest in fruit with HH (11.8 %) compared to no HH (11.1 %) (Table A.2). No differences were found in soluble solids content as a result of fruit distance from pollinizer (Table A.3). Soluble solids content was highest in the last harvest data (Table A.4). Lycopene, pH, citrulline and arginine were similar in fruit with or without HH ($p>0.05$). No interactions were found for HH x group or HH x block ($p>0.05$).

Table A.6. Distance from pollinizer and number of fruit with and without hollow heart.

Group	**HH** (0 = no, 1= yes)	**Number of fruit** (Harvest 1)	**Number of fruit** (Harvest 2)	**Number of fruit** (Harvest 3)
1	0	3	35	29
(0-5 m from pollinizer)	1	5	18	18
2	0	1	16	18
(5-10 m from pollinizer)	1	4	18	26
3	0	0	18	26
(10-15 m from pollinizer)	1	0	11	11
4	0	0	8	9
(>15 m from pollinizer)	1	0	4	2

Fruit number are reported as LS-means. No significant differences were found in fruit number ($p > 0.05$).

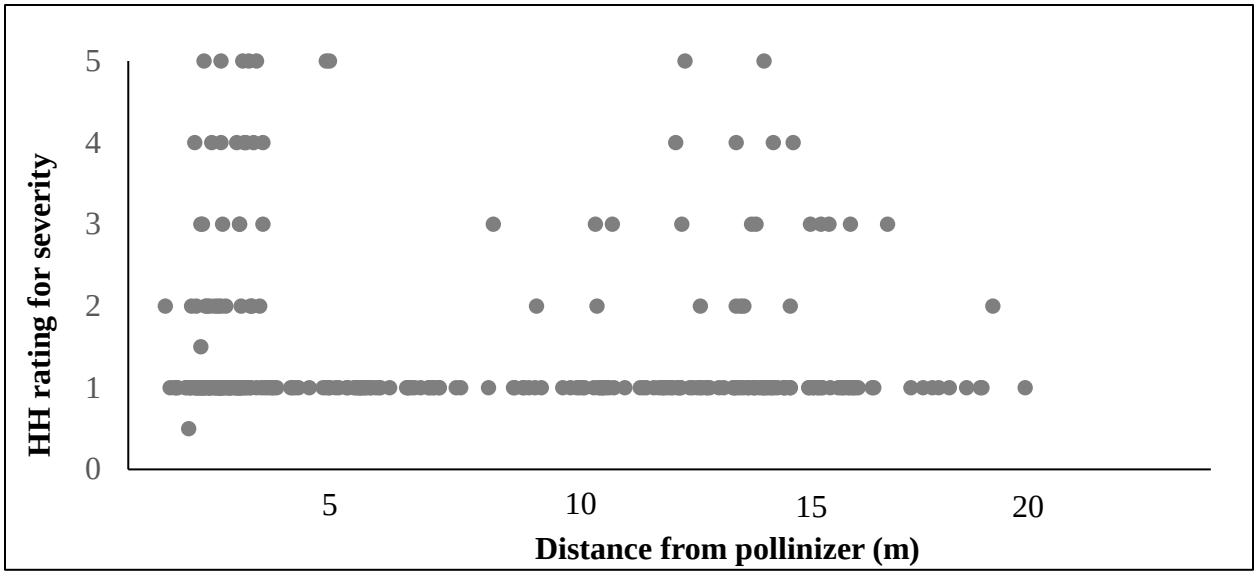

Figure A.1. Distance from pollinizer and severity of hollow heart. Severity of hollow heart is rated on a 1-5 scale, 1 = no or minor cavity and 5 severe. No differences in HH severity and distance from pollinizer were found ($p > 0.05$).

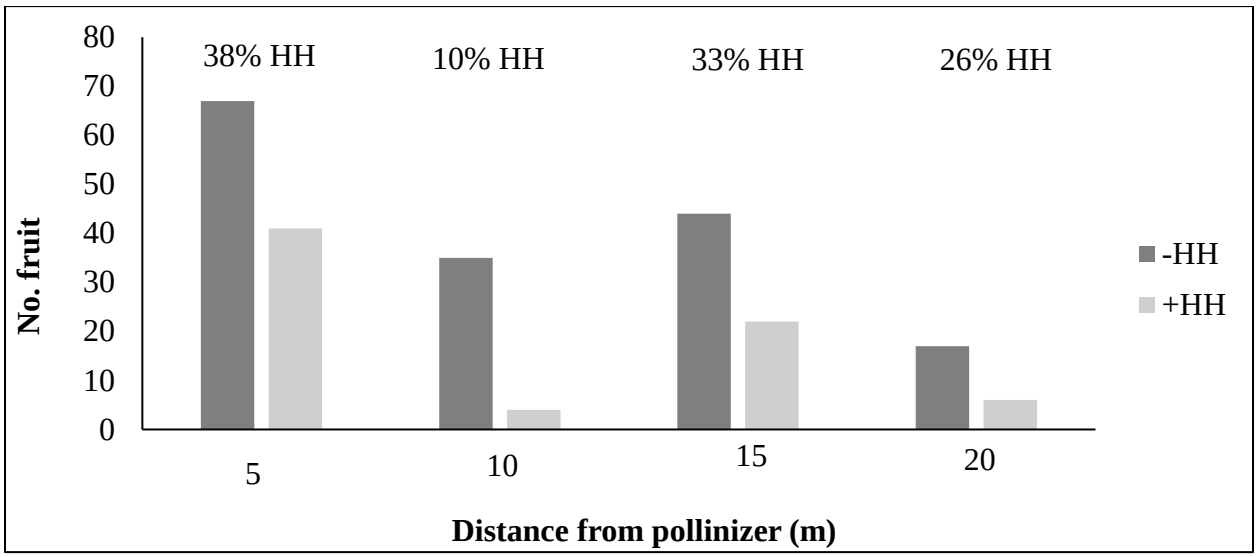

Figure A.2. Distance from pollinizer the number of fruit with and without hollow heart. The percentage of hollow heart is reported above each grouping. No fruit were harvested after 20 m from pollinizer plant.

Table A.7. Comparison of fruit with and without hollow heart on fruit quality attributes

HH	weight (kg)	length (cm)	Diameter (cm)	Heart firmness (N)	Locular firmness (N)	Soluble solids (ºBrix)	HH severity
0	5.8b	23.9b	18.8b	19.8a	20.6a	11.2b	0.00
1	7.5a	26.7a	20.7a	19.1a	20.6a	11.8a	2.27

Table A.8. Comparison of distance from pollinizer plants and effect on fruit quality in fruit with and without hollow heart.

Group distance	weight (kg)	length (cm)	Diameter (cm)	Heart firmness (N)	Locular firmness (N)	Soluble solids (ºBrix)	HH severity
Group 1 (0-5 m)	6.8ab	25.4ab	19.8a	19.6a	20.4a	11.4a	1.49a
Group 2 (5-10 m)	5.8bc	24.2bc	18.6b	19.5a	20.0a	11.1a	1.02b
Group 3 (10-15 m)	5.61c	23.6c	18.7b	19.7a	21.2a	11.4a	1.48a
Group 4 (>15 m)	7.3a	26.4a	20.0a	19.0a	20.9a	11.4a	1.30ab

Table A.9. Comparison of harvest date and fruit quality attributes in fruit with and without hollow heart.

Harvest	Weight (kg)	Length (cm)	Diameter (cm)	Heart firmness (N)	Locular firmness (N)	soluble solids (ºBrix)	HH severity
Harvest 1	7.0	26.5a	22.3a	19.2a	18.9b	11.1b	2.4a
Harvest 2	6.3	24.9a	19.2b	19.1a	19.9ab	11.1b	1.4b
Harvest 3	6.4	24.5a	19.2b	20.0a	21.4a	11.6a	1.3b

LS-means reported for hollow heart, fruit distance from pollinizer plants and harvest date. Tukey's honest significant test was done ($p < 0.05$); means with dissimilar letters are different.

Biases in experiment. The purpose of this study was to see if placing pollinizer plants at specific distances would affect the number of fruit and the incidence of hollow heart. Unfortunately there were two unexpected events at the site that were beyond our control. The first problem was a tendency of the crew to overwater. Overwatering can lead to uneven tissue expansion in the rind and heart (Johnson 2014; 2015), causing excess HH in fruit. Overwatering can also increase fruit size and may account for the differences seen in fruit size with and without HH.

Another issue with this experiment was the layout and location of the study. The experimental layout was two 100 m blocks (subdivided into reps 1,3 and 2,4). Reps 1 and 3 ended up being close to a watermelon cultivar study and bees were used to increase set in that study. The first block (reps 1 and 3) had far more fruit than the second block (reps 2 and 4). This strong block effect caused biases in the data as there were roughly 2-3 times more fruit from block 1 compared to block 2. It appears that bees may have inadvertently carried pollen from the watermelon cultivar study to block 1 and caused an increase in fruit set. In future studies with hollow heart, plots will need to be well quarantined from pollinators and other watermelon cultivar evaluations.

Summary

Despite biases in the data from plot overwatering and lack of complete control of pollinators, some results were found. By limiting the amount of diploid pollinizer plants (and amount of viable pollen) HH can be induced in triploid watermelon. HH did not affect fruit composition but it did affect fruit size (length and diameter, cm) and soluble solids content; fruit with HH had higher soluble solids. Future regression studies are needed to assess if increasing distance from the pollenizer increases the incidence and severity of HH.

References

1. Freeman, J., G.A. Miller, S.M. Olson and W.M. Stall. 2007c. Diploid watermelon pollenizer cultivars differ with respect to triploid watermelon yield. HortTechnology 17:518-523.

2. Johnson, G. 2014. These beautiful watermelon patterns are driving everyone crazy. [Online]. https://www.boredpanda.com/weird-watermelons-beautiful-hollow-heart/

3. Johnson, G. 2015. Research finds potential cause of hollow heart disorder in watermelon. PhysOrg. [Online]. https://phys.org/news/2015-06-potential-hollow-heart-disorder-watermelons.html

4. Schultheis, J.R. and B. Thompson. 2014. North Carolina State University Watermelon Cultivar Trials. No. 210. Pp 1-39. [Online]. https://gates.ces.ncsu.edu/wp-content/uploads/2015/01/NCSU-Watermelon-Cultivar-Booklet_2014.pdf?fwd=no
5. USDA. 2006. US Standards for Grades of Watermelon. Agricultural Marketing Services, Fruit and Vegetable Program, pp. 1-11.